Targeting Cell Wall Formation in the Oomycete Phytophthora cinnamomi for Disease Control

Amena Khatun

A thesis submitted to the University of Adelaide in fulfilment of the requirements for the degree of Doctor of Philosophy

School of Agriculture, Food and Wine
Faculty of Sciences, Engineering and Technology
The University of Adelaide

October 2023

“The most beautiful thing we can experience is the mysterious. It is the source of all true art and science”

Albert Einstein

(14 March 1879 – 18 April 1955)

Table of Contents

Abstract

The oomycete *Phytophthora* genus comprises microorganisms that cause devastating plant diseases, such as late blight and root rot diseases, leading to significant agricultural economic losses, and causing extensive damages to ecosystems. To date, no practical method is available to prevent these diseases. Furthermore, current strategies to control *Phytophthora*-induced diseases are ineffective in the long term. These strategies currently rely on different classes of chemicals. However, repeated use of the same chemicals can lead to development of pesticide resistance in phytopathogens. This concern, combined with an increased awareness of alternative approaches that have minimal impact on biodiversity and human health, highlights that efficient methods for controlling diseases caused by *Phytophthora* are urgently required. Targeting cell wall biosynthesis is a promising strategy to combat these pathogens. Indeed, the inhibition of enzymes involved in carbohydrate biosynthesis affects the growth and survival of these pathogens, offering a promising avenue for the development of effective treatments.

In recent years, plant antimicrobial peptides (AMPs) have been found to be effective against different phytopathogens. Well-known AMPs are plant defensins, a family of small cysteine-rich peptides that can bind to chitin and cell wall glucans in fungi. However, knowledge about the inhibitory role of plant defensins in oomycetes is limited. As such, this work investigates the effects of the plant defensin NaD1 (*Nicotiana alata* defensin 1) on *Phytophthora* species, which may reveal novel opportunities for controlling plant diseases.

Our findings demonstrate that NaD1 effectively inhibits the mycelial growth of *Phytophthora cinnamomi*, *Phytophthora cambivora*, *Phytophthora nicotianae*, and *Phytophthora citricola*. Exposure to NaD1 induced alterations in the growth and structure of *P. cinnamomi*, leading to suppressed apical dominance, hyper-branching, and changes in cell wall composition, likely due to disruption of calcium homeostasis. Transcriptomic analyses confirmed altered

expression of genes involved in cellulose synthesis and calcium transport (**Chapter 2**), and uncovered changes in the transcriptome across the entire genome in hyphal cells exposed to NaD1, shedding light on the mechanism of action of this AMP. These differentially expressed genes can serve as candidates to study the efficacy of NaD1 against *Phytophthora* species (**Chapter 4**).

In addition to NaD1, the effects of a chitin synthase inhibitor, nikkomycin Z, were also investigated. This study shows that nikkomycin Z causes strong growth inhibition of four *Phytophthora* species and induces abnormal hyphal growth. Exposure to this inhibitor decreases cellulose levels and affects the expression of genes related to vital functions such as cell wall biosynthesis, hexosamine biosynthesis and chitin deacetylation (**Chapter 3**).

Altogether, the present work reveals critical information about the fundamental inhibitory mechanisms of NaD1 and nikkomycin Z on *Phytophthora* species, with a focus on cell wall biosynthesis. This work paves the way for the development of novel effective targets for oomycete disease control.

Thesis declaration

I certify that this work contains no material which has been accepted for the award of any other degree or diploma in my name, in any university or other tertiary institution and, to the best of my knowledge and belief, contains no material previously published or written by another person, except where due reference has been made in the text. In addition, I certify that no part of this work will, in the future, be used in a submission in my name, for any other degree or diploma in any university or other tertiary institution without the prior approval of the University of Adelaide and where applicable, any partner institution responsible for the joint-award of this degree.

I acknowledge that copyright of published works contained within this thesis resides with the copyright holder(s) of those works.

I also give permission for the digital version of my thesis to be made available on the web, via the University's digital research repository, the Library Search and also through web search engines, unless permission has been granted by the University to restrict access for a period of time.

Amena Khatun

June 2023

Acknowledgments

This PhD thesis work was performed from November 2019 to June 2023 at the School of Agriculture, Food and Wine at The University of Adelaide. I would like to express my deepest appreciation to all those who continuously supported me during this period of time.

First and foremost, I am deeply indebted to my former supervisor and current co-supervisor, Prof. Vincent Bulone, for his constant support, encouragement, and guidance throughout my PhD thesis. I am incredibly grateful for his intense suggestions, contributions to proofreading manuscripts and presentations, and prompt actions when help was needed. He continuously encouraged me and was always willing to assist me. I would like to extend my most profound appreciation to my co-supervisor Dr Julian Schwerdt for his intensive contribution to data analysis of RNA sequencing experiments, proofreading of manuscripts, and always providing me emotional support by saying “nearly there”. His expertise in bioinformatics and insightful teaching helped me to understand and learn bioinformatics. I am also grateful to my co-supervisor Dr Caterina Selva for her continuous support during the development of the methods for cell wall preparations of *Phytophthora* species. I also appreciate her constant support and insightful discussion during my research work, thesis writing, and manuscript preparation. Special thanks to my postgraduate coordinator, Associate Professor Kenneth Chalmers, for PhD consultation and for helping with the administration.

Many thanks go to Dr Natalie Betts, Dr Alan Little, Dr Helen Collins and Dr. Bryan Coad, who provided an excellent starting point for this journey. I sincerely thank my current supervisor Dr Helen Collins for her silent but intense emotional support throughout these years; without this support, it would have been a lot harder for me to finish this journey. Furthermore, I would like to express my gratitude to Dr Long Yu and Jelle Lahnstein for teaching and helping me with cell wall analyses.

I extend my heartfelt appreciation and gratitude to Prof. Marilyn Anderson and Dr James McKenna from La Trobe University for providing the NaD1 peptide. I want to thank all members of the Burton Laboratory, past and present. I am grateful for the technical support provided by Sandy Khor, Chao Ma, Dr James Cowley, and Dr Ghazwan Karem when I joined the School. I would also like to express my sincerest thanks to Dr Gwenda Mayo for her assistance with different types of microscopy at Adelaide Microscopy. Further thanks to my workplace, Noakhali Science and Technology University in Bangladesh, for permitting me to undertake study leave to enhance my skills.

Thanks to my strong Mom and Dad for listening to my whining and giving me advice whenever life becomes hard for me. I also appreciate the continuous support of my husband, Zohirul Hoque Bapy, throughout my PhD. His sacrifice, encouragement, and appreciation helped me to overcome difficulties in this challenging journey. I would like to express my gratitude to my elder brothers, sisters-in-law, my nieces and nephews for their enormous emotional support and care. To my dearest uncle, Karim Kakku, who cared about me like my father throughout my life and during this PhD thesis. Even though you suddenly passed away in 2022, you will always be in my heart.

I must thank my friends Daniel Clayton-Cuch, Belinda Akomeah, and Dr Charity Chidzanga for encouraging me during tough times. I would like to extend a special thanks to Daniel Clayton-Cuch for his unwavering support and for being a dependable shoulder to cry on throughout the tough times of this PhD thesis.

Lastly, I thankfully acknowledge the financial support from the University of Adelaide during my PhD.

Publications

1. **Khatun A**, Selva C, Schwerdt JG, Betts N, Yu L and Bulone V. The plant defensin NaD1 inhibits the growth of *Phytophthora* species by interfering with cell wall structure and calcium transport (unpublished and unsubmitted work written in manuscript style).

2. **Khatun A**, Schwerdt JG, Selva C, Betts N, Yu L and Bulone V. Analysis of the effect of the chitin synthase inhibitor nikkomycin Z on *Phytophthora* species (unpublished and unsubmitted work written in manuscript style).

3. **Khatun A**, Schwerdt JG, and Bulone V. Global transcriptomic analysis of the *Phytophthora cinnamomi* response to treatment with the plant defensin NaD1 (unpublished and unsubmitted work written in manuscript style).

Conference proceedings

1. **Khatun, A**., Selva, C., Schwerdt, J., Betts, N., Yu, L. and Bulone, V. (2022). The plant defensin NaD1 inhibits the growth of *Phytophthora* species by interfering with cell wall structure and calcium transport. *The 21st Annual Meeting of the Oomycete Molecular Genetics Network,* Brno, Czech Republic. Invited speaker.

Thesis aims

The main objective of this study was to determine the inhibitory effect of the antimicrobial peptide Defensin 1 from the plant *Nicotiana alata* (NaD1) and of the chitin synthase inhibitor nikkomycin Z on the growth and development of *Phytophthora cinnamomi*, *Phytophthora cambivora*, *Phytophthora citricola*, and *Phytophthora nicotianae*. Particular emphasis was placed on *P. cinnamomi*, which represents a significant threat to the Australian ecosystems.

The research was designed to address the following aims:

1. Assess the sensitivity of *Phytophthora* species to the plant defensin NaD1;

3. Identify and characterise the effects of NaD1 and nikkomycin Z on hyphal morphology, growth, development, and cell wall constituents of *P. cinnamomi*;

4. Determine the effectiveness of a chitin synthase inhibitor, nikkomycin z, as a control agent of *P. cinnamomi*;

5. Understand the biological activity of NaD1 against *P. cinnamomi* by profiling whole transcriptional changes;

Thesis context

To assist readers in the navigation of this Thesis, an overview outlining the content of the main Chapters is provided below.

In this Thesis, Chapter 1 is intended to provide the background and framework for this work. This Chapter comprises a Literature Review on oomycetes and expands on their economic importance, biology and the structure and biosynthesis of oomycete cell walls. A detailed description of cell walls in oomycetes will enable readers to understand their diversity across lineages. Chapter 1 also provides an overview of current oomycete disease management strategies and the potential effectiveness of cell wall inhibitors. Several promising methods for managing oomycete diseases, including transgenic techniques, antimicrobial peptides (AMPs), dsRNA, biological control measures, and genome editing, have been introduced as potential avenues to pursue for improved disease management.

This study focused on the devastating phytopathogenic oomycete genus *Phytophthora*. Chapter 2 presents the growth inhibitory effects of the AMP defensin 1 from the plant *Nicotiana alata* (NaD1) on four species of this genus. The restricted hyphal growth of *P. citricola*, *P. cambivora*, *P. nicotianae* and *P. cinnamomi* validated the capability of NaD1 to inhibit the growth of this genus of plant pathogens. Afterwards, morphological, developmental, structural, and transcriptional changes caused by exposure of *Phytophthora cinnamomi* to NaD1 were analysed using a combination of molecular and biochemical techniques, and transcriptomic analysis by RNA sequencing. Together, it is clear that NaD1 acts as an inhibitor against *Phytophthora* species, and we show that this AMP holds the potential for developing new solutions to control these devastating phytopathogens.

In Chapter 3, the chitin synthase inhibitor nikkomycin Z was tested as a potential control agent against *Phytophthora* species. Nikkomycin Z is a secondary metabolite derived from

Streptomyces tendae. This compound has shown potential as an antifungal therapy due to its ability to inhibit chitin synthase activity in fungi, thereby interfering with chitin synthesis. This Chapter shows that nikkomycin Z is also active on *Phytophthora* species and modifies the cell wall structure of *P. cinnamomi*. As in Chapter 2 and 3, molecular and biochemical techniques, and transcriptomic analysis by RNA sequencing were used to study the impact of nikkomycin Z on *P. cinnamomi*. Identification of the differentially expressed genes provided insights into the inhibitory mechanism of nikkomycin Z.

Chapter 4 reports a global transcriptomic analysis for in-depth genome-wide understanding of the action mechanism of NaD1 in *P. cinnamomi*. The identified differentially expressed genes provide interesting candidates that might be targeted to develop new control strategies.

Chapter 5 provides a general conclusion of this thesis, followed by contribution to knowledge and recommendations for future directions.

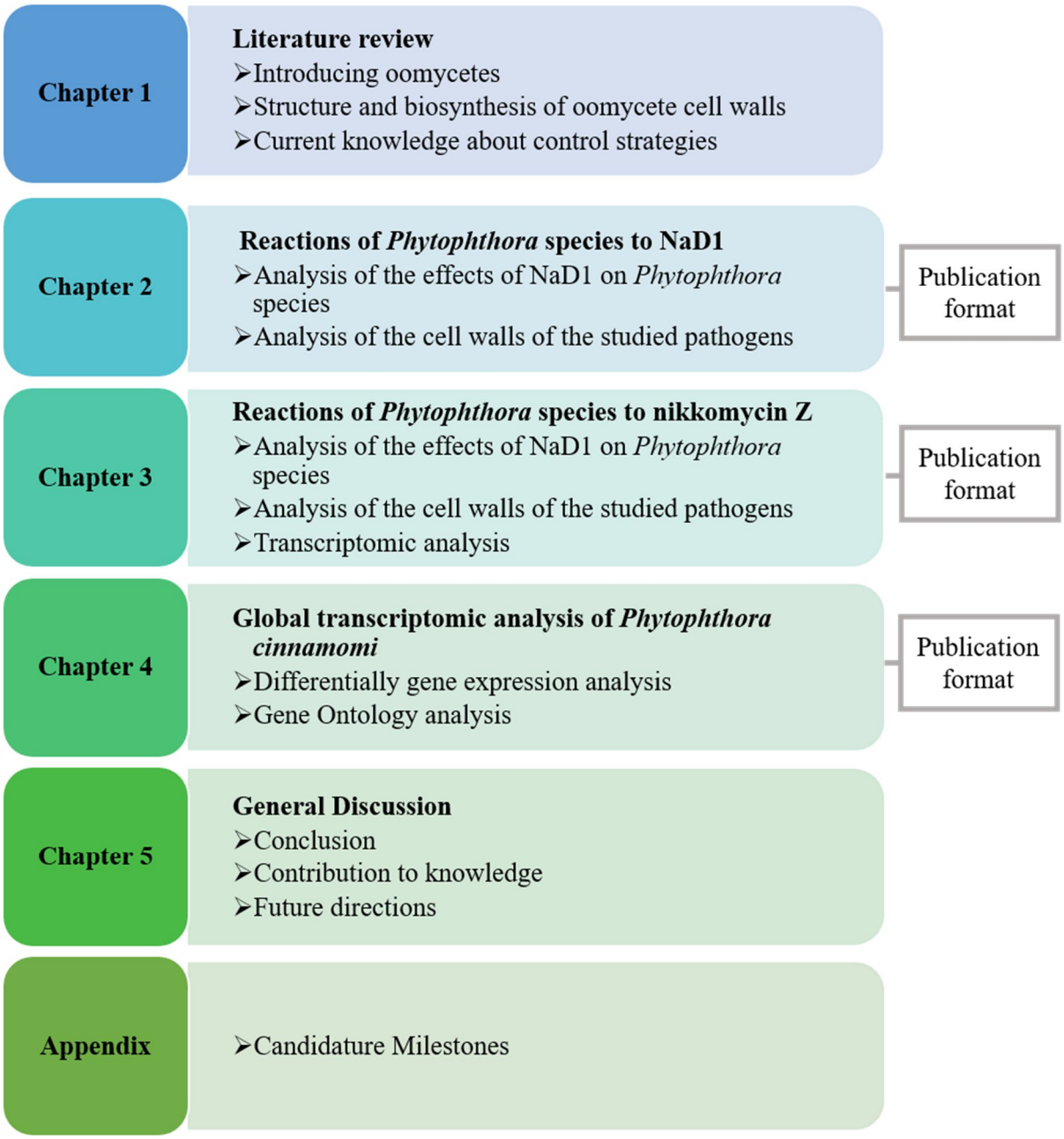

Figure 1. A schematic overview of the thesis structure.

Chapter 1

Insights into Oomycete Cell Walls and Implications for Oomycete Disease Management Strategies: Literature review

1 Introduction to oomycetes

Oomycetes are a class of eukaryotic microorganisms that live in different environments, including marine, freshwater, and terrestrial ecosystems (Bridge *et al.*, 2008; Hughes *et al.*, 2003; Mirzaee *et al.*, 2009; Thines, 2018). Certain species of oomycetes are adapted to thrive in specific habitats, while others can survive in a variety of conditions. Like fungi, oomycetes are heterotrophic organisms with saprophytic or parasitic (necrotrophic) modes of nutrition. Saprophytic oomycetes contribute to the decomposition of organic matter and participate in nutrient cycling. On the other hand, many terrestrial oomycetes are parasites of vascular plants and include several devastating phytopathogens, such as *Phytophthora*, *Pythium*, and *Aphanomyces* (*Aphanomyces euteiches*), which cause several root rot or foliar diseases like downy mildew, stem rot, and blight. In addition, some aquatic necrotrophic oomycetes cause devastating diseases in salmon, crayfish, and catfish. Some beneficial oomycetes defined as 'mycoparasitic oomycetes' can parasitise other phytopathogenic fungi and oomycetes. For example, *Pythium oligandrum* can protect crop plants from phytopathogenic fungi such as *Rhizoctonia solani*, *Botrytis cinerea*, and *Fusarium solani*, and from pathogenic oomycetes, e.g., *Phytophthora parasitica* and *Pythium ultimum* (Berry *et al.*, 1993; Bradshaw-Smith *et al.*, 1991; Laing & Deacon, 1991; Picard *et al.*, 2000). Owing to these properties, *P. oligandrum* has been used for years in the Slovak Republic as a commercial biocontrol agent known as 'Polygardron' (Brožová, 2002).

The Peronosporales and Saprolegniales are the most studied orders of oomycetes. The Peronosporales comprise *Phytophthora* as the largest genus, with more than 120 described plant pathogenic species (Kamoun, 2006; Kasuga *et al.*, 2012) that pose a significant threat to agricultural crops and natural ecosystems (Hansen *et al.*, 2012; Judelson, 2012; Jung *et al.*, 2013; Yang *et al.*, 2017). *Phytophthora* attracted attention after causing the potato famine in Ireland during 1845–1846. In 1876, *Phytophthora infestans* was identified as the causative agent of the potato late blight disease (Bourke *et al.*, 1993). In 2009, another late blight epidemic due to *P. infestans* was observed in tomato fruit in the Eastern United States (Fry, 2013), where the infection still costs US $507 per hectare annually in fungicide (Guenthner *et al.*, 2001). Globally, this pathogen causes more than $6 billion economic loss yearly (Derevnina *et al.*, 2016). In Australia, it has been reported that more than 5,000 native plant species are susceptible to the soilborne species *Phytophthora cinnamomi*, which has been identified as a serious threat to Australian native plants and the overall ecosystem of the country (Cahill *et al*., 2008; Jung *et al*., 2013; Kamoun *et al*., 2015). In the southern part of Western Australia, over 40% of indigenous plant species are identified as vulnerable encompassing numerous members of the

Proteaceae family. The risk is further amplified for endangered plant species, as approximately 56% of them are deemed susceptible *P. cinnamomi* (Shearer *et al*., 2004).

Besides pathogens of plants, the Peronosporales order comprises some animal and human pathogens responsible for severe diseases. For example, a life-threatening infectious human disease called 'Pythiosis' is increasingly diagnosed worldwide and becoming a concern as an emerging threat to human health caused by *Pythium insidiosum* (Permpalung, Worasilchai, & Chindamporn, 2020). The Saprolegniales more generally comprise pathogenic species of animals. *Saprolegnia parasitica* is an example of an aquatic oomycete that causes saprolegniosis, a disease responsible for significant economic losses in aquaculture and declines of fish populations in the wild. The intensive use of fungicides associated to large-scale outbreaks of pathogenic oomycetes can lead to environmental contaminations and important economic losses. Considering these adverse impacts, the development of successful and non-toxic anti-oomycete drugs is urgently required to suppress or mitigate the devastating threats caused by pathogenic oomycetes in agriculture, the environment and human and animal health.

Table 1: Impact of pathogenic oomycetes on agriculture, aquaculture and human health.

Hosts	Pathogen	Disease	Known hosts	Impact	References
Plants	*Phytophthora infestans*	Late blight	Potato & Tomato	Annual global loss of US $6 billion	(Derevnina *et al.*, 2016)
	Phytophthora palmivora	Black pod disease	Cocoa	Annual global loss of US $1 billion	(Drenth & Guest, 2004)
	Phytophthora capsici	Root rot	Pepper	Annual global loss > US $100 million	(Bosland, 2008)
	Phytophthora sojae	Damping off	Soybean	Annual global loss of US $1-2 billion	(Tyler, 2007)
	Phytophthora cinnamomi	Root rot	Avocado	Annual loss > US $40 million in California	(Ploetz, 2013)
		dieback	About 5000 species	Chestnut and holm oak forests in Europe; natural forests in Australia	(Hardham & Blackman, 2018)
	Plasmopara viticola	Downy mildew	Grape	Annual loss of A$ 140 million in Australia	(Taylor & Cook, 2018)

	Aphanomyces euteiches	Root rot	Pea, lentil, alfalfa, trifolium, and other Fabaceae species	Annual loss of US $600 million in Europe and the United States.	(Allmaras *et al.*, 1998)
	Aphanomyces cochlioides	Root rot	Sugar beet	Annual loss of US $42.8 million in the USA	(Becking *et al.*, 2022)
Fish and other aquatic animals	*Aphanomyces astaci*	Crayfish plague	Freshwater crayfish species	Significant annual loss worldwide, but no overall estimation available	(Becking *et al.*, 2022)
	Aphanomyces invadans	Epizootic Ulcerative Syndrome	Wild and farmed fish	Loss of US $110 million between the late 80s and early 90s	(Syndrome, 1998)
	Saprolegnia parasitica and *Saprolegnia monoica*	Saprolegniosis and winter kill	Salmon, catfish	Annual loss of US $40 million due to saprolegniosis and $50 million due to winter kill in the catfish industry in the USA	(Bly & Clem, 1992; Torto-Alalibo *et al.*, 2005)
Humans and animals	*Pythium insidiosum*	Pythiosis	Humans, cattle, canines, equines, felines	Causes life-threatening conditions with high mortality rate. Pythiosis is emerging as a deadly disease in humans in tropical, sub-tropical, and temperate regions.	(Chitasombat *et al.*, 2020)

2 Phylogenetic position of oomycetes

Historically, oomycetes were misclassified as lower fungi and still sometimes incorrectly considered as fungi. The confusion regarding their classification essentially lies in their similar filamentous growth pattern and ecological roles as true fungi. In addition, oomycetes and fungi are both heterotrophic and exhibit an osmotrophic mode of nutrition, which involves the

secretion of enzymes to break down nutrients for their further absorption (Beakes & Thines, 2016; Wijayawardene *et al.*, 2020). Furthermore, these organisms commonly produce sexual and asexual spores (Judelson, 2012). According to pioneering research by Aronson *et al*. in 1967 and Bartnicki-Garcia in 1968, oomycete cell walls are primarily composed of cellulose and devoid of chitin, while fungal cell walls are chitinous (Aronson *et al.*, 1967; Bartnicki-Garcia, 1968). However, this general dogma is no longer valid as chitin has been shown to occur in the cell walls of some oomycetes species, albeit in small amounts not exceeding 1-5% (see e.g., Bulone *et al.*, 1992; Mélida *et al.*, 2013). Unlike oomycetes, fungal cell walls contain higher amounts of chitin, typically up to 20 %, and lack cellulose in their cell walls (see Table 2 in Section 4). With advancements in molecular phylogenetics and genetic analysis, it became evident that oomycetes belong to a distinct lineage, the Stramenopiles or Heterokonts, separate from the true fungi (Beakes *et al.*, 2012). A distinctive evolutionary study proved that oomycetes are closely related to diatoms and brown algae within the heterokonts (Beakes *et al.*, 2012; Phillips *et al.*, 2008) (Fig. 1). Genome comparison between oomycetes and diatoms revealed the photosynthetic ancestry of oomycetes, although oomycetes lost chloroplast in all three clades through evolution (Adl *et al.*, 2005; Cavalier-Smith & Chao, 2006; Tsui *et al.*, 2009). The phylogenetic relationship within the oomycetes shows the presence of early diverging basal lineages, which mainly consist of obligate parasites of marine organisms like seaweed, crustaceans, and algae (Beakes *et al.*, 2012). The basal orders evolved successively into the saprolegnian line (mainly freshwater parasites), with the main divergent order being the peronosporalean (mainly soilborne plant/animal parasites). After landing from sea to land, mycelial growth pattern and sexual reproduction were acquired by this divergent group of oomycetes (Beakes *et al.*, 2012) (Figure 1).

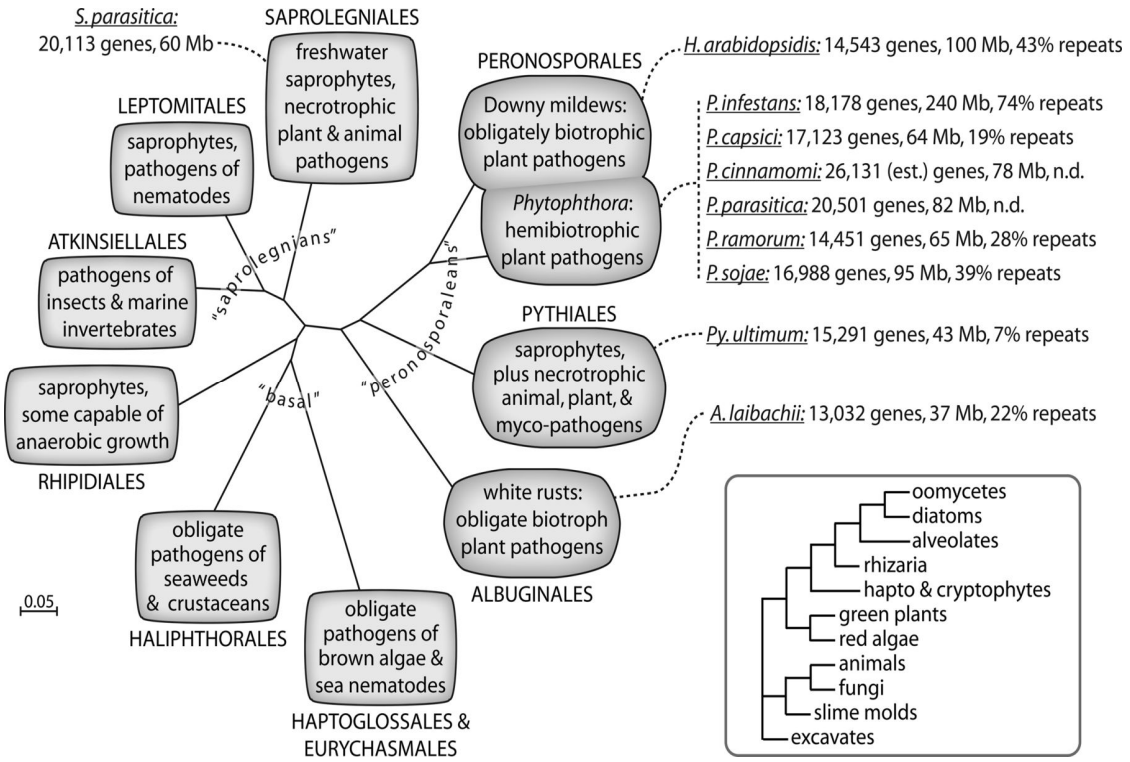

Figure 1: Evolutionary history of orders of oomycetes including the Saprolegniales and Peronosporales. (Reprinted with permission from {Judelson *et al*., 2012}. Copyright {2012} American Society for Microbiology.)

3 Life cycles of oomycetes

The basal lineages of the oomycetes have simplified morphological attributes and lifestyles compared to the species belonging to the Peronosporales and Saprolegniales orders. All known oomycetes of the basal lineages can produce sporangia from holocarpic thalli, and they are found to not produce oospores through sexual reproduction (Beakes *et al.*, 2017; Dick, 2013). However, a few genera of early lineages show evidence of a non-canonical form of sexual reproduction, e.g., *Olpiodiopsis*, *Eurychasma*, and *Anisolpidium*, which are marine species considered a potential threat to the cultivation of algae and therefore the seaweed industry (Badis *et al.*, 2020; Gachon *et al.*, 2017; Tsirigoti *et al.*, 2013). These species can produce oospore-like structures through the fusion of two thalli of different size by a form of sexual reproduction which is not clearly understood (Buaya & Thines, 2020; Cornu, 1872; Sparrow & Ellison, 1949). In their asexual stage, most species produce tubular or spherical thalli, which are branched or unbranched, and which can produce single or multiple tube-like sporangial structures to release zoospores (Buaya & Thines, 2019, 2019, 2020). After release, the zoospores can swim for several minutes and disperse readily in the environment (Perrott, 1960; Sparrow, 1960). The sporangia of these early lineages form primary zoospores only, which exhibit a pyriform shape and are bi-flagellate, except for *Anisolpidium.*

Species from the Saprolegniales order have a relatively complex life cycle compared to their counterpart from early lineages, and have distinct asexual and sexual life stages. In the sexual stage, nuclei fusion takes place between the haploid male antheridium and the female oogonium to produce a resting spore called 'oospore'. In the asexual stage, the mycelium can produce spike-shaped sporangia, which produce primary bi-flagellate zoospores. These zoospores are less stable than the zoospores produced by the early lineage species, but they encyst within a minute after release. The resulting primary cysts then germinate to produce secondary zoospores, which are better swimmers that primary zoospores and can survive for many hours before encystment, and the subsequent production of fully matured zoospores or mycelium (Bruno *et al.*, 2011; Walker & van West, 2007). *Aphanomyces*, *Saprolegnia* and *Achlya* are the three genera belonging to the Saprolegniales order. They can cause diseases in many organisms. The *Aphanomyces* genus comprises three major clades: one clade causes diseases in aquatic animals, e.g., crayfish plague in freshwater crayfish by *Aphanomyces astaci*; a second clade causes plant diseases, e.g., root rot in legume crops by *Aphanomyces euteiches*; and the third clade consists of saprophytes that cause diseases in nematodes (Diéguez-Uribeondo *et al.*, 2009) (Table 1). *Saprolegnia parasitica* is one of the most destructive oomycetes and a threat to fish farming in both freshwater and the ocean. Out of the 80 known *Achlya* species, about 20 are pathogens of fish (Choi *et al.*, 2019).

The order Peronosporales contains obligate biotrophs, e.g., *Albuginales* and *Plasmopara*, as well as hemi-biotrophs and saprotrophs, e.g., *Phytophthora*, *Halophytophthora*, *Pythium*, and *Phytopythium*. The outstanding feature of this lineage is that some of the saprophytes from the genus *Pythium* do not have asexual reproduction, while some produce multinucleate and immotile asexual spores. As a result of the evolutionary process, some species of this lineage have lost their potential to produce zoospores. However, *Phytophthora* still produces bi-flagellated zoospores through asexual reproduction. These are able to find their host cells by chemotaxis (Hosseini *et al.*, 2014) (Figure 2). Indeed, these zoospores can chemotactically sense compounds present in plant leaf or root exudates, such as pectins and amino acids. Thus, once zoospores are released, they actively swim towards the leaves or roots of the host plant and colonize the host tissues before competitive anamorphic fungi can establish themselves in the host. After attachment to the host surface (roots or other plant organs), the zoospores promptly shed their flagella and rapidly encyst by developing a cell wall within 10 minutes (Desjardins *et al.*, 1973). Cysts produce germ tubes and an infection structure named 'appressorium' to infect the host cells (Ristaino *et al.*, 1992).

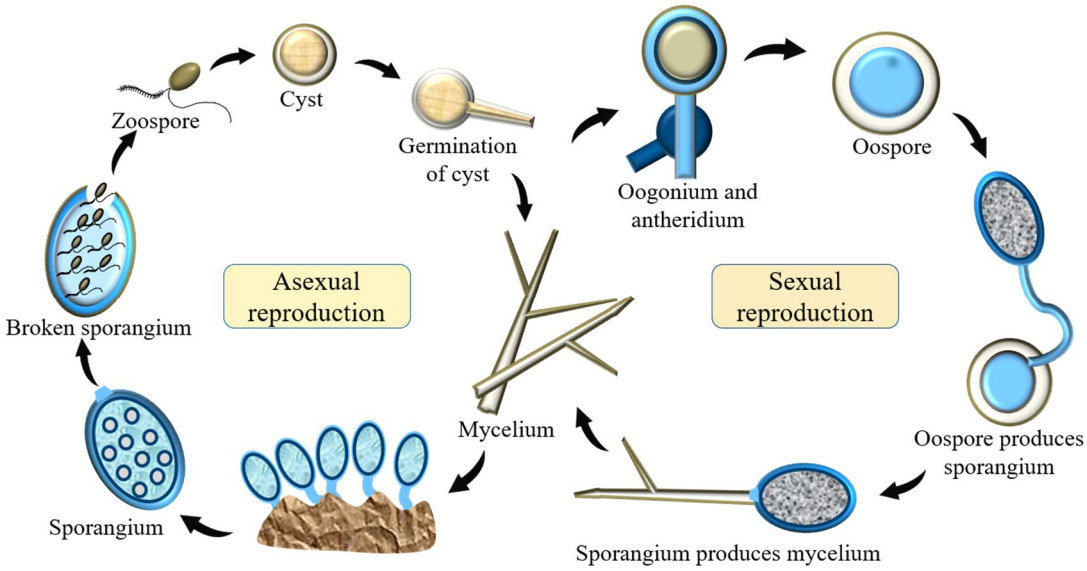

Figure 2: Life cycle of *Phytophthora* including sexual and asexual reproduction.

In unfavourable conditions (e.g., hot, dry weather), the mycelium produces hardier chlamydospores instead of sporangia, which can survive without a host for more than 100 days (Jung *et al.*, 2013) due to encapsulation by a cell wall. *Phytophthora* sp. can also reproduce sexually by producing gametangia, i.e., oogonium and antheridium; subsequent successful mating produces oospores, which remain alive during overwintering and produce a sporangium or germ tube under favourable conditions (Figure 2) (Savage *et al.*, 1968).

4 Oomycete cell walls

The cell wall is the cell's outermost layer and is the organism's first point of contact with the environment. Therefore, it is a primary player in the physical and chemical interactions with other cells or organisms. The principal role of the cell wall is to maintain cell shape and provide support for cell growth (Latge, 2007), but it is also a critical component in signalling pathways between hosts and pathogens that mediates pathogen attachment, entry, colonisation and defence against the host immune response. In turn, a plant host alters the composition of its cell wall to better resist infection and produce anti-microbial compounds.

The cell walls of fungi are well-studied compared to their oomycete counterparts. The cell wall polysaccharide composition of different fungal species varies significantly. However, they all contain chitin, most commonly associated with different ratios of (1→3)-β-glucans, (1→6)-β-glucans, (1→3; 1→6)-β-glucans, (1→3)-α-glucans, and mannoproteins (Free, 2013; Klis *et al.*, 2002) (Table 2). In the yeast *Saccharomyces cerevisiae*, chitin and (1→3)-β-glucans are mainly

found in the inner layer of the cell wall, making up 50-60% of its total dry weight and providing mechanical strength (Dallies *et al.*, 1998; Hartland *et al.*, 1994; Lipke & Ovalle, 1998). Cell wall proteins are mainly found in the outer layer of the fungal cell wall (FCW), where they facilitate interactions with cell walls from other micro-organisms and response to the environment, including abiotic factors such as excessive water, heat, and cold (Cappellaro *et al.*, 1994; Lipke & Kurjan, 1992; Reynolds & Fink, 2001; Teunissen & Steensma, 1995). The outer layer of the FCW also serves as a protective barrier for the inner layer of the cell wall and plasma membrane. Some of the structural proteins are covalently linked to (1→3)-β-glucans and chitin, either directly or through (1→6)-β-glucans. This complex network of cross-linked polysaccharides and proteins as well as the countless non-covalent interactions that take place within the network, lead to the formation of a malleable and mechanically robust cell wall. For example, the appressoria of some plant pathogens, such as *Magnaporthe oryzae*, can withstand an internal turgor pressure of up to 20 MPa, making them the most robust cell walls in nature. The turgor pressure produced allows the hyphae to penetrate the target host cell by applying mechanical force (Money, 2001, 2008). Besides structural proteins, such as mannoproteins, the FCW contains enzymes such as hydrolases and transglycosidases (Bowman & Free, 2006; Mouyna *et al.*, 2000). The coordinated action of these enzymes and membrane-bound glycosyltransferases (GT) ensures the proper assembly and constant remodelling of fungal cell wall components (Mouyna *et al.*, 2000).

Table 2: Major differences between the cell walls of two examples of oomycetes and true fungi

Polysaccharide	**Fungal species**		**Oomycete species**		
	Saccharomyces cerevisiae	*Aspergillus fumigatus*	*Phytophthora infestans*	*Saprolegnia parasitica*	*Aphanomyces euteiches*
Chitin: polymer of (1→4)-linked β-*N*-acetylglucosaminyl residues	1 to 2%	10-20%	None detected	2%	10%
Polymer of (1→6)-*N*-acetylglucosaminyl residues (most likely β anomery)	None detected	None detected	None detected	None detected	Present
(1→3)-β-glucans	50 to 55%	20 to 35%	20%	23%	28%
Cellulose: polymer of (1→4)-β-glucosyl residues	None detected	None detected	34%	51%	35%
(1→6)-β-glucans	10 to 15%	None detected	2%	10%	4%

(1→3; 1→6)-β-glucans			18%	5%	14%
(1→3; 1→4)-β-glucans	None detected	Present	Present	Present	None detected
Mannan	Present	Present	Present	Present	Present

Different oomycete cell walls are generally composed of different amounts of cellulose, (1→3)-β-glucans, (1→6)-β-glucans and (1→3; 1→6)-β-glucans (Mélida *et al.*, 2013) (Figure 4, Table 2). Besides these polysaccharides, chitin is found as an order-specific or species-specific cell wall component in some oomycetes (Bartnicki-Garcia, 1968; Cameron & Taylor, 1976; Mélida *et al.*, 2013; Novaes-Ledieu *et al.*, 1967; Reiskind & Mullins, 1981; Sietsma *et al.*, 1969). The oomycete cell wall (OCW) mainly comprises 80-90% glucans, 5-10% proteins and 1-2% lipids (Tokunaga & Bartnicki-Garcia, 1971). Although the presence of cellulose in the OCW was historically recognised as a characteristic feature of oomycetes, pioneering biochemical approaches suggested that cellulose is a relatively minor component (4-21%) whereas (1→3)-β-glucans and (1→6)-β-glucans were reported to represent 60-80% of the total cell wall carbohydrates (Bartnicki-Garcia, 1968; Cameron & Taylor, 1976; Reiskind & Mullins, 1981; Sietsma *et al.*, 1969; Sietsma *et al.*, 1975; Zevenhuizen & Bartnicki-Garcia, 1969). However, techniques such as glycosidic linkage analysis by gas chromatography coupled to mass spectrometry were not frequently used in this pioneering research, so the actual amount of cellulose was underestimated in several instances where the specific detection of (1→4)-β-linked glucosyl residues was not accounted for. In addition, no chitin was found in any of these studies. Ultrastructural analysis by electron microscopy confirmed the presence of two distinct layers within the OCW, similar to the organisation of the FCW. Early studies revealed that the inner layer of the OCW contains cellulose microfibrils, possibly cross-linked with other types of glucans, and an outer layer consisting mainly β-1,3-glucans with β-1,6 linkages (Hunsley & Burnett, 1970; Sietsma *et al.*, 1975).

In a more recent study by Mélida *et al*. (2013), a comprehensive analysis of OCW was performed to characterise the extracellular carbohydrates found in ten species belonging to the Peronosporales and Saprolegniales orders. Unlike the pioneering work mentioned above, Mélida *et al*. (2013) employed a combination of solvent-specific extractions and linkage analysis that enabled the identification and quantification of crystalline and non-crystalline cell wall polysaccharides and the glycosidic linkages they contain. This approach revealed a significantly higher percentage of cellulose (30-50%) within the oomycete cell wall glucans (Mélida *et al.*, 2013). The quantity of non-cellulosic glucans, predominantly (1→3)-β-glucans,

accounted for approximately 20-30% of the total glucans present in the OCW (Mélida *et al.*, 2013). The researchers proposed three distinct types of cell walls across the 10 species analysed, based on the distinctive features of their carbohydrate content. The cell wall of *Phytophthora* species was classified as type I, which is characterised by the absence of chitin but the presence of >3% mannosyl and glucuronosyl residues (small amounts) in the alkali-soluble fraction compared to the other two cell wall types. The cell walls of the Saprolegniales genera *Achlya*, *Leptolegnia*, *Saprolegnia* and *Dictyuchus* were classified as type II. In these cell walls, a small amount of chitin was detected (<5%) together with unexpected 1,3,4-linked glucosyl residues, implying the existence of cross-links between β-1,3-glucans and cellulose. The cell walls from another Saprolegniales, *Aphanomyces*, were classified as type III, characterised by a higher content of chitin (>5%), which distinguishes them from the type II OCW. Interestingly, the type III cell wall also contained 1,6-linked GlcNAc residues, which had been previously reported only in some bacterial polysaccharides. Although Mélida *et al*. (2013) provided valuable insights into the OCW composition, their study included two *Phytophthora* species only and no other Peronosporomycetes. Therefore, would be interesting to perform further similar carbohydrate analyses on different Peronosporomycetes, including species responsible for downy mildews, i.e., species from the Pythiales, Albuginales, Rhipidiales and Leptomitales orders, as well as members from the early diverging Haliphthorales and Haptoglossales orders, which have not been researched to date. However, the obligate lifestyle and holocarpic nature of some oomycetes may limit our ability to purify their cell wall material without contaminations from the host cell walls.

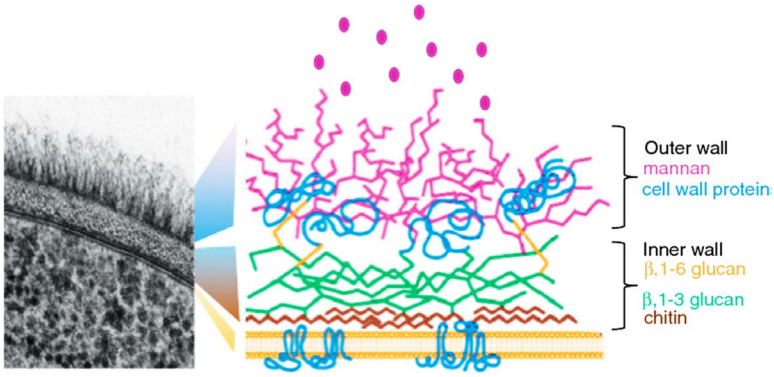

Figure 3: Cell wall model of the fungus *Candida albicans* **(Adapted from Gow *et al*., 2012)**

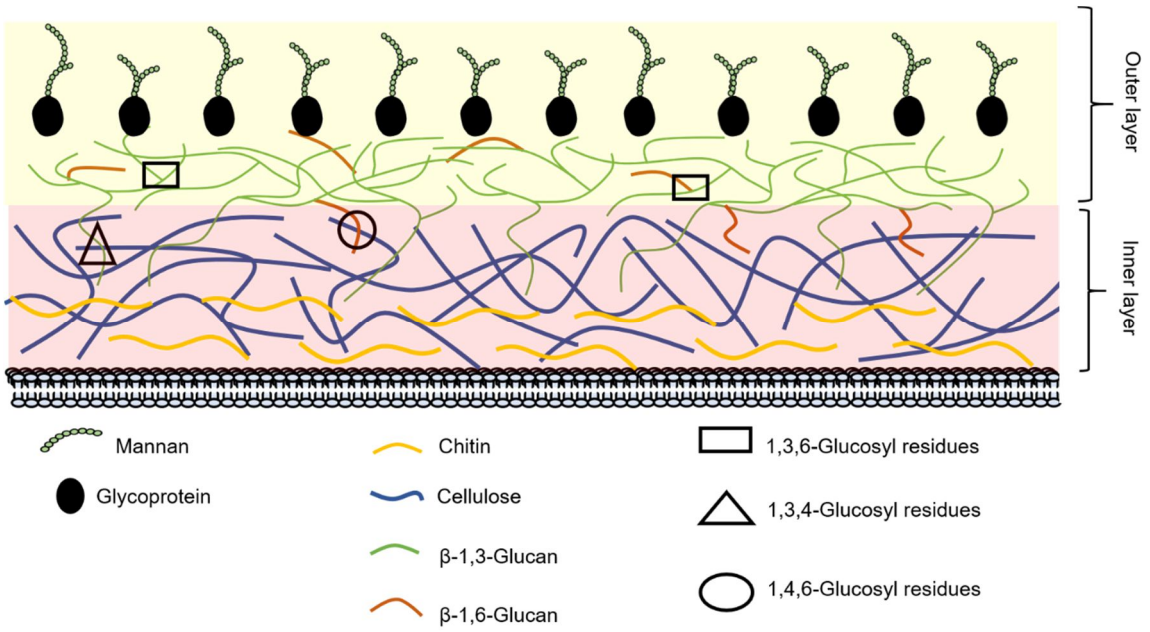

Figure 4: Model of an oomycete cell wall. The inner cell wall layer (pink shade) is cellulose-rich and may contain small amounts of chitin depending on the species. The outer cell wall layer (yellow shade) contains essentially β-glucans and mannoproteins.

In general, cell wall models of fungi and oomycetes derived from the experimental results summarised above indicate that the crystalline polymers such as chitin in fungi (Figure 3) and cellulose in oomycetes (Figure 4) occur essentially in the inner layers of the corresponding cell walls, while the outer layers of the cell walls largely consist of the less crystalline polymers (1→3)-β-glucans and mannans.

4.1 Cellulose: a linear chain of (1→4)-β-glucosyl residues

Cellulose is a biopolymer found in various organisms such as plants, algae, oomycetes, bacteria and some invertebrate marine animals from the tunicate phylum. It consists of linear chains of glucosyl residues linked by β-(1→4) linkages (Figure 5), stabilised by intramolecular H bonds. Owing to the β-(1→4) stereochemistry, each residue is rotated by 180° with respect to its neighbour (Figure 5). The length of the cellulose chains varies depending on the source and extraction techniques (Rajinipriya *et al.*, 2018; Somerville, 2006). Individual chains aggregate via many intermolecular H bonds to form mechanically strong, water-insoluble crystalline microfibrils, which stabilise the cell wall as well as the cell structure, tissues, and entire plant (Jarvis, 2003). Plant cell walls are typically rich in cellulose, ranging from around 20% to 40% in primary cell walls to up to over 50% in secondary cell walls of woody tissues, and 95% in cotton fibres (Cosgrove & Jarvis, 2012; Jarvis, 2003; Zhong & Ye, 2014).

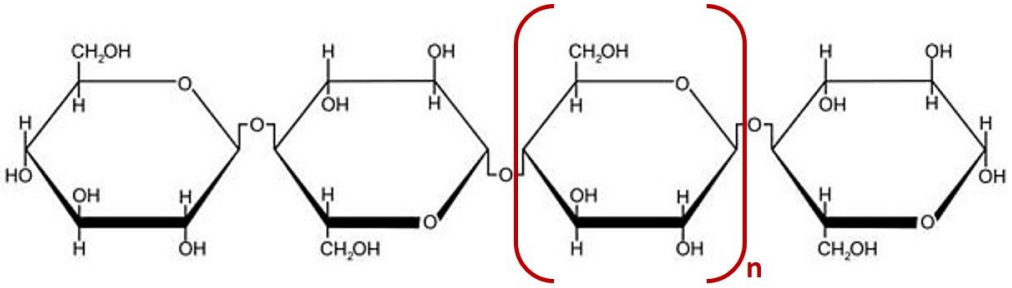

Figure 5: Cellulose structure. Cellulose consists of linear chains of glucosyl residues linked through (1→4)-β-glycosidic bonds (Reprinted with permission from {Rajinipriya *et al.*, 2018}. Copyright {2018} American Chemical Society.)

Crystalline cellulose may occur as four distinct allomorphs, as demonstrated by X-ray diffraction and solid-state ^{13}C-NMR, referred to as cellulose I, II, III, and IV (Moon *et al.*, 2011) (Figure 6). Cellulose I is the native form of cellulose that occurs in nature. Two allomorphs of cellulose, designated cellulose Iα and Iβ, are distinguishable by subtle differences in H bonding which result in a slightly different crystalline phase. Cellulose Iβ is predominant in plant cell walls whereas cellulose Iα is the major allomorph found in bacterial cellulose (Atalla & Vanderhart, 1984). However, both forms typically co-exist in the same biological source, albeit one form is usually much more abundant in a given organism than the other.

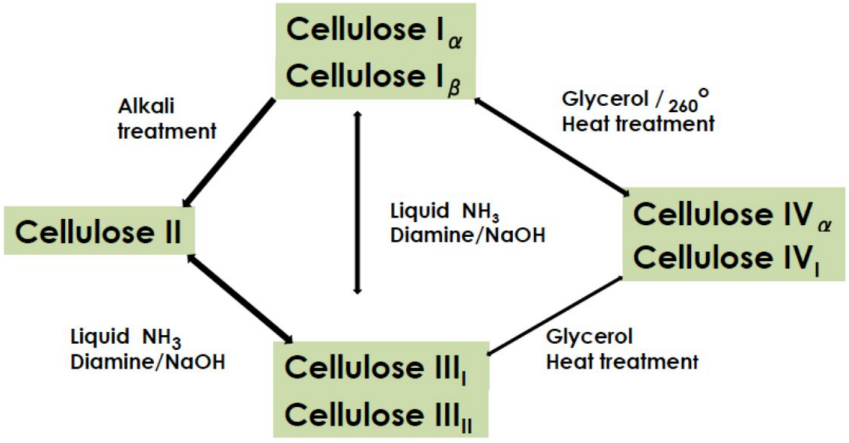

Figure 6: Allomorphs of cellulose. Allomorphs II, III and IV derive from cellulose I, the native form of cellulose found in nature. (Reprinted with permission from {Ulaganathan *et al*, 2015}. Copyright {2015} Bentham Science Publishers.)

Cellulose I microfibrils consist of parallel chains, i.e., the reducing ends of all cellulose chains point in the same direction, whereas cellulose II comprises anti-parallel chains. The alkali treatment of cellulose I changes the direction of the chains of cellulose I and reorganise the

chains into an anti-parallel orientation (Klemm *et al.*, 2005) (Figure 6). This process is poorly understood, but it is believed that the alkaline treatment provokes a swelling of cellulose or a complete dissociation of individual chains, with disruption of H bonds, to form the more metastable cellulose II. This allomorph is well-known for its smooth texture and is widely utilised as so-called 'regenerated cellulose fibres' in the textile industry. Cellulose II has been reported in very rare occasions in nature, e.g., in one algal species (Sisson, 1938) and one bacterial strain grown in high-viscosity medium (Kuga *et al.*, 1993). Cellulose III is an intermediate form between cellulose I and cellulose II and can be produced by chemical treatment of either cellulose I or cellulose II (Figure 6). Cellulose IV is a disorganised form of cellulose I (Wada *et al.*, 2004) found in the cell wall of oomycetes and primary cell walls of plants (Bulone *et al.*, 1992; Chanzy *et al.*, 1979; Helbert *et al.*, 1997). This allomorph can also be chemically derived from cellulose I and cellulose III by heat treatment in presence of glycerol (Figure 6) (Dai *et al.*, 2018; El Seoud *et al.*, 2019; Ulaganathan *et al.*, 2015).

4.2 Glucans: (1→3)-β- and (1→3, 1→6)-β-Glucans

(1→3)-β-Glucans are one of the main components of both fungal and oomycete cell walls. This type of polysaccharide provides tensile strength and contributes to the stabilisation of the size and shape of cells. In the yeast *S. cerevisiae*, (1→3)-β-glucan chains comprise approximately 1500 glucosyl units linked by β-1,3-linkages. The chains are moderately branched, and the polymer represents 50-55% of the cell wall dry weight (Klis *et al.*, 2002; Manners *et al.*, 1973; Xie & Lipke, 2010). Both fungi and oomycetes contain branched (1→3)-β-glucans, with the branching points taking place on the C6 of some of the main-chain β-1,3-linked glucosyl residues (Figure 7). These branched (1→3)-β-glucans are stabilised in the cell wall matrix by hydrogen bonding between neighbouring polymers (Klis *et al.*, 2006; Latgé, 2007). In fungi, the (1→6)-β-branches are irregularly distributed along the (1→3)-β-glucan chains, which prevents crystallisation of the polymers (Klis *et al.*, 2002).

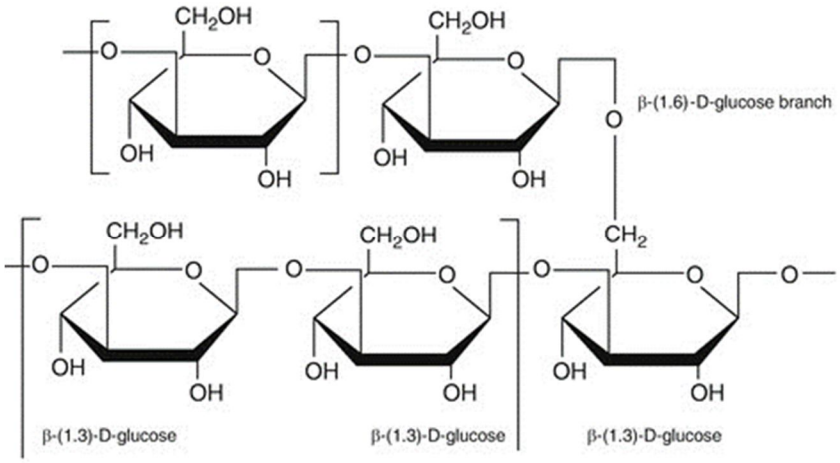

Figure 7: Chemical structure of (1→3)-β-glucans with a branching point at position 6. (Reprinted with permission from {Abuajah, 2017}. Copyright {2017} Springer Nature.)

In oomycetes, it has been reported that *Phytophthora* species contain higher proportions of (1→3)-β-glucans and branched (1→3, 1→6)-β-glucans, i.e., about 40% altogether of the whole cell wall carbohydrates (Table 2) compared to linear (1→6)-β-glucans, which represent no more than 3% of the cell wall (Melida *et al.*, 2013; Rahar *et al.*, 2011; Rouhier *et al.*, 1995; Tondolo *et al.*, 2017). Linear (1→3)-β-linked glucans play an important stabilising role during the formation and remodelling of the cell wall at different growth stages of *Phytophthora* sp., and also trigger plant immune responses during infection (Bartnicki-Gracia, 1983; Doke & Tomiyama, 1980; Waldmüller *et al.*, 1992). In addition, Zeković *et al*. (2008) showed that branched (1→3, 1→6)-β-glucans act as storage carbohydrates in oomycetes (Zeković *et al.*, 2005).

4.3 Chitin: a linear chain of (1→4)-β-linked *N*-acetylglucosaminyl residues

Chitin is a homopolymer of β-1,4-linked *N*-acetyl-D-glucosaminyl (GlcNAc) residues (Figure 8). It is found in all fungal species, but some oomycetes have also been shown to contain small amounts of chitin, not exceeding a few percent (Table 2) (Berezina, 2016).

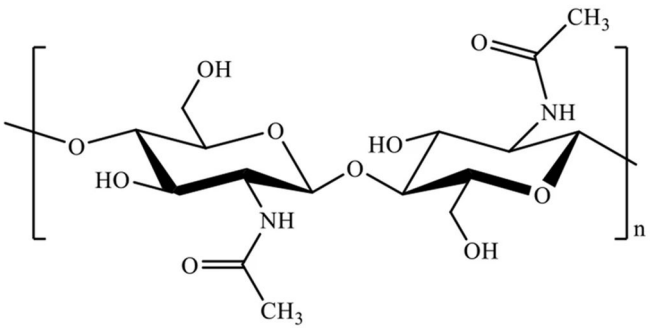

Figure 8: Chemical structure of chitin, a polymer of β-1,4-linked N-acetyl-D-glucosaminyl residues (GlcNAc). (Reprinted with permission from {Nasrollahzadeh *et al*., 2023}. Copyright {2023} Springer Nature.)

For example, the cell walls of *Saprolegnia* species contain 1-2% GlcNAc residues, while the *Aphanomyces euteiches* cell walls contain more than 5% GlcNAc residues. This is one of the features used to distinguish the oomycete types II and III cell walls (Mélida *et al.*, 2013). On the other hand, the Peronosporales *P. infestans* and *P. parasitica* lack GlcNAc residues in their cell walls (Table 2), suggesting that they are devoid of chitin (Melida *et al.*, 2013). As opposed to the situation in oomycetes, chitin is found in all fungal cell walls, such as Ascomycetes, Basidiomycetes, Deuteromycetes, and Zygomycetes (Elsoud & El Kady, 2019). It is important to note that, across all oomycetes, the presence of chitin has been reported only in some members of the Saprolegniales order (Badreddine *et al.*, 2008; Bulone *et al.*, 1992; Guerriero *et al.*, 2010). However, it remains elusive whether all genera of Peronosporomycetes are devoid of chitin. A recent study based on the use of wheat germ agglutinin (WGA) showed the presence of chitin in zoospores and released sporangia from *P. capsici* and *P. sojae* (Cheng *et al.*, 2019). However, the results are not entirely conclusive as WGA is not strictly specific for chitin and they contradict the findings of Mélida *et al*. (2013), which are based on more direct chemical evidence.

4.4 Mannans

Mannans are minor components of the OCW, present only in alkali-soluble cell wall extracts (Mélida *et al.*, 2013). The highest amounts of mannans are found in the type I OCW. it has been suggested that most of the detected mannans arise from surface glycoproteins such as mannoproteins, which are separable by alkali or hot water extraction (Ayers *et al.*, 1976; Keen & Legrand, 1980). Compared to the OCW, the well-characterised cell walls of the yeast *S. cerevisiae* and fungus *C. albicans* contain higher proportions of glycosylated proteins,

including mannoproteins, a high proportion of which are synthesised in the form of glycosylphosphatidylinositol (GPI) anchored protein (Ibe & Munro, 2021). In addition, some mannoproteins in fungal species are covalently linked to β-1,3-glucans via oligosaccharide sidechains. Similar to the situation in fungi, it has been proposed that the GPI-anchors present in the oomycete plasma membranes are involved in the attachment and/or subsequent release of glycosylated proteins and mannans in the cell wall (Jiang *et al.*, 2006; Kharel *et al.*, 2021). In oomycetes, mannoproteins are historically considered to not only cement β-glucans within the cell wall, but also to act as adhesive substances through which zoospores attach to the host cell during infection (Erwin *et al.*, 1983).

5 Cell wall biosynthesis in oomycetes

As indicated in the previous section, the main constituents of the OCW are cellulose and (1→3)-β-glucans. In addition, some species contain small amounts of chitin. These three types of carbohydrate polymers are synthesized by membrane-bound enzymes, which belong to the glycosyltransferase (GT) family. The GTs involved in the biosynthesis of cellulose, (1→3)-β-glucans and chitin catalyse the repetitive transfer of glycosyl residues from activated sugar donors, i.e., UDP-glucose or UDP-*N*-acetylglucosamine, to the acceptor polysaccharidic chains, thereby forming new glycosidic bonds and elongating individual chains (Saxena *et al.*, 1995). There are 116 GT families present in the carbohydrate-active enzyme (CAZy) database (www.cazy.org). The cellulose (CESA) and chitin (CHS) synthases belong to GT family 2, whereas the 1,3-β-glucan synthases (FKS) are classified in GT family 48. This classification is based on sequence similarities, mode of catalytic action and, where available, structural information.

5.1 Cellulose biosynthesis

The oomycete CESA enzymes use UDP-glucose as a substrate to extend the polysaccharide chains of (1→4)-β-glucans, a mechanism accompanied by an inversion of the configuration of the anomeric carbon from α in the sugar donor (UDP-glucose) to β in the acceptor (cellulose) (Aloni *et al.*, 1982; Bureau & Brown, 1987; Graf *et al.*, 2013; Lairson *et al.*, 2008). CESA proteins for multimeric complexes in the plasma membrane that can be visualised by electron microscopy. In plants these complexes are designated as ‘rosettes’ owing to their six-fold symmetry whereas bacterial CESAs occur as linear arrays of proteins (Brown, 1996; Mueller & Brown, 1980). The arrangement of the cellulose synthase complexes (CSC) in brown algae, which are phylogenetically related to oomycetes, is linear but there is no experimental evidence of the arrangement of CSC in oomycetes (Brown, 1996; Mueller & Brown, 1980). It is assumed

that the size and shape of cellulose microfibrils are determined by the number of CESA proteins in CSC and the geometry of the CSC, e.g., rosettes in plants versus linear complexes in bacteria.

The first cellulose synthase gene (*CesA*) was identified in 1990 and shown to encode the catalytic subunit of the bacterium *Gluconacetobacter xylinus* CesA complex (Brown Jr & Lin, 1990; Wong *et al.*, 1990). This discovery led to the identification of many more *CesA* genes in a large diversity of organisms. In 2008, Grenville-Briggs *et al*. reported the presence of four *CesA* genes in *P. infestans* (Grenville-Briggs *et al.*, 2008), and the same number of *CesA* genes was also found later in the Saprolegniales *Pythium* (Blum *et al.*, 2010; Blum & Gisi, 2012; Grenville-Briggs *et al.*, 2008). By comparison, the model plant *Arabidopsis thaliana* contains 10 *CesA* genes, among which seven (*CesA1*, *CesA2*, *CesA3, CesA4*, *CesA6*, *CesA7*, *CesA8*) have different roles in primary and secondary cell wall synthesis (Arioli *et al.*, 1998; Desprez *et al.*, 2007; Persson *et al.*, 2007). Interestingly, phylogenetic analysis showed that the *CesA* genes of *Phytophthora* group together in a separate clade, distinct from both plant and bacterial *CesA*s, but relatively close to cyanobacterial *CesA* genes (Figure 9) (Fugelstad *et al.*, 2009; Grenville-Briggs *et al.*, 2008).

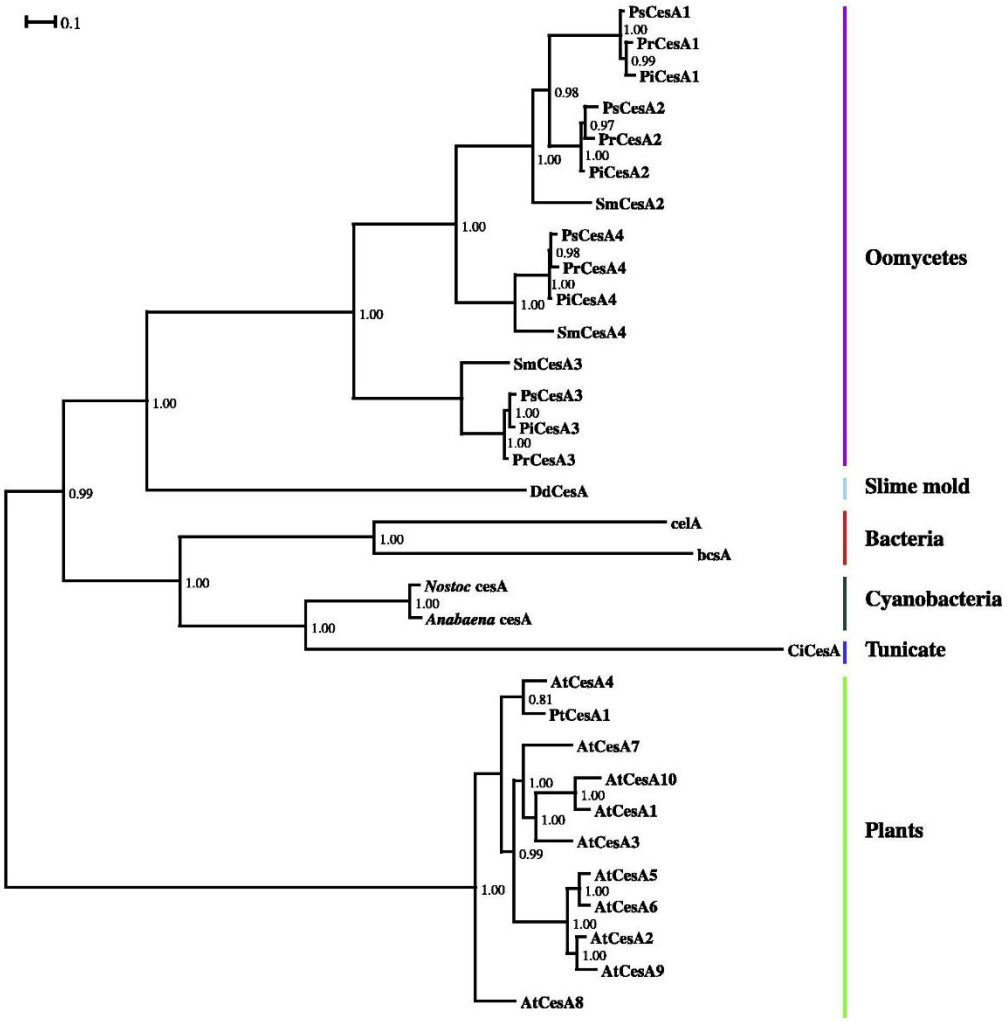

Figure 9: Phylogenetic analysis of cellulose synthase (*CesA*) genes. Pi, *Phytophthora infestans*; Pr, *Phytophthora ramorum*; Ps, *Phytophthora sojae*; Sm, *Saprolegnia monoica*; celA, CesA from *Agrobacterium tumefaciens*; bcsA, CesA from *Gluconacetobacter xylinus* ATCC 23769; Ci, *Ciona intestinalis*; Dd, *Dictyostelium discoideum*; At: *Arabidopsis thaliana*. (Reprinted with permission from {Fugelstad *et al*., 2009}. Copyright {2009} Fungal Genetics and Biology.)

The presence of cellulose in the OCW is vital and the polymer plays a key role in the different life stages by being involved in the strengthening or weakening of the cell wall to allow expansion when required (Grenville-Briggs *et al.*, 2008). Also, cellulose in *P. infestans* is crucial for the successful infection of potato epidermal cells (Mach, 2008). Expression profiling of *CesA* genes during different life cycle stages of *P. infestans* and infection of potato tissues indicated their upregulation during cysts and appressorium formation, both involved in the initiation of plant tissue colonisation by the pathogen (Grenville-Briggs *et al.*, 2008) (Figure 10).

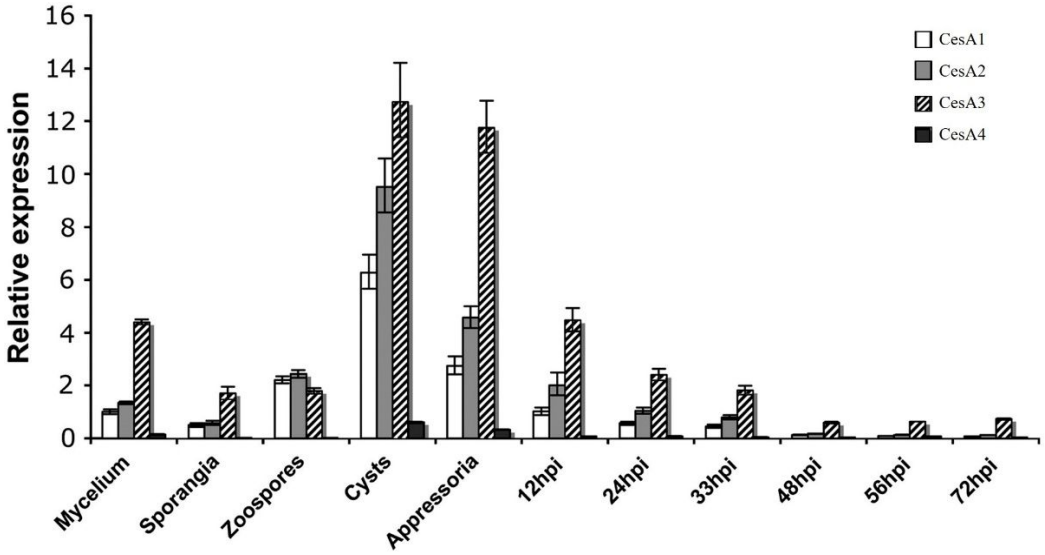

Figure 10. Expression of *CesA* genes during different stages (mycelium, sporangia, zoospores, cysts, and appressoria) of the life cycle of *P. infestans* and after 12, 24, 33, 48, 56, 72 h post-inoculation in a susceptible potato cultivar (adapted from Grenville-Briggs *et al.*, 2008). (Reprinted with permission from {Grenville-Briggs *et al*., 2008}. Copyright {2008} The Plant Cell.)

The study also showed that silencing by RNAi of the entire *CesA* gene family (*CesA1*, *CesA2*, *CesA3*, and *CesA4*) reduced cellulose content by more than 50% in the appressorial cell wall, significantly decreasing pathogenicity (Grenville-Briggs *et al.*, 2008). The results strongly suggested that the *CesA* genes have vital roles in appressorium formation, uniform cell wall structure and, indirectly, pathogenicity. However, the incomplete nature of the RNAi gene silencing approach used in this study makes the results difficult to fully interpret. Hence silencing of each individual gene is required to better understand the precise role of each *CesA* genes in *Phytophthora* throughout the life cycle and infection process.

In a more recent study, RNA silencing of the *CesA3* gene in *Hyaloperonospora arabidopsidis* revealed that this gene is crucial for the pathogenicity of this oomycete pathogen (Bilir *et al.*, 2019). In addition, it was also shown that *CesA1* is vital for cell wall formation, germination of cysts and successful infection (Li *et al.*, 2022; Pang *et al.*, 2020). The hyphae of *CesA1* knockout mutants present a thicker inner cell wall in *P. capsici* and higher sensitivity to carboxylic acid amide fungicides, which have been shown to bind directly to CESA proteins (CAAs) (Li *et al.*, 2022). Moreover, the deletion of *CesA1* is accompanied by an altered cell wall composition, i.e., a decrease in cellulose content and a lower extent of cross-linking between cell wall polysaccharides, revealed by lower amounts of 1,4,6-linked glucosyl residues

and 1,3,4-linked glucosyl residues compared to the wild-type *P. capsici* strain (Li *et al.*, 2022). In a different study on *P. capsici*, it was shown that the CESA1 protein produces cellobiose and interacts with other CESA proteins to form cellulose microfibrils in an unknown complex manner (Pang *et al.*, 2020). Compared to *CesA1* and *CesA3*, the *CesA2* and *CesA4* genes have been less studied in oomycetes and their roles still needs to be elucidated. Interestingly, unlike CESA proteins from other taxonomic groups, all predicted oomycete CESA proteins, except for CESA3, contain an N-terminal Pleckstrin Homology (PH) domain, which has been suggested to be involved in the regulation, trafficking and/or targeting of the CESA proteins to the plasma membrane (Fugelstad *et al.*, 2012).

5.2 (1→3)-β-Glucan biosynthesis

(1→3)-β-Glucan synthases from GT family 48 are found in plants, fungi, and oomycetes (Douglas et al., 1994; Li et al., 2003). All use UDP-glucose as a substrate and, in fungi, some require the presence of GTP to catalyse the formation of (1→3)-β-glucans (Shematek *et al.*, 1980). Silencing both the *Fks1* and *Fks2* genes encoding these enzymes is lethal in *S. cerevisiae* (Beauvais *et al.*, 2001; Douglas, 2001). Furthermore, a recent study on the biochemical, structural and functional characterisation of FKS1 in the yeast showed that the enzymatic activity of the protein is sensitive to the membrane environment (Hu *et al*., 2023). The structure of FKS was solved by cryo electron microscopy, which revealed a membrane-embedded part consisting of 17 transmembrane (TM) helices connected by elongated loops, and a large catalytic cytosolic part (Figure 11). The latter separates TM helices ‘1 to 6’ from helices ‘7 to 17’ and includes an N-terminal domain and a conserved GT48 domain (Hu *et al.*, 2023; Lairson *et al.*, 2008). The crystal structure of the protein revealed a close interaction with lipids from the plasma membrane (Figure 11). Interestingly, purified FKS enzymes from *S. cerevisiae* solubilised using glyco-diosgenin (GDN) and CHAPS as detergents showed different biochemical activities, which was attributed to the mode of interaction of the detergents with the membrane environment, hence lipids, indirectly affecting the activity of the protein. The membrane environment was also shown to play a role in echinocandin resistance observed in clinically important fungi (Healey *et al.*, 2012; Hu *et al.*, 2023; Satish *et al.*, 2019).

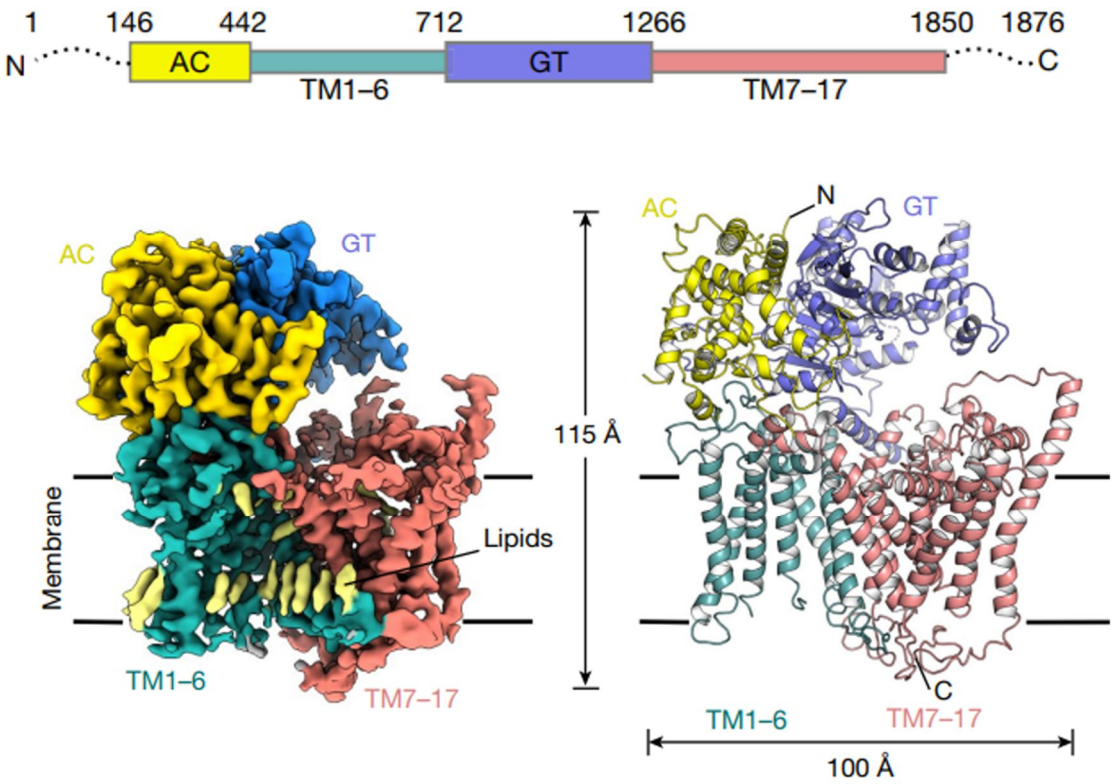

Figure 11: Cryo-EM map of FKS1 from *S. cerevisiae* viewed parallel to the membrane. The map is segmented into four parts shown in the figure with different colours to highlight the domain organisation of FKS1. (Reprinted with permission from {Hu *et al*., 2023}. Copyright {2008} Springer Nature.)

Like fungi, oomycetes genomes from the Peronosporales and Saprolegniales orders contain multiple *Fks* orthologs (Klinter, 2021). However, there is no experimental evidence for the function and architecture of FKS proteins in oomycetes. In fungi, FKS knockout mutants showed a decreased amount of β-1,3-glucans in the cell wall, which resulted in defective hyphae and spore production with a decreased formation of functional appressoria (Hu *et al.*, 2023; Oliveira-Garcia & Deising, 2013). However, the consequences of *Fks* gene deletion in oomycetes are unknown. To date, *P. insidiosum* is the only oomycete species that has been found to be susceptible to the fungal FKS inhibitors from the echinocandin family (Yolanda & Krajaejun, 2020). With the availability of an increasing number of oomycete genomes and progress made on the optimisation of CRISPR-Cas9 gene editing in oomycetes, it is expected that the functional characterisation of cell wall biosynthetic genes will become possible in the near future. Indeed, the difficulty to genetically manipulate oomycetes, including the challenges associated with the generation of stable mutants, has been a bottleneck in the functional characterisation of oomycete genes.

In yeast, the *Kre5* and *Kre6* genes are required for the biosynthesis of (1→6)-β-glucans and for the formation of β-(1→6) branching points in (1→3)-β-glucans (Lesage & Bussey, 2006; Roemer *et al.*, 1994). RNAi silencing of both genes in the ascomycete *Colletotricum graminicola* was accompanied by the formation of morphologically altered appressoria, including phenotypes such as swelling, bursting and reduced adhesion capability, which are similar to the phenotypes of FKS knockdown mutants (Oliveira-Garcia & Deising, 2016; Oliveira Silva *et al.*, 2022). Although the function of *Kre5* and *Kre6* is not fully understood, experimental data suggest that they play a role in processing or modifying β-glucans, possibly by transglycosylation to introduce branching points and/or cross-links with other polysaccharides. The products of these genes belong to the glycoside hydrolase family 16, which further suggests that they may be involved in breaking down or modifying glucan chains by transglycosylation. There are currently no studies available on the oomycete orthologs of the *Kre5* and *Kre6* genes, hence whether these are involved in the biosynthesis of (1→6)-β-glucans remains to be determined.

In summary, genes involved in the biosynthesis of linear (1→3)-β-glucans, (1→6)-β-glucans and branched (1→3; 1→6)-β-glucans in oomycetes are yet to be firmly identified and characterised to ultimately establish their role in cell growth and development, reproduction, pathogenicity, and disease establishment and progression.

5.3 Chitin biosynthesis in oomycetes

Chitin synthase (*Chs*) genes are present in both fungi and oomycetes. Some of these genes have specialized functions during different stages of the life cycles, with various levels of expression during specific developmental phases (Cheng *et al.*, 2019; Guerriero *et al.*, 2010; Kong *et al.*, 2012; Papi *et al.*, 2016; Shaw *et al.*, 1991; Weber *et al.*, 2005). For example, *S. cerevisiae* has three distinct CHS isoforms, namely *Sc*CHS1, *Sc*CHS2, and *Sc*CHS3, which have distinct biological roles and biochemical properties: *Sc*CHS1 is involved in the repair of cell wall scars following cell division (Cabib *et al.*, 1989); *Sc*CHS2 facilitates the creation of the septum before cell division (Sburlati & Cabib, 1986; Shaw *et al.*, 1991); and *Sc*CHS3 contributes to cell wall chitin synthesis under environmental stress (Valdivia & Schekman, 2003).

Most Saprolegniales have 5 or, less frequently, 6 *Chs* genes, and early diverging oomycetes, like *Eurychasmales dicksonii*, have 6 *Chs* genes (Klinter *et al.*, 2019). Interestingly, 1-2 *Chs* genes are found in *Phytophthora* species, although the presence of chitin in *Phytophthora* cell walls has not been demonstrated (Mélida *et al.*, 2013). In *P. infestans*, the use of the chitin synthase inhibitor nikkomycin Z leads to cell death despite the absence of detectable chitin the

the cell wall of the micro-organism. Contradicting with this situation, *P. sojae* whose genome contains two *Chs* paralogues (Tyler *et al*., 2006; Cheng *et al*., 2019) is not affected by the presence of nikkomycin Z (Hinkel & Ospina-Giraldo, 2017) and is able to tolerate gene disruption during host infection (Cheng *et al.*, 2019). Hence the function of *Chs* genes in different oomycete species from the same genus is elusive.

In a recent study, however, the first structure of an oomycete CHS protein was determined, showing that CHS1 from *P. sojae* consists of two main domains, an N-terminal cytoplasmic domain and a C-terminal membrane-embedded domain (Chen *et al.*, 2022), which confirmed the earlier predictive bioinformatic data (Briolay *et al.*, 2009; Guerriero *et al.*, 2010). The N-terminal end of the cytoplasmic domain designated NTD ('N-terminal domain) contains several sub-domains, i.e., a signal peptide (SP), a so-called microtubule-interacting and trafficking domain (MIT), and a linkage domain (LG) (Figure 12). The NTD domain is followed by a cytoplasmic GT domain, whose active site comprises a substrate-binding site and a so-called 'cave', which is the synthetic reaction site of the protein. The C-terminal membrane domain consists of 7 transmembrane (TM) helices, which form a translocating channel to discharge the growing chitin chain to the extracellular cell wall compartment (Figure 12) (Chen *et al.*, 2022).

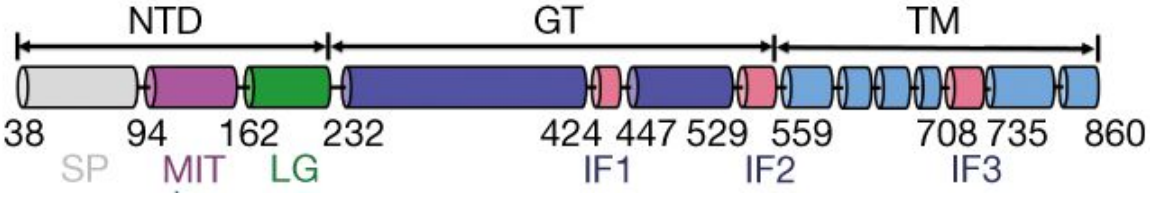

Figure 12: Domain architecture of chitin synthase 1 (CHS1) from ***Phytophthora sojae*** **(adapted from Chen *et al*, 2022).**

A flexible swinging loop acts as a 'gate-lock' in the doorway of the translocating channel to ensure that only one UDP-GlcNAc donor is present between the catalytic site and the gateway of the translocating channel. The swinging loop blocks the entrance of the substrate binding pocket, preventing the binding of more than one UDP-GlcNAc substrate during the biosynthetic reaction. After catalysis, the swinging loop opens to allow the entrance of another UDP-GlcNAc molecule while the extended chain is translocated across the translocating channel. This catalytic/translocation cycle is repeated multiple times to form long chains of chitin that are ultimately fully extruded and released in the extracellular space until biosynthesis is complete. The study proposed that the translocating channel can accommodate a chitin chain that consists of 7 (1→4)-β-linked GlcNAc residues. The chitin synthesized *in vitro* by the *P.*

sojae CHS1 protein has been shown to be α-chitin, which consists of anti-parallel chains of chitin (Chen *et al.*, 2022). In several earlier studies, it was hypothesised that chitin synthase activity is activated by free GlcNAc (Keller & Cabib, 1971; Orlean, 2012; Sburlati & Cabib, 1986), which may act as a positive effector for chitin biosynthesis (Horsch *et al.*, 1996; Mcmurrough *et al.*, 1971). However, Chen *et al*. (2022) showed that GlcNAc alone does not significantly impact the enzymatic activity of CHS1. However, the concomitant addition of GlcNAc and divalent cations is accompanied by an increase in the enzymatic activity of CHS1 (Chen *et al*., 2022).

A unique feature of oomycetes CHS proteins, compared to any other known CHS from other organisms, is the presence of an N-terminal MIT domain (Brown *et al.*, 2016; Guerriero *et al.*, 2010; Jiang *et al.*, 2013; Klinter *et al.*, 2019). It was suggested that the MIT domain plays a role in the dimerization of CHS1 in *P. sojae* (Chen *et al.*, 2022) and that it is involved in intracellular transport, interaction with the abundant membrane component phosphatidic acid, and regulation of oomycete CHS enzymes (Brown *et al.*, 2022; Brown *et al.*, 2016; Guerriero *et al.*, 2010; Rzeszutek *et al.*, 2019). In addition, it was suggested that the dimeric form of CHS1 in *P. sojae* may facilitate the formation of chitin sheets by aligning single chitin chains in a parallel fashion (Chen *et al.*, 2022). However, it remains that the chitin polymer has not been detected in *Phytophthora* species through biochemical analysis (Mélida *et al.*, 2013), hence the actual ability of CHS proteins to form chitin *in vivo* remains to be demonstrated.

Researchers have discovered a functional connection between CHS enzymes and chitin deacetylases (CDA) in fungi. CDA proteins modify chitin to produce its deacetylated form called chitosan. Typically, chitosan contains at least than 50% deacetylated residues, i.e., glucosamine, but the proportion of these with respect to GlcNAc residues varies to a large extent depending on the microbial origin of the chitosan polymer. In fungi, the deletion of CDA leads to the same phenotype as in strains where some CHS genes have been deleted (Geoghegan & Gurr, 2016; Odenbach *et al.*, 2009). It is hypothesized that pathogenic fungi can reduce the risk of detection by the host by modifying chitin into chitosan, thereby promoting successful infection. Another study showed that mutant *Oryza sativa* plants that produce a bacterial chitosanase (chitosan degrading enzyme) exhibit improved resistance to the rice blast fungus *Magnaporthe oryzae*, implying that chitosan helps fungi evade the plant immune response by acting as a weaker activator of the host defense pathways compared to chitin (Kouzai *et al.*, 2012). This proposed strategy of chitin deacetylation to evade the host immune response has not been studied in oomycetes. Interestingly, a recent study identified putative CDA genes in

the plant-pathogenic oomycetes *P. sojae* and *P. aphanidermatum*, but orthologs of these genes are not present in the oomycete fish pathogen *S. parasitica*, suggesting that CDA proteins are specific to plant pathogens and might play a similar tole as in fungal phytopathogens (Leonard *et al.*, 2018). Mutation of CDA genes by RNAi or CRISPR-Cas9 will help to determine the role of CDA and chitosan in oomycetes.

5.4 Mannan biosynthesis

In fungi, mannans are present either on the cell wall surface or within the cell wall, covalently bound to glucans or chitin (Fontaine *et al.*, 2000). The cell surface mannans play an important resistance role against antifungal drugs and the host immune response (Gow & Hube, 2012). Genes encoding mannosyltransferases, such as *Mnn1-2, 4-6, 9*, *12*, and *14*, are essential for maintaining the structure and function of the cell wall in *C. albicans* (Gentzsch & Tanner, 1997; Hall *et al*., 2013). However, fungal mannans confer less rigidity to the cell wall compared to other major polysaccharides and they do not influence cell shape (Garcia-Rubio *et al.*, 2020). Although some mannans are present in alkali soluble fractions of oomycete cell walls (Mélida *et al.*, 2013), mannosyltransferase genes have not been identified in oomycetes. The recently published genomes of different fish and plant pathogenic oomycetes offer an opportunity to identify genes orthologs to fungal mannosyltransferase genes. A comparative analysis of *Phytophthora* genomes shows that species from this genus contain putative mannosyltransferase genes which are similar to the *S. cerevisiae* genes that code for mannosyltransferases from GT families 32, 62, and 71, i.e., *Och1*, *Amp1*, *Mnn1,2,5*, respectively (Gao *et al.*, 2021). The products of these genes may be present in Golgi membranes and contain N-terminal transmembrane domains as proposed for their fungal counterparts (Figure 13). It has been hypothesised that the catalytic domains sit in the Golgi lumen where GDP-mannose is used as a substrate to produce mannan chains (Gao *et al.*, 2021). Similar to the role of chitosan in fungi, it has been proposed that the cell surface mannoproteins from *P. megasperma* suppress the immune response of the plant host, but this has to be firmly demonstrated (Gao *et al.*, 2021). Further studies are required to decipher the role of mannans in the OCW and their biosynthesis process.

In summary, based on the information available to date and summarised in the previous sections, significant progress has been made about the genes and proteins involved in the formation of the OCW. However, much remains to be investigated and experimentally demonstrated to elucidate the precise function of the identified genes in cell growth, cell wall integrity and infection of animals and plants, and the mode of action of their products. Figure

13 shows a schematic of the different biosynthetic enzymes involved in OCW formation, their domain organisation and subcellular location, and their connection to the nucleotide-sugar biosynthetic and interconversion pathway.

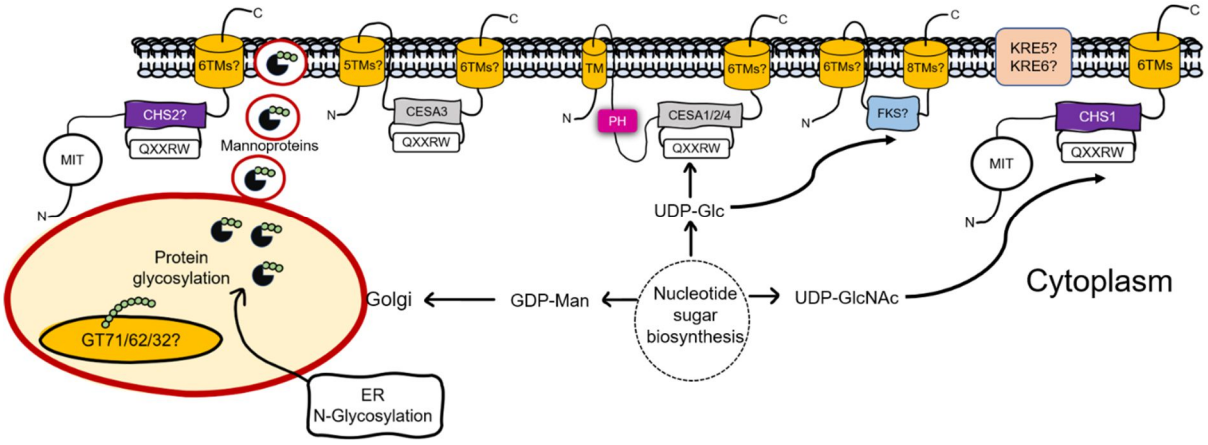

Figure 13: Proposed model summarising the biosynthesis of oomycete cell wall polysaccharides. ER: Endoplasmic reticulum, TM: Transmembrane helix, PH: Pleckstrin homology domain, MIT: Microtubule interacting and trafficking domain, CESA: cellulose synthase protein, FKS: glucan synthase protein, CHS: chitin synthase, GDP-Man: GDP-mannose, UDP-Glc: UDP-glucose, UDP-GlcNAc: UDP-*N*-acetylglucosamine, GT: Glycosyltransferase.

6 Current strategies for the control of oomycete diseases

Various approaches can be utilised to prevent and manage the dissemination of oomycetes that cause disease in a wide range of aquatic and terrestrial organisms. Principles and methods for plant disease management were first introduced by Whetzel in 1929 (Whetzel, 1929) and are considered essential to tackle the devastating effects of pathogenic oomycetes in crop production and aquaculture.

Avoidance is an approach to prevent disease by selecting a time or location where there is no inoculum, or the environment is not favourable for infection. A pathogen can be avoided by selecting unfavourable conditions for pathogen growth, spread, and transmission or by manipulating the environment to create such conditions. In Australia, the management of *P. cinnamomi* involves opening the canopy structure to allow sunlight to reach the ground and inhibit the growth of *Phytophthora* and *Pythium* species in seedlings (Panth *et al.*, 2020). In fish farming, avoidance tactics are employed by selecting locations, water sources, and fish species that are less prone to infection (Benavent-Celma *et al.*, 2022). However, the ability to

use avoidance methods to control the spread of fish pathogens like *Saprolegnia* species in aquaculture may be limited by climate change (Benavent-Celma *et al.*, 2022). Exclusion is another important method for controlling oomycete diseases. This process prohibits the introduction of diseased inoculum into an unaffected area. Strict hygiene should be maintained to avoid the dispersal of oomycetes in unaffected agricultural fields, forests, and fish farms (Benavent-Celma *et al.*, 2022; Hayden *et al.*, 2013). Once a pathogenic oomycete enters a site, such as an agricultural plot, eradication must be implemented to eliminate the pathogen before its dispersal in the farm. Combining approaches, such as removing the host plant by burning or uprooting, and soil fumigation by using metham sodium, can eradicate the newly introduced pathogen (Dunstan *et al.*, 2010; Hansen, 2008). However, the success of eradication methods is generally limited for pathogenic oomycetes due to the rapid dispersal characteristics of this class of micro-organisms in the environment (Derevnina *et al.*, 2016).

After the establishment of an oomycete pathogen in a forest, crop field or fish farm, protection and therapy can be used based on the principle of disease management, which typically relies on the use of chemicals (Whetzel, 1929). Fungicides like phosphonates, phenylamides and copper compounds are frequently applied in agricultural fields to control plant pathogenic oomycetes (Hayden *et al.*, 2013) (Table 3).

Table 3: Commonly used fungicides to control plant and fish pathogenic oomycetes. The risk of resistance is described according to the Fungicide Resistance Action Committee (FRAC) (www.frac.info).

Chemicals	Advantage	Disadvantage	Resistance risk	Reference
Phosphonates - fosetyl aluminium - potassium salts of phosphorous acid	Inhibition of plant pathogens and stimulation of host defense	Unable to fully eradicate the pathogen	Low	(Garbelotto *et al.*, 2009; King *et al.*, 2010; Pilbeam *et al.*, 2011)
Phenylamides - metalaxyl - mefenoxam	Inhibition of sporangia production in *Phytophthora* species	Limited use to avoid negative impacts on the environment	High	(Cohen & Coffey, 1986; Erwin & Ribeiro, 1996)
Copper compounds	Protection of the host plant, but no lasting effect	Causes heavy metal toxicity	Low	(Hayden *et al.*, 2013)
Agricultural lime ($CaCO_3$)	Reduces infection caused by *Aphanomyces invadans* in fish	Unable to eradicate the pathogen	Low	(Kamilya & Baruah, 2014)
Carboxylic Acid Amide (CAA) fungicides	Interfere with cellulose biosynthesis leading to reduced hyphal growth	Unable to eradicate the pathogen	Moderate	(Gisi & Sierotzki, 2015)

Malachite green is a well-known chemical that can control *Saprolegnia parasitica*, a devastating fish pathogen, but this dye has been banned in many countries due to its carcinogenic effect (Culp *et al.*, 2006; Meyer & Jorgenson, 1983; Srivastava *et al.*, 2004). None of the available fungicides are as effective as malachite green. Developing resistant plant varieties is another conventional method to control oomycete diseases. However, the long-term effectiveness of resistant plant varieties is limited due to the adaptation capacity of pathogenic oomycete strains (Sharma *et al.*, 2021). Overall, the current control strategies for oomycetes are either not entirely efficient or not environmentally friendly. This situation has spurred an ongoing pursuit for new and alternative approaches to manage pathogenic oomycetes. Interestingly, the polysaccharides found in the OCW are vital for the micro-organisms. Thus, cell wall biosynthesis is an excellent target for disease control, e.g., through inhibition of the glycosyltransferases involved in the polymerisation of essential cell wall polysaccharides.

7 Cell wall biosynthesis as a target for disease control

The major components of the OCW, such as cellulose and β-1,3-glucans, as well as minor polysaccharides like chitin that play an essential role in cell integrity, represent an ideal target for anti-oomycete drugs. In this section, we discuss the main compounds that are currently available and have an effect on cell wall biosynthesis.

7.1 Inhibitors of cellulose biosynthesis

Mandipropamid (MPD) is a carboxylic acid amide (CAA) fungicide that shows inhibitory effects on phytopathogenic oomycetes by affecting cellulose biosynthesis (Blum *et al.*, 2010). Studies have shown that MPD causes abnormal hyphal morphology and defects in germ tube formation in oomycetes (Blum *et al.*, 2010; Cai *et al.*, 2021). MPD targets CESA3 in Peronosporomycetes. Mutations in one of the transmembrane domains of the enzyme confers moderate resistance against MPD and other CAA compounds, suggesting that these inhibitors interfere with the stability of the membrane-spanning domains of CESA3 (Blum & Gisi, 2012). Other CAA fungicides such as dimethomorph, flumorph, iprovalicarb, and benthiavalicarb are used to control oomycetes, but all confer a moderate resistance risk in oomycetes, mainly Peronosporomycetes (Gisi & Sierotzki, 2015).

2,6-Dichlorobenzonitrile (DCB) is an inhibitor of cellulose biosynthesis that decreases the number of cellulose synthesizing complexes in the plasma membrane of plant cells by interfering with their mobility (DeBolt *et al.*, 2007; Liu *et al.*, 2017). While mycelial growth of

P. infestans was not affected at concentrations as high as 100 µM (Grenville-Briggs *et al.*, 2008), *S. monoica* mycelial growth was reduced by 40% when treated with 200 µM DCB (Fugelstad *et al.*, 2009). However, a similar concentration of DCB blocks the release of zoospores and germ tube formation in encysted zoospores of *P. infestans* (Grenville-Briggs *et al*., 2008). The difference in DCB susceptibility between these two organisms (Fugelstad *et al.*, 2009; Grenville-Briggs *et al.*, 2008) may be due to differences in their cell wall composition, including the amount of cellulose and the branching pattern of cell wall carbohydrates such as (1→3)-β- and (1→3, 1→6)-β-glucans. However, the actual mode of action of DCB against oomycetes, including whether it does interfere with cellulose biosynthesis, remains unknown.

7.2 Inhibitors of β-glucan biosynthesis

Echinocandins are a well-known class of antifungal agents that inhibit the enzymes responsible for the formation of β-glucans in the cell walls of fungi (Odds *et al.*, 2003). Among this class of antifungal agents, caspofungin, anidulafungin, and micafungin are three well-characterised echinocandins that have powerful activity against fungal pathogens of humans, for example, *Aspergillus*, *Candida*, and *Pneumocystis* species (Gil-Alonso *et al.*, 2015; Perfect, 2017; Souza & Amaral, 2017). Treatment with echinocandins disrupt the cohesive association of (1→3)-β-glucans and (1→6)-β-glucans in the cell wall and eventually causes the death of fungal cells as a result of the inhibition of (1→3)-β-glucan biosynthesis (Kathiravan *et al.*, 2012; Song & Stevens, 2016). Caspofungin binds the fungal glucan synthase FKS1 and acts as a non-competitive inhibitor of the enzyme. Studies on *C. albicans* suggest that (1→3)-β-glucans are unmasked in the presence of this inhibitor, which leads to an increased detection of the glucans by the immune receptor dectin-1, which ultimately enhances the host immune response (Eschenauer *et al.*, 2007; Goncalves *et al.*, 2016; Marakalala *et al.*, 2013). Moreover, exposure to caspofungin seems to not only cause changes in the glucan network but also reduces ergosterol content and, most strikingly, increases chitin content, which results in a relatively thicker cell wall (Pfaller *et al.*, 2008). These observations highlight a range of effects on the fungal cells, but the precise underlying molecular mechanisms are unclear, some of which might be an indirect effect of the inhibition of (1→3)-β-glucan synthases. It remains that the combined effect of caspofungin and CHS inhibitors may result in effective disease control, but this has yet to be tested against fish of plant pathogenic oomycetes.

Based on the efficiency of caspofungin on several fungal species, it was suggested that this type of inhibitor might be efficient against oomycetes. A first study evaluated the susceptibility of the pathogenic oomycete *P. insidiosum* to caspofungin (Pereira *et al.*, 2007). It was shown that

the use of caspofungin decreased lesion size in infected rabbits, but this positive effect did not last upon termination of exposure to the compound (Pereira *et al.*, 2007). Later, the assessment of caspofungin, anidulafungin and micafungin to control pythiosis was tested in humans and other mammals. Caspofungin was the most efficient compound at the lowest concentrations tested, with morphological alterations observed in the pathogen (Argenta *et al.*, 2010; Jesus *et al.*, 2015; Jesus *et al.*, 2014; Loreto *et al.*, 2014; Pereira *et al.*, 2007; Permpalung *et al.*, 2019; Permpalung *et al.*, 2015; Susaengrat *et al.*, 2019; Worasilchai *et al.*, 2018; Zanette *et al.*, 2015). However, echinocandins showed no inhibitory effect on pathogenic *Saprolegnia* species, despite the presence of at least 10 putative glucan synthases in these micro-organisms. Differences in susceptibility to echinodandins observed between oomycetes and fungi may reflect different properties of their glucan synthases.

Poacic acid is a recently discovered natural antifungal isolated from hydrolysates of grasses (Piotrowski *et al.*, 2015). It was shown that this compound is active against both oomycetes and fungi, and that it acts by inhibiting the remodelling of (1→3)-β-glucans through direct binding to the polysaccharide chains (Piotrowski *et al.*, 2015). Furthermore, poacid acid significantly alters hyphal growth of *P. sojae* grown in axenic conditions for 7 days (Piotrowski *et al.*, 2015). Interestingly, the combined application of poacic acid and caspofungin revealed a synergistic effect on fungal growth, but the same was not observed when the echinocandin was replaced with the chitin synthase inhibitor nikkomycin Z (Piotrowski *et al.*, 2015). It was suggested that poacic acid targets the cell wall through a mechanism that is distinct from that of caspofungin, i.e., that poacic acid affects cell wall integrity through a non-specific mechanism rather than by direct binding to (1→3)-β-glucans (Piotrowski *et al.*, 2015). Despite these promising observations, the inhibitory effect of poacic acid has not been tested on other pathogenic oomycetes such as members of the Saprolegniales order. Further research is therefore needed to determine whether the inhibitory effect of poacic acid can be generalised to multiple oomycete species, and also to gain further insight into the precise mode of action of the inhibitor.

7.3 Inhibitors of chitin biosynthesis

Despite chitin being a minor cell wall component of some oomycetes, this polymer plays a vital role in the growth and development of the species in which it is found (Badreddine *et al.*, 2008; Cheng *et al.*, 2019; Klinter *et al.*, 2019; Rzeszutek *et al.*, 2019). Thus, CHS inhibitors are expected to be efficient against the oomycete species that have been shown to contain chitin in

their cell walls. Nikkomycin Z and polyoxin D are structural analogues of UDP-GlcNAc, the substrate of CHS, and some of the most efficient inhibitors of fungal CHS.

Nikkomycins were isolated from the bacterium *Streptomyces tendae* in the 1970's. This group of competitive inhibitors of CHS show high affinity for the enzyme (Behr *et al.*, 2001). Nikkomycin Z is the most potent inhibitor and was shown to inhibit CHS1 and CHS3 in yeast, but its efficiency against CHS2 required the use of much higher concentrations of the inhibitor (Gaughran *et al.*, 1994). Similar inhibitory activity has been reported *in vitro* in the oomycetes *S. parasitica* and *S. monoica* (Guerriero *et al.*, 2010; Rzeszutek *et al.*, 2019). In these species, inhibition of CHS activity by nikkomycin Z results in decreased hyphal growth and hyphal tip bursting. Despite the absence of chitin in *Phytophthora* species, nikkomycin Z has a similar inhibitory effect on *Phytophthora* hyphal growth as in *Saprolegnia* species, except for *P. sojae* (Fuechtbauer *et al*., 2018; Guerriero *et al*., 2010; Hinkel & Ospina-Giraldo, 2017). However, in a recent study in which the crystal structure of CHS1 was solved, biochemical assays performed *in vitro* on the purified enzyme from *P. sojae* showed that nikkomycin Z does inhibit CHS1 activity; in addition the detailed mode of interaction of the inhibitor with the protein was deduced from the structure of the enzyme-inhibitor complex (Chen *et al*., 2022). Despite the demonstration of the efficacy of nikkomycin Z against several pathogenic oomycetes, the inhibitor is not used in agriculture and aquaculture essentially because of its high costs of production. Interestingly, a synergistic effect has been observed against *Aspergillus*, *Rhizopus* and *Candida* species when nikkomycin Z is used in combination with echinocandins such as caspofungin (Walker *et al.*, 2010), but this combination of cell wall biosynthesis inhibitors has not been tested on oomycetes.

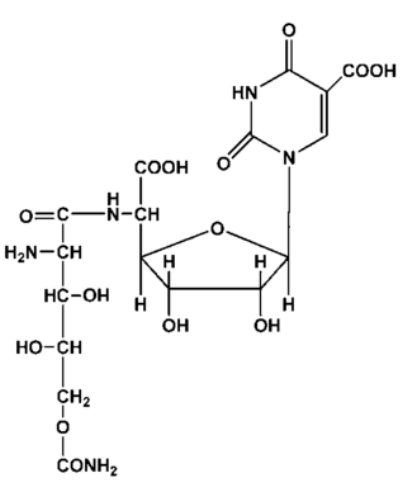

Polyoxin D

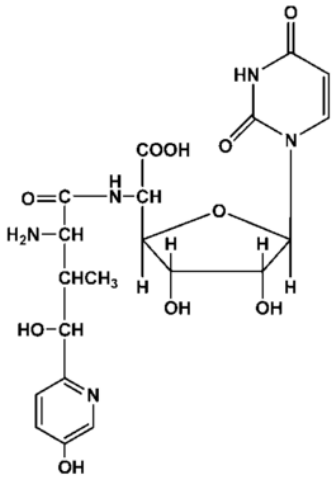

Nikkomycin Z

Figure 14: Structure of nikkomycin Z and polyoxin D (adapted from Li *et al*., 2009). (Reprinted with permission from {Li *et al*., 2009}. Copyright {2009} Microbiology Society.)

Polyoxin D is another specific CHS inhibitor that efficiently blocks the growth of pathogenic fungi and yeasts. In addition, it was shown that polyoxin D reduced mycelial growth and cell wall chitin content in *Saprolegnia monoica*, but without any impact on the morphology of hyphal cells (Bulone *et al.*, 1992). Similar observations were made in other oomycetes, i.e., *Leptomitus*, *Apodachlyella*, and *Apodachlya* (Dietrich & Campos, 1978; Huizar & Aronson, 1985; Huizar & Aronson, 1986). However, amore recent study showed that polyoxin D has no efficacy in controlling fruit rot disease of apples caused by *Phytophthora cactorum* under field conditions (Hill & Hausbeck, 2008). Another CHS inhibitor, plagiochin, is a derivative of bis-bibenzyl that significantly alters the expression of *Chs* genes in fungi, but its effect on oomycetes has not been investigated (Guo *et al.*, 2008; Wu *et al.*, 2010; Wu *et al.*, 2008).

8 The future of oomycete disease control

Currently, the most effective approaches to control oomycete diseases rely on the use of chemicals. However, using repeatedly the same chemical agent can result in genetic changes and development of resistance to pesticides in pathogens. Hence novel alternative strategies that have minimal impact on the environment and human health are needed for the management of pathogenic oomycetes. In this section, we present alternative approaches that hold potential for the control of oomycete diseases, such as transgenic approaches, antimicrobial peptides (AMP), double stranded RNA (dsRNA), biological control, and genome editing (Figure 15).

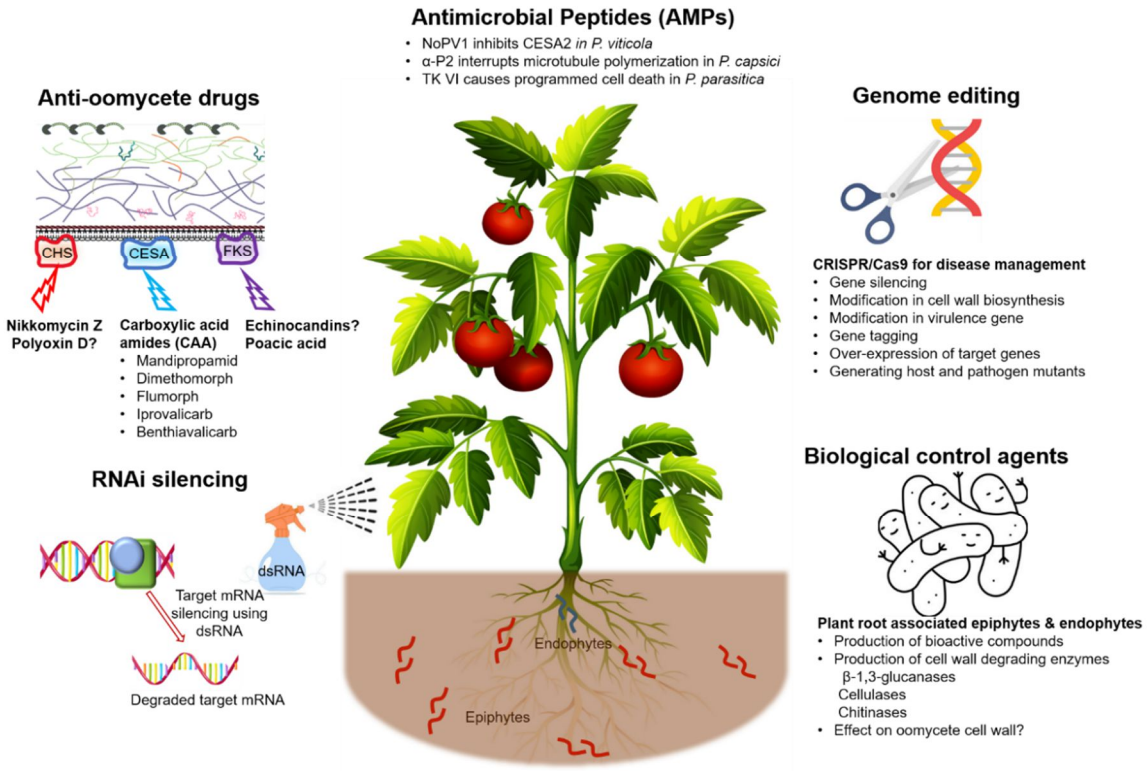

Figure 15: Potential strategies for the control of oomycete diseases. CHS: Chitin synthase; CESA: Cellulose synthase; FKS: β-1,3-Glucan synthase; NoPV1: a novel peptide aptamer named 'No *Plasmopora viticola* 1'; α-P2: phage number 1 against α-tubulin; TK VI: Trichokonin VI.

8.1 RNA silencing

Gene silencing using RNA interference (RNAi) was first introduced in 1998 (Fire *et al.*, 1998). This approach uses double-stranded RNAs (dsRNAs) to prepare small interfering RNA (siRNA) duplexes that bind the target mRNA, which subsequently degrades, leading to 'gene silencing'. It can be applied to the treatment of diseases caused by bacteria, viruses, and fungi (Whitten, 2019).

In 2006, a first study showed the efficacy of dsRNA in plant disease management (Wang *et al.*, 2016). Dicer-like 1 (DCL1) and Dicer-like 2 (DCL2) are plant proteins that process dsRNA to form siRNA duplexes. It was shown that the combined application of DCLs and dsRNA on plants infected by *Botrytis cinerea* significantly decreased the growth and development of the fungus (Wang *et al.*, 2016). A more recent study showed that genes involved in vesicle trafficking are good targets to tackle various pathogenic fungi and oomycetes. Indeed, RNAi applied to this type of genes resulted in successful control of the downy mildew disease in grape plants caused by *Plasmopara viticola* (Cai *et al.*, 2021; Haile *et al.*, 2021; Qiao *et al.*, 2021). Since cell wall biosynthetic enzymes are vital for cell growth and development, research has

been undertaken to target the corresponding mRNA using RNAi. For example, it was shown that RNAi-mediated silencing of the *Chs1* gene severely affects the growth of *B. cinerea* (Nerva *et al.*, 2020). In another study, about 50% of the cellulose content was reduced in the cell wall of *P. infestans* when the entire family of *CesA* genes were silenced using RNAi, resulting in decreased infection in potato (Grenville-Briggs *et al.*, 2008). These data indicate that genes related to cell wall biosynthesis and modification are promising targets. However, the success of RNAi gene silencing for plant disease management mostly depends on uptake rate of dsRNAs by the pathogenic cells. For example, low level of dsRNAs uptake has been observed in *P. infestans* (Gebremichael *et al.*, 2021; Qiao *et al.*, 2021). Moreover, the formulation of dsRNA used and the environment in the field, such as exposure to UV light, heat, and microbial interactions, are major factors that affect the delivery of dsRNAs into target cells. Hence, more research is required to better understand and determine dsRNAs uptake in different pathogenic oomycetes, and efficient sprayable formulations need to be developed.

8.2 Antimicrobial peptides

Antimicrobial peptides (AMPs) are produced by various organisms in response to biotic and abiotic stresses (Montesinos, 2007). AMPs are charged, hydrophobic and highly structurally stable peptides of 10–50 amino acid long, which translates into a molecular mass of 2–9 kDa (Pelegrini *et al.*, 2011). They are synthesised by plant cells as a response to, e.g., drought, salinity, cold, wounding and pathogen invasion (Montesinos, 2007). Various classes of AMPs have been identified in plants, such as defensins, thionins, snakins, cyclotides, lipid transfer proteins, heveins, knottins, harpinins, and 2S albumins. These are effective against different phytopathogens. For example, several cysteine-rich and circular AMPs from the defensin family that exhibit strong antifungal activity have been identified in the last 10 years (Nawrot *et al.*, 2014) (Table 4). Some exert their lethal effect through binding to chitin and/or glucans in the fungal cell wall (Bleackley *et al.*, 2019). The plant defensin NaD1 (*Nicotiana alata* defensin 1) kills *Fusarium oxysporum* cells by interacting first with β-1,3-glucans in the fungal cell wall (Van Der Weerden *et al.*, 2008). The data suggest that NaD1 subsequently permeabilizes cell membranes and eventually causes cells death through the increased production of reactive oxygen species (ROS) and cytoplasmic granulation. The presence of β-1,3-glucans in the OCW suggests that NaD1 and other plant AMPs with similar activity may be active against pathogenic oomycetes.

Table 4 : Examples of plant defensins and susceptible phytopathogenic fungi and oomycetes.

Defensin	Source	Binding to cell wall polysaccharide			Activity against pathogen		Reference
		Chitin	Glucan	Cellulose	Fungi	Oomycetes	
NaD1	*Nicotiana alata*	Yes	Yes	Not known	Damages the (1→3)-β-glucan-rich layer, initiates ROS production, disrupts cytoplasm, activates high osmolarity glycerol (HOG) pathway, but has no effect on the cell wall integrity (CWI) pathway, can cause cell death of *Fusarium oxysporum* and *Saccharomyces cerevisiae*	Not known	(Bleackley *et al.*, 2019; Hayes *et al.*, 2013; Van Der Weerden *et al.*, 2008)
DmAMP1	*Dahlia merkii*	No	No	Not known	Binds sphingolipids, sparks higher K^+ efflux and Ca^{2+} uptake, activates the CWI pathway, causes cell death of *Candida albicans*	Expression of DmAMP1 in papaya increases resistance against *P. palmivora*	(Parisi *et al.*, 2019; Zhu *et al.*, 2007)
RsAFP2	*Raphanus sativa*	Not known	Not known	Not known	Triggers the MAPK signalling cascade, which induces the CWI pathways, causes apoptosis in *C. albicans*	Agrobacterium mediated transformation of tomato plants showed resistance against *P. infestans*	(El-Siddig *et al.*, 2011; Thevissen *et al.*, 2012)
Msdef1	*Medicago sativa*	Not known	Not known	Not known	Interacts with glucosylceramides, activates the MAPK signalling cascade and CWI pathway, disrupts homeostasis due to Ca^{2+} uptake and eventually causes excessive branching of hyphae in *Fusarium graminearum*	Not known	(Muñoz *et al.*, 2014; Ramamoorthy *et al.*, 2007; Spelbrink *et al.*, 2004)
Lm-def	*Lepidium meyenii*	Not known	Not known	Not known	Not known	Recombinant NusA:Lm-def protein inhibits hyphal growth of *P. infestans*.	(Solis *et al.*, 2007)
cdef1	*Capsicum annum*	Not known	Not known	Not known	Transgenic tomato plants expressing cdef1 show resistance against *Fusarium* sp.	Transgenic tomato plants expressing cdef1 show resistance against *P. infestans.*	(Zainal *et al.*, 2009)

A recent study showed that a synthetic plant defensin named NoPV1 (No *Plasmopara viticola* 1) could specifically suppress *P. viticola* in infected grapevine (Colombo *et al.*, 2020; Colombo *et al.*, 2015). NoPV1 disrupts cellulose biosynthesis by binding to the CESA2 protein of *P. viticola*, which indirectly affects germ tube formation by zoospores (Colombo *et al.*, 2020). Another synthetic defensin, α_P2, significantly inhibits *P. capsici* by interrupting microtubule

polymerization (Lee *et al.*, 2019). Future detailed studies of the effect of combinations of multiple dsRNAs with cell wall inhibitors and AMPs may allow the development of new integrated pest management (IPM) systems for plant pathogens.

8.3 Biological control

Biological control is a technique based on the use of living organisms, such as epiphytic or endophytic bacteria and mycoparasites, to control disease-causing agents, e.g., pathogenic fungi or oomycetes (Stenberg *et al.*, 2021). For example, *Trichoderma* is a well-known fungus that is commercially available and used to control *P. infestans* and fungal diseases (Kariuki *et al.*, 2020; Stephan *et al.*, 2005). *Pythium oligandrum* is a mycoparasitic oomycete that uses effectors and enzymes to cause cell wall degradation in plant pathogenic fungi and oomycetes (Gerbore *et al.*, 2014; Liang *et al.*, 2020). Other examples of efficient biocontrol agents include antagonistic bacterial species active against oomycetes such as root-associated epiphytic or endophytic bacteria. Some *Pseudomonas* and *Bacillus* species are well-studied antagonistic bacteria with inhibitory characteristics against different species of *Phytophthora* (Figure 15). Such bacteria can be isolated based on their direct inhibition of hyphal growth in *in vitro* cultures of the target pathogen. This approach has facilitated the identification of many antagonistic bacteria that can reduce the rate of hyphal growth, cause lysis of zoospores, and interrupt germ tube formation in cysts of *P. infestans*, *P. capsici*, and many other oomycete species (Bailly & Weisskopf, 2017; Caulier *et al.*, 2018; De Vrieze *et al.*, 2020; Joller *et al.*, 2020; Khatun *et al.*, 2018). Bacterial biocontrol agents produce bioactive compounds and enzymes that contribute to the disintegration of the cell walls of plant pathogens, such as (1→3)-β-glucanases, cellulases, and chitinases (Fadiji & Babalola, 2020). For example, the chitinase released by *Streptomyces hygroscopicus* stops hyphal growth of a wide range of pathogenic fungi by degrading chitin as a key structural component of fungal cell walls (Haggag & Abdallh, 2012). Such approaches are highly promising for the treatment of plant diseases caused by oomycetes.

8.4 Genome editing

CRISPR/Cas9 is one of the gene editing methods that opens opportunities for the efficient treatment of diseases of plants, animals, and humans. In 2016, the method was adapted and applied for the first time to an oomycete species, *P. sojae* (Fang *et al.*, 2017; Fang & Tyler, 2016). Later, mutations of *Chs1* generated by CRISPR/Cas9 in *P. capsici* and *P. sojae* led to compromised hyphal growth and impaired pathogenicity (Cheng *et al.*, 2019). Furthermore, a recent study identified several genetic factors which could be used for producing CRISPR/Cas9

knockdowns to increase resistance in wheat against fungal diseases (Taj *et al.*, 2022). Similar studies are required for pathogenic oomycetes to develop resistant plant varieties, for instance by targeting genetic factors that control cellulose, glucan and chitin biosynthesis, as well as other cell wall-related signalling pathways. Unlike traditional genetic modifications of organisms that involve transgenes, CRISPR/Cas9 does not introduce foreign genes into the plant genome. As a result, plants that have been genetically altered using this technique are less subject to legal restrictions.

9 Conclusion

Compared to fungi, oomycetes and their cell walls have been extensively less studied. However, the cell walls of oomycetes are excellent targets for the development of novel strategies for disease control, as presented above. Hence considerable efforts are currently made to decipher cell wall biosynthesis in oomycetes as well as other vital pathways in these micro-organisms. It is expected that efficient disease management will arise from this research by combining several of the approaches presented in the previous sub-sections and that these will be applicable to animal and plant diseases caused by a diversity of oomycete species. The topic of this PhD thesis falls within this scope, with the study of the cell wall of *Phytophthora cinnamomi* and the mode of action of a cell wall inhibitor and an AMP that blocks the growth of the pathogen.

10 Outstanding questions for future areas of research

- The OCW is a complex network of polysaccharides, mainly composed of cellulose and other β-glucans. How are these polysaccharides distributed in different layers of the OCW and how do they interact to form a coherent extracellular matrix?
- What are the critical roles of mannans and mannoproteins in the regulation of oomycete growth, development, and pathogenicity?
- What are the enzymes responsible for the biosynthesis of (1→3)-β-glucans and branched (1→3; 1→6)-β-glucans in oomycetes? Are these enzymes vital for the growth, development, and pathogenesis of oomycetes?
- The presence of crosslinks between cellulose, (1→3)-β-glucans and (1→3; 1→6)-β-glucans has been shown using fine cell wall polysaccharide analyses. Which events/enzymes are required for the formation of these crosslinks and how is there activity regulated?

- The presence of chitin deacetylases in the oomycete genome has been shown using *in-silico* analysis. Do these enzymes have any role in cell wall structure and modification in oomycetes?
- Which combination of cell wall inhibitor(s) and modern biotechnological approaches (RNAi silencing/biological control agents/gene editing) is most efficient for disease control?
- Do plants produce antimicrobial peptides as a response to infection by oomycetes and how efficient are these for protection against infection? How do plant AMPs interact with molecular components of pathogenic oomycetes?

References

Abuajah, C.I. (2017). *Functional Components and Medicinal Properties of Food.* In: Mérillon, JM., Ramawat, K. (eds) Bioactive Molecules in Food. Reference Series in Phytochemistry. Springer, Cham.

Adl, S. M., Simpson, A. G., Farmer, M. A., Andersen, R. A., Anderson, O. R., Barta, J. R., Bowser, S. S., Brugerolle, G., Fensome, R. A. & Fredericq, S. (2005) The new higher level classification of eukaryotes with emphasis on the taxonomy of protists. *Journal of Eukaryotic Microbiology*, 52(5), 399-451.

Allmaras, R., Fritz, V., Pfleger, F. & Copeland, S. (1998) 'Common root rot of pea (*Pisum sativum* L.): oat pre-crop and traffic compaction effects in fine-textured mollisols', *Root Demographics and Their Efficiencies in Sustainable Agriculture, Grasslands and Forest Ecosystems: Proceedings of the 5th Symposium of the International Society of Root Research, held 14–18 July 1996 at Madren Conference Center, Clemson University, Clemson, South Carolina, USA*. Springer.

Aloni, Y., Delmer, D. P. & Benziman, M. (1982) Achievement of high rates of in vitro synthesis of 1,4-beta-D-glucan: activation by cooperative interaction of the Acetobacter xylinum enzyme system with GTP, polyethylene glycol, and a protein factor. *Proceedings of the National Academy of Sciences*, 79(21), 6448-6452.

Argenta, J. S., Alves, S. H., Silveira, F., Maboni, G., Pereira, D. I., Spanamberg, A., Santurio, J. M. & Ferreiro, L. (2010) In vitro paradoxical growth of Pythium insidiosum in the presence of caspofungin. *Veterinary Microbiology*, 145(3-4), 321-323.

Arioli, T., Peng, L. C., Betzner, A. S., Burn, J., Wittke, W., Herth, W., Camilleri, C., Hofte, H., Plazinski, J., Birch, R., Cork, A., Glover, J., Redmond, J. & Williamson, R. E. (1998) Molecular analysis of cellulose biosynthesis in Arabidopsis. *Science*, 279(5351), 717-720.

Aronson, J. M., Cooper, B. A. & Fuller, M. S. (1967) Glucans of oomycete cell walls. *Science*, 155(3760), 332-335.

Atalla, R. H. & Vanderhart, D. L. (1984) Native cellulose: a composite of two distinct crystalline forms. *Science*, 223(4633), 283-285.

Ayers, A. R., Ebel, J. r., Valent, B. & Albersheim, P. (1976) Host-pathogen interactions: X.

Fractionation and biological activity of an elicitor isolated from the mycelial walls of Phytophthora megasperma var. sojae. *Plant Physiology*, 57(5), 760-765.

Badis, Y., Klochkova, T. A., Brakel, J., Arce, P., Ostrowski, M., Tringe, S. G., Kim, G. H. & Gachon, C. M. (2020) Hidden diversity in the oomycete genus Olpidiopsis is a potential hazard to red algal cultivation and conservation worldwide. *European Journal of Phycology*, 55(2), 162-171.

Badreddine, I., Lafitte, C., Heux, L., Skandalis, N., Spanou, Z., Martinez, Y., Esquerre-Tugaye, M. T., Bulone, V., Dumas, B. & Bottin, A. (2008) Cell wall chitosaccharides are essential components and exposed patterns of the phytopathogenic oomycete Aphanomyces euteiches. *Eukaryotic Cell*, 7(11), 1980-1993.

Bailly, A. & Weisskopf, L. (2017) Mining the volatilomes of plant-associated microbiota for new biocontrol solutions. *Frontiers in Microbiology*, 8, 1638.

Bartnicki-Garcia, S. (1968) Cell wall chemistry, morphogenesis, and taxonomy of fungi. *Annual Review of Microbiology*, 22, 87-108.

Bartnicki-Gracia, S. (1983) Biochemical aspects of morphogenesis in Phytophthora. *Phytophthora : Its Taxonomy, Ecology and Pathology*, 121-137.

Beakes, G., Thines, M., Archibald, J., Simpson, A., Slamovits, C., Margulis, L., Melkonian, M., Chapman, D. & Corliss, J. (2017) Handbook of the protists. *Hyphochytriomycota and Oomycota*, 1-71.

Beakes, G. W., Glockling, S. L. & Sekimoto, S. (2012) The evolutionary phylogeny of the oomycete "fungi". *Protoplasma*, 249(1), 3-19.

Beakes, G. W. & Thines, M. (2016) Hyphochytriomycota and Oomycota, in Archibald, J. M., Simpson, A. G. B., Slamovits, C. H., Margulis, L., Melkonian, M., Chapman, D. J. & Corliss, J. O. (eds), *Handbook of the Protists*. Cham: Springer International Publishing, 1-71.

Beauvais, A., Bruneau, J. M., Mol, P. C., Buitrago, M. J., Legrand, R. & Latge, J. P. (2001) Glucan synthase complex of Aspergillus fumigatus. *Journal of Bacteriology*, 183(7), 2273-2279.

Becking, T., Kiselev, A., Rossi, V., Street-Jones, D., Grandjean, F. & Gaulin, E. (2022)

Pathogenicity of animal and plant parasitic Aphanomyces spp and their economic impact on aquaculture and agriculture. *Fungal Biology Reviews*, 40, 1-18.

Behr, J.-B., Gautier-Lefebvre, I., Mvondo-Evina, C., Guillerm, G. & Ryder, N. S. (2001) Inhibition of chitin synthetase from Saccharomyces cerevisiae by a new UDP-GlcNAc analogue. *Journal of Enzyme Inhibition*, 16(2), 107-112.

Benavent-Celma, C., López-García, N., Ruba, T., Ściślak, M. E., Street-Jones, D., van West, P., Woodward, S. & Witzell, J. (2022) Current practices and emerging possibilities for reducing the spread of oomycete pathogens in terrestrial and aquatic production systems in the European Union. *Fungal Biology Reviews*, 40, 19-36

Berezina, N. (2016) Production and application of chitin. *Physical Sciences Reviews*, 1(9), 20160048.

Berry, L., Jones, E. & Deacon, J. (1993) Interaction of the mycoparasite Pythium oligandrum with other Pythium species. *Biocontrol Science and Technology*, 3(3), 247-260.

Bilir, Ö., Telli, O., Norman, C., Budak, H., Hong, Y. & Tör, M. (2019) Small RNA inhibits infection by downy mildew pathogen Hyaloperonospora arabidopsidis. *Molecular Plant Pathology*, 20(11), 1523-1534.

Bleackley, M. R., Dawson, C. S., Payne, J. A. E., Harvey, P. J., Rosengren, K. J., Quimbar, P., Garcia-Ceron, D., Lowe, R., Bulone, V., van der Weerden, N. L., Craik, D. J. & Anderson, M. A. (2019) The interaction with fungal cell wall polysaccharides determines the salt tolerance of antifungal plant defensins. *The Cell Surface*, 5, 100026.

Blum, M., Boehler, M., Randall, E., Young, V., Csukai, M., Kraus, S., Moulin, F., Scalliet, G., Avrova, A. O., Whisson, S. C. & Fonne-Pfister, R. (2010) Mandipropamid targets the cellulose synthase-like PiCesA3 to inhibit cell wall biosynthesis in the oomycete plant pathogen, Phytophthora infestans. *Molecular Plant Pathology*, 11(2), 227-243.

Blum, M. & Gisi, U. (2012) Insights into the molecular mechanism of tolerance to carboxylic acid amide (CAA) fungicides in Pythium aphanidermatum. *Pest Management Science*, 68(8), 1171-1183.

Bly, J. E. & Clem, L. W. (1992) Temperature and teleost immune functions. *Fish & Shellfish*

Immunology, 2(3), 159-171.

Bosland, P. W. (2008) Think global, breed local: specificity and complexity of Phytophthora capsici, *19th International Pepper Conference. Atlantic City, NJ*.

Bourke, A., Hill, J. R. & Ó Gráda, C. (1993) *The visitation of God? : the potato and the great Irish famine*. Dublin, Ireland: Lilliput Press

Bowman, S. M. & Free, S. J. (2006) The structure and synthesis of the fungal cell wall. *BioEssays*, 28(8), 799-808.

Bradshaw-Smith, R., Whalley, W. & Craig, G. (1991) Interactions between Pythium oligandrum and the fungal footrot pathogens of peas. *Mycological Research*, 95(7), 861-865.

Bridge, P., Newsham, K. & Denton, G. (2008) Snow mould caused by a Pythium sp.: a potential vascular plant pathogen in the maritime Antarctic. *Plant Pathology*, 57(6), 1066-1072.

Brown, C., Patrick, J., Liebau, J. & Mäler, L. (2022) The MIT domain of chitin synthase 1 from the oomycete Saprolegnia monoica interacts specifically with phosphatidic acid. *Biochemistry and Biophysics Reports*, 30, 101229.

Brown, C., Szpryngiel, S., Kuang, G., Srivastava, V., Ye, W., McKee, L. S., Tu, Y., Mäler, L. & Bulone, V. (2016) Structural and functional characterization of the microtubule interacting and trafficking domains of two oomycete chitin synthases. *The FEBS Journal*, 283(16), 3072-3088.

Brown Jr, R. M. & Lin, F. C. (1990) Multiribbon microbial cellulose. Google Patents.

Brown, R. M. (1996) The biosynthesis of cellulose. *Journal of Macromolecular Science-Pure and Applied Chemistry*, A33(10), 1345-1373.

Brožová, J. (2002) Exploitation of the mycoparasitic fungus Pythium oligandrum in plant protection. *Plant Protection Science*, 38(1), 29-35.

Bruno, D. W., West, P. v. & Beakes, G. W. (2011) Saprolegnia and other oomycetes, *Fish diseases and disorders. Volume 3: viral, bacterial and fungal infections* CABI Wallingford UK, 669-720.

Buaya, A. T. & Thines, M. (2019a) Diatomophthoraceae – a new family of olpidiopsis-like

diatom parasitoids largely unrelated to Ectrogella. *Fungal Systematics and Evolution*, 5, 113-118.

Buaya, A. T. & Thines, M. (2019b) Miracula moenusica, a new member of the holocarpic parasitoid genus from the invasive freshwater diatom Pleurosira laevis. *Fungal Systematics and Evolution*, 3, 35-40.

Buaya, A. T. & Thines, M. (2020a) Bolbea parasitica gen. et sp. nov., a cultivable holocarpic parasitoid of the early-diverging Saprolegniomycetes. *Fungal Systematics and Evolution*, 6, 129 - 137.

Buaya, A. T. & Thines, M. (2020b) An overview on the biology and phylogeny of the early-diverging oomycetes. *Philippine Journal of Systematic Biology*, 14, 1-20.

Bulone, V., Chanzy, H., Gay, L., Girard, V. & Fevre, M. (1992) Characterization of chitin and chitin synthase from the cellulosic cell wall fungus Saprolegnia monoica. *Experimental Mycology*, 16(1), 8-21.

Bureau, T. E. & Brown, R. M. (1987) In vitro synthesis of cellulose II from a cytoplasmic membrane fraction of Acetobacter xylinum. *Proceedings of the National Academy of Sciences*, 84(20), 6985-6989.

Cabib, E., Sburlati, A., Bowers, B. & Silverman, S. J. (1989) Chitin synthase 1, an auxiliary enzyme for chitin synthesis in Saccharomyces cerevisiae. *The Journal of cell biology*, 108(5), 1665-1672.

Cahill, D. M., Rookes, J. E., Wilson, B. A., Gibson, L. & McDougall, K. L. (2008) Phytophthora cinnamomi and Australia's biodiversity: impacts, predictions and progress towards control. *Australian Journal of Botany*, 56(4), 279-310.

Cai, M., Li, T., Lu, X., Chen, L., Wang, Q. & Liu, X. (2021) Multiple mutations in the predicted transmembrane domains of the cellulose synthase 3 (CesA3) of Phytophthora capsici can confer semi-dominant resistance to carboxylic acid amide fungicides. *International Journal of Biological Macromoleculesl*, 193(Pt B), 2343-2351.

Cameron, D. S. & Taylor, I. E. (1976) Quantitative microanalysis of cell walls of Saprolegnia diclina Humphrey and Tremella mesenterica Fries. *Biochimica et Biophysica Acta*

(BBA)-General Subjects, 444(1), 212-222.

Cappellaro, C., Baldermann, C., Rachel, R. & Tanner, W. (1994) Mating type-specific cell-cell recognition of Saccharomyces cerevisiae: cell wall attachment and active sites of a-and alpha-agglutinin. *The EMBO journal*, 13(20), 4737-4744.

Caulier, S., Gillis, A., Colau, G., Licciardi, F., Liépin, M., Desoignies, N., Modrie, P., Legrève, A., Mahillon, J. & Bragard, C. (2018) Versatile antagonistic activities of soil-borne Bacillus spp. and Pseudomonas spp. against Phytophthora infestans and other potato pathogens. *Frontiers in Microbiology*, 9, 143.

Cavalier-Smith, T. & Chao, E. E. (2006) Phylogeny and megasystematics of phagotrophic heterokonts (kingdom Chromista). *Journal of Molecular Evolution*, 62, 388-420.

Chanzy, H., Imada, K., Mollard, A., Vuong, R. & Barnoud, F. (1979) Crystallographic aspects of sub-elementary cellulose fibrils occurring in the wall of rose cells culturedin vitro. *Protoplasma*, 100(3), 303-316.

Chen, W., Cao, P., Liu, Y., Yu, A., Wang, D., Chen, L., Sundarraj, R., Yuchi, Z., Gong, Y., Merzendorfer, H. & Yang, Q. (2022) Structural basis for directional chitin biosynthesis. *Nature*, 610(7931), 402-408.

Cheng, W., Lin, M., Qiu, M., Kong, L., Xu, Y., Li, Y., Wang, Y., Ye, W., Dong, S., He, S. & Wang, Y. (2019) Chitin synthase is involved in vegetative growth, asexual reproduction and pathogenesis of Phytophthora capsici and Phytophthora sojae. *Environmental Microbiology*, 21(12), 4537-4547.

Chitasombat, M. N., Jongkhajornpong, P., Lekhanont, K. & Krajaejun, T. (2020) Recent update in diagnosis and treatment of human pythiosis. *PeerJ*, 8, e8555.

Cohen, Y. & Coffey, M. D. (1986) Systemic fungicides and the control of oomycetes. *Annual Review of Phytopathology*, 24(1), 311-338.

Colombo, M., Masiero, S., Rosa, S., Caporali, E., Toffolatti, S. L., Mizzotti, C., Tadini, L., Rossi, F., Pellegrino, S. & Musetti, R. (2020) NoPv1: a synthetic antimicrobial peptide aptamer targeting the causal agents of grapevine downy mildew and potato late blight. *Scientific Reports*, 10(1), 17574.

Colombo, M., Mizzotti, C., Masiero, S., Kater, M. M. & Pesaresi, P. (2015) Peptide aptamers:

The versatile role of specific protein function inhibitors in plant biotechnology. *Journal of Integrative Plant Biology*, 57(11), 892-901.

Cornu, M. (1872) *Monographie des Saprolégniées: étude physiologique et systématique*, *5*E. Martinet.

Cosgrove, D. J. & Jarvis, M. C. (2012) Comparative structure and biomechanics of plant primary and secondary cell walls. *Frontiers in Plant Science*, 3, 204.

Culp, S. J., Mellick, P. W., Trotter, R. W., Greenlees, K. J., Kodell, R. L. & Beland, F. A. (2006) Carcinogenicity of malachite green chloride and leucomalachite green in B6C3F1 mice and F344 rats. *Food and Chemical Toxicology*, 44(8), 1204-1212.

Dai, S., Chu, Y., Liu, D., Cao, F., Wu, X., Zhou, J., Zhou, B., Chen, Y. & Huang, J. (2018) Intrinsically ionic conductive cellulose nanopapers applied as all solid dielectrics for low voltage organic transistors. *Nature Communications*, 9(1), 2737.

Dallies, N., François, J. & Paquet, V. (1998) A new method for quantitative determination of polysaccharides in the yeast cell wall. Application to the cell wall defective mutants of Saccharomyces cerevisiae. *Yeast*, 14(14), 1297-1306.

De Vrieze, M., Varadarajan, A. R., Schneeberger, K., Bailly, A., Rohr, R. P., Ahrens, C. H. & Weisskopf, L. (2020) Linking comparative genomics of nine potato-associated Pseudomonas isolates with their differing biocontrol potential against late blight. *Frontiers in Microbiology*, 11, 857.

DeBolt, S., Gutierrez, R., Ehrhardt, D. W. & Somerville, C. (2007) Nonmotile cellulose synthase subunits repeatedly accumulate within localized regions at the plasma membrane in Arabidopsis hypocotyl cells following 2,6-dichlorobenzonitrile treatment. *Plant Physiol*, 145(2), 334-338.

Derevnina, L., Petre, B., Kellner, R., Dagdas, Y. F., Sarowar, M. N., Giannakopoulou, A., De la Concepcion, J. C., Chaparro-Garcia, A., Pennington, H. G. & Van West, P. (2016) Emerging oomycete threats to plants and animals. *Philosophical Transactions of the Royal Society B: Biological Sciences*, 371(1709), 20150459.

Desjardins, P. R., Wang, M. C. & Bartnicki-Garcia, S. (1973) Electron microscopy of zoospores and cysts of Phytophthora palmivora: Morphology and surface texture. *Archiv für*

Mikrobiologie, 88(1), 61-70.

Desprez, T., Juraniec, M., Crowell, E. F., Jouy, H., Pochylova, Z., Parcy, F., Hofte, H., Gonneau, M. & Vernhettes, S. (2007) Organization of cellulose synthase complexes involved in primary cell wall synthesis in Arabidopsis thaliana. *Proceedings of the National Academy of Sciences of the United States of America*, 104(39), 15572-15577.

Dick, M. W. (2013) *Straminipilous Fungi: systematics of the Peronosporomycetes including accounts of the marine straminipilous protists, the plasmodiophorids and similar organisms*, Springer Science & Business Media.

Dietrich, S. M. C. & Campos, G. M. A. (1978) Effect of Polyoxin D on Achlya radiosa. *Microbiology*, 105(1), 161-164.

Doke, N. & Tomiyama, K. (1980) Effect of hyphal wall components from Phytophthora infestans on protoplasts of potato tuber tissues. *Physiological Plant Pathology*, 16(2), 169-176

Douglas, C. M. (2001) Fungal β(1,3)-d-glucan synthesis. *Medical Mycology*, 39(1), 55-66.

Drenth, A. & Guest, D. I. (2004) Diversity and management of Phytophthora in southeast Asia. Monographs, Australian Centre for International Agricultural Research, 114060.

Dunstan, W. A., Rudman, T., Shearer, B. L., Moore, N. A., Paap, T., Calver, M. C., Dell, B. & Hardy, G. E. S. J. (2010) Containment and spot eradication of a highly destructive, invasive plant pathogen (Phytophthora cinnamomi) in natural ecosystems. *Biological Invasions*, 12, 913-925.

El-Siddig, M. A., El-Hussein, A. A. & Saker, M. M. (2011) Agrobacterium-mediated transformation of tomato plants expressing defensin gene. *International Journal of Agricultural Research*, 6(4), 323-334.

El Seoud, O. A., Kostag, M., Jedvert, K. & Malek, N. I. (2019) Cellulose in ionic liquids and alkaline solutions: advances in the mechanisms of biopolymer dissolution and regeneration. *Polymers (Basel)*, 11(12).

Elsoud, M. M. A. & El Kady, E. (2019) Current trends in fungal biosynthesis of chitin and chitosan. *Bulletin of the National Research Centre*, 43(1), 1-12.

Erwin, D. C., Bartnicki-Garcia, S. & Tsao, P. H, eds. (1983) *Phytophthora: its biology,*

taxonomy, ecology, and pathology, American Phytopathological Society Press, Saint Paul, Minnesota.

Erwin, D. C. & Ribeiro, O. K. (1996) *Phytophthora diseases worldwide*, American Phytopathological Society Press, Saint Paul, Minnesota.

Eschenauer, G., DePestel, D. D. & Carver, P. L. (2007) Comparison of echinocandin antifungals. *Therapeutics and Clinical Risk Management*, 3(1), 71-97.

Fadiji, A. E. & Babalola, O. O. (2020) Elucidating mechanisms of endophytes used in plant protection and other bioactivities with multifunctional prospects. *Frontiers in Bioengineering and Biotechnology*, 8, 467.

Fang, Y., Cui, L., Gu, B., Arredondo, F. & Tyler, B. M. (2017) Efficient genome editing in the oomycete Phytophthora sojae using CRISPR/Cas9. *Current Protocols in Microbiology*, 44, 21A.1.1-21A.1.26.

Fang, Y. & Tyler, B. M. (2016) Efficient disruption and replacement of an effector gene in the oomycete Phytophthora sojae using CRISPR/Cas9. *Molecular Plant Pathology*, 17(1), 127-139.

Fire, A., Xu, S., Montgomery, M. K., Kostas, S. A., Driver, S. E. & Mello, C. C. (1998) Potent and specific genetic interference by double-stranded RNA in Caenorhabditis elegans. *Nature*, 391(6669), 806-811.

Fontaine, T., Simenel, C., Dubreucq, G., Adam, O., Delepierre, M., Lemoine, J., Vorgias, C. E., Diaquin, M. & Latgé, J.-P. (2000) Molecular organization of the alkali-insoluble fraction ofAspergillus fumigatus cell wall. *Journal of Biological Chemistry*, 275(36), 27594-27607

Free, S. J. (2013) Fungal cell wall organization and biosynthesis. *Advanced Genetics*, 81, 33-82.

Fry, W. E. (2013) The 2009 late blight pandemic in the eastern United States - Causes and Results (vol 97, pg 296, 2013). *Plant Disease*, 97(5), 696-696.

Fuechtbauer, W., Yunusov, T., Bozsóki, Z., Gavrin, A., James, E. K., Stougaard, J., Schornack, S. & Radutoiu, S. (2018) LYS12 LysM receptor decelerates Phytophthora palmivora

disease progression in Lotus japonicus. *The Plant Journal*, 93(2), 297-310.

Fugelstad, J., Bouzenzana, J., Djerbi, S., Guerriero, G., Ezcurra, I., Teeri, T. T., Arvestad, L. & Bulone, V. (2009) Identification of the cellulose synthase genes from the Oomycete Saprolegnia monoica and effect of cellulose synthesis inhibitors on gene expression and enzyme activity. *Fungal Genetics and Biology*, 46(10), 759-767.

Fugelstad, J., Brown, C., Hukasova, E., Sundqvist, G., Lindqvist, A. & Bulone, V. (2012) Functional characterization of the pleckstrin homology domain of a cellulose synthase from the oomycete Saprolegnia monoica. *Biochemical and Biophysical Research Communications*, 417(4), 1248-1253.

Gachon, C. M., Strittmatter, M., Badis, Y., Fletcher, K. I., West, P. V. & Müller, D. G. (2017) Pathogens of brown algae: culture studies of Anisolpidium ectocarpii and A. rosenvingei reveal that the Anisolpidiales are uniflagellated oomycetes. *European Journal of Phycology*, 52(2), 133-148.

Gao, R.-F., Wang, J.-Y., Liu, K.-W., Yoshida, K., Hsiao, Y.-Y., Shi, Y.-X., Tsai, K.-C., Chen, Y.-Y., Mitsuda, N., Liang, C.-K., Wang, Z.-W., Wang, Y., Zhang, D.-Y., Huang, L., Zhao, X., Zhong, W.-Y., Cheng, Y.-H., Jiang, Z.-D., Li, M.-H., Sun, W.-H., Yu, X., Hu, W., Zhou, Z., Zhou, X.-F., Yeh, C.-M., Katoh, K., Tsai, W.-C., Liu, Z.-J., Martin, F. & Zhang, G.-M. (2021) Comparative analysis of Phytophthora genomes reveals oomycete pathogenesis in crops. *Heliyon*, 7(2), e06317.

Garbelotto, M., Harnik, T. & Schmidt, D. (2009) Efficacy of phosphonic acid, metalaxyl-M and copper hydroxide against Phytophthora ramorum in vitro and in planta. *Plant Pathology*, 58(1), 111-119.

Garcia-Rubio, R., de Oliveira, H. C., Rivera, J. & Trevijano-Contador, N. (2020) The fungal cell wall: Candida, Cryptococcus, and Aspergillus species. *Frontiers in Microbiology*, 10, 2993.

Gaughran, J. P., Lai, M. H., Kirsch, D. R. & Silverman, S. J. (1994) Nikkomycin Z is a specific inhibitor of Saccharomyces cerevisiae chitin synthase isozyme Chs3 in vitro and in vivo. *Journal of Bacteriology*, 176(18), 5857-5860.

Gebremichael, D. E., Haile, Z. M., Negrini, F., Sabbadini, S., Capriotti, L., Mezzetti, B. & Baraldi, E. (2021) RNA interference strategies for future management of plant

pathogenic fungi: prospects and challenges. *Plants*, 10(4), 650.

Gentzsch, M. & Tanner, W. (1997) Protein-O-glycosylation in yeast: protein-specific mannosyltransferases. *Glycobiology*, 7(4), 481-486.

Geoghegan, I. A. & Gurr, S. J. (2016) Chitosan mediates germling adhesion in Magnaporthe oryzae and is required for surface sensing and germling morphogenesis. *PLoS Pathogens*, 12(6), e1005703.

Gerbore, J., Benhamou, N., Vallance, J., Le Floch, G., Grizard, D., Regnault-Roger, C. & Rey, P. (2014) Biological control of plant pathogens: advantages and limitations seen through the case study of Pythium oligandrum. *Environmental Science and Pollution Research*, 21, 4847-4860.

Gil-Alonso, S., Jauregizar, N., Cantón, E., Eraso, E. & Quindós, G. (2015) In vitro fungicidal activities of anidulafungin, caspofungin, and micafungin against Candida glabrata, Candida bracarensis, and Candida nivariensis evaluated by time-kill studies. *Antimicrobial Agents and Chemotherapy*, 59(6), 3615-3618.

Gisi, U. & Sierotzki, H. (2015) Oomycete fungicides: Phenylamides, quinone outside inhibitors, and carboxylic acid amides. *Fungicide resistance in plant pathogens: principles and a guide to practical management*, 145-174.

Goncalves, S. S., Souza, A. C. R., Chowdhary, A., Meis, J. F. & Colombo, A. L. (2016) Epidemiology and molecular mechanisms of antifungal resistance in Candida and Aspergillus. *Mycoses*, 59(4), 198-219.

Gow, N. A. & Hube, B. (2012) Importance of the Candida albicans cell wall during commensalism and infection. *Current Opinion in Microbiology*, 15(4), 406-412.

Graf, M. M. H., Bren, U., Haltrich, D. & Oostenbrink, C. (2013) Molecular dynamics simulations give insight into d-glucose dioxidation at C2 and C3 by Agaricus meleagris pyranose dehydrogenase. *Journal of Computer-Aided Molecular Design*, 27(4), 295-304.

Grenville-Briggs, L. J., Anderson, V. L., Fugelstad, J., Avrova, A. O., Bouzenzana, J., Williams, A., Wawra, S., Whisson, S. C., Birch, P. R. & Bulone, V. (2008a) Cellulose synthesis in Phytophthora infestans is required for normal appressorium formation and

successful infection of potato. *The Plant Cell*, 20(3), 720-738.

Guenthner, J. F., Michael, K. C. & Nolte, P. (2001) The economic impact of potato late blight on US growers. *Potato Research*, 44(2), 121-125.

Guerriero, G., Avino, M., Zhou, Q., Fugelstad, J., Clergeot, P.-H. & Bulone, V. (2010a) Chitin synthases from Saprolegnia are involved in tip growth and represent a potential target for anti-oomycete drugs. *PLoS Pathogens*, 6(8), e1001070.

Guerriero, G., Avino, M., Zhou, Q., Fugelstad, J., Clergeot, P. H. & Bulone, V. (2010b) Chitin synthases from Saprolegnia are involved in tip growth and represent a potential target for anti-oomycete drugs. *Plos Pathogens*, 6(8).

Guo, X. L., Leng, P., Yang, Y., Yu, L. G. & Lou, H. X. (2008) Plagiochin E, a botanic-derived phenolic compound, reverses fungal resistance to fluconazole relating to the efflux pump. *Journal of Applied Microbiology*, 104(3), 831-838.

Haggag, W. M. & Abdallh, E. (2012) Purification and characterization of chitinase produced by endophytic Streptomyces hygroscopicus against some phytopathogens. *Journal of Microbiology Research*, 2(5), 145-151.

Haile, Z. M., Gebremichael, D. E., Capriotti, L., Molesini, B., Negrini, F., Collina, M., Sabbadini, S., Mezzetti, B. & Baraldi, E. (2021) Double-stranded RNA targeting dicer-like genes compromises the pathogenicity of Plasmopara viticola on grapevine. *Frontiers in Plant Science*, 12, 667539.

Hall, R. A., Bates, S., Lenardon, M. D., MacCallum, D. M., Wagener, J., Lowman, D. W., Kruppa, M. D., Williams, D. L., Odds, F. C. & Brown, A. J. (2013) The Mnn2 mannosyltransferase family modulates mannoprotein fibril length, immune recognition and virulence of Candida albicans. *PLoS Pathogens*, 9(4), e1003276.

Hansen, E. M. (2008) Alien forest pathogens: Phytophthora species are changing world forests. *Boreal Environment Research*, 13, 33-41

Hansen, E. M., Reeser, P. W. & Sutton, W. (2012) Phytophthora beyond agriculture. *Annual Review of Phytopathology*, 50, 359-378.

Hardham, A. R. & Blackman, L. M. (2018) Phytophthora cinnamomi. *Molecular Plant*

Pathology, 19(2), 260-285.

Hartland, R. P., Vermeulen, C. A., Sietsma, J. H., Wessels, J. G. & Klis, F. M. (1994) The linkage of (1–3)-β-glucan to chitin during cell wall assembly in Saccharomyces cerevisiae. *Yeast*, 10(12), 1591-1599.

Hayden, K. J., Hardy, G. E. S. J. & Garbelotto, M. (2013) Oomycete diseases, *Infectious forest diseases*, CABI Wallingford UK, 519-546.

Hayes, B. M. E., Bleackley, M. R., Wiltshire, J. L., Anderson, M. A., Traven, A. & van der Weerden, N. L. (2013) Identification and mechanism of action of the plant defensin NaD1 as a new member of the antifungal drug arsenal against Candida albicans. *Antimicrobial Agents and Chemotherapy*, 57(8), 3667-3675.

Healey, K. R., Katiyar, S. K., Raj, S. & Edlind, T. D. (2012) CRS–MIS in C andida glabrata: sphingolipids modulate echinocandin–Fks interaction. *Molecular Microbiology*, 86(2), 303-313.

Helbert, W., Sugiyama, J., Ishihara, M. & Yamanaka, S. (1997) Characterization of native crystalline cellulose in the cell walls of Oomycota. *Journal of Biotechnology*, 57(1), 29-37.

Hill, S. N. & Hausbeck, M. K. (2008) Virulence and fungicide sensitivity of Phytophthora cactorum isolated from American ginseng gardens in Wisconsin and Michigan. *Plant Disease*, 92(8), 1183-1189.

Hinkel, L. & Ospina-Giraldo, M. D. (2017) Structural characterization of a putative chitin synthase gene in Phytophthora spp. and analysis of its transcriptional activity during pathogenesis on potato and soybean plants. *Current Genetics*, 63(5), 909-921.

Horsch, M., Mayer, C. & Rast, D. M. (1996) Stereochemical requirements of chitin synthase for ligand binding at the allosteric site for N-acetylglucosamine. *European Journal of Biochemistry*, 237(2), 476-482.

Hosseini, S., Heyman, F., Olsson, U., Broberg, A., Funck Jensen, D. & Karlsson, M. (2014) Zoospore chemotaxis of closely related legume-root infecting Phytophthora species towards host isoflavones. *Plant Pathology*, 63(3), 708-714.

Hu, X., Yang, P., Chai, C., Liu, J., Sun, H., Wu, Y., Zhang, M., Zhang, M., Liu, X. & Yu, H.

(2023) Structural and mechanistic insights into fungal β-1,3-glucan synthase FKS1. *Nature*, 616(7955), 190-198.

Hughes, K. A., Lawley, B. & Newsham, K. K. (2003) Solar UV-B radiation inhibits the growth of Antarctic terrestrial fungi. *Applied and Environmental Microbiology*, 69(3), 1488-1491.

Huizar, H. E. & Aronson, J. M. (1985) Chitin synthase of Apodachlya sp. *Experimental Mycology*, 9(4), 302-309.

Huizar, H. E. & Aronson, J. M. (1986) Aspects of cellulin deposition and chitin biosynthesis in the Leptomitaceae. *Mycologia*, 78(3), 489-492.

Hunsley, D. & Burnett, J. H. (1970) The ultrastructural architecture of the walls of some hyphal fungi. *Microbiology*, 62(2), 203-218.

Ibe, C. & Munro, C. A. (2021) Fungal cell wall: An underexploited target for antifungal therapies. *PLoS Pathogens*, 17(4), e1009470

Jarvis, M. (2003) Cellulose stacks up. *Nature*, 426(6967), 611-612.

Jesus, F. P., Ferreiro, L., Bizzi, K. S., Loreto É, S., Pilotto, M. B., Ludwig, A., Alves, S. H., Zanette, R. A. & Santurio, J. M. (2015) In vitro activity of carvacrol and thymol combined with antifungals or antibacterials against Pythium insidiosum. *Journal of Medical Mycology*, 25(2), e89-93.

Jesus, F. P., Ferreiro, L., Loreto, É. S., Pilotto, M. B., Ludwig, A., Bizzi, K., Tondolo, J. S., Zanette, R. A., Alves, S. H. & Santurio, J. M. (2014) In vitro synergism observed with azithromycin, clarithromycin, minocycline, or tigecycline in association with antifungal agents against Pythium insidiosum. *Antimicrobial Agents and Chemotherapy*, 58(9), 5621-5625.

Jiang, R. H., de Bruijn, I., Haas, B. J., Belmonte, R., Löbach, L., Christie, J., van den Ackerveken, G., Bottin, A., Bulone, V. & Díaz-Moreno, S. M. (2013) Distinctive expansion of potential virulence genes in the genome of the oomycete fish pathogen Saprolegnia parasitica. *PLoS Genetics*, 9(6), e1003272.

Jiang, R. H., Tyler, B. M., Whisson, S. C., Hardham, A. R. & Govers, F. (2006) Ancient origin of elicitin gene clusters in Phytophthora genomes. *Molecular Biology and Evolution*,

23(2), 338-351.

Joller, C., De Vrieze, M., Moradi, A., Fournier, C., Chinchilla, D., L'Haridon, F., Bruisson, S. & Weisskopf, L. (2020) S-methyl methanethiosulfonate: promising late blight inhibitor or broad range toxin? *Pathogens*, 9(6), 496.

Judelson, H. S. (2012) Dynamics and innovations within oomycete genomes: insights into biology, pathology, and evolution. *Eukaryotic Cell*, 11(11), 1304-1312.

Jung, T., Colquhoun, I. J. & Hardy, G. E. S. (2013) New insights into the survival strategy of the invasive soilborne pathogen Phytophthora cinnamomi in different natural ecosystems in Western Australia. *Forest Pathology*, 43(4), 266-288.

Kamilya, D. & Baruah, A. (2014) Epizootic ulcerative syndrome (EUS) in fish: history and current status of understanding. *Reviews in Fish Biology and Fisheries*, 24(1), 369-380.

Kamoun, S. (2006) A catalogue of the effector secretome of plant pathogenic oomycetes. *Annual Review of Phytopathology*, 44, 41-60.

Kamoun, S., Furzer, O., Jones, J. D., Judelson, H. S., Ali, G. S., Dalio, R. J., Roy, S. G., Schena, L., Zambounis, A., Panabières, F., Cahill, D., Ruocco, M., Figueiredo, A., Chen, X. R., Hulvey, J., Stam, R., Lamour, K., Gijzen, M., Tyler, B. M., Grünwald, N. J., Mukhtar, M. S., Tomé, D. F., Tör, M., Van Den Ackerveken, G., McDowell, J., Daayf, F., Fry, W. E., Lindqvist-Kreuze, H., Meijer, H. J., Petre, B., Ristaino, J., Yoshida, K., Birch, P. R. & Govers, F. (2015) The Top 10 oomycete pathogens in molecular plant pathology. *Molecular Plant Pathology*, 16(4), 413-434.

Kariuki, W., Mungai, N., Otaye, D., Thuita, M., Muema, E., Korir, H. & Masso, C. (2020) Antagonistic effects of biocontrol agents against Phytophthora infestans and growth stimulation in tomatoes. *African Crop Science Journal*, 28(s1), 55-70.

Kasuga, T., Kozanitas, M., Bui, M., Huberli, D., Rizzo, D. M. & Garbelotto, M. (2012) Phenotypic diversification is associated with host-induced transposon derepression in the sudden oak death pathogen Phytophthora ramorum. *Plos One*, 7(4).

Kathiravan, M. K., Salake, A. B., Chothe, A. S., Dudhe, P. B., Watode, R. P., Mukta, M. S. & Gadhwe, S. (2012) The biology and chemistry of antifungal agents: a review.

Bioorganic & Medicinal Chemistry, 20(19), 5678-5698.

Keen, N. & Legrand, M. (1980) Surface glycoproteins: evidence that they may function as the race specific phytoalexin elicitors of Phytophthora megasperma f. sp. glycinea. *Physiological Plant Pathology*, 17(2), 175-192.

Keller, F. A. & Cabib, E. (1971) Chitin and yeast budding: Properties of chitin synthetase from Saccharomyces Carlsbergensis. *Journal of Biological Chemistry*, 246(1), 160-166.

Kharel, A., Islam, M. T., Rookes, J. & Cahill, D. (2021) How to unravel the key functions of cryptic oomycete elicitin proteins and their role in plant disease. *Plants (Basel)*, 10(6), 1201.

Khatun, A., Farhana, T., Sabir, A. A., Islam, S. M. N., West, H. M., Rahman, M. & Islam, T. (2018) Pseudomonas and Burkholderia inhibit growth and asexual development of Phytophthora capsici. *Zeitschrift fuer Naturforschung C*, 73(3-4), 123-135.

King, M., Reeve, W., Van der Hoek, M. B., Williams, N., McComb, J., O'Brien, P. A. & Hardy, G. E. S. J. (2010) Defining the phosphite-regulated transcriptome of the plant pathogen Phytophthora cinnamomi. *Molecular Genetics and Genomics*, 284, 425-435.

Klemm, D., Heublein, B., Fink, H.-P. & Bohn, A. (2005) Cellulose: Fascinating Biopolymer and Sustainable Raw Material. *Angewandte Chemie International Edition*, 44(22), 3358-3393.

Klinter, S. (2021) Identification and characterisation of chitin and cellulose synthases in oomycetes : New tools for biochemical studies and structure determination (PhD dissertation, KTH Royal Institute of Technology).

Klinter, S., Bulone, V. & Arvestad, L. (2019) Diversity and evolution of chitin synthases in oomycetes (Straminipila: Oomycota). *Molecular Phylogenetics and Evolution*, 139, 106558.

Klis, F. M., Boorsma, A. & De Groot, P. W. (2006) Cell wall construction in Saccharomyces cerevisiae. *Yeast*, 23(3), 185-202

Klis, F. M., Mol, P., Hellingwerf, K. & Brul, S. (2002) Dynamics of cell wall structure in Saccharomyces cerevisiae. *FEMS Microbiology Reviews*, 26(3), 239-256.

Kong, L.-A., Yang, J., Li, G.-T., Qi, L.-L., Zhang, Y.-J., Wang, C.-F., Zhao, W.-S., Xu, J.-R.

& Peng, Y.-L. (2012) Different chitin synthase genes are required for various developmental and plant infection processes in the rice blast fungus Magnaporthe oryzae. *PLoS Pathogens*, 8(2), e1002526.

Kouzai, Y., Mochizuki, S., Saito, A., Ando, A., Minami, E. & Nishizawa, Y. (2012) Expression of a bacterial chitosanase in rice plants improves disease resistance to the rice blast fungus Magnaporthe oryzae. *Plant Cell Reports*, 31, 629-636.

Kuga, S., Takagi, S. & Brown, R. M. (1993) Native folded-chain cellulose II. *Polymer*, 34(15), 3293-3297.

Laing, S. & Deacon, J. (1991) Video microscopical comparison of mycoparasitism by Pythium oligandrum, P. nunn and an unnamed Pythium species. *Mycological Research*, 95(4), 469-479.

Lairson, L. L., Henrissat, B., Davies, G. J. & Withers, S. G. (2008) Glycosyltransferases: Structures, Functions, and Mechanisms. *Annual Review of Biochemistry*, 77(1), 521-555.

Latge, J. P. (2007) The cell wall: a carbohydrate armour for the fungal cell. *Molecular Microbiology*, 66(2), 279-290.

Lee, S.-C., Kim, S.-H., Hoffmeister, R. A., Yoon, M.-Y. & Kim, S.-K. (2019) Novel peptide-based inhibitors for microtubule polymerization in Phytophthora capsici. *International Journal of Molecular Sciences*, 20(11), 2641.

Leonard, G., Labarre, A., Milner, D. S., Monier, A., Soanes, D., Wideman, J. G., Maguire, F., Stevens, S., Sain, D., Grau-Bové, X., Sebé-Pedrós, A., Stajich, J. E., Paszkiewicz, K., Brown, M. W., Hall, N., Wickstead, B. & Richards, T. A. (2018) Comparative genomic analysis of the 'pseudofungus' Hyphochytrium catenoides. *Open Biology*, 8(1), 170184.

Lesage, G. & Bussey, H. (2006) Cell wall assembly in Saccharomyces cerevisiae. *Microbiology and Molecular Biology Reviews*, 70(2), 317-343.

Li, R., Xie, Z., Tian, Y., Yang, H., Chen, W., You, D., Liu, G., Deng, Z. & Tan, H. (2009) polR, a pathway-specific transcriptional regulatory gene, positively controls polyoxin biosynthesis in Streptomyces cacaoi subsp. asoensis. *Microbiology (Reading)*, 155(Pt

6), 1819-1831.

Li, T., Cai, M., Wang, W., Dai, T., Zhang, C., Zhang, B., Shen, J., Wang, Y. & Liu, X. (2022) PcCesA1 is involved in the polar growth, cellulose synthesis, and glycosidic linkage crosslinking in the cell wall of Phytophthora capsici. *International Journal of Biological Macromolecules*, 208, 720-730.

Liang, D., Andersen, C. B., Vetukuri, R. R., Dou, D. & Grenville-Briggs, L. J. (2020) Horizontal gene transfer and tandem duplication shape the unique CAZyme complement of the mycoparasitic oomycetes Pythium oligandrum and Pythium periplocum. *Frontiers in Microbiology*, 11, 581698.

Lipke, P. N. & Kurjan, J. (1992) Sexual agglutination in budding yeasts: structure, function, and regulation of adhesion glycoproteins. *Microbiological Reviews*, 56(1), 180-194.

Lipke, P. N. & Ovalle, R. (1998) Cell wall architecture in yeast: new structure and new challenges. *Journal of Bacteriology*, 180(15), 3735-3740.

Liu, D., Zehfroosh, N., Hancock, B. L., Hines, K., Fang, W., Kilfoil, M., Learned-Miller, E., Sanguinet, K. A., Goldner, L. S. & Baskin, T. I. (2017) Imaging cellulose synthase motility during primary cell wall synthesis in the grass Brachypodium distachyon. *Scientific Reports*, 7(1), 15111.

Loreto, É. S., Tondolo, J. S., Pilotto, M. B., Alves, S. H. & Santurio, J. M. (2014) New insights into the in vitro susceptibility of Pythium insidiosum. *Antimicrobial Agents and Chemotherapy*, 58(12), 7534-7537.

Mach, J. (2008) Cellulose synthesis in Phytophthora infestans pathogenesis. *The Plant Cell*, 20(3), 500-500.

Manners, D. J., Masson, A. J. & Patterson, J. C. (1973) The structure of a beta-(1 leads to 3)-D-glucan from yeast cell walls. *Biochemical Journal*, 135(1), 19-30.

Marakalala, M. J., Vautier, S., Potrykus, J., Walker, L. A., Shepardson, K. M., Hopke, A., Mora-Montes, H. M., Kerrigan, A., Netea, M. G. & Murray, G. I. (2013) Differential adaptation of Candida albicans in vivo modulates immune recognition by dectin-1. *PLoS Pathogens*, 9(4), e1003315.

Mcmurrough, I., Floresca.A & Bartnick.S (1971) Pathway of chitin synthesis and cellular

localization of chitin synthetase in Mucor Rouxii. *Journal of Biological Chemistry*, 246(12), 3999-4007.

Melida, H., Sandoval-Sierra, J. V., Dieguez-Uribeondo, J. & Bulone, V. (2013) Analyses of extracellular carbohydrates in oomycetes unveil the existence of three different cell wall types. *Eukaryotic Cell*, 12(2), 194-203.

Meyer, F. P. & Jorgenson, T. A. (1983) Teratological and other effects of malachite green on development of rainbow trout and rabbits. *Transactions of the American Fisheries Society*, 112(6), 818-824.

Mirzaee, M., Abbasi, M. & Mohammadi, M. (2009) Albugo candida causing white rust on Erysimum crassicaule in Iran. *Australasian Plant Disease Notes*, 4(1), 124-125.

Money, N. P. (2001) Biomechanics of invasive hyphal growth. *Biology of the Fungal Cell*, 3-17.

Money, N. P. (2008) Insights on the mechanics of hyphal growth. *Fungal Biology Reviews*, 22(2), 71-76.

Montesinos, E. (2007) Antimicrobial peptides and plant disease control. *FEMS Microbiology Letters*, 270(1), 1-11.

Moon, R. J., Martini, A., Nairn, J., Simonsen, J. & Youngblood, J. (2011) Cellulose nanomaterials review: structure, properties and nanocomposites. *Chemical Society Reviews*, 40(7), 3941-3994.

Mouyna, I., Fontaine, T., Vai, M., Monod, M., Fonzi, W. A., Diaquin, M., Popolo, L., Hartland, R. P. & Latgé, J. P. (2000) Glycosylphosphatidylinositol-anchored glucanosyltransferases play an active role in the biosynthesis of the fungal cell wall. *Journal of Biological Chemistry*, 275(20), 14882-14889.

Mueller, S. C. & Brown, R. M., Jr. (1980) Evidence for an intramembrane component associated with a cellulose microfibril-synthesizing complex in higher plants. *The Journal of Cell Biology*, 84(2), 315-326.

Muñoz, A., Chu, M., Marris, P. I., Sagaram, U. S., Kaur, J., Shah, D. M. & Read, N. D. (2014) Specific domains of plant defensins differentially disrupt colony initiation, cell fusion and calcium homeostasis in N eurospora crassa. *Molecular Microbiology*, 92(6), 1357-

1374.

Nasrollahzadeh, M., Soleimani, F., Nezafat, Z. Orooji, Y & Ahmadpoor, F. (2023) Facile synthesis of Cu nanoparticles supported on magnetic lignin-chitosan blend as a highly effective catalyst for the preparation of 5-aryl-1H-tetrazoles. *Biomass Conversion and Biorefinery*, 13, 12451–12465.

Nawrot, R., Barylski, J., Nowicki, G., Broniarczyk, J., Buchwald, W. & Goździcka-Józefiak, A. (2014) Plant antimicrobial peptides. *Folia Microbiologica*, 59(3), 181-196.

Nerva, L., Sandrini, M., Gambino, G. & Chitarra, W. (2020) Double-stranded RNAs (dsRNAs) as a sustainable tool against gray mold (Botrytis cinerea) in grapevine: Effectiveness of different application methods in an open-air environment. *Biomolecules*, 10(2), 200.

Novaes-Ledieu, M., Jiménez-Martínez, A. & Villanueva, J. R. (1967) Chemical composition of hyphal wall of Phycomycetes. *The Journal of General Microbiology*, 47(2), 237-245.

Odds, F. C., Brown, A. J. & Gow, N. A. (2003) Antifungal agents: mechanisms of action. *Trends in Microbiology*, 11(6), 272-279.

Odenbach, D., Thines, E., Anke, H. & Foster, A. J. (2009) The Magnaporthe grisea class VII chitin synthase is required for normal appressorial development and function. *Molecular Plant Pathology*, 10(1), 81-94.

Oliveira-Garcia, E. & Deising, H. B. (2013) Infection structure-specific expression of β-1,3-glucan synthase is essential for pathogenicity of Colletotrichum graminicola and evasion of β-glucan-triggered immunity in maize. *Plant Cell*, 25(6), 2356-2378.

Oliveira-Garcia, E. & Deising, H. B. (2016) Attenuation of PAMP-triggered immunity in maize requires down-regulation of the key β-1, 6-glucan synthesis genes KRE 5 and KRE 6 in biotrophic hyphae of Colletotrichum graminicola. *The Plant Journal*, 87(4), 355-375.

Oliveira Silva, A., Aliyeva-Schnorr, L., Wirsel, S. G. R. & Deising, H. B. (2022) Fungal pathogenesis-related cell wall biogenesis, with emphasis on the maize anthracnose fungus Colletotrichum graminicola. *Plants (Basel)*, 11(7).

Orlean, P. (2012) Architecture and biosynthesis of the Saccharomyces cerevisiae cell wall. *Genetics*, 192(3), 775-818.

Pang, Z., McKee, L. S., Srivastava, V., Klinter, S., Díaz-Moreno, S. M., Orlean, P., Liu, X. &

Bulone, V. (2020) Analysis of a cellulose synthase catalytic subunit from the oomycete pathogen of crops Phytophthora capsici. *Cellulose*, 27(15), 8551-8565.

Panth, M., Hassler, S. C. & Baysal-Gurel, F. (2020) Methods for management of soilborne diseases in crop production. *Agriculture*, 10(1), 16.

Papi, M., Palmieri, V., Bugli, F., De Spirito, M., Sanguinetti, M., Ciancico, C., Braidotti, M. C., Gentilini, S., Angelani, L. & Conti, C. (2016) Biomimetic antimicrobial cloak by graphene-oxide agar hydrogel. *Scientific Reports*, 6(1), 12.

Parisi, K., Shafee, T. M. A., Quimbar, P., van der Weerden, N. L., Bleackley, M. R. & Anderson, M. A. (2019) The evolution, function and mechanisms of action for plant defensins. *Seminars in Cell & Developmental Biology*, 88, 107-118.

Pelegrini, B., del Sarto, R., Silva, O., Franco, O. & Grosside-Sa, M. (2011) Antibacterial peptides from plants: what they are and how they probably work. *Biochemistry Research International*, 2011: 250349.

Pereira, D. I. B., Santurio, J. M., Alves, S. H., Argenta, J. S., Pötter, L., Spanamberg, A. & Ferreiro, L. (2007) Caspofungin in vitro and in vivo activity against Brazilian Pythium insidiosum strains isolated from animals. *Journal of Antimicrobial Chemotherapy*, 60(5), 1168-1171.

Perfect, J. R. (2017) The antifungal pipeline: a reality check. *Nature Reviews Drug Discovery*, 16(9), 603-616.

Permpalung, N., Worasilchai, N., Manothummetha, K., Torvorapanit, P., Ratanawongphaibul, K., Chuleerarux, N., Plongla, R. & Chindamporn, A. (2019) Clinical outcomes in ocular pythiosis patients treated with a combination therapy protocol in Thailand: a prospective study. *Medical Mycology*, 57(8), 923-928.

Permpalung, N., Worasilchai, N., Plongla, R., Upala, S., Sanguankeo, A., Paitoonpong, L., Mendoza, L. & Chindamporn, A. (2015) Treatment outcomes of surgery, antifungal therapy and immunotherapy in ocular and vascular human pythiosis: a retrospective study of 18 patients. *Journal of Antimicrobial Chemotherapy*, 70(6), 1885-1892.

Perrott, P. E. (1960) The ecology of some aquatic Phycomycetes. *Transactions of the British*

Mycological Society, 43(1), 19-30.

Persson, S., Paredez, A., Carroll, A., Palsdottir, H., Doblin, M., Poindexter, P., Khitrov, N., Auer, M. & Somerville, C. R. (2007) Genetic evidence for three unique components in primary cell-wall cellulose synthase complexes in Arabidopsis. *Proceedings of the National Academy of Sciences of the United States of America*, 104(39), 15566-15571.

Pfaller, M. A., Boyken, L., Hollis, R. J., Kroeger, J., Messer, S. A., Tendolkar, S. & Diekema, D. J. (2008) In vitro susceptibility of invasive isolates of Candida spp. to anidulafungin, caspofungin, and micafungin: six years of global surveillance. *Journal of Clinical Microbiology*, 46(1), 150-156.

Phillips, A. J., Anderson, V. L., Robertson, E. J., Secombes, C. J. & van West, P. (2008) New insights into animal pathogenic oomycetes. *Trends in Microbiology*, 16(1), 13-19.

Picard, K., Tirilly, Y. & Benhamou, N. (2000) Cytological effects of cellulases in the parasitism of Phytophthora parasitica by Pythium oligandrum. *Applied and Environmental Microbiology*, 66(10), 4305-4314.

Pilbeam, R. A., Howard, K., Shearer, B. L. & Hardy, G. E. S. J. (2011) Phosphite stimulated histological responses of Eucalyptus marginata to infection by Phytophthora cinnamomi. *Trees*, 25, 1121-1131.

Piotrowski, J. S., Okada, H., Lu, F., Li, S. C., Hinchman, L., Ranjan, A., Smith, D. L., Higbee, A. J., Ulbrich, A., Coon, J. J., Deshpande, R., Bukhman, Y. V., McIlwain, S., Ong, I. M., Myers, C. L., Boone, C., Landick, R., Ralph, J., Kabbage, M. & Ohya, Y. (2015) Plant-derived antifungal agent poacic acid targets β-1,3-glucan. *The Proceedings of the National Academy of Sciences*, 112(12), E1490-E1497.

Ploetz, R. C. (2013) *Phytophthora root rot of Avocado*, CABI International.

Qiao, L., Lan, C., Capriotti, L., Ah-Fong, A., Nino Sanchez, J., Hamby, R., Heller, J., Zhao, H., Glass, N. L. & Judelson, H. S. (2021) Spray-induced gene silencing for disease control is dependent on the efficiency of pathogen RNA uptake. *Plant Biotechnology Journal*, 19(9), 1756-1768.

Rajinipriya, M., Nagalakshmaiah, M., Robert, M. & Elkoun, S. (2018) Importance of agricultural and industrial waste in the field of nanocellulose and recent industrial developments of wood based nanocellulose: A review. *ACS Sustainable Chemistry &*

Engineering, 6(3), 2807-2828.

Ramamoorthy, V., Cahoon, E. B., Li, J., Thokala, M., Minto, R. E. & Shah, D. M. (2007) Glucosylceramide synthase is essential for alfalfa defensin-mediated growth inhibition but not for pathogenicity of Fusarium graminearum. *Molecular Microbiology*, 66(3), 771-786.

Reiskind, J. B. & Mullins, J. (1981) Molecular architecture of the hyphal wall of Achlya ambisexualis Raper. II. Ultrastructural analyses and a proposed model. *Canadian Journal of Microbiology*, 27(10), 1100-1105.

Reynolds, T. B. & Fink, G. R. (2001) Bakers' yeast, a model for fungal biofilm formation. *Science*, 291(5505), 878-881.

Ristaino, J. B., Hord, M. J. & Gumpertz, M. L. (1992) Population densities of Phytophthora capsici in field soils in relation to drip irrigation, rainfall, and disease incidence. *Plant Disease*, 76(10), 1017-1024.

Roemer, T., Paravicini, G., Payton, M. A. & Bussey, H. (1994) Characterization of the yeast (1-->6)-beta-glucan biosynthetic components, Kre6p and Skn1p, and genetic interactions between the PKC1 pathway and extracellular matrix assembly. *Journal of Cell Biology*, 127(2), 567-79.

Rouhier, P., Bruneteau, M. & Michel, G. (1995) Structural analysis on β-d-Glucans from Phytophthora capsici. *Journal of Carbohydrate Chemistry*, 14(2), 247-254.

Rzeszutek, E., Díaz-Moreno, S. M. & Bulone, V. (2019) Identification and characterization of the chitin synthase genes from the fish pathogen Saprolegnia parasitica. *Frontiers in Microbiology*, 10(2873).

Satish, S., Jiménez-Ortigosa, C., Zhao, Y., Lee, M. H., Dolgov, E., Krüger, T., Park, S., Denning, D. W., Kniemeyer, O. & Brakhage, A. A. (2019) Stress-induced changes in the lipid microenvironment of β-(1, 3)-d-glucan synthase cause clinically important echinocandin resistance in Aspergillus fumigatus. *MBio*, 10(3), e00779-19.

Savage, E., Clayton, C., Hunter, J., Brenneman, J., Laviola, C. & Gallegly, M. (1968) Homothallism, heterothallism, and interspecific hybridization in the genus.

Phytophthora. *Phytopathology*, 58(7), 1004-1021.

Saxena, I. M., Brown, R. M., Jr., Fevre, M., Geremia, R. A. & Henrissat, B. (1995) Multidomain architecture of beta-glycosyl transferases: implications for mechanism of action. *Journal of Bacteriology*, 177(6), 1419-1424.

Sburlati, A. & Cabib, E. (1986) Chitin synthetase-2, a presumptive participant in septum formation in Saccharomyces-Cerevisiae. *Journal of Biological Chemistry*, 261(32), 5147-5152.

Sharma, S., Sundaresha, S. & Bhardwaj, V. (2021) Biotechnological approaches in management of oomycetes diseases. *3 Biotech*, 11(6), 274.

Shaw, J. A., Mol, P. C., Bowers, B., Silverman, S. J., Valdivieso, M. H., Durán, A. & Cabib, E. (1991) The function of chitin synthases 2 and 3 in the Saccharomyces cerevisiae cell cycle. *The Journal of Cell Biology*, 114(1), 111-123.

Shearer, B. L. , Crane, C. E. & Cochrane, A. (2004) Quantification of the susceptibility of the native flora of the South-West Botanical Province, Western Australia, to Phytophthora cinnamomi. *Australian Journal of Botany*, 52(4), 435-443.

Shematek, E. M., Braatz, J. A. & Cabib, E. (1980) Biosynthesis of the yeast cell wall: I. Preparation and properties of β-(1→3)glucan synthetase. *Journal of Biological Chemistry*, 255(3), 888-894.

Sietsma, J., Eveleigh, D. & Haskins, R. (1969) Cell wall composition and protoplast formation of some oomycete species. *Biochimica et Biophysica Acta (BBA)-General Subjects*, 184(2), 306-317.

Sietsma, J. H., Child, J. J., Nesbitt, L. R. & Haskins, R. H. (1975) Chemistry and ultrastructure of the hyphal walls of Pythium Acanthicum. *Microbiology*, 86(1), 29-38.

Sisson, W. A. (1938) The existence of mercerized cellulose and its orientation in halicystis as indicated by x-ray diffraction analysis. *Science*, 87(2259), 350.

Solis, J., Medrano, G. & Ghislain, M. (2007) Inhibitory effect of a defensin gene from the Andean crop maca (Lepidium meyenii) against Phytophthora infestans. *Journal of Plant Physiology*, 164(8), 1071-1082.

Somerville, C. (2006) Cellulose synthesis in higher plants. *Annual Review of Cell and*

Developmental Biology, 22, 53-78.

Song, J. C. & Stevens, D. A. (2016) Caspofungin: Pharmacodynamics, pharmacokinetics, clinical uses and treatment outcomes. *Critical Reviews in Microbiology*, 42(5), 813-846.

Souza, A. C. O. & Amaral, A. C. (2017) Antifungal therapy for systemic mycosis and the nanobiotechnology era: Improving efficacy, biodistribution and toxicity. *Frontiers in Microbiology*, 8.

Sparrow, F. & Ellison, B. (1949) Olpidiopsis Schenkiana and its hyperparasite Ectrogella Besseyi N. Sp. *Mycologia*, 41(1), 28-35

Sparrow, F. K. (1960) Aguatic phycomycetes. *AIBS Bulletin*, 10(6), 40.

Spelbrink, R. G., Dilmac, N., Allen, A., Smith, T. J., Shah, D. M. & Hockerman, G. H. (2004) Differential antifungal and calcium channel-blocking activity among structurally related plant defensins. *Plant Physiology*, 135(4), 2055-2067.

Srivastava, S., Sinha, R. & Roy, D. (2004) Toxicological effects of malachite green. *Aquatic Toxicology*, 66(3), 319-329.

Stenberg, J. A., Sundh, I., Becher, P. G., Björkman, C., Dubey, M., Egan, P. A., Friberg, H., Gil, J. F., Jensen, D. F. & Jonsson, M. (2021) When is it biological control? A framework of definitions, mechanisms, and classifications. *Journal of Pest Science*, 94(3), 665-676.

Stephan, D., Schmitt, A., Carvalho, S. M., Seddon, B. & Koch, E. (2005) Evaluation of biocontrol preparations and plant extracts for the control of Phytophthora infestans on potato leaves. *European Journal of Plant Pathology*, 112, 235-246.

Susaengrat, N., Torvorapanit, P., Plongla, R., Chuleerarux, N., Manothummetha, K., Tuangsirisup, J., Worasilchai, N., Chindamporn, A. & Permpalung, N. (2019) Adjunctive antibacterial agents as a salvage therapy in relapsed vascular pythiosis patients. *International Journal of Infectious Diseases*, 88, 27-30

Syndrome, E. U. (1998) Technical Handbook. *Bangkok. The Aquatic*.

Taj, M., Sajjad, M., Li, M., Yasmeen, A., Mubarik, M. S., Kaniganti, S. & He, C. (2022) Potential targets for CRISPR/Cas knockdowns to enhance genetic resistance against

some diseases in wheat (*Triticum aestivum* L.). *Frontiers in Genetics*, 13, 926955.

Taylor, A. S. & Cook, D. C. (2018) An economic assessment of the impact on the Western Australian viticulture industry from the incursion of grapevine downy mildew. *Journal of Plant Diseases and Protection*, 125(4), 397-403.

Teunissen, A. & Steensma, H. (1995) the dominant flocculation genes of Saccharomyces cerevisiae constitute a new subtelomeric gene family. *Yeast*, 11(11), 1001-1013.

Thevissen, K., de Mello Tavares, P., Xu, D., Blankenship, J., Vandenbosch, D., Idkowiak-Baldys, J., Govaert, G., Bink, A., Rozental, S. & De Groot, P. W. (2012) The plant defensin RsAFP2 induces cell wall stress, septin mislocalization and accumulation of ceramides in Candida albicans. *Molecular Microbiology*, 84(1), 166-180

Thines, M. (2018) Oomycetes. *Current Biology*, 28(15), R812-R813.

Tokunaga, J. & Bartnicki-Garcia, S. (1971) Structure and differentiation of the cell wall of Phytophthora palmivora: Cysts, hyphae and sporangia. *Archives of Microbiology*, 79(4), 293-310.

Tondolo, J. S. M., Ledur, P. C., Loreto, É. S., Verdi, C. M., Bitencourt, P. E. R., de Jesus, F. P. K., Rocha, J. P., Alves, S. H., Sassaki, G. L. & Santurio, J. M. (2017) Extraction, characterization and biological activity of a (1,3)(1,6)-β-d-glucan from the pathogenic oomycete Pythium insidiosum. *Carbohydrate Polymers*, 157, 719-727.

Torto-Alalibo, T., Tian, M., Gajendran, K., Waugh, M. E., Van West, P. & Kamoun, S. (2005) Expressed sequence tags from the oomycete fish pathogen *Saprolegnia parasitica* reveal putative virulence factors. *Bmc Microbiology*, 5(1), 1-13.

Tsirigoti, A., Kuepper, F. C., Gachon, C. M. & Katsaros, C. (2013) Filamentous brown algae infected by the marine, holocarpic oomycete Eurychasma dicksonii: first results on the organization and the role of cytoskeleton in both host and parasite. *Plant Signaling and Behavior*, 8(11), e26367.

Tsui, C. K., Marshall, W., Yokoyama, R., Honda, D., Lippmeier, J. C., Craven, K. D., Peterson, P. D. & Berbee, M. L. (2009) Labyrinthulomycetes phylogeny and its implications for the evolutionary loss of chloroplasts and gain of ectoplasmic gliding. *Molecular*

Phylogenetics and Evolution, 50(1), 129-140.

Tyler, B. M. (2007) Phytophthora sojae: root rot pathogen of soybean and model oomycete. *Molecular Plant Pathology*, 8(1), 1-8.

Ulaganathan, K., Goud, B. S., Reddy, M. M., Kumar, V. P., Balsingh, J. & Radhakrishna, S. (2015) Proteins for breaking barriers in lignocellulosic bioethanol production. *Current Protein & Peptide Science*, 16(2), 100-134.

Valdivia, R. H. & Schekman, R. (2003) The yeasts Rho1p and Pkc1p regulate the transport of chitin synthase III (Chs3p) from internal stores to the plasma membrane. *Proceedings of the National Academy of Sciences*, 100(18), 10287-10292.

Van Der Weerden, N. L., Lay, F. T. & Anderson, M. A. (2008) The plant defensin, NaD1, enters the cytoplasm of Fusarium oxysporum hyphae. *Journal of Biological Chemistry*, 283(21), 14445-14452.

Wada, M., Heux, L. & Sugiyama, J. (2004) Polymorphism of cellulose I family: Reinvestigation of cellulose IVI. *Biomacromolecules*, 5(4), 1385-1391.

Waldmüller, T., Cosio, E. G., Grisebach, H. & Ebel, J. (1992) Release of highly elicitor-active glucans by germinating zoospores of Phytophthora megasperma f. sp. glycinea. *Planta*, 188(4), 498-505.

Walker, C. A. & van West, P. (2007) Zoospore development in the oomycetes. *Fungal biology reviews*, 21(1), 10-18.

Walker, L. A., Gow, N. A. & Munro, C. A. (2010) Fungal echinocandin resistance. *Fungal Genetics and Biology*, 47(2), 117-126.

Wang, P., Wang, L., Guo, J., Yang, W. & Shen, H. (2016) Molecular mapping of a gene conferring resistance to Phytophthora capsici Leonian race 2 in pepper line PI201234 (Capsicum annuum L.). *Molecular Breeding*, 36, 1-11.

Weber, I., Aßmann, D., Thines, E. & Steinberg, G. (2005) Polar localizing class v myosin chitin synthases are essential during early plant infection in the plant pathogenic fungus Ustilago maydis. *The Plant Cell*, 18(1), 225-242.

Whetzel, H. (1929) The terminology of phytopathology. *Proceedings of the International*

Congress of Plant Sciences, 2, 1204-1215.

Whitten, M. M. (2019) Novel RNAi delivery systems in the control of medical and veterinary pests. *Current Research in Insect Science*, 34, 1-6.

Wijayawardene, N. N., Hyde, K. D., Al-Ani, L. K. T., Tedersoo, L., Haelewaters, D., Rajeshkumar, K. C., *et al*. (2020) Outline of fungi and fungus-like taxa. *Mycosphere*, 11(1).

Wong, H. C., Fear, A. L., Calhoon, R. D., Eichinger, G. H., Mayer, R., Amikam, D., Benziman, M., Gelfand, D. H., Meade, J. H. & Emerick, A. W. (1990) Genetic organization of the cellulose synthase operon in Acetobacter xylinum. *Proceedings of the National Academy of Sciences*, 87(20), 8130-8134.

Worasilchai, N., Permpalung, N., Chongsathidkiet, P., Leelahavanichkul, A., Mendoza, A. L., Palaga, T., Reantragoon, R., Finkelman, M., Sutcharitchan, P. & Chindamporn, A. (2018) Monitoring anti-Pythium insidiosum IgG Antibodies and (1→ 3)-β-d-Glucan in vascular pythiosis. *Journal of Clinical Microbiology*, 56(8), e00610-18.

Wu, X.-Z., Chang, W.-Q., Cheng, A.-X., Sun, L.-M. & Lou, H.-X. (2010) Plagiochin E, an antifungal active macrocyclic bis (bibenzyl), induced apoptosis in Candida albicans through a metacaspase-dependent apoptotic pathway. *Biochimica et Biophysica Acta (BBA)-General Subjects*, 1800(4), 439-447.

Wu, X.-z., Cheng, A.-x., Sun, L.-m. & Lou, H.-x. (2008) Effect of plagiochin E, an antifungal macrocyclic bis (bibenzyl), on cell wall chitin synthesis in Candida albicans. *Acta Pharmacologica Sinica*, 29(12), 1478-1485.

Xie, X. & Lipke, P. N. (2010) On the evolution of fungal and yeast cell walls. *Yeast*, 27(8), 479-488.

Yang, X., Tyler, B. M. & Hong, C. X. (2017) An expanded phylogeny for the genus Phytophthora. *Ima Fungus*, 8(2), 355-384.

Yolanda, H. & Krajaejun, T. (2020) Review of methods and antimicrobial agents for susceptibility testing against Pythium insidiosum. *Heliyon*, 6(4), e03737.

Zainal, Z., Marouf, E., Ismail, I. & Fei, C. K. (2009) Expression of the Capsicuum annum (Chili) defensin gene in transgenic tomatoes confers enhanced resistance to fungal

pathogens. *American Journal of Plant Physiology*, 4(2), 70-79Zanette, R., Jesus, F., Pilotto, M., Weiblen, C., Pötter, L., Ferreiro, L., Alves, S. & Santurio, J. (2015) Micafungin alone and in combination therapy with deferasirox against Pythium insidiosum. *Journal de Mycologie Medicale*, 25(1), 91-94.

Zeković, D. B., Kwiatkowski, S., Vrvić, M. M., Jakovljević, D. & Moran, C. A. (2005) Natural and modified (1→ 3)-β-D-glucans in health promotion and disease alleviation. *Critical Reviews in Biotechnology*, 25(4), 205-230.

Zevenhuizen, L. & Bartnicki-Garcia, S. (1969) Structure of the insoluble hyphal wall glucan of Phytophthora cinnamomi. *Biochemistry*, 8(4), 1496-1502.

Zhong, R. & Ye, Z.-H. (2014) Secondary cell walls: Biosynthesis, patterned deposition and transcriptional regulation. *Plant and Cell Physiology*, 56(2), 195-214.

Zhu, Y. J., Agbayani, R. & Moore, P. H. (2007) Ectopic expression of Dahlia merckii defensin DmAMP1 improves papaya resistance to Phytophthora palmivora by reducing pathogen vigor. *Planta*, 226(1), 87-97.

Chapter 2

The plant defensin NaD1 inhibits the growth of *Phytophthora* species by interfering with cell wall structure and calcium transport

Statement of Authorship

Title of Paper	**The plant defensin NaD1 inhibits the growth of *Phytophthora* species by interfering with cell wall structure and calcium transport**
Publication status	Unpublished and unsubmitted work written in manuscript style

Principal Author

Name of Principal Author	Amena Khatun		
Contribution to the Paper	Designed and performed the experiments, Analysed and interpreted the results, performed bioinformatic analyses, and wrote the manuscript.		
Overall percentage (%)	80%		
Certification	This paper reports on original research I conducted during the period of my Higher Degree by Research candidature and is not subject to any obligations or contractual agreements with a third party that would constrain its inclusion in this thesis. I am the primary author of this paper.		
Signature		Date	29/06/2023

Co-author Contributions

By signing the Statement of Authorship, each author certifies that:

i. The candidate's stated contribution to the publication is accurate (as detailed above),
ii. Permission is granted for the candidate in include the publication in the thesis, and
iii. The sum of all co-author contributions is equal to 100% less the candidate's stated contribution.

Name of Co-Author	Caterina Selva		
Contribution to the paper	Helped in cell wall preparation, guided primers design, and reviewed the manuscript. I hereby certify that the Statement of Authorship is accurate.		
Signature		Date	29/06/2023

Name of Co-Author	Julian Schwerdt		
Contribution to the paper	Conducted RNA-Seq data analyses, helped in bioinformatic analyses for gene prediction and reviewed the manuscript. I hereby certify that the Statement of Authorship is accurate.		
Signature		Date	29/06/2023

Name of Co-Author	Natalie Betts		
Contribution to the paper	Helped in primer design at the early stages of the PhD, and also gene expression analysis by qRT-PCR and RNA extraction. I hereby certify that the Statement of Authorship is accurate.		
Signature		Date	29/06/2023

Name of Co-Author	Long Yu		
Contribution to the paper	Helped in cell wall analysis by using GC-MS and HPLC and reviewed the manuscript. I hereby certify that the Statement of Authorship is accurate.		
Signature		Date	29/06/2023

Name of Co-Author	Vincent Bulone		
Contribution to the paper	Conceived the project, designed experiments, revised and edited the manuscript; corresponding author. I hereby certify that the Statement of Authorship is accurate.		
Signature		Date	29/06/2023

The plant defensin NaD1 inhibits the growth of *Phytophthora* species by interfering with cell wall structure and calcium transport

Amena Khatun, Caterina Selva[§], Julian Schwerdt[§], Natalie Betts, Long Yu[§] and Vincent Bulone[§,*]

School of Agriculture, Food and Wine, The University of Adelaide, Waite Campus, Urrbrae, South Australia 5064, Australia

[§]Present address: *College of Medicine and Public Health, Flinders University, Bedford Park South Australia 5042, South Australia, Australia*

[*]*To whom correspondence should be addressed: vincent.bulone@flinders.edu.au*

Abstract

The *Nicotiana alata* Defensin 1 (NaD1) antimicrobial peptide has demonstrated antifungal activity but its mode of action in oomycetes remains unknown. Here we investigated whether NaD1 exerts a similar inhibitory activity against phytopathogenic oomycetes and combined multiple approaches to shed light on its mechanism of action. The effect of NaD1 was tested against four different *Phytophthora* species, with further focus on *Phytophthora cinnamomi*. Exposure to the peptide led to cytoplasmic granulation, hyper-branching, and suppression of apical dominance. Scanning and transmission electron microscopy revealed changes in cell wall thickness and morphology, while glycosidic linkage analysis revealed a difference in cellulose content, suggesting an altered cell wall composition and ultrastructure in NaD1-treated hyphae. In fungi, hyper-branching and suppression of apical dominance are linked to disrupted Ca^{2+} channel activity. Interestingly, our data show that the NaD1-induced inhibition of hyphal growth in *P. cinnamomi* is rescued by addition of extracellular Ca^{2+}, while K^+ and Na^+ were ineffective. In addition, analysis of cytosolic Ca^{2+} by fluorescence microscopy using Fluo-3-AM revealed a disruption in calcium homeostasis by NaD1. Results from RNA sequencing experiments were consistent with this observation, showing a decreased expression of genes encoding cellulose synthase and Ca^{2+} transport proteins in treated hyphae. Our data suggest that NaD1 inhibits the growth of *Phytophthora* species by interfering with intracellular Ca^{2+} homeostasis and by modifying cell wall biosynthesis and properties. This information can be exploited to develop new successful control strategy.

Keywords: Antimicrobial peptides; calcium transport; cell wall; defensin; hyphal growth; oomycetes; *Phytophthora*.

Introduction

The oomycetes are a class of Heterokonts morphologically and ecologically analogous to the fungi. They have colonised every continent on the planet as saprotrophs and obligate biotrophs (Yang, 2017). Terrestrial oomycetes are primarily parasites of vascular plants and comprise many devastating pathogens including causative agents of common root rot, or foliar diseases such as downy mildew, stem rot, and leaf blight (Derevnina *et al.*, 2016). The most well-known terrestrial genus is *Phytophthora* ("plant destroyer"), discovered through the investigation of the catastrophic European potato blight of the 1840s, which contains ~142 species (Kamoun, 2006; Kasuga *et al.*, 2012). Globally, the economic cost to agriculture due to *Phytophthora* infections is estimated to be USD ~7 billion per annum (Derevnina *et al.*, 2016; Fisher *et al.*, 2012; Haverkort *et al.*, 2008). However, aggressive and invasive *Phytophthora* species also present a significant danger to natural ecosystems (Hansen *et al.*, 2012; Judelson, 2012; Jung *et al.*, 2013; Yang *et al.*, 2017). Illustrative of this threat is *Phytophthora cinnamomi,* a species that infects a large diversity of crops, including cultivated fruit and vegetables, and ~5000 woody tree species worldwide (Kamoun *et al.*, 2015). In Australia, more than 2500 native plant species are susceptible to this soil-borne pathogen (Hardham, 2005). Understanding the biology of *Phytophthora* is of high importance for the management of biodiversity and ecological stability (Wilson *et al*., 2020).

With these economic and ecological impacts in mind, numerous studies conducted over the last decades have detailed the mechanisms that have underpinned the extraordinary expansion of oomycetes, especially their strategies to overcome host resistance. These include a malleable mating system through sexual and interspecific hybridization; an enhanced fitness through production of larger population; variations in ploidy to enhance vigour and pathogenicity; and the use of effectors to mitigate plant defense responses (Bozkurt *et al.*, 2012; McDonald & Linde, 2002; Schornack *et al.*, 2009; Thines, 2014). Anti-infective strategies have emerged from these studies. However, given the paucity of resistance genes in hosts of invasive *Phytophthora,* implementing breeding and transgenic programmes is complex, costly and laborious (Ramalingam *et al*., 2020; Vega-Arreguín *et al*. 2017). Chemical pesticides have had impact in reducing yield losses due to *Phytophthora*, but several have been banned because of their detrimental effects on human health and the environment (Cabras & Angioni, 2000; Nicolopoulou-Stamati *et al.*, 2016). Accordingly, there is currently a strong incentive to

develop novel, sustainable and targeted methods to control *Phytophthora*. In recent years, plant antimicrobial peptides (AMPs) have been the focus of several research groups for their inhibitory activity against the growth of a wide range of pathogenic fungi (Hayes *et al.*, 2013; Lay & Anderson, 2005; Poon *et al.*, 2014). But how efficacious AMPs are against challenging *Phytophthora* infectious species remains unknown.

AMPs are a structurally diverse class of bioactive compounds deployed by many organisms as central components of their innate immunity (Bulet *et al*., 2004; Koehback and Craik, 2019). Defensins are among the largest AMP families. Typically 45–54 amino acid residues long, they are non-toxic to plant cells and can be rapidly marshalled at infection sites (Stotz *et al.*, 2009), or in response to environmental stress (Lay *et al.*, 2003). Understanding the biochemistry of plant defensins is a significant undertaking given their broad range of activities, which include binding to specific lipids to induce anti-fungal activities; conferral of heavy metal tolerance; synthesis of reactive oxygen species; and membrane permeabilisation (Parisi *et al*., 2019). Several models have been proposed, e.g., carpet and toroidal pore models, to describe how defensins interact with the negatively charged plasma membrane (Brogden, 2005). The increase in cell permeability subsequent to alteration of the stability of the plasma membrane is known to cause cell leakage and death (Teixeira *et al.*, 2012). *Nicotiana alata* Defensin (NaD1) is a defensin synthesised by ornamental tobacco to protect its reproductive organs from diverse pathogenic fungi. It is active against a diversity of fungal species not limited to plant pathogens, e.g., *Botrytis cinerea*, *Candida albicans*, *Aspergillus niger*, *Saccharomyces cerevisiae* and *Fusarium oxysporum* (Hayes *et al.*, 2013; Lay *et al.*, 2003; Lay & Anderson, 2005; Poon *et al.*, 2014; van der Weerden *et al.*, 2008). NaD1 activity involves binding to the fungal cell surface, followed by membrane permeabilization and cell death through induced oxidative damage (Hayes *et al.*, 2013). Evidence also exists that NaD1 interacts with the membrane by binding to phosphatidic acid (Järvå *et al.*, 2018). Furthermore, NaD1 has been shown to exert its anti-fungal activity through the inhibition of the high-osmolarity glycerol (HOG) pathway (Hayes *et al.*, 2013; Tam *et al.*, 2015).

The wide range of targets and broad activities of NaD1 highlights its remarkable potential as a therapeutic tool. As yet, no study has determined whether NaD1 exhibits an inhibitory effect on oomycetes. Here, we investigated the effect of NaD1 on *Phytophthora* species and gained knowledge into its probable mechanism of action. We demonstrate that NaD1 arrests hyphal growth and sporangia development, modifies cell wall composition and biosynthesis, destabilises calcium homeostasis, suppresses apical dominance, and affects intracellular

organelles in *P. cinnamomi*. RNA-Seq results revealed that NaD1 significantly affects the expression of calcium transport and cellulose biosynthesis genes. In addition, retarded hyphal growth and suppression of apical dominance were observed in three other *Phytophthora* species, *P. cambivora*, *P. nicotianae*, and *P. citricola*, which suggests broad activity against the *Phytophthora* genus and provides a foundation for the development of a *Phytophthora* control strategy.

Materials and Methods

Source and cultures of *Phytophthora* species

Phytophthora cinnamomi (DAR 77502), *P. citricola* (DAR 64697), *P. cambivora* (DAR 67503), and *P. nicotianae* (DAR 63044) strains were purchased from the Plant Pathology & Mycology Herbarium in New South Wales, Australia. All species were maintained on potato dextrose agar (PDA), V8-agar, or pea broth agar (PBA) at 25°C in the dark. Cultures for experimental work were prepared by placing seven-day-old mycelial plugs at the centre of Petri dishes containing V8-agar medium and sterilized poppy seeds distributed over the surface of the Petri dishes. After 5 days of culture at 25°C in the dark, each poppy seed covered with mycelium was transferred into a well of 24-well plates (Corning Inc., AZ, USA) containing 500 µl of potato dextrose broth (PDB). The plates were used for diverse experiments, as described in the following sections.

NaD1 treatment

The NaD1 peptide used in our work was a generous gift from Professor Marilyn Anderson (La Trove University, Australia). For NaD1 treatment, individual wells of 24-well plates prepared as described above were supplemented with 1.625, 3.125, 6.25, 12.5, 25, 50, 75, 80 and 100 µM NaD1 dissolved in water. The selection of the dose range was based on a prior study conducted on *Candida albicans* (Hayes *et al*., 2018). A control was performed in the same conditions in the absence of NaD1. The inhibitory activity of NaD1 on the growth of all 4 *Phytophthora* strains was quantified as described by Reyes-Chilpa *et al*. (1997) after 48 h of incubation, using 3 replicates for each concentration of NaD1 and the following formula:

$$\% \text{ Inhibition} = (A - B) / A \times 100$$

where, A is the colony diameter in the control performed in the absence of NaD1 (expressed in cm), and B is the colony diameter measured in the presence of NaD1. Morphological alterations were observed using an Olympus ix70 inverted microscope. Based on the results obtained from these assays, 50 µM NaD1 was selected as the optimal concentration providing significant

inhibition (percent growth inhibition >70%), but not preventing growth, for all other experiments.

Effect of NaD1 on the formation of sporangia

Poppy seeds covered with mycelium from *P. cinnamomi* were incubated in the dark for three days at 25 °C in wells of 24-well plates containing 500 µl sterilized Milli-Q water in the absence (control) and presence of 50 µM NaD1 (Corning Inc, US). The mycelium in each cell was washed three times with water, transferred to new wells containing 500 µl sterilized Milli-Q water and incubated for three more days. The presence of sporangia was assessed three biological replicates using an Olympus ix70 inverted microscope.

Scanning (SEM) and Transmission (TEM) Electron Microscopy

Mycelial cells were collected from the periphery of colonies and fixed for 24 h in 2.5% (v/v) glutaraldehyde, 4% sucrose and 4% formaldehyde (Solarbio, Beijing, China). Samples for TEM were stained in 2% osmium tetroxide for 2 h at room temperature and pre-embedded in 1% agarose. The agarose blocks and the samples for SEM were subsequently dehydrated in 5 consecutive steps of 30 min each using a series of aqueous ethanol solutions (30%, 50%, 70%, 80%, 90%, v/v). The 90% ethanol solution was then replaced with a 1:1 mixture of ethanol:propylene oxide and the samples were incubated for 30 min in this solution, followed by 1 h incubation in 100% propylene oxide (ProScieTech C156). A Leica EM CPD300 critical point dryer was used to dry the SEM samples, which were subsequently coated with ultra-thin carbon and observed using a FEI ESEM Quanta 450 FEG microscope. SEM images were recorded from two biological replicates. After dehydration, the TEM agarose blocks were embedded in 100% Procure Araldite resin (ProScieTech, Australia) and polymerization was carried out for 24 h in a 60°C oven. The resin blocks were sectioned using a Leica UC6 ultramicrotome fitted with a diamond knife to obtain slices of 70-80 nm, which were deposited on carbon-coated TEM grids and observed with a FEI Tecnai G2 Spirit TEM microscope.

Preparation and fractionation of cell wall polysaccharides

Four biological replicates of the control and NaD1-treated mycelia from *P. cinnamomi* were collected after 48 h of growth and used for cell wall preparation as described earlier (Mélida *et al.*, 2013). Briefly, the samples were snap-frozen and ground in liquid nitrogen using a mortar and pestle. The resulting powder was extracted at room temperature under constant agitation using 70% (v/v) ethanol for 6, 8, and 12 h, and the ethanol-insoluble material was recovered by centrifugation at 4,000 × g for 10 min at 4°C. The pellets were resuspended in 70% ethanol and

filtered through glass-fiber filters (GF/A; Whatman), washed 6 times with 70% ethanol, 6 times with acetone and kept overnight in a fume hood at room temperature to dry completely. The dried cell walls were fractionated into an alkali-soluble fraction (ASF) and an alkali-insoluble fraction (AIF) (Mélida *et al.*, 2013). For this purpose, 50 mg of dried cell walls was mixed with 15 ml of 80% (vol/vol) methanol containing 5% (wt/vol) KOH and 0.1% (wt/vol) $NaBH_4$, and the samples were heated for 15 min at 100°C. After cooling, the ASF and AIF fractions were collected by centrifugation at 4,000 × g for 10 min and the extraction step in methanolic KOH was repeated three times. The AIF material was washed three times with 0.5 M acetic acid to neutralize the excess of KOH. The first wash was added to the ASF solution and the pH was adjusted to 6 with glacial acetic acid. The AIF and ASF solutions were dialyzed (SnakeSkin™ Dialysis Tubing, 3.5K MWCO, 22 mm) against Milli-Q water, freeze-dried and stored in a desiccator prior to monosaccharide and glycosidic linkage analyses.

Monosaccharide and glycosidic analysis

Monosaccharide analysis was performed as described by Comino *et al*. (2013), with some modifications. The freeze-dried ASF and AIF samples (1-2 mg) from the four independent biological replicates were hydrolysed with 2 M trifluoroacetic acid (TFA) at 121°C for 3 h. The TFA-resistant materials from each sample were further hydrolysed with 6 N HCl at 100°C for 16 h, and the resulting solution was dried in a centrifugal vacuum concentrator (Melida *et al*., 2013). For each sample, TFA and HCL aliquots were diluted 20 times with distilled water and derivatized with 1-phenyl-3-methyl-5-pyrazolone (PMP). Ten µL of 0.5 mM 2-deoxy glucose was added to each sample as an internal standard. The derivatized monosaccharides were separated using an Agilent 1200 high performance liquid chromatography (HPLC) fitted with a Phenomenex Kinetex C18 column (2.6 µm C18 100 × 3 mm 100Å). Ten microlitres of each sample were injected and the separation was carried out at 30 °C using a gradient of eluents A (10% acetonitrile, 40 mM ammonium acetate pH ~6.8) and B (70% acetonitrile) at a flow rate of 0.8 mL/min. The elution gradient was 8 to 16% B over 12 min and the derivatized monosaccharides were detected at 250 nm. The molar percentage of each monosaccharide in the samples was calculated based on standard curves obtained from solutions of the following reference monosaccharides: mannose, ribose, rhamnose, glucosamine, glucuronic acid, galacturonic acid, glucose, galactose, xylose, arabinose, and fructose.

Glycosidic linkage analysis was performed as described earlier (Pettolino *et al.*, 2012) on the ASF and AIF fractions from three biological replicates of the control and NaD1-treated mycelia. The freeze dried ASF and AIF materials (0.5 mg) were suspended in 200 µl of dry dimethyl

sulfoxide (DMSO) to pre-swell the samples, in particular cellulose, prior to the addition of 10 µl of a DMSO solution containing sulphur dioxide (0.3 mg sulphur dioxide/l DMSO) and 5 µl of diethyl amine. The samples were then sonicated in a sonicator bath for 30 min and permethylated alditol acetates were prepared as described earlier (Mélida *et al.*, 2013). The sugar derivatives were analyzed on an Agilent 7890B/5977B GC–MS instrument fitted with a VF-23 ms capillary column (30 m × 0.25 mm, 0.25µm) (Agilent Technologies, CA, USA) using helium as the carrier gas. The following temperature program was used: 165°C to 175°C at 1°C /min; 175°C to 195°C at 0.5°C/min; 195°C to 210 °C at 2 °C/min; 210 °C to 250°C at 10 °C /min, followed by a plateau at 250°C for 6.5 min (total run time 68 min). The permethylated alditol acetates were fragmented by electron-impact mass spectrometry and the mass spectra from the resulting fragments were compared to those available in the CCRC Spectral Database (glygen.ccrc.uga.edu) for identification of glycosidic linkages.

RNA sequencing

To identify genes that are differentially expressed during the NaD1 treatment, we performed a transcriptomics analysis by RNA sequencing (RNA-Seq). RNA was successively extracted from a two-day-old mycelium using the Spectrum™ Plant total RNA Kit (Sigma-Aldrich, MO, USA), treated with DNase I (New England Biolabs, MA, USA) and cleaned and concentrated using the RNA Clean & Concentrator Kit (Zymo research, CA, USA). The quality of extracted RNA was checked by spectrophotometry using a Thermo Scientific Nanodrop (Thermo Fisher Scientific, MA, USA) and an Agilent 2100 Bioanalyzer. Library construction and RNA-Seq were performed at the South Australian Genomics Centre (SAGC) using their fee-for-service facility. Briefly, RNA samples were run on a Novaseq 6000 S1 Lane (2x100 bp, v1.5 chemistry). Stranded polyA libraries were prepared using the Nugen Universal Plus mRNA-seq kit (Part No. 0508, M01442 v2). Denaturing and on-board clustering was done using Illumina protocol 15048776 v15 according to the manufacturer's protocol. The quality of sequencing reads was assessed using FASTQC (www.bioinformatics.babraham.ac.uk/projects/fastqc/). RNA-seq reads from five technical replicates were aligned to the *P. cinnamomi* reference genome ASM1869171v1 using STAR 2.7.8a in 2-pass mode (Dobin *et al.*, 2012). Gene count values were determined using the featureCounts program (Liao *et al.*, 2013). SAM/BAM file manipulation was performed using Samtools (Danecek *et al.*, 2021) and BamTools (Barnett *et al.*, 2011). The detection of differentially expressed genes (DEGs) between the NaD1 treated and control samples was performed using the DESeq2 pipeline with the count matrix data derived from the featureCounts output.

Identification, phylogenetic and expression analysis by qPCR of genes encoding voltage gated calcium channels and cell wall biosynthetic enzymes

Genes encoding Voltage Gated Calcium Channels (VGCC) were preliminary identified as differentially expressed based on RNA-Seq data. In addition, Blast searches were performed against different types of VGCC, i.e., L-, P/Q-, T-, R-, and N-type, to construct a phylogenetic tree and analyse the predicted structural differences between the *Phytophthora* sequences and similar sequences from the following species: *Homo sapiens*, *Gorilla gorilla*, *Nomascus leucogenys*, *Malassezia restricta*, *Selaginella moellendorffii*, *Pongo abelii*, *Pan troglodytes*, *Cimex lectularius*, *Zymoseptoria tritici*, *Entomortierella parvispora*, and *Mus musculus*. Sequences were aligned with the *P. cinnamomi* VGCC sequences and InterProScan, together with manual inspection of published crystal structures, was used to confirm domain structure (Gauberg *et al*., 2022; Zheng & Mackrill, 2016). In addition to *VGCC* genes, a gene encoding a putative stretch-activated ion channel involved in calcium influx and homeostasis was found to be differentially expressed in *P. cinnamomi*. The product of this genes, MID1, was therefore included in our bioinformatic and qPCR analyses.

Data from cell wall analyses suggested differences in polysaccharide content. Hence we also performed Blast searches against the NCBI databases to identify genes that code for key putative cell wall related enzymes in *P. cinnamomic* and other oomycetes, *i.e*., chitin synthases (*Chs*), cellulose synthases (*CesA*) and glucan synthases (*Fks*). Phylogenetic analysis of these genes was performed by aligning the *P. cinnamomi* sequences with their orthologues followed by maximum likelihood estimation using FastTree (Geneious Prime version 2022.1.1).

For q-PCR analysis, cDNA was synthesised from purified RNA using the Invitrogen superscript IV kit (Invitrogen, CA, USA). The q-PCR was performed as described elsewhere (Burton *et al.*, 2008) using a Thermal cycler C1000 Touch instrument (Bio-Rad, USA). Reaction mixtures consisted of 2 µl cDNA (1:20 dilution in water) and 8 µl of iTaq Universal SYBR Green supermix. Primers were used at a concentration of 4 µM and the amplification conditions were as specified in Supplementary Table 1. Four reference genes were used as previosule described, namely *Ws21* (40S ribosomal protein S3A), *Tub-b* (β-tubulin), *Ubc* (Ubiquitin-conjugating enzyme), and *G6pdh* (glyceraldehyde-3-phosphate dehydrogenase) (Supplementary Table 2). The cell wall, VGCC and MID1 target genes were: *CesA1* (KAG6610888.1), *CesA2* (KAG6610748.1), *CesA3* (KAG6583257.1), *CesA4* (KAG6583016.1), *Chs1* (KAG6617362.1), *Chs2* (KAG6622452.1), *Fks1a* (KAG6621264.1), *Fks1b* (KAG6596129.1), *Fks1c*

(KAG6616379.1), *Fks1d* (KAG6616627.1), *Fks2a* (KAG6610049.1), *Mid1* (KAG6591006.1), *Pmca3* (KAG6587129.1), *Pmca1* (KAG6623208.1), *Pmca2* (KAG6614297.1), *Vgcc2* (KAG6604562.1), and *Vgcc3* (KAG6622298.1) (Supplementary Table 3).

Hyphal growth recovery using cations

As several *Vgcc* genes were found to be differentially expressed, we analyzed the effect of $CaCl_2$ on *P. cinnamomi* hyphae treated with NaD1, and investigated whether other cations, i.e., K^+ and Na^+, affected hyphal growth in a similar manner. For this purpose, individual poppy seeds covered with mycelium were transferred in wells of 24-well plates containing 500 µl PDB, 50 µM NaD1 and varying $CaCl_2$ concentrations (0, 12.5, 25, 50, 100 mM). Plates were incubated at 25°C for 48 h, after which growth was assessed by observation with an Olympus ix70 inverted microscope. A similar approach was used to test the effect of KCl (0, 12.5, 25, 50, 100 mM) and NaCl (0, 12.5, 25, 50, 100 mM).

An L-type Ca^{2+} channel blocker, nifedipine, was used as a positive control and tested on the mycelium in the same conditions as above at 4, 8, 15, 31, 62, 125, 250, 500 and 1000 µM. In addition, a test to rescue the inhibition by nifedipine and associated phenotype was performed by adding 3, 6, 12.5, 25, 50, 100, 200 mM $CaCl_2$ in the samples. The levels of free cytosolic calcium were estimated using the Fluo-3-AM probe after 48 h culture in PDB in the following conditions: 50 µM NaD1; 50 µM NaD1 + 50 mM $CaCl_2$; 250 µM nifedipine; 250 µM nifedipine + 25 mM $CaCl_2$. Fluo-3-AM was then added to each well at a final concentration of 150 µM and the cultures were incubated at 37°C for 1 h. The excess of dye was washed with 500 µl phosphate buffered saline (PBS) twice for 5 min and green fluorescence indicative of the presence of calcium was detected using a Nikon Ni-E fluorescence microscope fitted with a 450-490 nm excitation filter and a 520 nm emission filter. Images from three biological replicates were recorded using an exposure time of 40 ms.

Statistical analyses

All statistical analyses were performed using the SPSS software (version 26.0; Chicago, IL, USA). Numerical data are presented as the mean ± standard error of the mean (SEM). Independent T-test P-values ≤0.05 (*), ≤0.01 (**) and ≤0.001 (***) are shown to highlight significant differences.

Results

Effect of NaD1 on the growth of *Phytophthora* species and formation of sporangia

Hyphal growth of *P. citricola, P. cambivora*, *P. nicotianae* and *P. cinnamomi* was significantly inhibited in the presence of 50 µM NaD1 (Figure 1a). The extent of inhibition was similar for all species, with the strongest inhibition observed for *P. citricola* (86%) followed by *P. cambivora* (83%), *P. nicotianae* (75%), and *P. cinnamomi* (74%) (Figure 1a-1b). *P. cinnamomi* is a broad-host pathogen of crops and a serious threat to the ecosystem across all continents. Hence we decided to focus on this species for further analysis despite its relatively lower sensitivity to NaD1 compared to the other species tested. Observation of the mycelium under the inverted microscope revealed cytoplasmic granulation, irregular and hyper-branched hyphal cells in the NaD1-treated samples compared to the control performed in the absence of the peptide (Figure 1c). In addition, NaD1 completely inhibited the formation of sporangia in *P. cinnamomi* compared to the control (Figure 1d). Similar observations were made on the three other species tested (not shown).

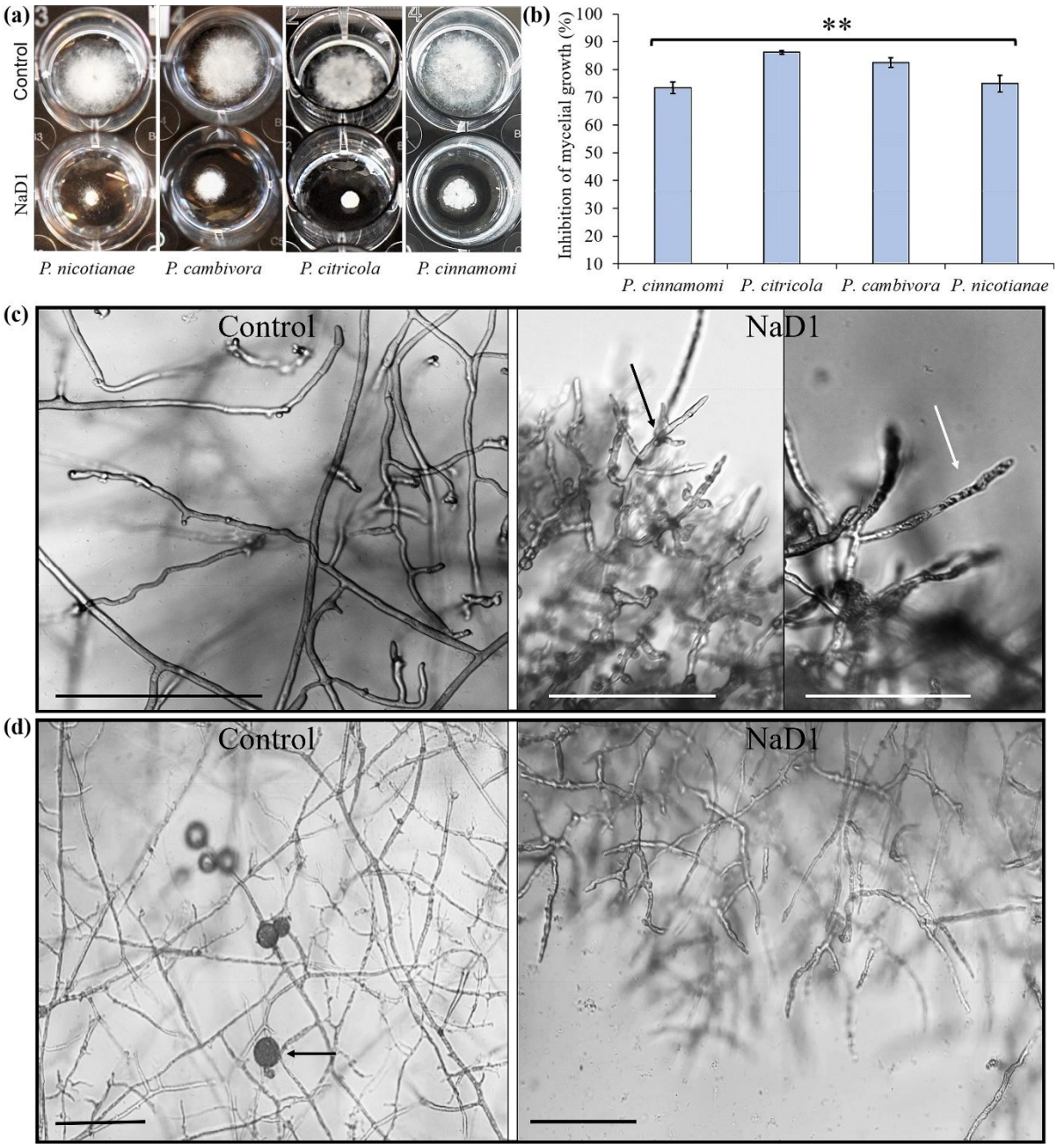

Figure 1: Effect of NaD1 on the growth and morphology of *Phytophthora* species.

(a) Hyphal growth of *P. cinnamomi, P. citricola, P. cambivora, and P. nicotianae* in the presence of 50 µM NaD1. (b) Percentage of inhibition of mycelial growth in the presence of 50 µM NaD1 (number of biological replicates = 5). (c) Morphology of hyphal cells of *P. cinnamomi* in the absence (control) and presence of NaD1. The NaD1 treatment induced suppression of apical dominance (black arrow) and cytoplasmic granulation (white arrow). (d) Sporangia development in *P. cinnamomi* in the absence and presence of NaD1. Scale bars = 100 µm.

Electron microscopy analysis of the effect of NaD1 on hyphal cells of *P. cinnamomi*

SEM observations showed that the control hyphal cells of *P. cinnamomi* appeared as tubular filaments with a smooth surface appearance (Figure 2a). In contrast, cells exposed to NaD1 had a shrivelled and uneven morphology, and some appeared as distorted filaments. In addition, most cells were covered by granular structures that seem to bulge out from the hyphal cells (Figure 2b).

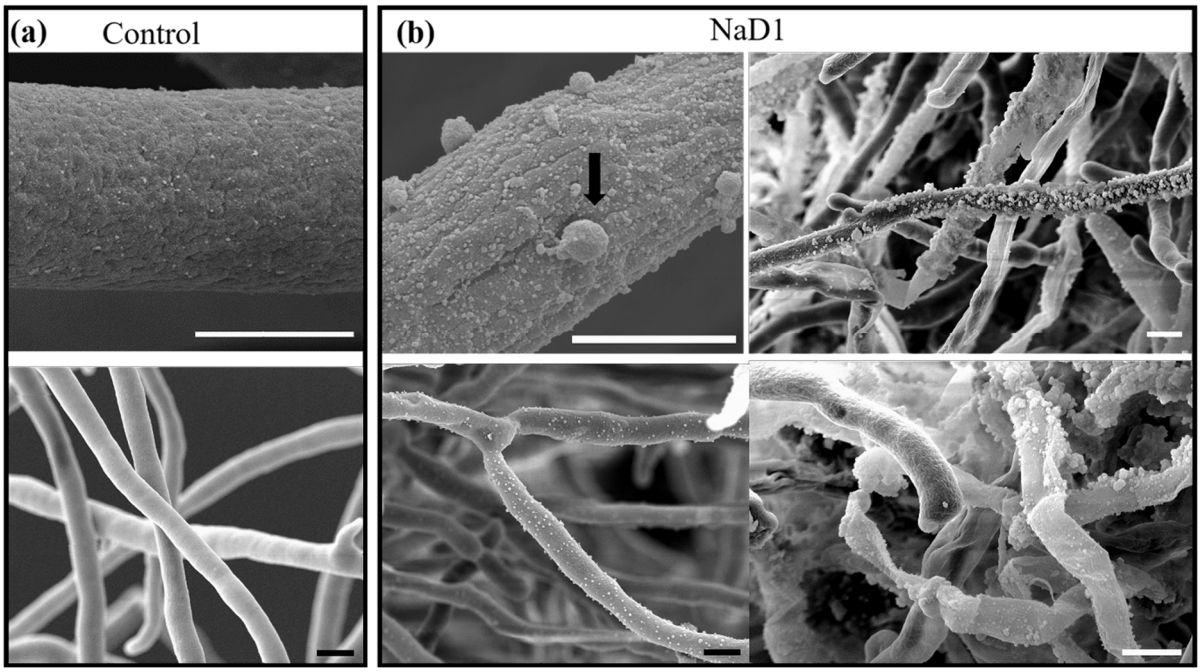

Figure 2: Scanning electron microscopy (SEM) imaging of hyphal cells of *P. cinnamomi*. Images show smooth mycelial surfaces in the absence of NaD1 (control, panel a), while exposure to NaD1 led to the formation of granular structures (black arrow, panel b) at the surface of the cells as well as distorted hyphae. Scale bars = 5 µm.

TEM was used to better understand the effect of NaD1 on the ultrastructure of the cells. Images showed a typical ultrastructure in the control hyphae, with an intact cell wall and cell membrane, normally distributed organelles, including mitochondria, nucleus, Golgi bodies, lysosomes, endoplasmic reticulum, and vacuoles (Figure 3a-3b). After treatment with NaD1, the cell wall was twice as thick compared to the untreated cells and slightly denser to electrons. The plasma membrane was also altered, exhibiting a significantly higher number of invaginations. Additionally, a higher density of vesicles was present in proximity to the plasma membrane compared to the control (Figure 3c-3d). Interestingly, the cell wall surface of the

treated hyphae was covered with electron-dense granular structures of irregular shape (Figure 3d), reminiscent of the extracellular granules observed by SEM (Figure 2b).

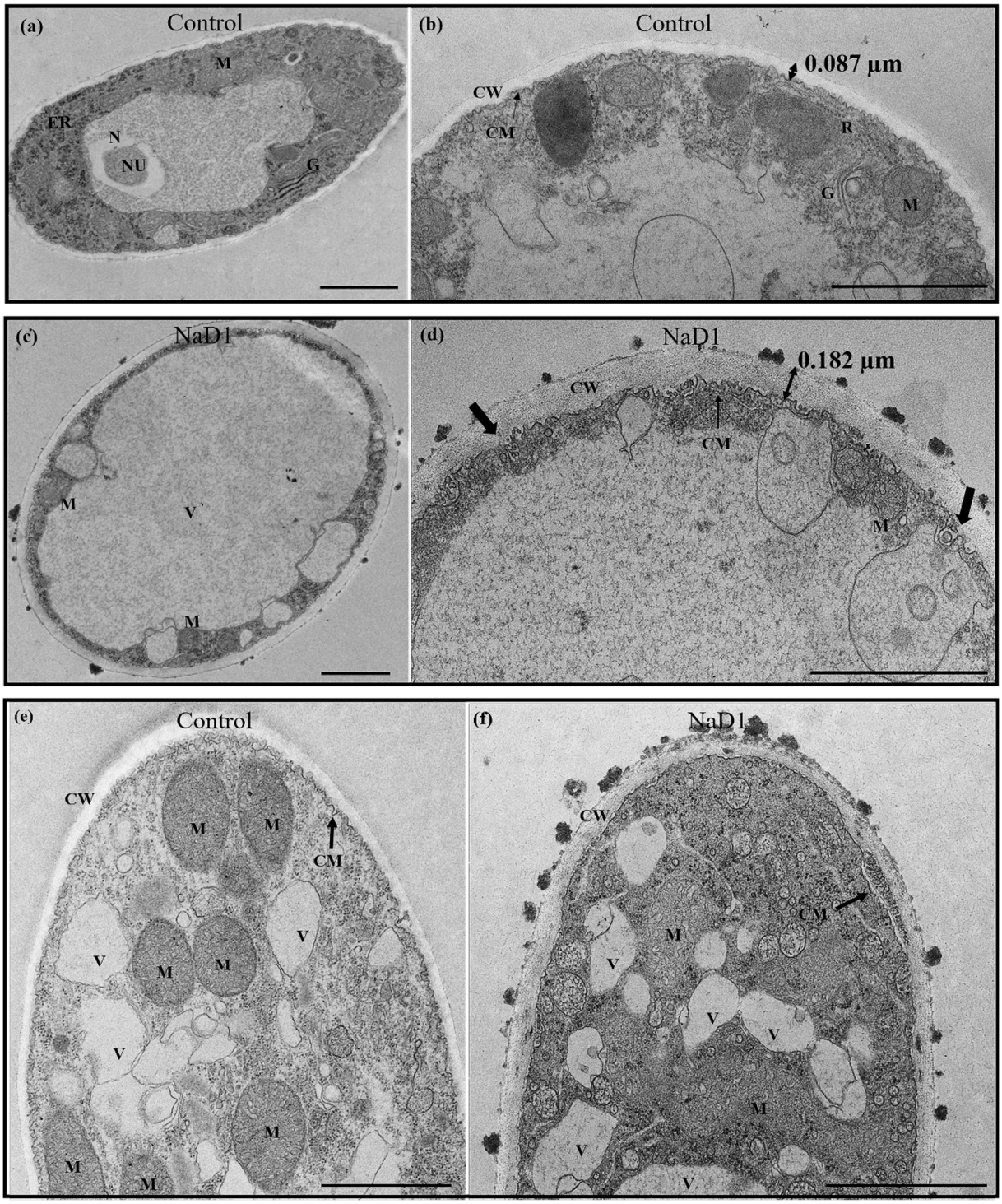

Figure 3: Transmission electron microscopy (TEM) imaging of hyphal cells of ***P. cinnamomi*****.**

TEM transversal (a-b) and longitudinal (e) sections of control cells not exposed to NaD1 and transversal (c-d) and longitudinal (f) sections of cells treated with the peptide. Black arrows indicate vesicles near the plasma membrane. Cell wall thickness was measured as indicated

with the double arrow spanning the wall of the control and NaD1-treated cells. M: mitochondria; V: vacuole; N: nucleus; NU: nucleolus; ER: endoplasmic reticulum; G: Golgi bodies; CM: cell membrane; CW: cell wall. Scale bars = 1 µm.

Effect of NaD1 treatment on the cell wall composition of *P. cinnamomi*

The total cell wall composition of the control cells and cells treated with NaD1 was reconstituted from the data obtained from the AIF and ASF fractions. As expected, monosaccharide analysis showed that glucose is the major component of the cell wall of *P. cinnamomi* hyphae, representing 89% (molar percentage) of the total ethanol insoluble material (Supplementary Figure 1). The other monosaccharides detected were mannose, galactose, glucuronic and galacturonic acids, with mannose (5% of the cell wall material) being the most abundant of these minor sugars. No acetylglucosamine indicative of the presence of chitin was detected, which is consistent with previous results on other *Phytophthora* species (Melida *et al*., 2013). The cell wall monosaccharide composition of the mycelium exposed to NaD1 was nearly identical to that of the control cells, with a minor increase in glucose content and a slight decrease in mannosyl residues (Supplementary Figure 1).

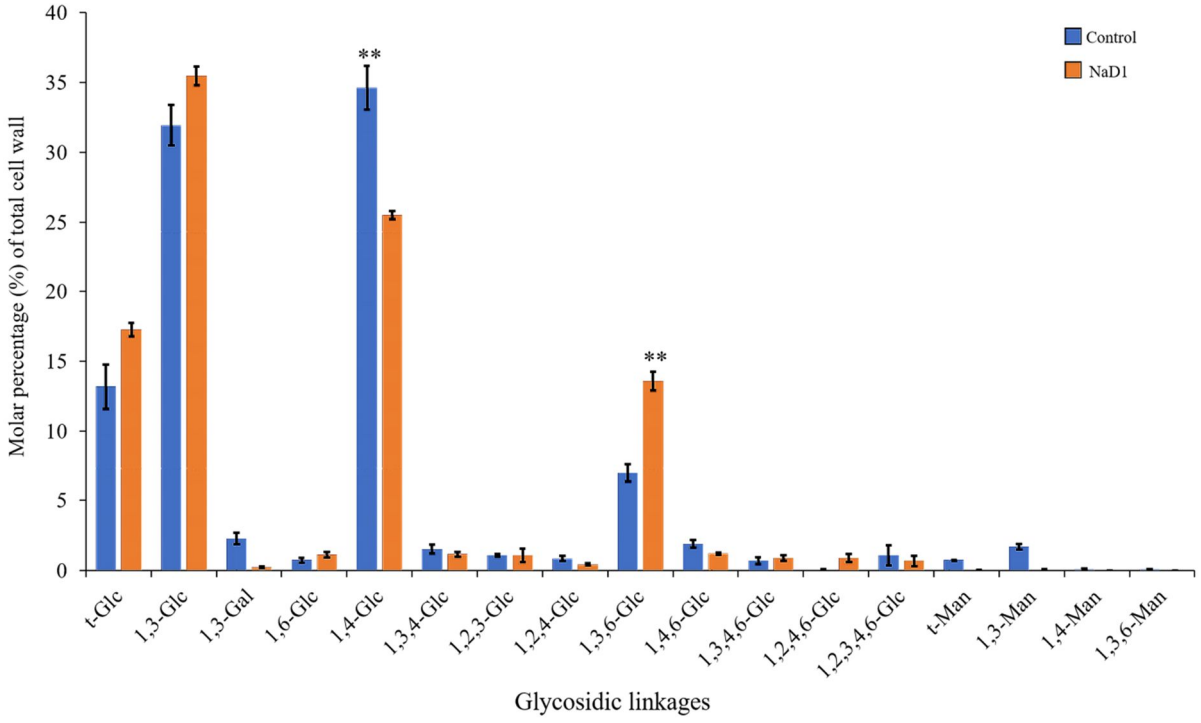

Figure 4: Glycosidic linkage analysis of cell wall polysaccharides from *P. cinnamomi* cells grown in the absence of NaD1 (control) and exposed to the peptide (NaD1).

The data are presented as the mean ± standard error of the mean, with n = 3 independent biological replicates. T-test P-values ≤0.01 (**) are shown for differences between the control and NaD1-treated cells.

To determine whether more subtle structural differences were induced by the NaD1 treatment, we performed a glycosidic linkage analysis on the AIF and ASF fractions of the cell walls from the control and NaD1-treated cells, and combined the data to reflect the amounts of each linkage type in the total cell walls (Figure 4). As expected, the major types of linkages detected in the control cells corresponded to 1,3-linked and 1,4-linked glucosyl residues, representing around 32% and 35% of the total cell wall linkages, respectively. Terminal glucosyl residues were the next most abundant (13%), followed by 3,6-linked glucosyl residues (7%). Each of the multiple remaining glycosidic linkage types detected did not exceed 2%. The total amount of linkages from glucosyl residues represents 95% of the total cell wall linkages, which is consistent with the data obtained by monosaccharide analysis. The 1,4-linked glucosyl residues can be considered as arising from cellulose since starch-like polysaccharides do not occur in oomycetes as evidenced by the observation that amylase treatment does not influence glucosidic linkage profiles in *Phytophthora* species (Mélida *et al.*, 2013). Interestingly, the NaD1 treatment led to a significant decrease in the content of 1,4-linked glucosyl residues, from 35% in the control cells to 25% in the NaD1 samples, which reveals a decrease in cellulose content. Conversely, the proportion of 1,3-linked glucosyl residues increased from 32% in the cell walls of the control cells to 36% in the NaD1-treated hyphae. A similar trend was observed for the terminal and 3,6-linked glucosyl residues, whose proportions were increased by 4% and 7%, respectively, compared to the control cells. The 3,6-linked glucosyl residues are indicative of the presence of 3,6-branching points in (1,3)-β-glucans, and terminal glucosyl residues reflect the proportion of branched chains in a polysaccharide as well as chain length. Hence the observed increase of both linkage types in the cell walls from the NaD1-treated cells strongly suggests an increase in the degree of branching of (1,3)-β-glucans compared to the control, possibly accompanied by a reduced chain length. In summary, these data indicate that the observed decreased in cellulose content in the NaD1-treated cells is compensated by an increased proportion of branched (1,3)-β-glucans.

Transcriptomic analysis by RNA-Seq and qPCR

The RNA-Seq data showed that the expression of 694 genes was significantly altered in the NaD1-treated cells compared to the control, including 103 up-regulated genes and 591 down-regulated genes (fold change ≥1.5 and adjusted P value <0.05). In light of the structural

differences observed after cell wall glycosidic linkage analysis, we specifically targeted genes involved in cell wall formation, in particular genes involved in cellulose and (1,3)-β-glucan biosynthesis, to determine whether their expression profile was altered following cell exposure to NaD1. Sequence homology searches and phylogenetic analyses showed that four putative cellulose synthase genes are found in *P. cinnamomi*, which we named *CesA1*, *CesA2*, *CesA3*, and *CesA4* based on their similarity with gene orthologues from other species. In addition, five putative glucan synthase genes named *Fks1a*, *b*, *c* and *d*, and *Fks2a*, as well as two chitin synthase genes named *Chs1* and *Chs2* were identified (Supplementary Figure 2). The RNA-Seq data revealed that *CesA1*, *CesA2*, *CesA3* and *Chs1* tend to be slightly downregulated upon cell exposure to NAD1, but not above a significant threshold (Figure 5a). Conversely, *Chs2* was slightly upregulated in the NaD1 treated hyphae as well as *Fks2a*, however were less robust in the latter case (Figure 5a). All other cell wall related genes analyzed (*CesA4*, *Fks1a*, *Fks1b*, *Fks1c*, *Fks1d*) were not differentially expressed (not shown).

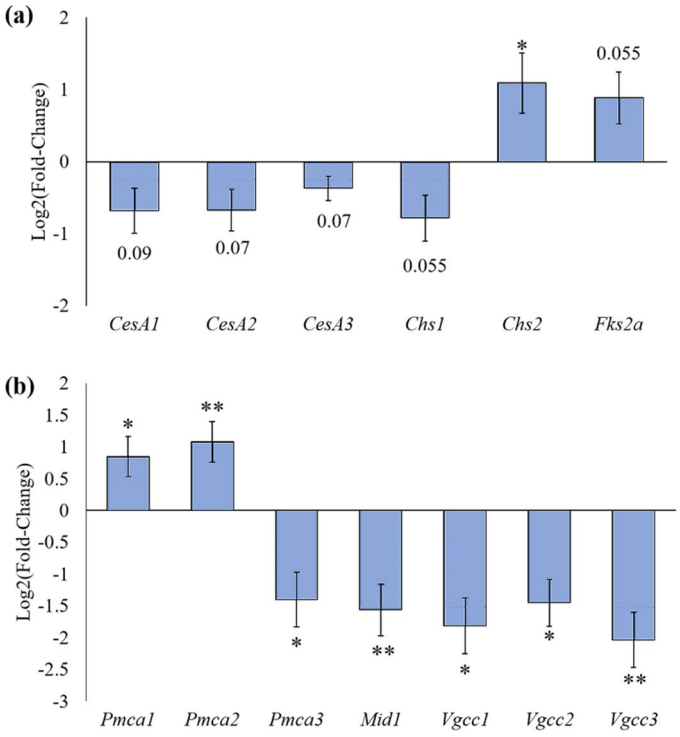

Figure 5: RNA-Seq analysis of genes involved in cell wall biosynthesis and calcium transport.

(a) Expression analysis of cell wall related genes, namely cellulose synthase (*CesA*), chitin synthase (*Chs*), and glucan synthase (*Fks*) genes. (b) As in (a) but for genes involved in calcium transport and homeostasis: *Pmca*, *Mid1* and *Vgcc* genes. All data are presented as the mean ± standard error of the mean (n = 5). T-test P-values ≤0.05 (*), ≤0.01 (**) or actual values are shown to highlight the most significant differences.

Interestingly, three of the four *Vgcc* genes identified in *P. cinnamomic*, namely *Vgcc1-3*, were significantly downregulated (Figure 5b). We also identified that NaD1 exposure led to downregulation of a gene encoding a plasma membrane Ca^{2+} ATPase named PMCA3, whereas the similar *Pmca1* and *Pmca2* genes were upregulated (Figure 5b). This class of proteins control calcium efflux in *P. cinnamomi* (Zheng & Mackrill, 2016). In addition, the expression of *Mid1*, a gene that encodes a calcium channel protein, was downregulated in the NaD1 treated cells. MID1 controls calcium homeostasis by uptaking calcium from the environment (Milhem, 2019). Overall these data suggest that the expression of diverse calcium transporters is differently affected when cells are exposed to NaD1.

To confirm the RNA-Seq data presented above, we performed qPCR analysis on 11 cell wall biosynthetic genes (*CesA1-4*, *Chs1-2*, *Fks1a-d*, *Fks2a*) and 6 genes involved in calcium transport and homeostasis *Pmca1* (KAG6614297.1), *Pmca2* (KAG6587129.1), *Pmca3* (KAG6623208.1), *Vgcc2* (KAG6604562.1), *Vgcc3* (KAG6622298.1), and *Mid1* (KAG6591006) (Figure 6). Despite extensive efforts to design primers for *Vgcc1* it was not possible to obtain data for this gene, hence it was excluded from the q-PCR analysis. In addition, *Vgcc4* was not found to be differentially expressed by RNA-Seq and was therefore not included in the q-PCR analysis.

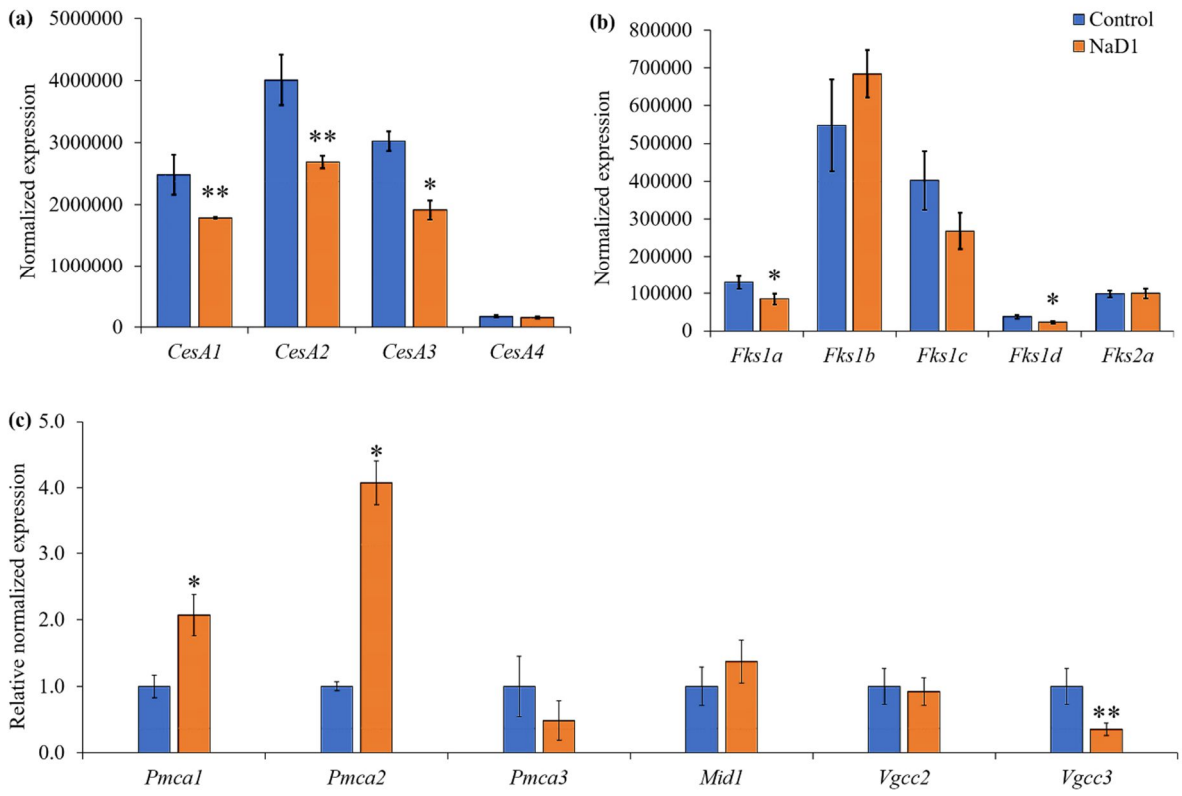

Figure 6: q-PCR analysis of putative *P. cinnamomi* genes involved in cell wall biosynthesis and calcium transport.

Relative normalized expression of *CesA* (a) and *Fks* (b) genes, and genes involved in calcium transport, i.e., *Vgcc*, *Pmca* and *Mid1* genes (c). The data are represented as the mean ± standard error of the mean (n = 3). T-test P-values ≤0.05 (*) and ≤0.01 (**) are indicated to highlight significant differences between the control and NaD1-treated samples.

The q-PCR data obtained for the cellulose synthase genes were in keeping with the RNA-Seq data, with a slight decrease in expression for *CesA1*, *CesA2*, and *CesA3*, but no difference for *CesA4* compared to the control cells (Figure 6a). The higher expression of *Chs2* and *Fks2a* observed in the RNA-Seq data (Figure 5a) was not confirmed by q-PCR (Supplementary Figure 4). Conversely, analysis by q-PCR of the *Fks1a-d* genes showed some differences in level of expression between the control and NaD1 cells, which were not observed by RNA-Seq (Figure 6b). However, statistical analysis of the q-PCR data suggests these differences are not significant. In agreement with the RNA-Seq data, the *Pmca1* and *Pmca2* genes related to calcium transport were confirmed by q-PCR to be upregulated, and *Vgcc3* to be downregulated. Although both RNA-seq and q-PCR data showed the same trend for the expression of *Pmca3* and *Vgcc2* genes (downregulation) the differences observed in the q-PCR experiments were not

significant (Figure 6c). In contrast to the decreased expression of *Mid1* observed in the RNA-Seq experiment, no difference was detected by q-PCR.

NaD1 affects calcium transport in *P. cinnamomi*

Following the demonstration that the expression of several genes involved in calcium transport and homeostasis is affected when cells of *P. cinnamomi* are exposed to NaD1, we next determined more directly whether calcium transport is indeed affected by the peptide. For this purpose, we first used several concentrations of nifedipine, a known L-type calcium channel blocker, to determine whether the phenotype observed in the presence of NaD1 is reproduced by exposure to the inhibitor. The data showed that the growth of hyphal cells of *P. cinnamomi* is severely affected in the presence of 250 µM nifedipine, to a similar extent as with NaD1 (Figure 7). Growth inhibition was reverted when the medium containing the inhibitor was supplemented by 25 mM calcium, showing that growth inhibition is indeed due to blockage of calcium transport by nifedipine (Figure 7). Interestingly, a similar result was obtained in these rescue experiments when nifedipine was replaced by NaD1, suggesting that NaD1 does affect calcium transport (Figure 7).

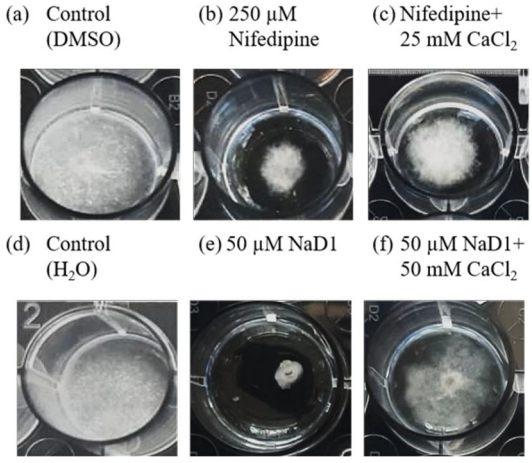

Figure 7: Effect of $CaCl_2$ on growth recovery of hyphal cells of *P. cinnamomi* exposed to NaD1 and nifedipine.

a) control (DMSO); b) 250 µM nifedipine; c) 250 µM nifedipine + 25 mM $CaCl_2$; d) control (water); e) 50 µM NaD1; f) 50 µM NaD1 + 50 mM $CaCl_2$

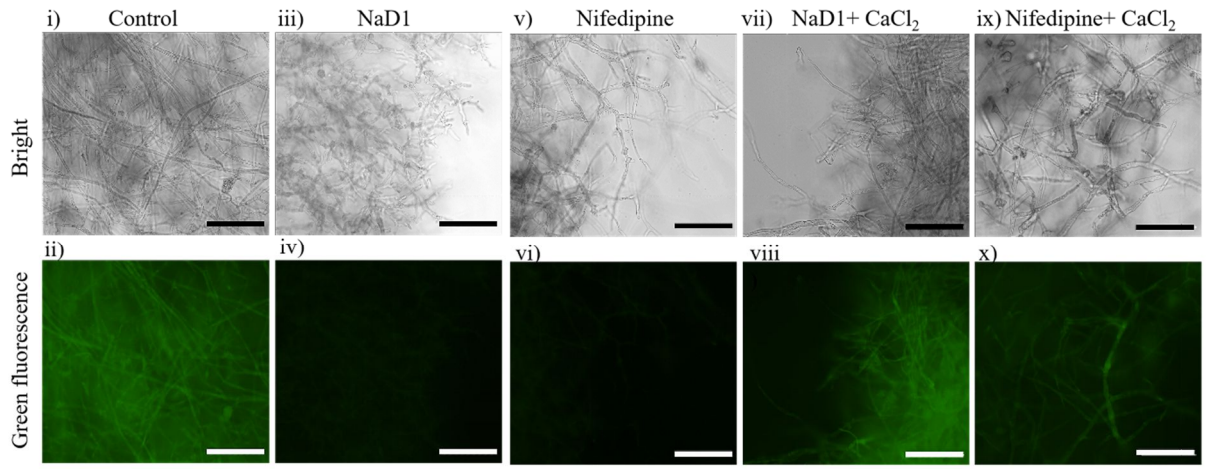

Figure 8: Effect of $CaCl_2$ on the recovery of *P. cinnamomi* cells exposed to nifedipine and NaD1 and assay of intracellular calcium by fluorescence microscopy. The green fluorescence intensities reflect the relative quantities of free cytosolic Ca^{2+}.
i-ii) control (cells in PDB medium); iii-iv) 50 µM NaD1; v-vi) 250 µM nifedipine; vii-viii) 50 µM NaD1 + 50 mM $CaCl_2$; ix-x) 250 µM Nifedipine + 25 mM $CaCl_2$. Cytosolic Ca^{2+} was detected by using the Fluo-3-AM fluorophore; the intensity of the green fluorescence reflects the concentration of free cytosolic Ca^{2+}. Scale bars = 100 µm.

The relative amount of free intracellular Ca^{2+} was evaluated by fluorescence microscopy using the Fluo-3-AM probe. Further substantiating an effect of NaD1 on calcium transport, the concentration of free cytosolic calcium was significantly decreased in the presence of NaD1 to a similar extent as with nifedipine, and this effect could be reverted when calcium ions were added in the medium (Figure 8). The observed effects of NaD1 on hyphal growth seem to be specific to alteration of calcium transport as neither KCl nor NaCl were able to revert the inhibitory effect of the peptide (Supplementary Figure 3).

Discussion

Plant defensins, and more generally antimicrobial peptides, represent a powerful resource for the development of next-generation therapeutics against microbial pathogens relevant to the agricultural, veterinary and medical sectors (Dracatos *et al.*, 2014; van der Weerden *et al.*, 2008) (Wang *et al.*, 2016). Their breadth of biochemical activities suggests a commensurate range of targets, from the enormous diversity of pathogenic micro-organisms to human tumour cells. However, many defensins remain uncharacterised and their mode of action undefined. The defensin NaD1 from *Nicotiana alata* has been shown to bind to cell wall lipids and cause membrane permeabilisation in filamentous fungi and tumour cells (Dracatos *et al.*, 2014; Lay

et al., 2003; van der Weerden & Anderson, 2013; van der Weerden *et al.*, 2008). However, the inhibitory effect of NaD1 or any other plant defensin against oomycetes has not been investigated and characterized at the biochemical level. Instead, prior studies have focused on transgenic plants that express *Nicotiana megalosiphon* defensin 2 (NmDef02) and an antifungal peptide from *Medicago sativa* (alfAFP). In these studies, NmDef02 was shown to increase resistance to *P. infestans* infection, but alfAFP was not efficient (Gao *et al.*, 2000; Portieles *et al.*, 2010). Since NaD1 is a well-characterized plant defensin and its mechanism of action is well-described in fungi (Hayes *et al.*, 2013; van der Weerden *et al.*, 2008), it offers a promising starting point to investigate the efficacy of this class of antimicrobial peptides against pathogenic oomycetes.

In this report, we have analysed the effect of NaD1 on hyphal growth of four different *Phytophthora* spp., namely *P. cinnamomi*, *P. citricola*, *P. cambivora* and *P. nicotianae*. The data showed that 50 µM NaD1 strongly suppressed apical dominance in all four species, which resulted in hyper-branched hyphae, and significantly reduced hyphal growth and colony area. These effects were accompanied by cytoplasmic granulation, extensive vacuolation and inhibition of sporangial development. This suggests that NaD1 can efficiently inhibit mycelial growth of multiple pathogenic *Phytophthora* species. We subsequently focused our work on *P. cinnamomi* as this species is considered one of the top ten most devastating oomycete phytopathogens (Kamoun *et al.*, 2015). As NaD1 is known to exhibit direct cytotoxic activities on pathogenic fungi by interacting with phospholipid bilayers (Payne *et al.*, 2016), we hypothesised that it may act in a similar manner on oomycetes. SEM observations of cells exposed to NaD1 revealed the presence of granular structures on the surface of hyphae. In other instances, the hyphae were severely distorted and leaked. TEM observations revealed that the cell wall, cell membrane, mitochondria, and vesicles activity of hyphae were affected in the presence of NaD1 (Figure 3c). Additionally, the accumulation of vesicles close to the plasma membranes suggests an increased vesicle trafficking and intensive secretion activity toward the cell wall (Figure 3d). In the filamentous fungus *Fusarium oxysporum,* NaD1 binds to the cell wall and permeabilizes the plasma membrane to affect the integrity of the fungal cells (van der Weerden *et al.*, 2008). Similarly, the electron-dense granular structures visible on the surface of the *P. cinnamomi* cells may reflect cytoplasmic leakage prior to cell death (Figure 3d).
TEM images revealed a thicker cell wall in the *P. cinnamomi* hyphae treated with NaD1, and glycosidic linkage analysis showed a significant decrease in 1,4-linked glucosyl residues, which is indicative of a reduced abundance of cellulose (Figure 4). Consistent with these observations, transcript abundance analysis of putative cellulose synthase genes revealed that *CesA1*, *CesA2*,

and *CesA3* were downregulated in both RNA-Seq (Figure 5a) and q-PCR experiments (Figure 6a). Further, we show that NaD1 caused a significant increase in 3,6-linked glucosyl residues, which indicates a higher degree of branching of the 1,3-glucans in the cell wall (Figure 4). Our report is consistent with a recent study that showed that *CesA1* knockout mutants in *P. capsici* had decreased cellulose content and altered glycosidic linkages indicative of branched polysaccharides and/or crosslinks between cell wall polysaccharides, i.e., 4,6-linked glucosyl residues, and 3,4- linked glucosyl residues (Li *et al.*, 2022).

In summary, our results suggest that NaD1 affects cellulose biosynthesis and the branching pattern of 1,3-linked glucans, resulting in mechanically weaker cell walls with reduced tensile strength and, potentially, an increase in cell wall permeability and cell death. Chitin is not detected in the cell walls of *Phytophthora* hyphal cells (Mélida et al., 2013), but it has been reported to occur in low abundance in zoospores and sporangia (Cheng *et al*., 2019). In keeping with the results from (Mélida *et al.*, 2013), no N-acetylglucosaminyl residues indicative of chitin were detected in our monosaccharide analysis of mycelial cells, and no significant or consistent variation in gene expression for the chitin synthase genes (*Chs*) was observed.

The growth, morphological and developmental effects of NaD1 on *Phytophthora* species described in this report are associated with calcium homeostasis in fungi (Naveena Lavanya Latha & Maruthi Mohan, 2011; Spelbrink *et al.*, 2004; Zheng & Mackrill, 2016). In fungal species, apical dominance is a key character which regulates the formation of lateral branching in vegetative hyphae (Rayner, 1991). It has been reported that a high calcium gradient in hyphal tips regulates apical dominance, and therefore branching pattern, in filamentous cells (Schmid & Harold, 1988). Hence a disturbance in calcium signalling typically causes hyperbranching in hyphal tips (da Silva Ferreira *et al.*, 2007). Some plant defensins have been shown to interact with calcium signalling pathways. For example, the defensin MsDef1 from *Medicago sativa* seeds was reported as a blocker of mammalian L-type calcium channels (Allen *et al.*, 2008; Ramamoorthy *et al.*, 2007; Ramamoorthy *et al.*, 2007; Spelbrink *et al.*, 2004). However, plant defensins are diverse and others, such as the Rs-AFP2 defensin from *Raphanus sativus* (radish) seeds and MtDef2 from *M. sativa*, have been shown to have no interaction with calcium transport (Spelbrink *et al.*, 2004). Although NaD1 has been extensively studied in fungi, its relationship with calcium signalling pathways has not been reported yet. In our study, 50 mM $CaCl_2$ was sufficient to decrease the inhibitory effect of NaD1 on hyphal growth (Figure 7), whereas no recovery was observed with either NaCl and KCl. Nifedipine, a well-known L-type calcium channel blocker, was used as positive control and mimicked the NaD1 phenotype on

P. cinnamomi hyphal growth. In *P. capsici* nifedipine blocks calcium channels, and it has been proposed that this could lead to decreased pathogenicity and virulence (Liu *et al.*, 2016). In *P. cinnamomi*, both NaD1 and nifedipine inhibited calcium transport inside the hyphal cells, resulting in lower intracellular calcium levels as detected with Fluo-3-AM (Figure 8). It is plausible that the NaD1-mediated disruption of Ca^{2+} homeostasis in *P. cinnamomi* causes the observed organelle abnormalities.

Our work demonstrates parallels between the biochemical activity of NaD1 in fungal and *Phytophthora* species. In fungi, NaD1 loses its anti-microbial activity in the presence of physiological salt (NaCl) at high concentrations (~100 mM) (Bleackley *et al.*, 2019; McColl *et al.*, 2018). In addition, the same reports indicate that decreased levels of 1,3-β-glucans restored anti-fungal activity of NaD1 within yeast cells. As shown in our work, NaCl and KCl additions in the medium did not decrease the NaD1 anti-microbial activity in *Phytophthora* species, as opposed to $CaCl_2$ (Supplementary Fig 3). These results indicate that the antagonistic mechanism of NaD1 is different in fungi and oomycete (*Phytophthora*) species.

In Fungi, Ca^{2+} ATPases (PMCAs) regulate and maintain calcium homeostasis by transporting Ca^{2+} ions (calcium efflux) from the cytosol to internal stores to circumvent calcium toxicity (Pittman, 2011). Interestingly, vacuolar PMCA is also required for pathogenesis caused by *Candida albicans* (Luna-Tapia *et al.*, 2019). Another plasma membrane protein, the stretch-activated Ca^{2+}-permeable channel component MID1, is an important channel for calcium influx in fungi (Ozeki-Miyawaki *et al.*, 2005), and is necessary for regulating vegetative growth (Cavinder *et al.*, 2011). Moreover, it has role in cell wall biosynthesis, host penetration, and virulence of fungi (Bormann & Tudzynski, 2009; Xie *et al.*, 2019). In our study, we propose that NaD1 altered gene transcript levels of the homologues of these proteins in *P. cinnamomi*, which consequently may be similarly correlated with decreased growth and development.

Voltage Gated Calcium channels (VGCC) are multi-subunit membrane-bound proteins that are activated by membrane depolarization (Moran & Zakon, 2014; Stephens *et al.*, 2015). The presence of VGCCs and their role in calcium influx and homeostasis is well-known in fungi (Lange & Peiter, 2019). However, oomycete VGCCs have not been well studied and their biochemistry is not well understood (Zheng & Mackrill, 2016). Oomycetes encode numerous VGCC homologs which bear a resemblance to vertebrate VGCCs and have been shown to act as Ca^{2+} channel inhibitors, suppressing apical dominance of mycelial growth in an aquatic oomycete *Achlya bisexualis* (Stephens *et al.*, 2015; Zheng & Mackrill, 2016). Some of the

identified putative *Vgcc*s in *P. cinnamomi* were downregulated in presence of NaD1, albeit with some discrepancies between the RNA-Seq and q-PCR data, suggesting that the activity of VGCC proteins in oomycetes is correlated with growth and development and, indirectly, pathogenicity. However, their precise molecular mechanism needs to be further investigated and direct evidence that NaD1 blocks calcium channel activity remains to be demonstrated. In summary, these results show that calcium homeostasis in *P. cinnamomi* was altered in the presence of NaD1, likely due to modified expression levels of genes involved in the regulation of calcium influx and efflux.

In conclusion, the work presented here provides a valuable foundation to understand the biochemical interaction between the plant defensin NaD1 and a devastating phytopathogenic oomycete, *P. cinnamomi*. The anti-oomycete activity of NaD1 demonstrated here alongside its known inhibitory effect on fungal cells show evident potential of NaD1 as an effective broad-spectrum anti-microbial agent.

Acknowledgments

We thank Dr. Gwenda Mayo from the Microscopy Centre at the University of Adelaide for support with electron microscopy observations and Professor Marilyn Anderson for generously providing the NaD1 peptide used in this work. The fee-for-service facility of the South Australian Genomics Centre (SAGC) was used for library construction and RNA sequencing. This work was supported by a grant to V.B. from the Australian Research Council (grant # DP180103974).

References

Allen, A., Snyder, A. K., Preuss, M., Nielsen, E. E., Shah, D. M. & Smith, T. J. (2008) Plant defensins and virally encoded fungal toxin KP4 inhibit plant root growth. *Planta*, 227(2), 331-339.

Barnett, D. W., Garrison, E. K., Quinlan, A. R., Strömberg, M. P. & Marth, G. T. (2011) BamTools: a C++ API and toolkit for analyzing and managing BAM files. *Bioinformatics*, 27(12), 1691-1692.

Bleackley, M. R., Dawson, C. S., Payne, J. A. E., Harvey, P. J., Rosengren, K. J., Quimbar, P., Garcia-Ceron, D., Lowe, R., Bulone, V., van der Weerden, N. L., Craik, D. J. & Anderson, M. A. (2019) The interaction with fungal cell wall polysaccharides determines the salt tolerance of antifungal plant defensins. *Cell Surface*, 5, 100026.

Bormann, J. & Tudzynski, P. (2009) Deletion of Mid1, a putative stretch-activated calcium channel in *Claviceps purpurea*, affects vegetative growth, cell wall synthesis and virulence. *Microbiology*, 155(12), 3922-3933.

Bozkurt, T. O., Schornack, S., Banfield, M. J. & Kamoun, S. (2012) Oomycetes, effectors, and all that jazz. *Current Opinion in Plant Biology*, 15(4), 483-492.

Burton, R. A., Jobling, S. A., Harvey, A. J., Shirley, N. J., Mather, D. E., Bacic, A. & Fincher, G. B. (2008) The genetics and transcriptional profiles of the cellulose synthase-like hvcslf gene family in barley. *Plant Physiology*, 146(4), 1821-1833.

Cabras, P. & Angioni, A. (2000) Pesticide residues in grapes, wine, and their processing products. *Journal of Agricultural and Food Chemistry*, 48(4), 967-973.

Cavinder, B., Hamam, A., Lew, R. R. & Trail, F. (2011) Mid1, a mechanosensitive calcium ion channel, affects growth, development, and ascospore discharge in the filamentous fungus *Gibberella zeae*. *Eukaryotic Cell*, 10(6), 832-841.

Comino, P., Shelat, K., Collins, H., Lahnstein, J. & Gidley, M. J. (2013) Separation and purification of soluble polymers and cell wall fractions from wheat, rye and hull less barley endosperm flours for structure-nutrition studies. *Journal of Agricultural and Food Chemistry*, 61(49), 12111-12122.

da Silva Ferreira, M. E., Heinekamp, T., Härtl, A., Brakhage, A. A., Semighini, C. P., Harris, S. D., Savoldi, M., de Gouvêa, P. F., de Souza Goldman, M. H. & Goldman, G. H. (2007) Functional characterization of the *Aspergillus fumigatus* calcineurin. *Fungal Genetics and Biology*, 44(3), 219-230.

Danecek, P., Bonfield, J. K., Liddle, J., Marshall, J., Ohan, V., Pollard, M. O., Whitwham, A., Keane, T., McCarthy, S. A., Davies, R. M. & Li, H. (2021) Twelve years of SAMtools and BCFtools. *GigaScience*, 10(2), giab008.

Derevnina, L., Petre, B., Kellner, R., Dagdas, Y. F., Sarowar, M. N., Giannakopoulou, A., De la Concepcion, J. C., Chaparro-Garcia, A., Pennington, H. G., van West, P. & Kamoun, S. (2016) Emerging oomycete threats to plants and animals. *Philosophical Transactions of the Royal Society B: Biological Sciences*, 371(1709).

Dobin, A., Davis, C. A., Schlesinger, F., Drenkow, J., Zaleski, C., Jha, S., Batut, P., Chaisson, M. & Gingeras, T. R. (2012) STAR: ultrafast universal RNA-seq aligner. *Bioinformatics*, 29(1), 15-21.

Dracatos, P. M., van der Weerden, N. L., Carroll, K. T., Johnson, E. D., Plummer, K. M. & Anderson, M. A. (2014) Inhibition of cereal rust fungi by both class I and II defensins derived from the flowers of *Nicotiana alata*. *Molecular Plant Pathology*, 15(1), 67-79.

Fisher, M. C., Henk, D. A., Briggs, C. J., Brownstein, J. S., Madoff, L. C., McCraw, S. L. & Gurr, S. J. (2012) Emerging fungal threats to animal, plant and ecosystem health. *Nature*, 484(7393), 186-194.

Gao, A.G., Hakimi, S. M., Mittanck, C. A., Wu, Y., Woerner, B. M., Stark, D. M., Shah, D. M., Liang, J. & Rommens, C. M. T. (2000) Fungal pathogen protection in potato by expression of a plant defensin peptide. *Nature Biotechnology*, 18(12), 1307-1310.

Gauberg, J., Elkhatib, W., Smith, C. L., Singh, A., & Senatore, A. (2022) Divergent Ca^{2+}/calmodulin feedback regulation of CaV1 and CaV2 voltage-gated calcium channels evolved in the common ancestor of Placozoa and Bilateria. *The Journal of Biological Chemistry*, 298(4), 101741.

Hansen, E. M., Reeser, P. W. & Sutton, W. (2012) Phytophthora beyond agriculture. *Annual Review of Phytopathology*, 50, 359-378.

Hardham, A. R. (2005) *Phytophthora cinnamomi*. *Molecular Plant Pathology*, 6(6), 589-604.

Haverkort, A. J., Boonekamp, P. M., Hutten, R., Jacobsen, E., Lotz, L. A. P., Kessel, G. J. T., Visser, R. G. F. & van der Vossen, E. A. G. (2008) Societal costs of late blight in potato and prospects of durable resistance through cisgenic modification. *Potato Research*, 51(1), 47-57.

Hayes, B. M., Bleackley, M. R., Wiltshire, J. L., Anderson, M. A., Traven, A. & van der Weerden, N. L. (2013) Identification and mechanism of action of the plant defensin NaD1 as a new member of the antifungal drug arsenal against *Candida albicans*. *Antimicrobial Agents and Chemotherapy*, 57(8), 3667-3675.

Hayes, B. M. E., Bleackley, M. R., Anderson, M. A., & van der Weerden, N. L. (2018) The plant defensin NaD1 enters the cytoplasm of *Candida albicans* via endocytosis. *Journal of fungi*, 4(1), 20.

Järvå, M., Lay, F. T., Phan, T. K., Humble, C., Poon, I. K. H., Bleackley, M. R., Anderson, M. A., Hulett, M. D. & Kvansakul, M. (2018) X-ray structure of a carpet-like antimicrobial defensin–phospholipid membrane disruption complex. *Nature Communications*, 9(1), 1962.

Judelson, H. S. (2012) Dynamics and innovations within oomycete genomes: insights into biology, pathology, and evolution. *Eukaryot Cell*, 11(11), 1304-1312.

Jung, T., Colquhoun, I. J. & Hardy, G. E. S. J. (2013) New insights into the survival strategy of the invasive soilborne pathogen *Phytophthora cinnamomi* in different natural ecosystems in Western Australia. *Forest Pathology*, 43(4), 266-288.

Kamoun, S. (2006) A catalogue of the effector secretome of plant pathogenic oomycetes. *Annual Review of Phytopathology*, 44, 41-60.

Kamoun, S., Furzer, O., Jones, J. D., Judelson, H. S., Ali, G. S., Dalio, R. J., Roy, S. G., Schena, L., Zambounis, A., Panabières, F., Cahill, D., Ruocco, M., Figueiredo, A., Chen, X. R., Hulvey, J., Stam, R., Lamour, K., Gijzen, M., Tyler, B. M., Grünwald, N. J., Mukhtar, M. S., Tomé, D. F., Tör, M., Van Den Ackerveken, G., McDowell, J., Daayf, F., Fry, W. E., Lindqvist-Kreuze, H., Meijer, H. J., Petre, B., Ristaino, J., Yoshida, K., Birch, P. R. & Govers, F. (2015a) The Top 10 oomycete pathogens in molecular plant pathology. *Molecular Plant Pathology*, 16(4), 413-34.

Kamoun, S., Furzer, O., Jones, J. D. G., Judelson, H. S., Ali, G. S., Dalio, R. J. D., Roy, S. G., Schena, L., Zambounis, A., Panabières, F., Cahill, D., Ruocco, M., Figueiredo, A., Chen, X.-R., Hulvey, J., Stam, R., Lamour, K., Gijzen, M., Tyler, B. M., Grünwald, N. J., Mukhtar, M. S., Tomé, D. F. A., Tör, M., Van Den Ackerveken, G., McDowell, J., Daayf, F., Fry, W. E., Lindqvist-Kreuze, H., Meijer, H. J. G., Petre, B., Ristaino, J., Yoshida, K., Birch, P. R. J. & Govers, F. (2015b) The Top 10 oomycete pathogens in molecular plant pathology. *Molecular Plant Pathology*, 16(4), 413-434.

Kasuga, T., Kozanitas, M., Bui, M., Hüberli, D., Rizzo, D. M. & Garbelotto, M. (2012) Phenotypic diversification is associated with host-induced transposon derepression in the sudden oak death pathogen *Phytophthora ramorum*. *PLoS One*, 7(4), e34728.

Lange, M. & Peiter, E. (2019) Calcium transport proteins in fungi: The phylogenetic diversity of their relevance for growth, virulence, and stress resistance. *Frontiers in Microbiology*, 10, 3100.

Lay, F. T., Brugliera, F. & Anderson, M. A. (2003) Isolation and properties of floral defensins from ornamental tobacco and petunia. *Plant Physiology*, 131(3), 1283-1293.

Lay, T. F. & Anderson, A. M. (2005) Defensins - Components of the innate immune system in plants. *Current Protein & Peptide Science*, 6(1), 85-101.

Li, T., Cai, M., Wang, W., Dai, T., Zhang, C., Zhang, B., Shen, J., Wang, Y. & Liu, X. (2022) PcCesA1 is involved in the polar growth, cellulose synthesis, and glycosidic linkage crosslinking in the cell wall of *Phytophthora capsici*. *International Journal of Biological Macromolecules*, 208, 720-730.

Liao, Y., Smyth, G. K. & Shi, W. (2013) featureCounts: an efficient general purpose program for assigning sequence reads to genomic features. *Bioinformatics*, 30(7), 923-930.

Liu, P., Gong, J., Ding, X., Jiang, Y., Chen, G., Li, B., Weng, Q. & Chen, Q. (2016) The l-type Ca^{2+} channel blocker nifedipine inhibits mycelial growth, sporulation, and virulence of *Phytophthora capsici*. *Frontiers in Microbiology*, 7.

Luna-Tapia, A., DeJarnette, C., Sansevere, E., Reitler, P., Butts, A., Hevener, K. E. & Palmer, G. E. (2019) The vacuolar Ca^{2+} ATPase pump Pmc1p is required for *Candida albicans* pathogenesis. *mSphere*, 4(1), e00715-18.

McColl, A. I., Bleackley, M. R., Anderson, M. A. & Lowe, R. G. T. (2018) Resistance to the plant defensin Nad1 features modifications to the cell wall and osmo-regulation pathways of yeast. *Frontiers in Microbiology*, 9.

McDonald, B. A. & Linde, C. (2002) Pathogen population genetics, evolutionary potential, and durable resistance. *Annual Review of Phytopathology*, 40(1), 349-379.

Mélida, H., Sandoval-Sierra, J. V., Diéguez-Uribeondo, J. & Bulone, V. (2013) Analyses of extracellular carbohydrates in oomycetes unveil the existence of three different cell wall types. *Eukaryot Cell*, 12(2), 194-203.

Moran, Y. & Zakon, H. H. (2014) The evolution of the four subunits of voltage-gated calcium channels: ancient roots, increasing complexity, and multiple losses. *Genome Biology and Evolution*, 6(9), 2210-2217.

Naveena Lavanya Latha, J. & Maruthi Mohan, P. (2011) Role of cell wall bound calcium in *Neurospora crassa*. *Microbiological Research*, 166(5), 419-429.

Nicolopoulou-Stamati, P., Maipas, S., Kotampasi, C., Stamatis, P. & Hens, L. (2016) Chemical pesticides and human health: The urgent need for a new concept in agriculture. *Frontiers in Public Health*, 4, 148.

Ozeki-Miyawaki, C., Moriya, Y., Tatsumi, H., Iida, H. & Sokabe, M. (2005) Identification of functional domains of Mid1, a stretch-activated channel component, necessary for localization to the plasma membrane and Ca^{2+} permeation. *Experimental Cell Research*, 311(1), 84-95.

Payne, J. A., Bleackley, M. R., Lee, T. H., Shafee, T. M., Poon, I. K., Hulett, M. D., Aguilar, M. I., van der Weerden, N. L. & Anderson, M. A. (2016) The plant defensin NaD1 introduces membrane disorder through a specific interaction with the lipid, phosphatidylinositol 4,5 bisphosphate. *Biochimica et Biophysica Acta (BBA) - Biomembranes*, 1858(6), 1099-1109.

Pettolino, F. A., Walsh, C., Fincher, G. B. & Bacic, A. (2012) Determining the polysaccharide composition of plant cell walls. *Nature Protocols*, 7(9), 1590-1607.

Pittman, J. K. (2011) Vacuolar Ca^{2+} uptake. *Cell Calcium*, 50(2), 139-146.

Poon, I. K. H., Baxter, A. A., Lay, F. T., Mills, G. D., Adda, C. G., Payne, J. A. E., Phan, T. K., Ryan, G. F., White, J. A., Veneer, P. K., van der Weerden, N. L., Anderson, M. A., Kvansakul, M. & Hulett, M. D. (2014) Phosphoinositide-mediated oligomerization of a defensin induces cell lysis. *eLife*, 3, e01808.

Portieles, R., Ayra, C., Gonzalez, E., Gallo, A., Rodriguez, R., Chacón, O., López, Y., Rodriguez, M., Castillo, J., Pujol, M., Enriquez, G., Borroto, C., Trujillo, L., Thomma, B. P. & Borrás-Hidalgo, O. (2010) NmDef02, a novel antimicrobial gene isolated from Nicotiana megalosiphon confers high-level pathogen resistance under greenhouse and field conditions. *Plant Biotechnology Journal*, 8(6), 678-690.

Ramamoorthy, V., Cahoon, E. B., Li, J., Thokala, M., Minto, R. E. & Shah, D. M. (2007a) Glucosylceramide synthase is essential for alfalfa defensin-mediated growth inhibition but not for pathogenicity of *Fusarium graminearum*. *Molecular Microbiology*, 66(3), 771-786.

Ramamoorthy, V., Zhao, X., Snyder, A. K., Xu, J. R. & Shah, D. M. (2007b) Two mitogen-activated protein kinase signalling cascades mediate basal resistance to antifungal plant defensins in *Fusarium graminearum*. *Cellular Microbiology*, 9(6), 1491-506.

Rayner, A. D. M. (1991) The challenge of the individualistic mycelium. *Mycologia*, 83(1), 48-71.

Reyes-Chilpa, R., Quiroz-Vazquez, R., Jiménez-Estrada, M., Navarro-Oca a, A. & Cassani-Hernández, J. (1997) Antifungal activity of selected plant secondary metabolites against *Coriolus versicolor*. *Journal of Tropical Forest Products*, 3, 110-113.

Schmid, J. & Harold, F. M. (1988) Dual roles for calcium ions in apical growth of *Neurospora crassa*. *Microbiology*, 134(9), 2623-2631.

Schornack, S., Huitema, E., Cano, L. M., Bozkurt, T. O., Oliva, R., Van Damme, M., Schwizer, S., Raffaele, S., Chaparro-Garcia, A., Farrer, R., Segretin, M. E., Bos, J., Haas, B. J., Zody, M. C., Nusbaum, C., Win, J., Thines, M., & Kamoun, S. (2009) Ten things to know about oomycete effectors. *Molecular Plant Pathology*, 10(6), 795-803.

Spelbrink, R. G., Dilmac, N., Allen, A., Smith, T. J., Shah, D. M. & Hockerman, G. H. (2004) Differential antifungal and calcium channel-blocking activity among structurally related plant defensins. *Plant Physiology*, 135(4), 2055-2067.

Stephens, R. F., Guan, W., Zhorov, B. S. & Spafford, J. D. (2015) Selectivity filters and cysteine-rich extracellular loops in voltage-gated sodium, calcium, and NALCN channels. *Frontiers in Physiology*, 6, 153.

Stotz, H. U., Thomson, J. G. & Wang, Y. (2009) Plant defensins: defense, development and application. *Plant Signaling and Behavior*, 4(11), 1010-1012.

Tam, J. P., Wang, S., Wong, K. H. & Tan, W. L. (2015) Antimicrobial peptides from plants. *Pharmaceuticals (Basel)*, 8(4), 711-757.

Teixeira, V., Feio, M. J. & Bastos, M. (2012) Role of lipids in the interaction of antimicrobial peptides with membranes. *Progress in Lipid Research*, 51(2), 149-177.

Thines, M. (2014) Phylogeny and evolution of plant pathogenic oomycetes—a global overview. *European Journal of Plant Pathology*, 138(3), 431-447.

van der Weerden, N. L. & Anderson, M. A. (2013) Plant defensins: Common fold, multiple functions. *Fungal Biology Reviews*, 26(4), 121-131.

van der Weerden, N. L., Lay, F. T. & Anderson, M. A. (2008) The plant defensin, NaD1, enters the cytoplasm of *Fusarium oxysporum* hyphae. *Journal of Biological Chemistry*, 283(21), 14445-14452.

Wang, C. K., King, G. J., Conibear, A. C., Ramos, M. C., Chaousis, S., Henriques, S. T. & Craik, D. J. (2016) Mirror images of antimicrobial peptides provide reflections on their functions and amyloidogenic properties. *Journal of the American Chemical Society*, 138(17), 5706-5713.

Xie, M., Zhou, X., Xia, Y. & Cao, Y. (2019) Mid1 affects ion transport, cell wall integrity, and host penetration of the entomopathogenic fungus *Metarhizium acridum*. *Applied Microbiology and Biotechnology*, 103(4), 1801-1810.

Yang, X., Tyler, B. M. & Hong, C. (2017) An expanded phylogeny for the genus *Phytophthora*. *IMA Fungus*, 8(2), 355-384.

Zheng, L. & Mackrill, J. J. (2016) Calcium signaling in oomycetes: An evolutionary perspective. *Frontiers in Physiology*, 7, 123.

Supplementary Figures

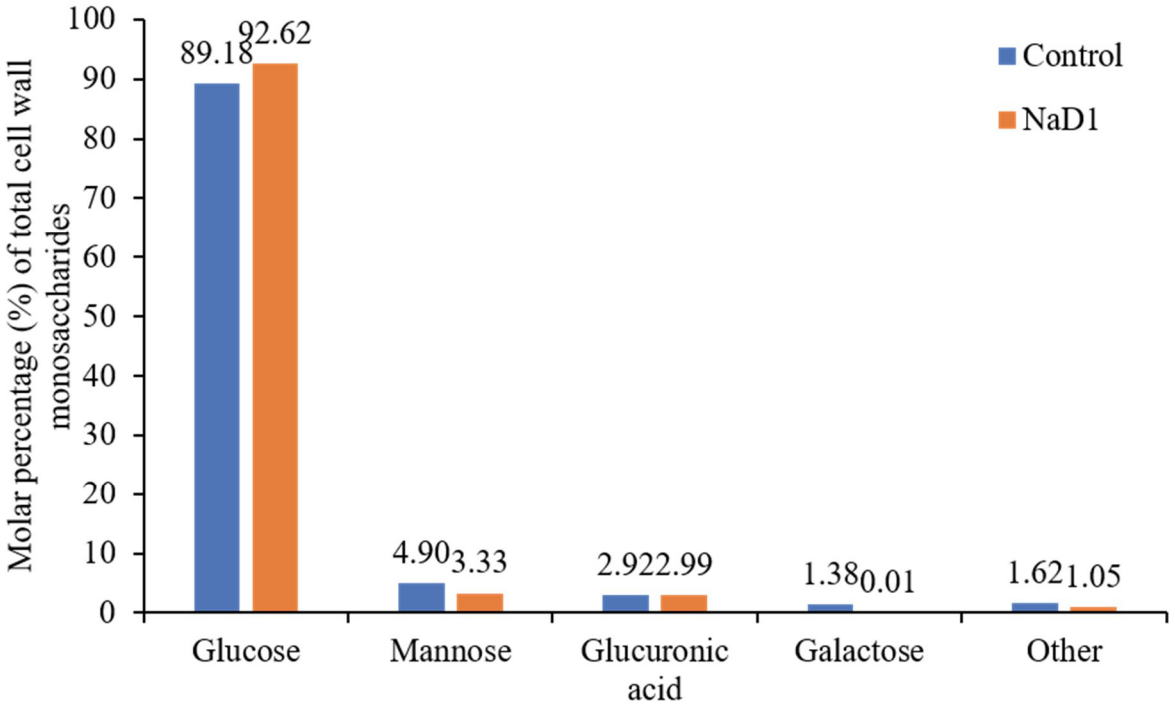

Supplementary Figure 1: Cell wall monosaccharide composition of *P. cinnamomi* cells grown in the absence (Control) and presence of NaD1.

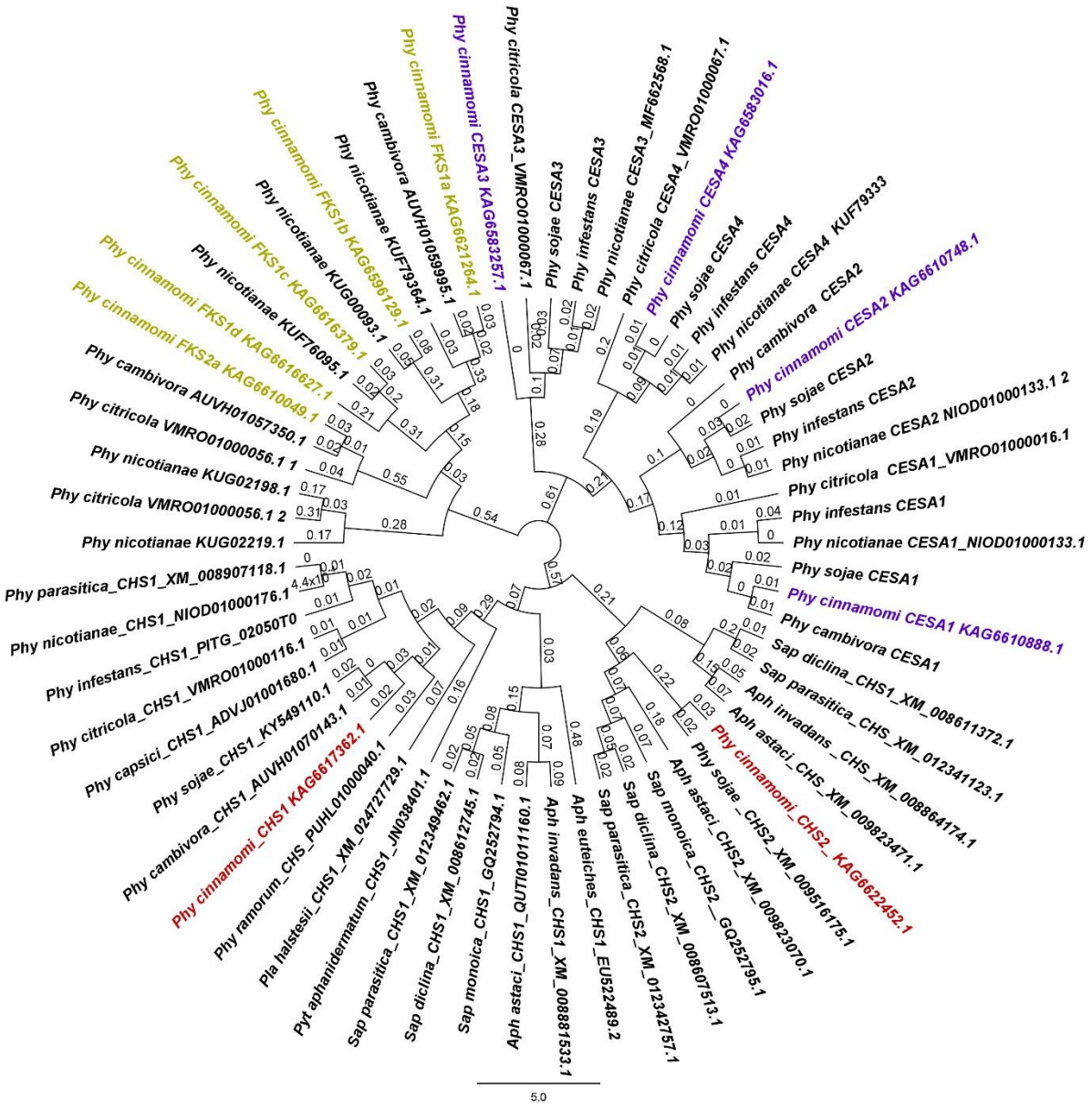

Supplementary Figure 2: Phylogenetic analysis of genes involved in cell wall biosynthesis from different oomycete species.

Phy = *Phytophthora*; Sap = *Saprolegnia*; Aph = *Aphanomyces*; Pyt = *Pythium*; Pla = *Plasmopara*. The tree was generated using alignment-based algorithm followed by maximum likelihood estimation using FastTree. The *CesA*, *Chs*, and *Fks* genes of *P. cinnamomi* are highlighted in purple, red, and pale green, respectively.

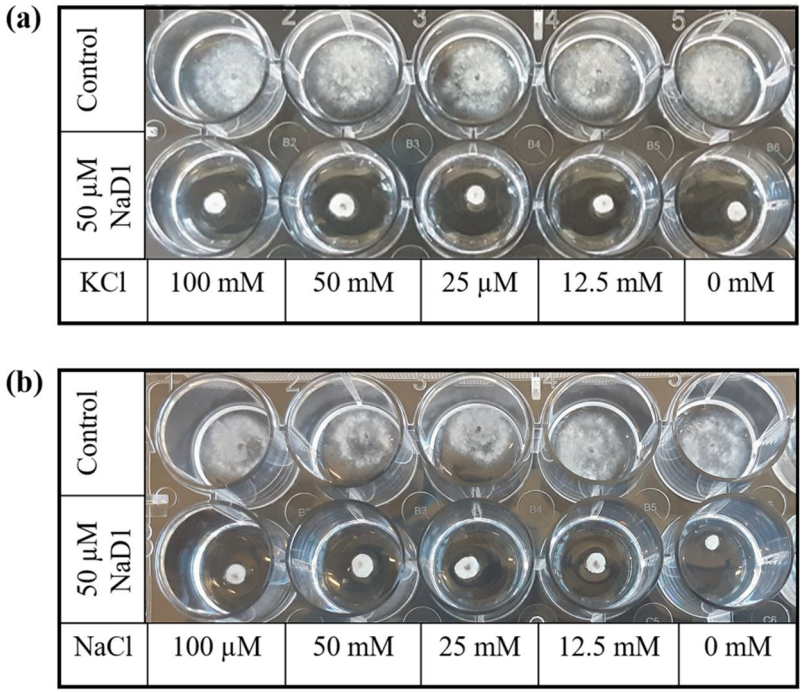

Supplementary Figure 3: Recovery assays showing that the addition of KCl (a) and NaCl (b) in cultures of *P. cinnamomi* cells exposed to NaD1 did not revert growth inhibition. Control: cells grown in the absence of NaD1.

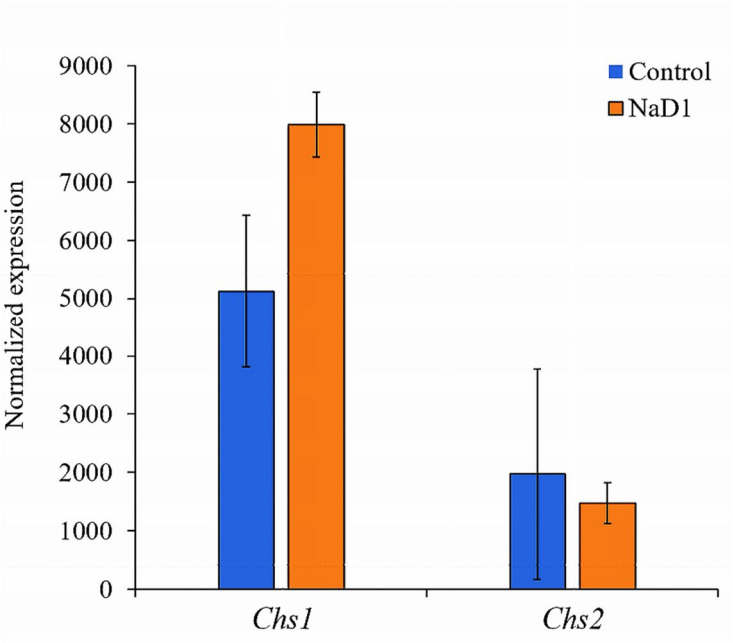

Supplementary Figure 4: q-PCR analysis of putative chitin synthase (*Chs*) genes from *P. cinnamomi*.

Relative normalized expression of the two putative *Chs* genes identified in *P. cinnamomi*. The data are represented as the mean ± standard error of the mean (n = 3).

Supplementary Tables

Supplementary Table 1: Thermal cycling conditions for each gene used for q-PCR analysis.

Gene name	Gene ID	Initial denaturation	Denaturation	Annealing	Extension	End of extension
Ws21 *Tub-B* *Ubc* *G6pdh*	KAG6576187.1 KAG6611174.1 KAG6597952.1 KAG6611192.1	95 °C for 3 min	95 °C for 10s	55 °C for 10s	72 °C for 30s	84 °C for 15s
Chs1 *Chs2*	KAG6617362.1 KAG6622452.1	95 °C for 3 min	95 °C for 10s	55 °C for 10s	72 °C for 30s	83 °C for 15s
CesA1 *CesA2* *CesA3* *CesA4*	KAG6610888.1 KAG6610748.1 KAG6583257.1 KAG6583016.1	95 °C for 3 min	95 °C for 10s	60 °C for 10s	72 °C for 30s	80 °C for 15s
Fks1a *Fks1b* *Fks1c* *Fks1d* *Fks2a*	KAG6621264.1 KAG6596129.1 KAG6616379.1 KAG6616627.1 KAG6610049.1	95 °C for 3 min	95 °C for 10s	65 °C for 10s	72 °C for 30s	84 °C for 15s
Vgcc2 *Vgcc3* *Pmca2* *Pmca3*	KAG6604562.1 KAG6622298.1 KAG6614297.1 KAG6587129.1	95 °C for 3 min	95 °C for 10s	58 °C for 10s	72 °C for 30s	84 °C for 15s
Pmca1 *Mid1*	KAG6623208.1 KAG6591006.1	95 °C for 3 min	95 °C for 10s	58 °C for 10s	72 °C for 30s	85 °C for 15s

Supplementary Table 2: Primers corresponding to each of the reference genes used in q-PCR analysis.

Gene name	Gene ID	FW primer sequence (5'-3')	REV primer sequence (5'-3')
Ws21	KAG6576187.1	TGGCAAGGAGATCGAGAAGGCC	TCGACTCCACCAGCTGGTCCTCC
Tub-B	KAG6611174.1	CCCAACAACATCAAGGCTAGCG	GGTGGCGTCCTGGTACTGCTGG
Ubc	KAG6597952.1	CCACTGCAACATCAACGCCAACG	GGCGTACTTGGCGGTCCATTCGC
G6pdh	KAG6611192.1	GGCAAGCAGGCCGCATTCGTGCG	GTTCACCAGCTCGTCGCTCTCC

Supplementary Table 3: Primers specific to the cell wall related genes analyzed by q-PCR.

Gene name	Gene ID	FW primer sequence (5'-3')	REV primer sequence (5'-3')
Chs1	KAG6617362.1	CCGGTGCTGTACATCTTCGTGGC	CGCTGGTCCTCTGCGAGGGCGGC
Chs2	KAG6622452.1	ACGTACTTCGTGTCGAGCTCGTGC	CTTGTAGTGCGCCTGCCACTCGG
CesA1	KAG6610888.1	CGGTGACTCGATGCTGTGCGC	CCAACAGCGATGGAGATGGAGCCC
CesA2	KAG6610748.1	AACAGCATCCAGACGTCGCACGG	CCACGACGTTGCCCTGGTCC
CesA3	KAG6583257.1	TTCTTGCCCGTGACGTTCTGCCG	GTCTTTGCCCGTCACACGCGCC

CesA4	KAG6583016.1	CCTGGCAAGTCAGCTGGGCCCC	TACCCGAAGATGGAGTGGTTGGGC
Fks1a	KAG6621264.1	GAAGATGCGCAAGGACGCCGAGGC	TGCCTGCGAGCCGTTGAGTGTCCG
Fks1b	KAG6596129.1	GACTTGTCCGCCACGAACGCCGAGC	CCGGGTACTGCTGCGACTGCAGG
Fks1c	KAG6616379.1	GCACCAAGGGCGAGATGGAGGC	TCTATGGTGCGCTGCCAGCAGG
Fks1d	KAG6616627.1	CGCGCAAGTCGCAACACACGG	TGGACAGCTTGACGATACGAGCGC
Fks2a	KAG6610049.1	GCCATCATGTCGGAGGAGGAGCG	GAATGGCGGAGAAATCGCTCGTGG
Vgcc2	KAG6604562.1	ACGTTTGCCAATGTATGAAGGCG	GCCGTCGTCGTCACAACTG
Vgcc3	KAG6622298.1	ACGTTTGCCAATGTATGAAGGCG	GCCGTCGTCGTCACAACTG
Pmca1	KAG6623208.1	AAACTGAGCTTCGCCGCGC	CGCCGCCAATCTGCTCCTT
Pmca2	KAG6614297.1	ACAGTGCACTAACAGCGCGC	CCTCAGCAGCTTGTGGCTG
Pmca3	KAG6587129.1	TGTTGACGTTCAGCAGCGCC	CCCCTGGATAACGCGCGTA
Mid1	KAG6591006.1	GACCAGCAAGACCGCCGC	CCGTCCGAGTCGCGCTTG

Chapter 3

Analysis of the effect of the chitin synthase inhibitor nikkomycin Z on *Phytophthora* species

Statement of Authorship

Title of Paper	**Analysis of the effect of the chitin synthase inhibitor nikkomycin Z on *Phytophthora* species**
Publication status	Unpublished and unsubmitted work written in manuscript style

Principal Author

Name of Principal Author	Amena Khatun		
Contribution to the Paper	Designed and performed the experiments, Analysed and interpreted the results, wrote the manuscript.		
Overall percentage (%)	80%		
Certification	This paper reports on original research I conducted during the period of my Higher Degree by Research candidature and is not subject to any obligations or contractual agreements with a third party that would constrain its inclusion in this thesis. I am the primary author of this paper.		
Signature		Date	29/06/2023

Co-author Contributions

By signing the Statement of Authorship, each author certifies that:

i. The candidate's stated contribution to the publication is accurate (as detailed above),

ii. Permission is granted for the candidate in include the publication in the thesis, and

iii. The sum of all co-author contributions is equal to 100% less the candidate's stated contribution.

Name of Co-Author	Julian Schwerdt		
Contribution to the paper	Conducted RNA-Seq data analyses and reviewed the manuscript. I hereby certify that the Statement of Authorship is accurate.		
Signature		Date	29/06/2023

Name of Co-Author	Caterina Selva		
Contribution to the paper	Helped in cell wall preparation and reviewed the manuscript. I hereby certify that the Statement of Authorship is accurate.		
Signature		Date	29/06/2023

Name of Co-Author	Natalie Betts		
Contribution to the paper	Helped with primers design at the early stage of the PhD, and also gene expression analysis by qRT-PCR and RNA extraction. I hereby certify that the Statement of Authorship is accurate.		
Signature		Date	29/06/2023

Name of Co-Author	Long Yu		
Contribution to the paper	Helped in cell wall analysis by using GC-MS and HPLC. I hereby certify that the Statement of Authorship is accurate.		
Signature		Date	29/06/2023

Name of Co-Author	Vincent Bulone		
Contribution to the paper	Conceived the project, designed experiments, revised and edited the manuscript; corresponding author. I hereby certify that the Statement of Authorship is accurate.		
Signature		Date	29/06/2023

Analysis of the effect of the chitin synthase inhibitor nikkomycin Z on *Phytophthora* species

Amena Khatun, Julian Schwerdt[§], Caterina Selva[§], Natalie Betts, Long Yu[§] and Vincent Bulone[§,*]

School of Agriculture, Food and Wine, The University of Adelaide, Waite Campus, Urrbrae, South Australia 5064, Australia

[§]Present address: *College of Medicine and Public Health, Flinders University, Bedford Park South Australia 5042, South Australia, Australia*

[*]*To whom correspondence should be addressed: vincent.bulone@flinders.edu.au*

Abstract

Chitin is a biopolymer that plays an essential role in the growth and development of fungi and some oomycete species. Paradoxically, the cell walls of oomycetes from the *Phytophthora* genus are devoid of chitin despite the presence of putative chitin synthase genes in their genomes, and hyphal growth of these micro-organisms is severely affected by nikkomycin Z, a competitive inhibitor of chitin synthases. Here, we aimed to determine the mode of action of nikkomycin Z in *Phytophthora* species and shed light on the function of the chitin synthase genes in these micro-organisms. We first confirmed that nikkomycin Z inhibits mycelial growth of several species, namely *Phytophthora cinnamomi*, *Phytophthora cambivora*, *Phytophthora citricola*, and *Phytophthora nicotianae*. Further characterisation using *P. cinnamomi* as a model species revealed that exposure to nikkomycin Z is accompanied by tip bursting and abnormal hyphal growth as well as a decreased level of cellulose in the hyphal cell walls. In addition, treatment with the inhibitor affected the level of expression of genes playing vital roles in the micro-organism, i.e., genes related to cell wall biosynthesis, the uridine diphosphate N-acetylglucosamine pathway, glycosylphosphatidylinositol (GPI) anchored proteins, effector proteins, and chitin deacetylases. Our data suggest that nikkomycin Z has a wide range of effects on *Phytophthora* species that might be useful in guiding the development of future anti-oomycete drugs.

Keywords: Chitin synthase, hyphal growth, nikkomycin Z, oomycetes, *Phytophthora*, RNA-Seq.

Introduction

Phytophthora cinnamomi is a notorious oomycete phytopathogen infecting ~5000 plant species and is among the most devastating invasive species currently known, posing a significant threat to both natural ecosystems and horticulture worldwide (Cahill *et al.*, 2008; Jung *et al.*, 2013; Kamoun *et al.*, 2015). The pathogen is distributed throughout temperate and tropical regions. However, it is most destructive in Mediterranean climates (Shearer *et al.*, 2007). The scale of the threat posed by *P. cinnamomi* is exemplified by the situation in the South-West botanical province of Western Australia, a region renowned for biodiversity, where 40% of the 5710 recorded plant species is vulnerable. Aware of this significant problem, the 1999 Australian Environment Protection and Biodiversity Conservation (EPBC) Act includes provisions to protect native plants from the dieback disease caused by *P. cinnamomi*. Recommendations include an integrated disease management approach which includes the use of hygiene measures and chemicals, such as phosphonates, potassium phosphite and phenylamide fungicides (Belisle *et al.*, 2019; "Environment protection and biodiversity conservation act," 1999; Hu *et al.*, 2010). Carboxylic acid amide (CAA) fungicides are also being used to control *Phytophthora* diseases, and the Fungicide Resistance Action Committee (FRAC) is proposing new recommendations each year for optimal usage of CAA fungicides to avoid the risk of resistance development. However, in recent years insensitivity to these chemicals has been reported in oomycete phytopathogens, including several species of *Phytophthora* (Cai *et al.*, 2021; Chen *et al.*, 2012; *FRAC Recommendations for CAA fungicides 2023*; Gent *et al.*, 2020; González-Tobón *et al.*, 2020; Rubin *et al.*, 2008). Indeed, one significant drawback of these compounds is that they cannot completely eradicate *Phytophthora* from an infected area, which increases the risk of emergence of resistance. Consequently, existing procedures to protect native plants from *Phytophthora* infections largely depend on hygiene measures, e.g., regular sanitation, the use of disease free-soil and plant materials, optimized fertilization processes, and adequate drainage. Enforcing these measures in agricultural fields and native forests, where these pathogens are most easily spread, presents many insurmountable challenges. It is therefore necessary to develop new methodologies to control *Phytophthora* species so that we can safeguard crops and protect natural ecosystems already challenged by human activities and (a)biotic stresses.

Cell walls are extracellular polysaccharide-rich matrices that surround the cells of many organisms, providing mechanical support and protection from the external environment. In microbial pathogens, cell walls are the primary point of contact with the host. Cell wall composition is highly diverse and complex, even among closely related species. In oomycetes

and other microbial pathogens this diversity presents a challenge for developing effective and broad-spectrum antimicrobial agents. However, it also offers opportunities for developing targeted therapies that exploit the unique features of specific cell wall structures. A promising approach for controlling oomycete diseases involves targeting the enzymes responsible for the biosynthesis of major cell wall polysaccharides such as cellulose and β-1,3-glucans, and, in some oomycetes, chitin (Blum *et al.*, 2010; Blum & Gisi, 2012; Guerriero *et al.*, 2010; Hinkel & Ospina-Giraldo, 2017; Piotrowski *et al.*, 2015).

The composition of a typical *Phytophthor*a cell wall consists of approximately 34% cellulose, 20% β-1,3-glucan, and 18% β-1,3;1,6-glucan (Li *et al.*, 2022; Mélida *et al.*, 2013). At the time of writing, no N-acetylglucosamine (GlcNAc), the constituent monosaccharide of chitin, has been detected in the cell wall of *Phytophthora* hyphae through biochemical analysis (Li *et al.*, 2022; Mélida *et al.*, 2013). Despite this observation, *Phytophthora* species contain 1 to 2 chitin synthase genes, nominally chitin synthase 1 (*Chs1*) and chitin synthase 2 (*Chs2*) (Klinter *et al.*, 2019). It has been reported that the *Chs1* gene in *P. sojae*, which is an ortholog of the *Chs* genes found in other *Phytophthora* species that have only one *Chs* gene (Klinter *et al.*, 2019), exhibits significantly high expression levels during asexual reproduction, including during sporangia development, formation of mature zoospores, and germination of encysted zoospores (cysts) (Cheng *et al.*, 2019; Hinkel & Ospina-Giraldo, 2017). Furthermore, Cheng *et al*. (2019) demonstrated that asexual reproduction stages exhibited fluorescence signals when stained with wheat germ agglutinin (WGA), indicating the presence of chitin in the cell walls formed during this part of the cell cycle. Thus, it can be hypothesised that chitin biosynthesis may occur during asexual reproduction to strengthen the cell coat of specialised cells such as zoospores, whose composition differs from the typical composition of oomycete cells from other life stages (Bartnicki-Garcia, 1983).

Interestingly, even though the mycelial growth stage is devoid of chitin in *Phytophthora* species, this class of micro-organisms shows sensitivity to the chitin synthase inhibitor nikkomycin Z (Cheng *et al.*, 2019; Fuechtbauer *et al.*, 2018; Hinkel & Ospina-Giraldo, 2017). Nikkomycin Z is a natural compound produced by *Streptomyces* species that shows promise as an antifungal agent and is currently undergoing Phase 1 clinical trials for the treatment of fungal diseases in humans and animals (Larwood, 2020). In fungi, nikkomycin Z competitively binds the catalytic domain of chitin synthases (CHS), affecting chitin biosynthesis and overall fungal growth (Bentz *et al.*, 2021; Sass *et al.*, 2021). Similarly, most tested *Phytophthora* species have been found to be sensitive to nikkomycin Z, but some, such as *P. sojae*, are less sensitive to the compound (Cheng *et al.*, 2019; Hinkel & Ospina-Giraldo, 2017). However, a recent study

showed that nikkomycin Z blocks the activity of a recombinant form of CHS1 from *P. sojae*, which was expressed and purified from HEK293F cells following recombinant plasmid transfection (Chen *et al.*, 2022). Therefore, further research is necessary to understand the precise mechanism and conditions by which nikkomycin Z inhibits mycelial growth in *Phytophthora* species, particularly in the absence or limited presence of chitin biosynthesis. A comprehensive analysis of this phenomenon is required to understand the role of chitin biosynthesis in *Phytophthora* and discover potential new target sites for designing future anti-oomycete drugs to control this phytopathogenic group.

Here, we provide a detailed examination of the effects of nikkomycin Z on the devastating phytopathogen *P. cinnamomi.* We first examined the effect of nikkomycin Z on the growth and ultrastructure of *P. cinnamomi* hyphal cells using optical and electron microscopy. This was followed by the characterization of the cell wall composition of *P. cinnamomi* and transcriptomic analysis to investigate the effect of the inhibitor on gene expression. The data shed light on the different cell and biochemical processes affected by nikkomycin Z, which paves the way for the development of novel anti-oomycete compounds.

Materials and Methods

Phytophthora strains

Four *Phytophthora* species, i.e., *P. cinnamomi*, *P. citricola*, *P. cambivora*, and *P. nicotianae*, were obtained from the Plant Pathology & Mycology Herbarium in New South Wales, Australia. Mycelial cultures of all species were maintained in Petri dishes containing potato dextrose agar (PDA) as a growth medium on which sterilized poppy seeds were evenly distributed. After 5 days of culture at 25°C in the dark, the seeds covered by mycelium were used as an inoculum for liquid medium.

Nikkomycin Z treatment

Individual poppy seeds covered with mycelium from each of the four *Phytophthora* species were transferred to each well of 24-well plates (Corning Inc, US) containing 500 µl of liquid potato dextrose broth (PDB) and different concentrations of nikkomycin Z: 65, 125, 250, 500 and 1000 µM. A control was performed in the absence of nikkomycin Z. After 48 h incubation, the minimal inhibitory dose of nikkomycin Z was determined by observing the inhibitory effect of the molecule on mycelial growth and the percentage of growth inhibition was determined as described earlier (Reyes-Chilpa *et al.*, 1997). This experiment was repeated three times for each *Phytophthora* species.

Optical and electron microscopy observations

Based on the growth inhibition rate, the selected dose of Nikkomycin Z was tested on the four *Phytophthora* species. At first, an Olympus ix70 inverted microscope was used to observe any morphological difference in *Phytophthora* species exposed to nikkomycin Z. The control and nikkomycin Z treated mycelia of *P. cinnamomi* were subjected to both Scanning Electron Microscopy (SEM) and Transmission Electron Microscopy (TEM) analysis. The mycelia were grown for two days and incubated in a fixative solution containing 2.5% (v/v) glutaraldehyde, 4% formaldehyde and 4% sucrose overnight. TEM and SEM samples were incubated in 2% osmium tetroxide for 2 h and the TEM samples were pre-embedded in a 1% agar block. After fixation, a series of aqueous ethanol solutions of 30%, 50%, 70%, 80%, 90% (v/v) was used to dehydrate the SEM and TEM samples (30 min incubation in each ethanol solution). Samples were then washed with ethanol: propylene oxide (1:1) (30 min) and 100% propylene oxide (ProScieTech C156) (1 h). SEM samples were dried using a Leica EM CPD300 critical point dryer and the agar pre-embedded TEM samples were embedded in 100% resin (Procure Araldite, ProScieTech, AUS) at 60°C in an oven for one day. An ultramicrotome (Leica EM UC6) was used for sectioning the TEM samples, which were subsequently deposited carbon-coated TEM grids. Besides, SEM samples were securely mounted on SEM stubs following ultra-thin carbon coating. Finally, the samples were observed using a FEI Tecnai G2 Spirit TEM microscope and a FEI Quanta 450 FEG Environmental SEM microscope.

Preparation of cell wall polysaccharides

The control and nikkomycin Z treated mycelia from *P. cinnamomi* (48 h old) were collected separately from three replicates and washed five times with sterilised Milli-Q water. Mycelia from multiple control and nikkomycin Z wells were pooled into respective groups, and cell walls were prepared as described earlier (Mélida *et al*., 2013). For this purpose, the control and nikkomycin Z samples were snap-frozen and ground in liquid nitrogen using a mortar and pestle, and cell walls were prepared by incubating the powders in 70% (vol/vol) ethanol for 6, 8 and 12 h on a rotator at room temperature (RT). The cell wall materials were successively recovered by centrifugation at 4,000 × g for 10 min at 4°C, resuspended and washed 6 times by filtration through glass-fibre filters (GF/A; Whatman) using 70% ethanol and 100% acetone. The cell walls were dried overnight at RT after the last wash with acetone. About 15 ml of 80% (vol/vol) CH_3OH containing 5% (wt/vol) potassium hydroxide and 0.1% (wt/vol) sodium borohydride was added to 50 mg of the cell walls from each sample type (control and nikkomycin Z treated). The suspensions were heated for 15 min at 100°C and the resulting

alkali soluble fraction (ASF) and alkali insoluble fraction (AIF) were recovered by centrifugation at 4,000 × g for 10 min. This step was repeated three times. After the third extraction, 5 ml of 0.5 M acetic acid was added to the AIF material to wash the alkali insoluble fractions. Next, the wash solution was added to the ASF. The pH of the ASF was then adjusted to 6 with acetic acid. The AIF and ASF fractions were dialyzed against 25 litres of Milli-Q water using SnakeSkin™ dialysis tubes of 3.5K MWCO and 22 mm diameter. The dialyzed AIF and ASF fractions were stored at RT until further analysis. The entire process was repeated three times to prepare samples from three independent biological replicates.

Monosaccharide analysis

Total sugar analysis of the AIF and ASF fractions were performed as described by Comino *et al*. (2013) with some amendments. Approximately 1-2 mg of AIF and ASF material from the control cells and their counterpart exposed to nikkomycin Z was hydrolysed in two subsequent steps using 2 M trifluoroacetic acid (TFA) at 121°C followed by 6 N HCl at 100°C (Mélida *et al*., 2013). The hydrolysates were diluted 20 times in distilled water and the PMP (1-phenyl-3-methyl-5-pyrazolone)/ammonia reagent was used to derivatize the monosaccharides in the hydrolyzates. An internal standard (0.5 mM 2-deoxy glucose) was added to each sample and the excess of PMP was removed by two consecutive extractions with di-butyl ether. The PMP derivatives were then separated using an Agilent 1200 high-performance liquid chromatography (HPLC) fitted with a C18 Phenomenex Kinetex column (particle size: 2.6 µm; pore size: 100 Å; column dimension 100 × 3 mm;). A sample volume of 10 µl was injected, and the eluent flow rate was 0.8 mL/min at a temperature of 30°C. Eluent A consisted of 10% acetonitrile and 40 mM ammonium acetate pH 6.8, while Eluent B consisted of 70% acetonitrile. The elution gradient was increased from 8 to 16% (B) over 12 min, and absorbance was measured continuously at 250 nm. Standard curves were produced using monosaccharide standards (mannose, ribose, rhamnose, glucosamine, glucuronic acid, galacturonic acid, glucose, galactose, xylose, arabinose, fructose). The monosaccharide content of each sample was determined from peak areas relative to the standard curves and expressed as molar percentage.

Glycosidic linkage analysis

Glycosidic linkage analysis was performed as described earlier (Mélida *et al*., 2013). Firstly, 0.5 to 1 mg of ASF and AIF samples were separately immersed in 200 µL of dry dimethyl sulfoxide (DMSO) in a glass tube. Next, 10 µL of DMSO containing 0.3 mg L^{-1} sulphur dioxide and 5 µL of diethyl amine were added and the samples were sonicated for 20 min.

Permethylated alditol acetates were prepared as described earlier (Mélida *et al*., 2013) and analyzed on an Agilent 7890B/5977B GC–MS instrument fitted with a VF-23 ms capillary column (30 m × 0.25 mm, 0.25 μm) (Agilent Technologies, CA, USA) using helium as the carrier gas. The following temperature program was used: 165°C to 175°C at 1°C /min; 175°C to 195°C at 0.5°C/min; 195°C to 210 °C at 2 °C/min; 210 °C to 250°C at 10 °C /min, followed by a plateau at 250°C for 6.5 min (total run time 68 min). The permethylated alditol acetates were fragmented by electron-impact mass spectrometry and the mass spectra from the resulting fragments were compared to those available in the CCRC Spectral Database (glygen.ccrc.uga.edu) for identification of glycosidic linkages.

RNA extraction and cDNA synthesis

P. cinnamomi hyphae were grown for 48 h in 24-well plates with and without nikkomycin Z. The hyphae were washed with sterilized distilled water, and immediately pulverized in liquid nitrogen using a mortar and pestle. RNA extraction was performed using the Spectrum Plant Total RNA Kit (Signa-Aldrich, ST. Louis, MO, USA) by following the manufacturer's instructions, and DNA was hydrolyzed using DNase I (New England Biolabs, Ipswich, MA, USA). The RNA Clean & Concentrator Kit from Zymo Research (Irvine, CA, USA) was used to improve RNA purity. The quality of purified RNA was assessed using a Thermo Scientific Nanodrop (Thermo Fisher Scientific, Waltham, MA, USA) and Agilent 2100 Bioanalyzer. Library construction and RNA-Seq were performed at the South Australian Genomics Centre (SAGC) using their fee-for-service facility, as described below. cDNA was synthesized using the Invitrogen Superscript IV kit (Invitrogen, Carlsbad, CA, USA) and preserved at -20 °C for further analysis by q-PCR.

Library construction and RNA sequencing

The RNA samples prepared as described above were sequenced on a Novaseq 6000 S1 Lane using 2x100 bp, v1.5 chemistry. Nugen Universal Plus mRNA-seq kit (Part No. 0508, M01442 v2) was used to generate stranded polyA libraries. The Illumina protocol 15048776 v15 was followed for the process of denaturation and on-board clustering. FASTQC (www.bioinformatics.babraham.ac.uk/projects/fastqc/) was used to assess the quality of sequencing reads. STAR 2.7.8a in 2-pass mode (Dobin *et al.*, 2012) was used to align all reads (five technical replicates per treatment group) to the reference genome (ASM1869171v1) of *P. cinnamomi*. Gene count values were determined using featureCounts (Liao *et al.*, 2013). Samtools (Danecek *et al.*, 2021) and BamTools (Barnett *et al.*, 2011) were used to manipulate the SAM/BAM files. Differentially expressed genes (DEGs) were identified by comparing the

control and treatment sets using the DESeq2 pipeline. The count matrix data were obtained from the featureCounts output. In addition, to examine the replication of each group of transcriptomes, principal component analysis (PCA) was performed.

Gene Ontology enrichment analyses

The Blast2 GO software (https://www.blast2go.com/) was used to perform GO annotation. Adjusted p-value (padj) less than 0.05 and Log_2FC is the fold change) greater/less than 1.5 were used for screening DEGs. In addition, the WEGO and TopGO software were used for Gene Ontology (GO) enrichment analysis to elucidate GO functional classification, such as cellular components, molecular functions, and biological processes. We also used clusterProfiler to compare enriched terms in a dot plot image.

q-PCR analysis of cell wall biosynthetic genes identified as differentially expressed by RNA-Seq

qPCR analysis was performed as described earlier (Burton *et al.*, 2008). Three biological replicates were used for qPCR validation, and three technical replicates were included for the amplification reactions. Four reference genes selected based on the report from Yan *et al*. (2006) were used, i.e., *Ws21* (40S ribosomal protein S3A), *Tub-b* (β- tubulin), *Ubc* (Ubiquitin-conjugating enzyme), and *G6pdh* (glyceraldehyde-3-phosphate dehydrogenase). The following cellulose synthase (*CesA*), chitin synthase (*Chs*) and glucan synthase (*Fks*) genes involved in cell wall polysaccharide biosynthesis and identified as described in the previous Chapter of this Thesis were analysed: *CesA1* (KAG6610888.1), *CesA2* (KAG6610748.1), *CesA3* (KAG6583257.1), *CesA4* (KAG6583016.1), *Chs1* (KAG6617362.1), *Chs2* (KAG6622452.1), *Fks1a* (KAG6621264.1), *Fks1b* (KAG6596129.1), *Fks1c* (KAG6616379.1), *Fks1d* (KAG6616627.1), *Fks2a* (KAG6610049.1). The primers used for each gene were as described in the previous Chapter of this Thesis.

Statistical analyses

Graphical presentation and statistical analysis were made using the SPSS statistical software (version 26.0; Chicago, IL, USA) and GraphPad Prism (Version 9). The data are presented as the mean ± standard error of the mean (SEM). Significance levels for differences were determined using independent t-tests and one-way ANOVA, with * indicating $p \leq 0.05$, ** indicating $p \leq 0.01$, and *** indicating $p \leq 0.001$. The post hoc analysis, specifically Tukey's test, was utilized to determine if there were significant differences between specific groups.

Results

Nikkomycin Z inhibits hyphal growth and alters the morphology and ultrastructure of *Phytophthora* hyphae

The effect of nikkomycin Z, a well-known competitive inhibitor of chitin synthases, was analyzed on four *Phytophthora* species, *P. cinnamomi*, *P. citricola*, *P. cambivora*, and *P. nicotianae*. In the presence of 500 µM nikkomycin Z, *P. citricola* showed the highest growth inhibition (74%), followed by *P. cambivora* (70%), *P. cinnamomi* (51%), and *P. nicotianae* (30%) (Figure 1A-1B). This concentration of inhibitor severely affected the morphology of the hyphae compared to the control. Indeed, in the presence of nikkomycin Z, cells appeared thinner, distorted and their tips swelled before eventually bursting, leading to cell death (Figure 1C). These effects are similar to the previously reported effect of 200 µM nikkomycin Z on *Saprolegnia monoica*, a pathogenic oomycete of salmonids (Guerriero *et al.*, 2010). As indicated in the previous Chapter of this Thesis, we decided to focus the next parts of our study on *P. cinnamomi* because this species is economically and environmentally more important than the others. It is indeed a pathogen of a broader range of commercial crops and other plants occurring in a large diversity of ecosystems across all continents.

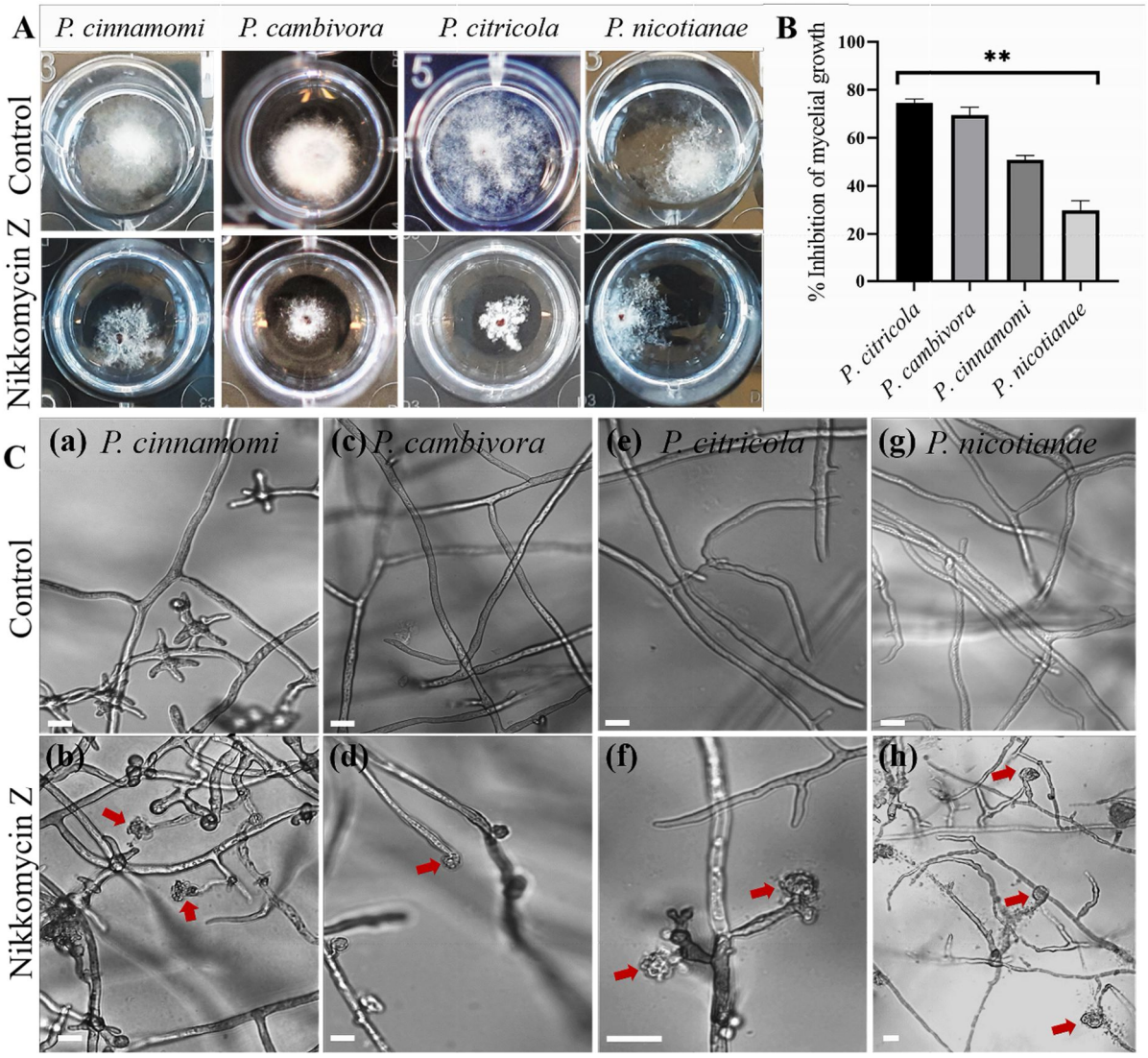

Figure 1: Effect of nikkomycin Z on mycelial growth and morphology of 4 selected *Phytophthora* species.

(A) Mycelial growth of *P. cinnamomi*, *P. cambivora*, *P. citricola*, and *P. nicotianae* after 48 h in a 24-well plate in the absence and presence of 500 µM nikkomycin Z. (B) Inhibition of mycelial growth (%) of each *Phytophthora* species compared to control. '**' indicates significant difference with $p \leq 0.01$ ($n = 5$). (C) Mycelial growth in the absence (panels a, c, e, g) and presence (b, d, f, h) of nikkomycin Z. Scale bars = 10 µm.

SEM observations of the *P. cinnamomi* hyphae grown in the absence of nikkomycin Z revealed a smooth and uniform cell surface (Figure 2A-2B). In the presence of the inhibitor (500 µM), the hyphal tips appeared shrivelled (Figure 2C), knotted (Figure 2D) and, confirming the observations by optical microscopy (Figure 1C), swelling followed by tip bursting occurred, leading to a loss of cell integrity and ultimately cell death (Figure 2E-2F).

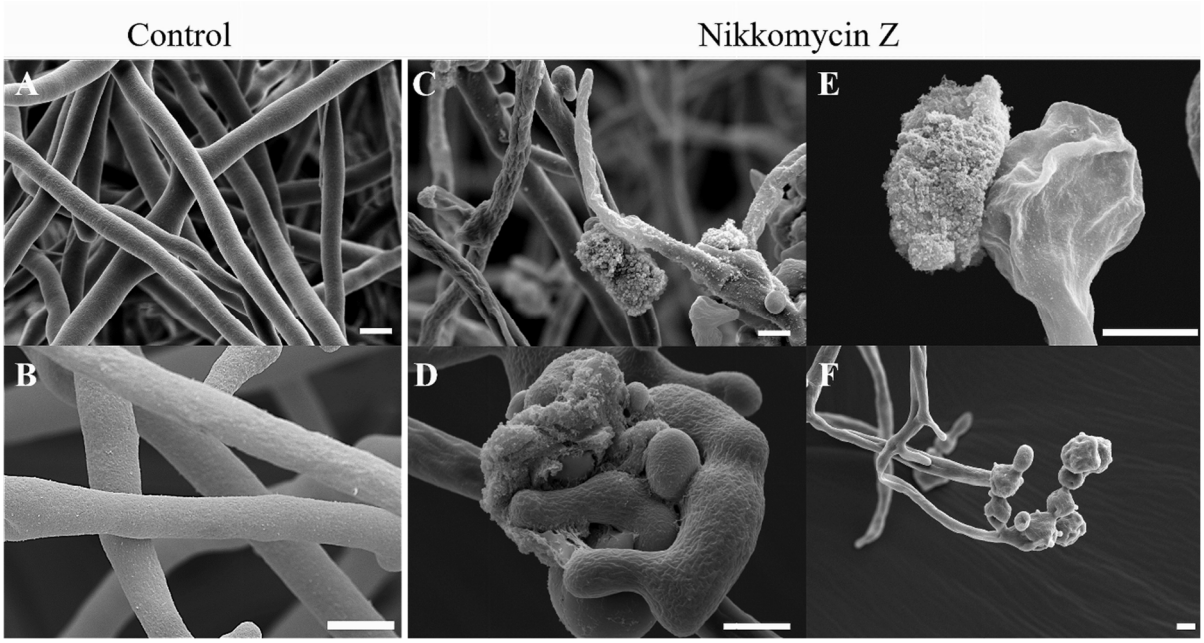

Figure 2: Scanning electron microscopy (SEM) showing the morphology of *P. cinnamomi* hyphal cells exposed to 500 µM nikkomycin Z.

(A, B) Control performed in the absence of nikkomycin Z. (C-F) Growth in the presence of nikkomycin Z showing: (C) Wrinkled and thinner hyphal cells resulting from hyphal tip bursting; (D) knotted hyphae; (E) hyphal tip bursting; and (F) swelled hyphal tip. The experiment was repeated two times. Scale bars = 5 µm.

TEM observations were made to gained further insight into the subcellular ultrastructural changes that accompany these morphological abnormalities. As expected, the untreated control hyphae were characterized by intact organelles, plasma membrane and cell wall (Figure 3A-3B). In the presence of the inhibitor, diverse detrimental effects on intracellular organelles and the cell wall were observed, such as extensive vacuolization (Figure 3C-3F), plasmolysis (Figure 3D) accompanying the extracellular release of the cytoplasmic content and organelles through the bursting area of the hyphal tip (Figure 3F), thicker and irregular cell walls (Figure 3E-3G; Supplementary Figure 1), and disorganised cellular components (Figure 3H). These results clearly demonstrate that nikkomycin Z severely affects hyphal growth, cell morphology, ultrastructure, and stability in *Phytophthora* species, despite the absence of detectable chitin in their cell walls (Mélida *et al.*, 2013).

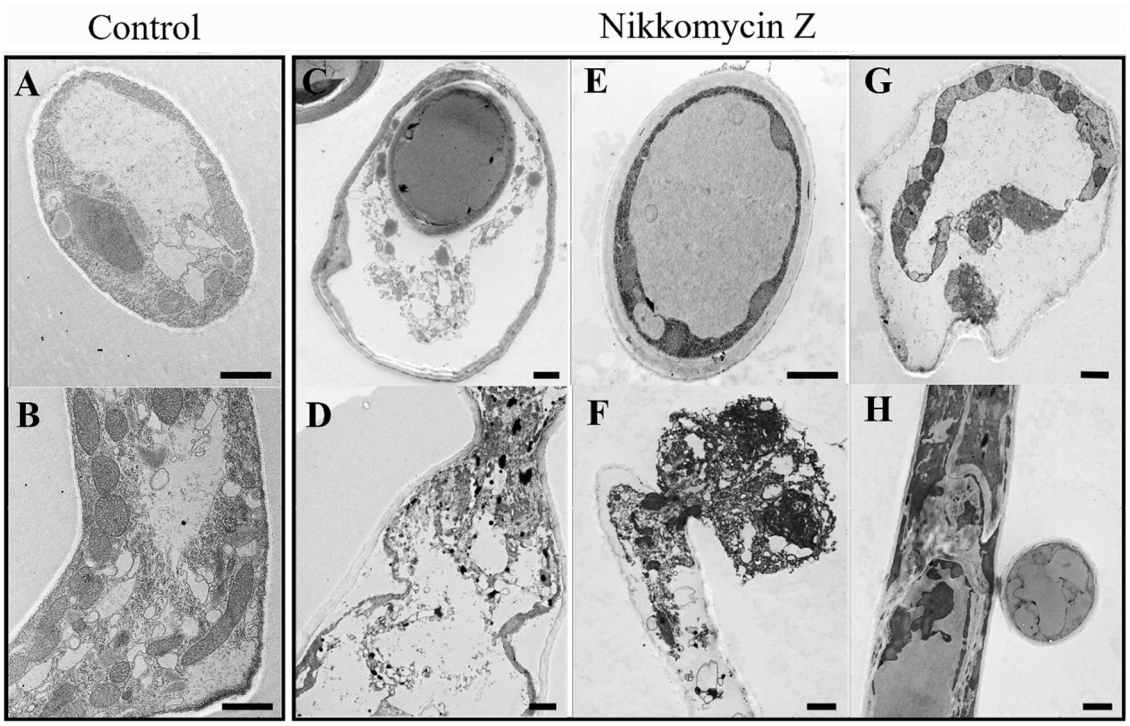

Figure 3: Transmission electron microscopy (TEM) images of *P. cinnamomi* hyphal cells in the presence of 500 µM nikkomycin Z.

Transverse (A) and longitudinal (B) sections of control cells not exposed to the inhibitor. Abnormal morphological and ultrastructural features in cells treated with nikkomycin Z (C-H). Scale bars = 1 µm.

Nikkomycin Z affects the cell wall composition of *P. cinnamomic* hyphal cells

Monosaccharide analysis was performed to determine whether the morphological effects of nikkomycin Z on the cell wall of *P. cinnamomi* reflect differences in cell wall polysaccharide composition. The nikkomycin Z-treated cells were characterized by a significantly decreased proportion of mannosyl residues and increased amounts of glucosyl residues in the ASF fraction (Figure 4), which represented about 25% of the total cell wall, the remaining 75% corresponding to the AIF material. Moreover, the proportion of glucuronosyl residues was significantly increased in both the AIF and ASF materials (Figure 4). No N-acetylglucosamine indicative of the presence of chitin was detected in these fractions, consistent with the earlier observation that hyphal cells of *Phytophthora* species are devoid of chitin (Mélida *et al.*, 2013).

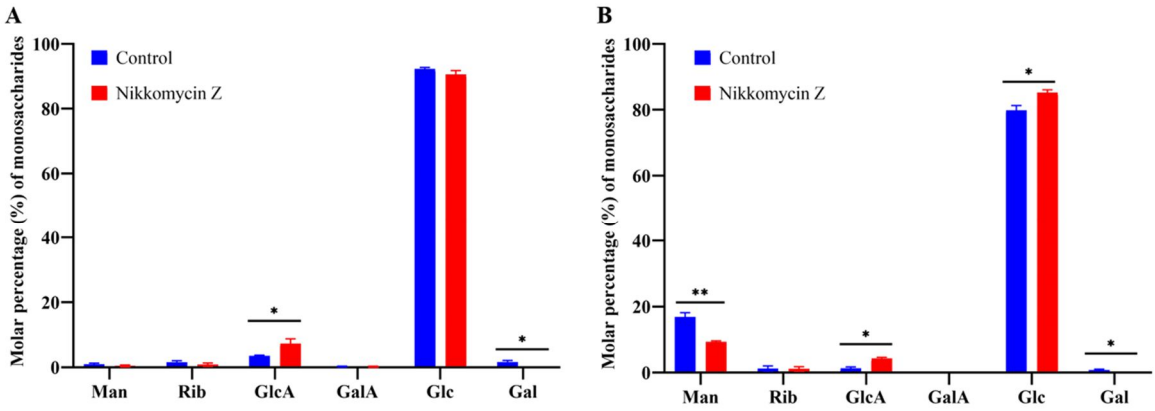

Figure 4: Monosaccharide composition of the mycelial cell wall of *P. cinnamomi* grown in the absence (control) and in the presence of 500 µM nikkomycin Z.

Carbohydrate analysis of (A) Alkali Insoluble Fraction (AIF) and (B) Alkali Soluble Fraction (ASF) from four independent biological replicates (N = 4). '*' indicates $p \leq 0.05$.

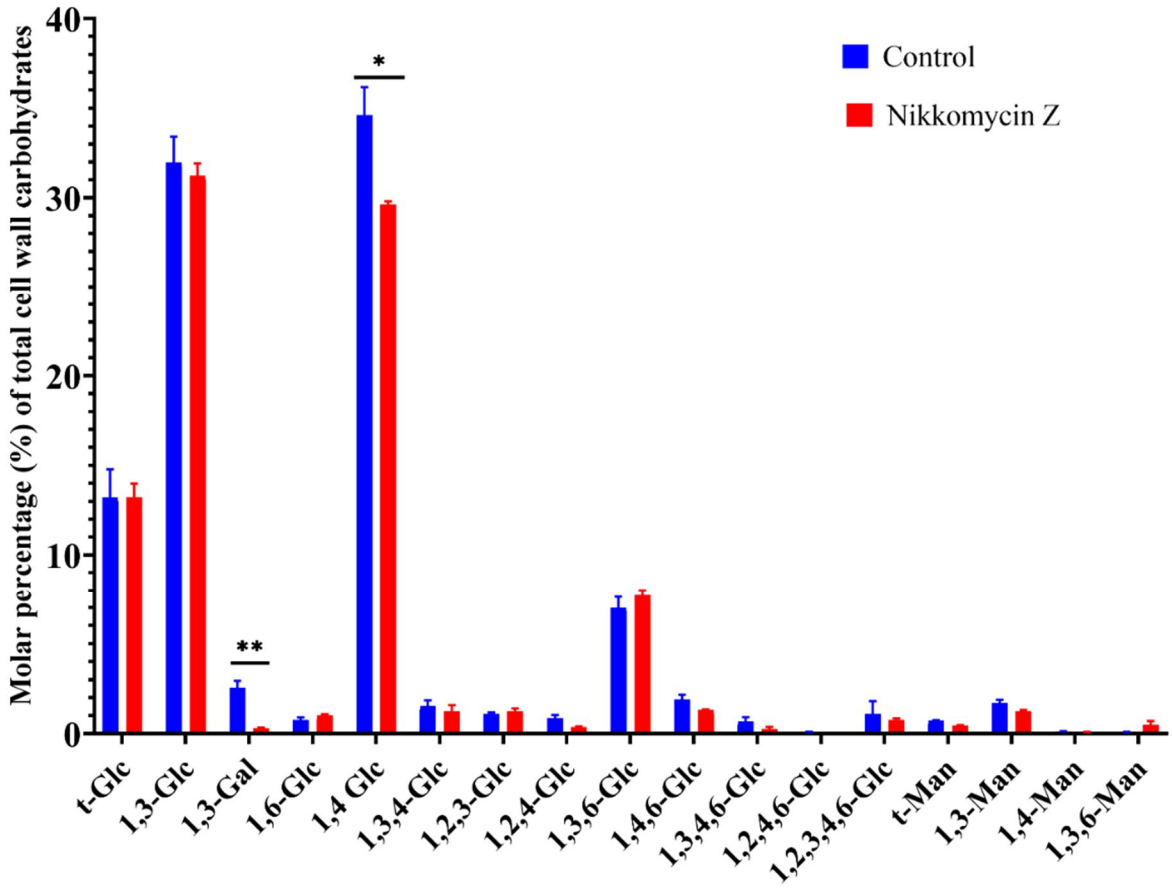

Figure 5: Carbohydrate composition of mycelial cell wall from *P. cinnamomi* grown in the absence (control) and in the presence of 500 µM nikkomycin Z.

Glycosidic linkage analysis was performed on three technical replicates from three independent biological replicates (N = 3). '**' indicates $p \leq 0.01$, and '*' indicates $p \leq 0.05$.

Glycosidic linkage analysis revealed that cell wall content in glucosyl and galactosyl residues changed significantly following treatment with nikkomycin Z. Indeed, the proportion of 1,4-linked glucosyl residues and 1,3-linked galactosyl residues significantly decreased. Owing to the decreased content in 1,4-linked glucosyl residues, which are most abundant in untreated control cells, 1,3-linked glucans became the most abundant polysaccharides in the cells exposed to nikkomycin Z (Figure 5).

RNA-Seq analysis reveals widespread shifts in gene expression upon nikkomycin Z exposure

To gain insight into the mechanism of nikkomycin Z inhibition of *P. cinnamomi*, RNA sequencing was performed to evaluate the differences in gene expression caused by exposure to the inhibitor. Principal component analysis (PCA) showed that the control and treated samples were clearly grouped into two independent clusters with good agreement between biological replicates (Figure 6A). The variance value for the first principal component (PC1) was 68% and 18% for the second principal component (PC2). In total 8928 DEGs were identified in *P. cinnamomi* after exposure to 500 µM nikkomycin Z for 48 h. Among these, 565 DEGs were upregulated, and 2057 DEGs were downregulated with a $\log_2$FC (fold change) ≥1.5 and adjusted *P* value (padj) ≤ 0.05 (Figure 6B).

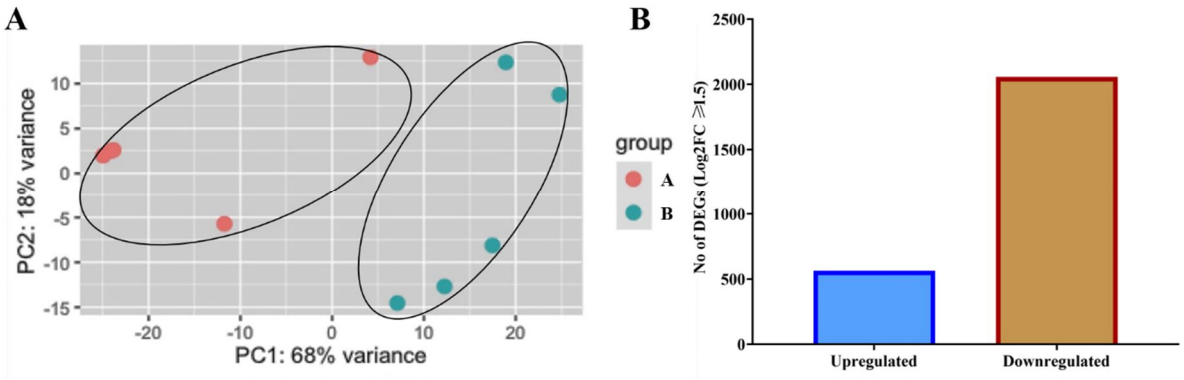

Figure 6: Principal component and Differentially Expressed Genes (DEGs) analysis of the *P. cinnamomi* hyphal cells grown in the presence of 500 µM nikkomycin Z.
(A) The analysis was performed on five biological replicates; orange dots = control; green dots = cells exposed to nikkomycin Z. (B) Number of DEGs in *P. cinnamomi* grown in the presence of nikkomycin Z (N = 5).

Out of the top 30 downregulated genes (Table 1), 6 genes were found to be uncharacterised; and of the top 30 upregulated genes, 7 were found uncharacterized (Table 2). The gene with the highest fold change (down) encoded 'Calcyphosin-like protein' (KAG6622322.1). In the top

30 upregulated gene list, the most differentially upregulated gene was isoflavone reductase P3 (KAG6613123.1) with 22.56 log_2FC. Another two genes encoding pyruvate phosphate di-kinase and acetyl-CoA acetyltransferase, were upregulated with 21.7577 and 19.739 log_2FC ratios, respectively. All the other upregulated genes with > 3 log_2FC are listed in Table 2.

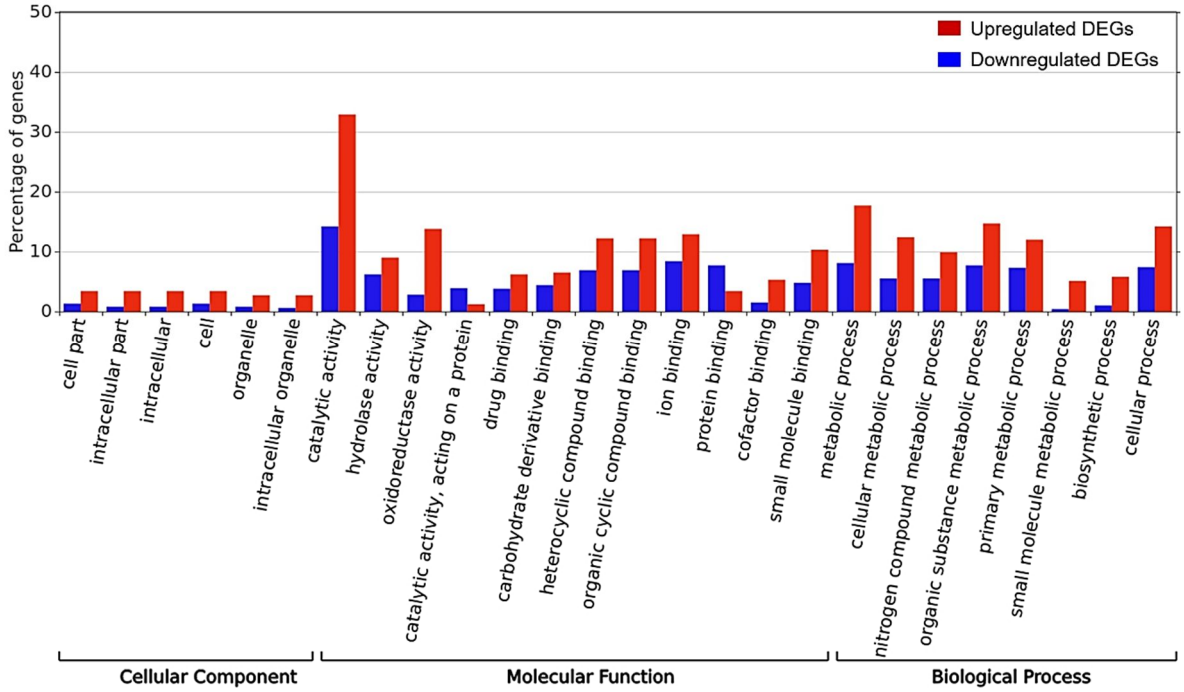

Figure 7: Gene Ontology (GO) enrichment analysis of differentially expressed genes (DEGs) in the mycelium of *P. cinnamomi* grown in the presence of 500 µM nikkomycin Z. The percentage of genes based on enriched terms in the cellular components, molecular functions, and biological processes are shown as an effect of cell exposure to nikkomycin Z. Blue bars indicate downregulated DEGs and red bars indicate upregulated DEGs.

However, only 58.76% (332 genes) of significantly upregulated DEGs and 39.20% (806 genes) of significantly downregulated DEGs were functionally annotated (Table 3) in the ASM1869171v1 reference genome. GO enrichment analysis revealed that 970 differentially expressed genes (277 up, 693 down) were associated with the molecular function ontology, 448 genes (128 up, 320 down) were associated with a biological process ontology, and 205 genes (63 up, 142 down) to the cellular component ontology (Table 3, Figure 7). The top 28 enriched GO terms were visualised in a dotplot, which shows the ratios between expected and observed gene counts for each GO process (Figure 8). These data indicate the highest number of genes of enzyme pathways ontologies were associated with peptidase activity, acyltransferase

activity, catalytic activity related to 'acting on RNA', structural molecular activity and acyltransferase activity (Figure 8).

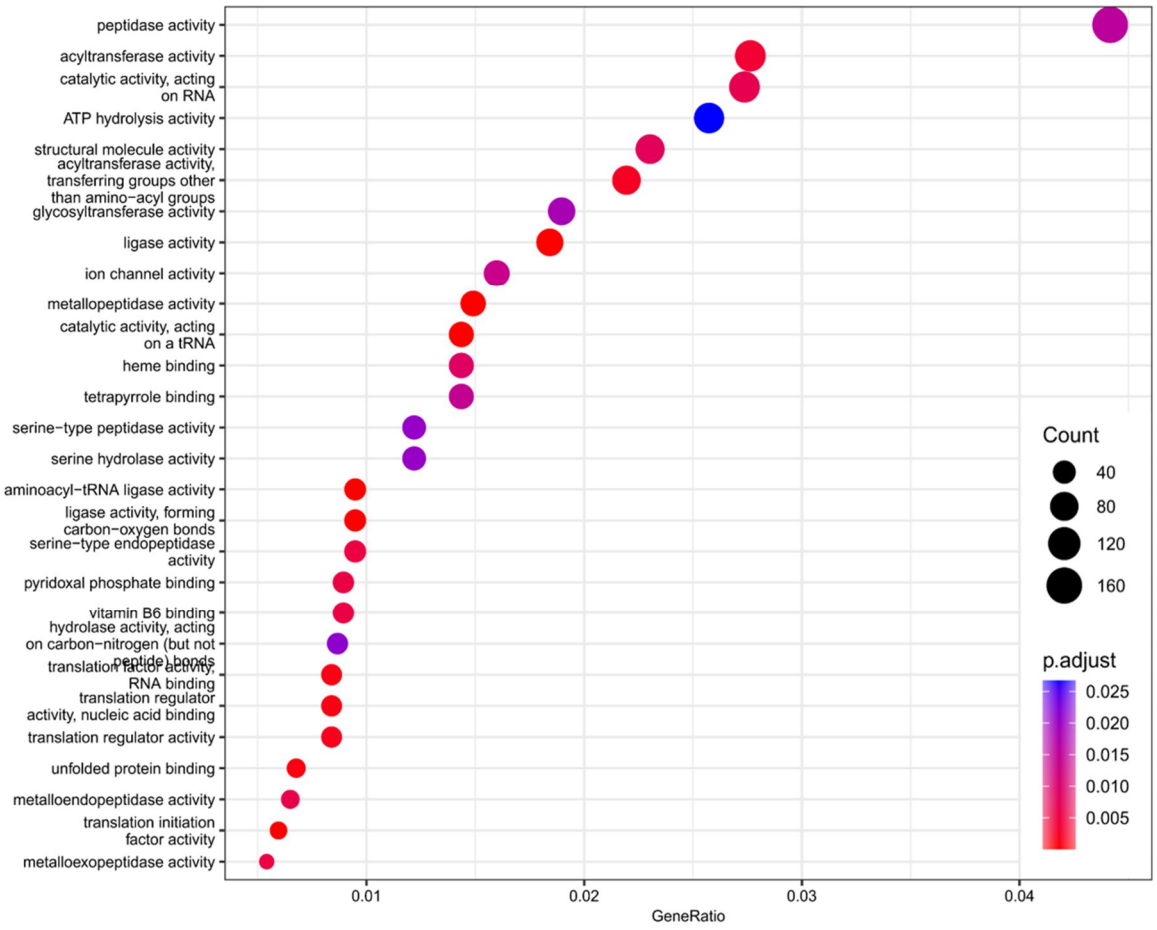

Figure 8: Dot plot of enriched Gene Ontology (GO) terms.

The figure depicts the 28 Gene Ontology (GO) processes with the highest gene ratios arranged in increasing order of gene ratio. The dots in the graph are scaled according to the number of genes in the significant Differentially Expressed Genes (DEGs) list linked with the specific GO term, while different colours of dots represent the adjusted p-values.

RNA-Seq shows modified gene expression in carbohydrate pathways and pathogenicity after nikkomycin Z treatment

As presented above, structural modifications were observed in the cell wall of *P. cinnamomic* hyphal cells exposed to nikkomycin Z. Thus, in our RNA-Seq analysis, particular attention was given to cell wall biosynthesis-related genes. Analysis of DEGs revealed that 3 cellulose synthase genes (*CesA1*, *CesA2*, *CesA3*), 2 glucan synthase genes (*Fks1b*, *Fks1c*), and the chitin synthase 1 gene (*Chs1*) were significantly downregulated in the cells exposed to nikkomycin

Z, whereas one glucan synthase gene (*Fks2a*) was upregulated in the presence of the inhibitor (Figure 9A).

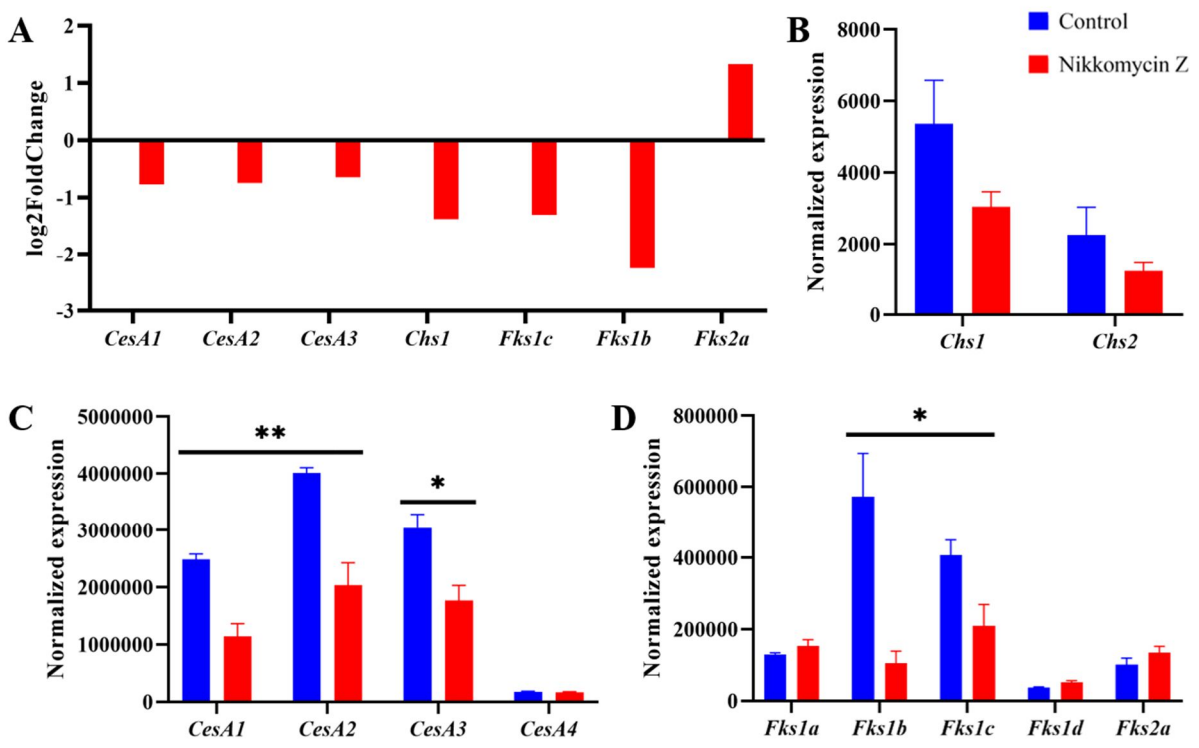

Figure 9: Gene expression analysis of cell wall genes by RNA-Seq (A) and q-PCR (B, C, D) in cells exposed to 500 µM nikkomycin Z.

The genes analyzed are cellulose synthase (*CesA*), chitin synthase (*Chs*), and 1,3-β-glucan synthase (*Fks*) genes (biological replicates: N = 5 for RNA-Seq and N = 3 for q-PCR analysis). '**' indicates $p \leq 0.01$, and '*' indicates $p \leq 0.05$.

UDP-GlcNAc is a nucleotide-sugar used as a substrate in the hexosamine biosynthetic pathway (HBP) leading to the biosynthesis of chitin. It is also a substrate of enzymes involved in the synthesis of various glycoconjugates such as GPI anchors and N- and O-linked glycans (Vetting *et al.*, 2005). The HBP is found in most eukaryotes and is composed of four highly conserved enzymes: Glutamine-fructose-6-phosphate aminotransferase (GFAT/GFA1), Phosphoglucomutase (PGM/AGM1), UDP-N-acetylglucosamine pyrophosphorylase (UAP/UAP1) and glucosamine-6-phosphate N-acetyltransferase (GNA1/GNA) (Milewski *et al.*, 2006). Our RNA-Seq experiment revealed that three of genes that code for these enzymes were up (*Uap1*) and downregulated (*Pgm* and *Gfat*) in the presence of nikkomycin Z (Table 4). GPI anchors are an end product of the HBP pathway, and we found 8 genes that code for putative GPI anchor proteins that were differentially up- (4 genes) or down- (4 genes) regulated (Table 5).

Phytophthora pathogens secrete effector proteins into host plants to facilitate infection (Jiang *et al.*, 2008; Wang & Jiao, 2019; Win *et al.*, 2007). These proteins have the ability to manipulate the host immune response and promote disease development (Qiao *et al.*, 2015). We found 87 DEGs of putative *Rxlr* effector genes, among which 82 were downregulated by up to 6-fold. Furthermore, 7 putative *Crn* effector genes were differentially expressed, all of which were significantly downregulated by up to 5-fold (Figure 9). In *Phytophthora* species, Necrosis-inducing Phytophthora proteins (NPP1) or necrosis inducing proteins (NIP) typically contain a secretion signal peptide at their N-terminus and belong to a superfamily of apoplastic effectors which are secreted and possess phytotoxic activity (Feng *et al.*, 2014). Among the 11 differentially expressed putative *Npp1* effector genes, 9 were significantly downregulated up to 4-fold (Figure 10). Disorganised cellular organelles were observed in treatment group (Figure 3C-3H) as presented above. Potentially related to this phenotype, RNA-Seq data revealed that 12 genes encoding intracellular organelle membrane-related proteins were downregulated and 3 genes were upregulated in the presence of nikkomycin Z (Table 6).

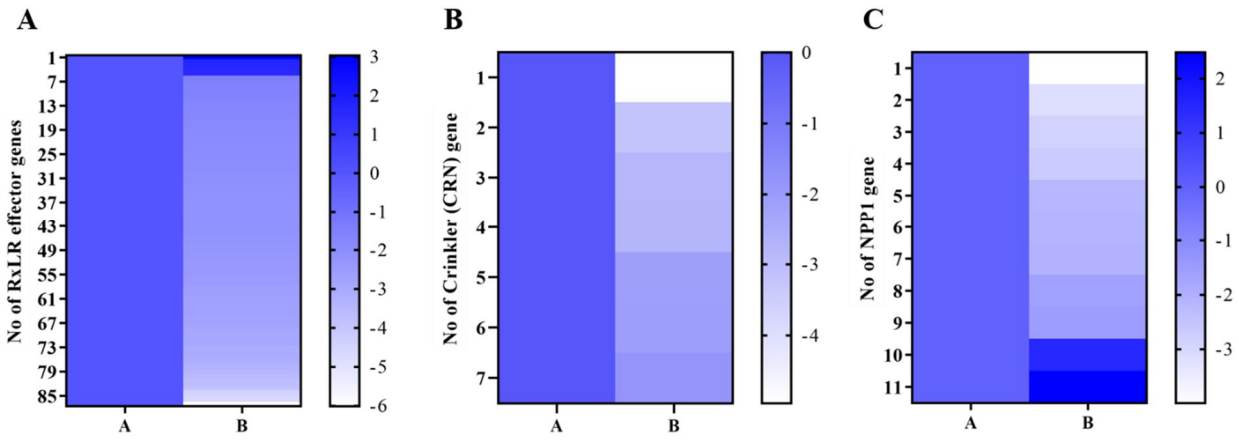

Figure 10: Heatmap of hierarchical clustering indicating differentially expressed genes (DEGs) involved in the pathogenicity of *P. cinnamomi* grown in the presence of nikkomycin Z.

Upregulation and downregulation of genes are indicated using a colour scale with each heatmap related to (A) RxLR effectors, (B) CRN effectors, and (C) Necrosis inducing phytophthora protein 1 (NPP1) genes using DEGs analysis. The numbers on the scales denote 'log2FoldChange'. Number of biological replicates = 5.

In addition, other top downregulated genes included those that encode five Retroelement pol Polyproteins, two Cobalamin synthesis proteins and single copies of unc-50 protein, Integrase catalytic core protein, Copia protein, putative secreted RxLR effector protein, CRN protein, protease inhibitor EpiC2B, putative endo-1,4-β-glucanase, myrosinase-binding protein, mucin-

like protein, L-threonine dehydratase biosynthetic IlvA, acidic fibroblast growth factor intracellular-binding protein, proline-rich protein, glutamate carboxypeptidase, sodium-dependent phosphate transporter, white protein (Table 1). The ratio of log_2FC ranged from 4 to 8 times for these genes after nikkomycin Z treatment.

Quantitative real-time PCR validation

A total of 11 genes associated with cell wall biosynthesis was selected for validation of RNA-Seq data by q-PCR (Figure 9B-D). Overall, transcriptional trends obtained by q-PCR were consistent with the RNA-Seq data (Figure 9B-D). In particular, the putative cellulose synthase genes *CesA1*, *CesA2* and *CesA3* were found to be significantly downregulated in both experiments, while *CesA4* transcript levels remained unaltered in both q-PCR and RNA-Seq (Figure 9A, 9C). In addition, both experiments showed significant downregulation of the putative glucan synthase genes *Fks1b* and *Fks1c* in the presence of nikkomycin Z, and no change in transcript levels for *Fks1a* and *Fks1d* (Figure 9A, 9D). Transcript levels of *Chs1* and *Fks2a* followed similar dynamics in both experiments after exposure to nikkomycin Z, but the change was not considered statistically significant in the q-PCR analysis, as opposed to the RNA-Seq data. The expression of *Chs2* was not significantly affected by nikkomycin Z in both experiments.

Discussion

Oomycetes are a class of organisms with morphologies and life strategies analogous to that of fungi, despite diverging about 500 Ma (Matari & Blair, 2014). A major distinction between the lineages is the composition of their cell walls, i.e., oomycetes have cell walls made primarily of cellulose and other glucans, while fungal cell walls are devoid of cellulose and characteristically contain chitin (Aronson *et al.*, 1967; Badreddine *et al.*, 2008; Bulone *et al.*, 1992; Guerriero *et al.*, 2010). In filamentous fungi, approximately 10-20% of the total cell wall (dry weight) is chitin, and their genomes contain ~3-10 chitin synthase genes (*Chs*) (Cohen, 2001; Lenardon *et al.*, 2010). Chitin is observed in some oomycetes too, although in very low abundance and its function in this class of micro-organisms remains obscure. Both *Aphanomyces* and *Saprolegnia* contain 4-5 *Chs* genes and a small amount of chitin/chitosaccharides can be detected in their hyphal cell walls by quantitative monosaccharide and linkage analyses (Badreddine *et al.*, 2008; Bulone *et al.*, 1992; Guerriero *et al.*, 2010; Mélida *et al.*, 2013). Indeed, the presence or absence of chitin in oomycete cell walls is a crucial distinction between two major oomycete taxonomic groups, the Saprolegniales and the Peronosporomycetes. Monosaccharide and glycosidic linkage analysis of the cell wall

of two *Phytophthora* species (*Phytophthora infestans* and *Phytophthora parasitica*) failed to detect GlcNAc residues (Mélida *et al.*, 2013). These results are supported by the carbohydrate analyses presented here. However, *Phytophthora* do harbour 1 to 2 *Chs* genes, and show vulnerability to the chitin synthase inhibitor nikkomycin Z. Only a few *Phytophthora* species have been tested against nikkomycin Z and many remain to be tested, notably *P. cinnamomi*. Additionally, how nikkomycin Z modifies the cell wall structure of *Phytophthora* species has not been examined. Our results demonstrate that nikkomycin Z not only affects the expression of chitin biosynthesis genes but also — presumably through secondary effects to gene expression — alters other cell wall biosynthetic pathways, ultimately changing cell wall structure and intracellular organisation of *P. cinnamomi*. The transcriptome analysis presented here shows that this inhibitor significantly affects the expression levels of cellulose and other glucan synthase genes, as well as the expression of genes that code for effectors and enzymes from the HBP pathway.

The precise role of chitin and consequently *Chs* in *Phytophthora* remains to be fully resolved. Several gene expression studies reveal *Chs1* to be expressed during the germination of cysts and zoospores, whilst *Chs2* showed very weak transcription levels across all life stages (Cheng *et al.*, 2019; Hinkel & Ospina-Giraldo, 2017). Therefore, *Chs1* in *Phytophthora* species may be involved in asexual reproduction and pathogenesis, whereas the probable function of *Chs2* remains obscure. The relationship between the copy number of *Chs genes*, functional differentiation of *Chs* homologues and nikkomycin Z sensitivity is puzzling. It has previously been observed that *P. sojae*, with two chitin synthase genes (*Chs1, Chs2*), exhibits reduced hyphal sensitivity to nikkomycin Z compared to species that contain single copies (*Chs1*), such as *P. capsici* (Cheng *et al.*, 2019; Hinkel & Ospina-Giraldo, 2017). This led to the conclusion that resistance to nikkomycin Z is modulated by gene copy number. However, in our study we show that *P. cinnamomi*, with two *Chs* genes, is less sensitive to nikkomycin Z than *P. nicotianae*, a species with a single *Chs* (Figure 1).

In *Saprolegnia* species, nikkomycin Z induces swelling and bursting of the hyphal tip, which may indicate the presence of chitin in this location (Guerriero *et al*., 2010). Similarly, we also observed some hyphal tips of newly formed branches swelled, eventually bursting in all tested *Phytophthora* species (Figure 1, 2 and 3). The higher susceptibility of hyphae grown from new branching points to nikkomycin Z may indicate that chitin synthase activity also occurs at the foremost area of growing hyphae, however additional delicate studies are required to prove this hypothesis on the functional role of chitin in *Phytophthora*.

It is well established that chitin produced by fungi induces immune responses in host plants and acts as a pathogen-associated molecular pattern (PAMP) during interactions between plants and fungi (Pusztahelyi, 2018; Sánchez-Vallet *et al.*, 2015). To avoid this recognition, some fungi produce chitin deacetylases that modify chitin to chitosan, which is less readily recognised as a PAMP (Oliveira-Garcia & Valent, 2015; Teixeira *et al.*, 2014). No direct evidence exists for the role of oomycete chitin deacetylases in host recognition. However, several studies suggest the presence of chitin deacetylase genes in *Phytophthora,* although their precise functional role remains undetermined (Cheng *et al.*, 2019; Leonard *et al.*, 2018). In our study we find that the *P. cinnamomi* genome contains three putative chitin deacetylases (Supplementary file 1, Supplementary Figure 3). We observed upregulation of two chitin deacetylases (*Cda1* and *Cda2*) in the presence of nikkomycin Z that may reflect their compensatory role for oomycete cell wall integrity in a similar response to that deployed by fungi (Baker *et al.*, 2007) (Supplementary Figure 3).

In fungi, it has been demonstrated that chitin is covalently linked to β-1,3-glucans in the cell wall (Bowman & Free, 2006; Latgé, 2007; Oliveira-Garcia & Deising, 2013; Ruiz-Herrera, 1991). In our study, nikkomycin Z did not affect the content in 1,3-linked glucosyl residues in the *P. cinnamomi* cell wall, however the proportions of 1,4-linked glucosyl residues (mainly derived from cellulose) and 1,3-linked galactosyl residues were significantly decreased (Figure 5). Both 1,4-linked glucosyl residues and 1,3-linked galactosyl residues were mainly derived from the alkali insoluble fraction (AIF), where chitin is primarily found in *Saprolegnia* and *Aphanomyces* (Mélida *et al*., 2013). However, whether chitin can be covalently linked to 1,4-β-glucans as a fundamental cell wall component or not in oomycetes is unknown. It remains for future work to understand how nikkomycin Z treatment modifies cellulose content in *Phytophthora* species. The inclusion of *Saprolegnia* and *Aphanomyces* species, which contain chitin in their cell wall, might be instructive.

It is known that chitin is synthesized in eukaryotes by the CHS enzyme, which uses UDP-GlcNAc as a sugar donor. This nucleotide-sugar is a product of the hexosamine biosynthetic pathway (HBP) and is also a constituent of glycoproteins and GPI anchors (Nishitani *et al.*, 2006; Ram *et al.*, 2004). There are four enzymes involved in the pathway: glutamine fructose-6-phosphate aminotransferase (GFAT), glucosamine-6-phosphate N-acetyltransferase (GNA1), phosphoacetylglucosamine mutase (PGM/AGM1), and UDP-GlcNAc pyrophosphorylase (UAP1) (Supplementary Figure 2). GFAT is considered the rate-limiting enzyme in the HBP pathway (McKnight *et al.*, 1992). It converts fructose-6P to glucosamine-6P. GNA1, which belongs to the GCN5-related acetyltransferase family (GNATs), then

converts glucosamine-6P to GlcNAc-6P. Next, AGMI/PGM performs the conversion of GlcNAc-6P to GlcNAc-1P, and UAP1 catalyzes the uridylation of GlcNAc-1P to form UDP-GlcNAc (Nishitani *et al.*, 2006; Raimi *et al.*, 2020). Inhibiting any of these enzymes could potentially disrupt the HBP, leading to a decrease in the availability of UDP-GlcNAc and consequently impede the biosynthesis of chitin and glycoconjugates (Candy & Kilby, 1962; Cohen, 2001). Indeed, the entire HBP pathway is vital for hyphal growth under *in vitro* conditions in *Aspergillus fumigatus* (Fang *et al.*, 2013; Fang *et al.*, 2013; Hu *et al.*, 2007). Deletion of the *Gna1* gene resulted in loss of fungal viability and disruption of the cell wall, indicating its essential role in fungal cell survival and integrity (Lockhart *et al.*, 2020). Similarly, studies on conditional mutants lacking *Agm1*/*Pgm* or *Uap1* demonstrated their importance for fungal cell growth and cell wall biosynthesis (Fang *et al.*, 2013). In this view, the downregulated expression of *Gfat* and *Agmi/Pgm* in our experiments may explain why cell stability and cell growth were affected (Table 4, Supplementary Figure 2). In addition, we observed an upregulation of *Uap1* in the presence of nikkomycin Z, which may reflect a compensation reaction to counter the affected HBP in *P. cinnamomi* exposed to nikkomycin Z (Supplementary Figure 2). These findings suggest that nikkomycin Z may not only act as a competitive inhibitor of CHS but also significantly alter the UDP-GlcNAc pathway in the tested species, resulting in the downregulation of GPI anchors and *Chs1* genes (Figure 9B, Table 4-5, Supplementary Figure 2). Thus, the development of HBP inhibitors holds promise for effectively controlling pathogenic oomycetes and could pave the way for innovative strategies in their management.

The disruption of the core cell wall architecture is an effective anti-microbial effect, however nikkomycin Z may also modify pathways specific to pathogenicity. *Phytophthora* species secrete effector proteins into the host cytoplasm while attacking host cells to modify the immune response of the host plant and ensure successful colonization (Amaro *et al.*, 2017). Among known cytoplasmic effectors, both CRN (Crinkling and necrosis) effectors and effectors harboring the RXLR motif at their N-terminus facilitate infection of host plants (Gascuel *et al.*, 2016; Schornack *et al.*, 2010; Whisson *et al.*, 2007). The downregulation of some of these effector genes (both *Rxlr* and *Crn*) and necrosis-inducing genes (*Npp1*) in our study suggests that nikkomycin Z may also depress the infectiousness of *P. cinnamomi*. The downregulation of some of the effector genes, combined with the observation that the expression of genes involved in other specific pathways, as observed in our study, suggests that nikkomycin Z affects multiple cellular and biochemical processes in *Phytophthora*, and that this inhibitor or analogues are potentially usable for disease control against pathogenic oomycetes. Indeed, the analysis of enriched GO terms highlights the large number of *P.*

cinnamomi biochemical pathways affected by nikkomycin Z (Figure 6-8). Many genes of this non-model organism remain functionally unannotated and therefore we anticipate that the number of modified pathways is a conservative estimate. Future genomic *P. cinnamomi* projects will likely discover additional pathways and what we present here is a foundation for future work on the response of this pathogen to nikkomycin Z. The two most enriched GO terms are indictive of the profound disruption caused by this compound: peptidase and acyltransferase activity (Figure 8). Acyltransferases are central to fundamental biological processes such as lipid metabolism and protein modification. One such enzyme catalyzes the production of triacylglycerol, which plays a key role in pathogenicity in fungi, e.g., *Colletotrichum gloeosporioides* and in oomycetes, e.g., *Phytophthora melonis* (Ahmad *et al.*, 2021; Sharma *et al.*, 2016). Peptidase activity is similarly core to organismal viability, implicated with, among other functions, protein metabolism and cellular homeostasis. Disruption of these fundamental pathways indicates the severe effect of nikkomycin Z on these organisms.

Due to the robust statistical methods used to analyse the RNA-Seq data, qRT-PCR was not performed to validate all expression data in the current study. Prior studies have verified that about 15–20% of genes displaying fold changes lower than 1.5 may have 'non-concordant' expression in RNA-Seq and q-PCR analyses (Coenye, 2021). Therefore, we validated only the cell wall-related *CesA*s, *Fks*s, and *Chs*s genes using q-PCR because of their overall low level of expression in the RNA-Seq experiment (Figure 9). Moreover, recent scientific studies have provided evidence that RNA-Seq results are reliable and do not necessitate independent validation, owing to the high level of consistency observed between RNA-Seq and q-PCR approaches (Coenye, 2021; Everaert *et al.*, 2017).

In conclusion, our comprehensive analysis has provided valuable insights into the profound effects of nikkomycin Z against one of the most destructive oomycete pathogens, *P. cinnamomi*. Our findings demonstrate that this inhibitor can disrupt the organization of the cell wall, impair the formation of new hyphal branches, and perturb the expression of genes involved in UDP-GlcNAc biosynthesis and pathogenicity. Moreover, our study highlights the significance of chitin biosynthesis in *P. cinnamomi*, as observed in other non-phytophthora oomycetes. We also observed a reduction in cellulose content within the cell wall, reduction of gene expression associated with this process, and an overall inhibition of cell viability and growth. These results hold great potential for future research endeavours aimed at developing alternative disease control strategies for *Phytophthora* diseases.

Acknowledgments

The fee-for-service facility of the South Australian Genomics Centre (SAGC) was used for library construction and RNA sequencing. This work was supported by a grant to V.B. from the Australian Research Council (grant # DP180103974).

References

Environment protection and biodiversity conservation act 1999, No. 91, C. 56. Available at: https://www.legislation.gov.au/Details/C2021C00182

FRAC Recommendations for CAA fungicides 2023. Available at: https://www.frac.info: Online publication.

Ahmad, A., Akram, W., Bashir, Z., Shahzadi, I., Wang, R., Abbas, H. M. K., Hu, D., Ahmed, S., Xu, X., Li, G. & Wu, T. (2021) Functional and structural analysis of a novel acyltransferase from pathogenic *Phytophthora melonis*. *ACS Omega*, 6(3), 1797-1808.

Amaro, T. M. M. M., Thilliez, G. J. A., Motion, G. B. & Huitema, E. (2017) A perspective on CRN proteins in the genomics age: Evolution, classification, delivery and function revisited. *Frontiers in Plant Science*, 8, 99.

Aronson, J. M., Cooper, B. A. & Fuller, M. S. (1967) Glucans of oomycete cell walls. *Science*, 155(3760), 332-335.

Badreddine, I., Lafitte, C., Heux, L., Skandalis, N., Spanou, Z., Martinez, Y., Esquerré-Tugayé, M. T., Bulone, V., Dumas, B. & Bottin, A. (2008) Cell wall chitosaccharides are essential components and exposed patterns of the phytopathogenic oomycete *Aphanomyces euteiches*. *Eukaryotic Cell*, 7(11), 1980-1993.

Baker, L. G., Specht, C. A., Donlin, M. J. & Lodge, J. K. (2007) Chitosan, the deacetylated form of chitin, is necessary for cell wall integrity in *Cryptococcus neoformans*. *Eukaryotic Cell*, 6(5), 855-867.

Barnett, D. W., Garrison, E. K., Quinlan, A. R., Strömberg, M. P. & Marth, G. T. (2011) BamTools: a C++ API and toolkit for analyzing and managing BAM files. *Bioinformatics*, 27(12), 1691-1692.

Bartnicki-Gracia, S. (1983) Biochemical aspects of morphogenesis in Phytophthora. In Phytophthora : Its Taxonomy, Ecology and Pathology, 121-137.

Belisle, R. J., Hao, W., McKee, B., Arpaia, M. L., Manosalva, P. & Adaskaveg, J. E. (2019) New oomycota fungicides with activity against *Phytophthora cinnamomi* and their potential use for managing avocado root rot in California. *Plant Disease*, 103(8),

2024-2032.

Bentz, M. L., Nunnally, N., Lockhart, S. R., Sexton, D. J. & Berkow, E. L. (2021) Antifungal activity of nikkomycin Z against Candida auris. *Journal of Antimicrobial Chemotherapy*, 76(6), 1495-1497.

Blum, M., Boehler, M., Randall, E., Young, V., Csukai, M., Kraus, S., Moulin, F., Scalliet, G., Avrova, A. O., Whisson, S. C. & Fonne-Pfister, R. (2010) Mandipropamid targets the cellulose synthase-like PiCesA3 to inhibit cell wall biosynthesis in the oomycete plant pathogen, *Phytophthora infestans*. *Molecular Plant Pathology*, 11(2), 227-243.

Blum, M. & Gisi, U. (2012) Insights into the molecular mechanism of tolerance to carboxylic acid amide (CAA) fungicides in *Pythium aphanidermatum*. *Pest Management Science*, 68(8), 1171-83.

Bowman, S. M. & Free, S. J. (2006) The structure and synthesis of the fungal cell wall. *Bioessays*, 28(8), 799-808.

Bulone, V., Chanzy, H. D., Girard, V. & Fěvre, M. (1992) Characterization of chitin and chitin synthase from the cellulosic cell wall fungus. *Experimental Mycology*, 16(1), 8-21.

Burton, R. A., Jobling, S. A., Harvey, A. J., Shirley, N. J., Mather, D. E., Bacic, A. & Fincher, G. B. (2008) The genetics and transcriptional profiles of the cellulose synthase-like HvCslF gene family in barley. *Plant Physiology*, 146(4), 1821-1833.

Cahill, D. M., Rookes, J. E., Wilson, B. A., Gibson, L. & McDougall, K. L. (2008) *Phytophthora cinnamomi* and Australia's biodiversity: impacts, predictions and progress towards control. *Australian Journal of Botany*, 56(4), 279-310.

Cai, M., Zhang, C., Wang, W., Peng, Q., Song, X., Tyler, B. M. & Liu, X. (2021) Stepwise accumulation of mutations in CesA3 in *Phytophthora sojae* results in increasing resistance to CAA fungicides. *Evolutionary Applications*, 14(4), 996-1008.

Candy, D. & Kilby, B. (1962) Studies on chitin synthesis in the desert locust. *Journal of Experimental Biology*, 39(1), 129-140.

Chen, L., Zhu, S., Lu, X., Pang, Z., Cai, M. & Liu, X. (2012) Assessing the risk that *Phytophthora melonis* can develop a point mutation (V1109L) in CesA3 conferring

resistance to carboxylic acid amide fungicides. *PLoS One*, 7(7), e42069.

Chen, W., Cao, P., Liu, Y., Yu, A., Wang, D., Chen, L., Sundarraj, R., Yuchi, Z., Gong, Y., Merzendorfer, H. & Yang, Q. (2022) Structural basis for directional chitin biosynthesis. *Nature*, 610(7931), 402-408.

Cheng, W., Lin, M., Qiu, M., Kong, L., Xu, Y., Li, Y., Wang, Y., Ye, W., Dong, S., He, S. & Wang, Y. (2019) Chitin synthase is involved in vegetative growth, asexual reproduction and pathogenesis of *Phytophthora capsici* and *Phytophthora sojae*. *Environmental Microbiology*, 21(12), 4537-4547.

Coenye, T. (2021) Do results obtained with RNA-sequencing require independent verification? *Biofilm*, 3, 100043.

Cohen, E. (2001) Chitin synthesis and inhibition: a revisit. *Pest Management Science*, 57(10), 946-950.

Comino, P., Shelat, K., Collins, H., Lahnstein, J. & Gidley, M. J. (2013) Separation and Purification of Soluble Polymers and Cell Wall Fractions from Wheat, Rye and Hull less Barley Endosperm Flours for Structure-Nutrition Studies. *Journal of Agricultural and Food Chemistry*, 61(49), 12111-12122.

Danecek, P., Bonfield, J. K., Liddle, J., Marshall, J., Ohan, V., Pollard, M. O., Whitwham, A., Keane, T., McCarthy, S. A., Davies, R. M. & Li, H. (2021) Twelve years of SAMtools and BCFtools. *GigaScience*, 10(2).

Dobin, A., Davis, C. A., Schlesinger, F., Drenkow, J., Zaleski, C., Jha, S., Batut, P., Chaisson, M. & Gingeras, T. R. (2012) STAR: ultrafast universal RNA-seq aligner. *Bioinformatics*, 29(1), 15-21.

Everaert, C., Luypaert, M., Maag, J. L., Cheng, Q. X., Dinger, M. E., Hellemans, J. & Mestdagh, P. (2017) Benchmarking of RNA-sequencing analysis workflows using whole-transcriptome RT-qPCR expression data. *Scientific Reports*, 7(1), 1559.

Fang, W., Du, T., Raimi, O. G., Hurtado-Guerrero, R., Mariño, K., Ibrahim, A. F., Albarbarawi, O., Ferguson, M. A., Jin, C. & Van Aalten, D. M. (2013) Genetic and structural validation of Aspergillus fumigatus N-acetylphosphoglucosamine mutase as

an antifungal target. *Bioscience Reports*, 33(5).

Feng, B. Z., Zhu, X. P., Fu, L., Lv, R. F., Storey, D., Tooley, P. & Zhang, X. G. (2014) Characterization of necrosis-inducing NLP proteins in *Phytophthora capsici*. *BMC Plant Biology*, 14, 126.

Fuechtbauer, W., Yunusov, T., Bozsóki, Z., Gavrin, A., James, E. K., Stougaard, J., Schornack, S. & Radutoiu, S. (2018) LYS12 LysM receptor decelerates *Phytophthora palmivora* disease progression in Lotus japonicus. *The Plant Journal*, 93(2), 297-310.

Gascuel, Q., Buendia, L., Pecrix, Y., Blanchet, N., Muños, S., Vear, F. & Godiard, L. (2016) RXLR and CRN Effectors from the sunflower downy mildew pathogen *Plasmopara halstedii* induce hypersensitive-like responses in resistant sunflower lines. *Frontiers in Plant Science*, 7, 1887.

Gent, D. H., Block, M. & Claassen, B. J. (2020) High levels of insensitivity to phosphonate fungicides in *Pseudoperonospora humuli*. *Plant Disease*, 104(5), 1400-1406.

González-Tobón, J., Childers, R., Olave, C., Regnier, M., Rodríguez-Jaramillo, A., Fry, W., Restrepo, S. & Danies, G. (2020) Is the phenomenon of mefenoxam-acquired resistance in *Phytophthora infestans* universal? *Plant Disease*, 104(1), 211-221.

Guerriero, G., Avino, M., Zhou, Q., Fugelstad, J., Clergeot, P.-H. & Bulone, V. (2010) Chitin synthases from Saprolegnia are involved in tip growth and represent a potential target for anti-oomycete drugs. *PLoS Pathogens*, 6(8), e1001070.

Hinkel, L. & Ospina-Giraldo, M. D. (2017) Structural characterization of a putative chitin synthase gene in *Phytophthora* spp. and analysis of its transcriptional activity during pathogenesis on potato and soybean plants. *Current Genetics*, 63(5), 909-921.

Hu, J., Hong, C., Stromberg, E. L. & Moorman, G. W. (2010) Mefenoxam sensitivity in *Phytophthora cinnamomi* isolates. *Plant Disease*, 94(1), 39-44.

Hu, W., Sillaots, S., Lemieux, S., Davison, J., Kauffman, S., Breton, A., Linteau, A., Xin, C., Bowman, J. & Becker, J. (2007) Essential gene identification and drug target prioritization in *Aspergillus fumigatus*. *PLoS Pathogens*, 3(3), e24.

Jiang, R. H., Tripathy, S., Govers, F. & Tyler, B. M. (2008) RXLR effector reservoir in two *Phytophthora* species is dominated by a single rapidly evolving superfamily with

more than 700 members. *Proceedings of the National Academy of Sciences*, 105(12), 4874-4879.

Jung, T., Colquhoun, I. & Hardy, G. S. J. (2013) New insights into the survival strategy of the invasive soilborne pathogen *Phytophthora cinnamomi* in different natural ecosystems in W estern Australia. *Forest Pathology*, 43(4), 266-288.

Kamoun, S., Furzer, O., Jones, J. D., Judelson, H. S., Ali, G. S., Dalio, R. J., Roy, S. G., Schena, L., Zambounis, A., Panabières, F., Cahill, D., Ruocco, M., Figueiredo, A., Chen, X. R., Hulvey, J., Stam, R., Lamour, K., Gijzen, M., Tyler, B. M., Grünwald, N. J., Mukhtar, M. S., Tomé, D. F., Tör, M., Van Den Ackerveken, G., McDowell, J., Daayf, F., Fry, W. E., Lindqvist-Kreuze, H., Meijer, H. J., Petre, B., Ristaino, J., Yoshida, K., Birch, P. R. & Govers, F. (2015) The Top 10 oomycete pathogens in molecular plant pathology. *Molecular Plant Pathology*, 16(4), 413-34.

Klinter, S., Bulone, V. & Arvestad, L. (2019) Diversity and evolution of chitin synthases in oomycetes (Straminipila: Oomycota). *Molecular Phylogenetics and Evolution*, 139, 106558.

Larwood, D. J. (2020) Nikkomycin Z-ready to meet the promise? *Journal of Fungi (Basel)*, 6(4).

Latgé, J. P. (2007) The cell wall: a carbohydrate armour for the fungal cell. *Molecular Microbiology*, 66(2), 279-290.

Lenardon, M. D., Munro, C. A. & Gow, N. A. (2010) Chitin synthesis and fungal pathogenesis. *Current Opinion in Microbiology*, 13(4), 416-23.

Leonard, G., Labarre, A., Milner, D. S., Monier, A., Soanes, D., Wideman, J. G., Maguire, F., Stevens, S., Sain, D., Grau-Bové, X., Sebé-Pedrós, A., Stajich, J. E., Paszkiewicz, K., Brown, M. W., Hall, N., Wickstead, B. & Richards, T. A. (2018) Comparative genomic analysis of the 'pseudofungus' Hyphochytrium catenoides. *Open Biology*, 8(1), 170184.

Li, T., Cai, M., Wang, W., Dai, T., Zhang, C., Zhang, B., Shen, J., Wang, Y. & Liu, X. (2022) PcCesA1 is involved in the polar growth, cellulose synthesis, and glycosidic linkage crosslinking in the cell wall of *Phytophthora capsici*. *International Journal of*

Biological Macromolecules, 208, 720-730.

Liao, Y., Smyth, G. K. & Shi, W. (2013) featureCounts: an efficient general purpose program for assigning sequence reads to genomic features. *Bioinformatics*, 30(7), 923-930.

Lockhart, D. E. A., Stanley, M., Raimi, O. G., Robinson, D. A., Boldovjakova, D., Squair, D. R., Ferenbach, A. T., Fang, W. & van Aalten, D. M. F. (2020) Targeting a critical step in fungal hexosamine biosynthesis. *Journal of Biological Chemistry*, 295(26), 8678-8691.

Matari, N. H. & Blair, J. E. (2014) A multilocus timescale for oomycete evolution estimated under three distinct molecular clock models. *BMC Evolutionary Biology*, 14(1), 101.

McKnight, G. L., Mudri, S. L., Mathewes, S. L., Traxinger, R. R., Marshall, S., Sheppard, P. O. & O'Hara, P. J. (1992) Molecular cloning, cDNA sequence, and bacterial expression of human glutamine:fructose-6-phosphate amidotransferase. *Journal of Biological Chemistry*, 267(35), 25208-12.

Mélida, H., Sandoval-Sierra, J. V., Diéguez-Uribeondo, J. & Bulone, V. (2013) Analyses of extracellular carbohydrates in oomycetes unveil the existence of three different cell wall types. *Eukaryotic Cell*, 12(2), 194-203.

Milewski, S., Gabriel, I. & Olchowy, J. (2006) Enzymes of UDP-GlcNAc biosynthesis in yeast. *Yeast*, 23(1), 1-14.

Nishitani, Y., Maruyama, D., Nonaka, T., Kita, A., Fukami, T. A., Mio, T., Yamada-Okabe, H., Yamada-Okabe, T. & Miki, K. (2006) Crystal structures of N-acetylglucosamine-phosphate mutase, a member of the alpha-D-phosphohexomutase superfamily, and its substrate and product complexes. *Journal of Biological Chemistry*, 281(28), 19740-7.

Oliveira-Garcia, E. & Deising, H. B. (2013) Infection structure-specific expression of β-1,3-glucan synthase is essential for pathogenicity of *Colletotrichum graminicola* and evasion of β-glucan-triggered immunity in maize. *Plant Cell*, 25(6), 2356-78.

Oliveira-Garcia, E. & Valent, B. (2015) How eukaryotic filamentous pathogens evade plant recognition. *Current Opinion in Microbiology*, 26, 92-101.

Piotrowski, J. S., Okada, H., Lu, F., Li, S. C., Hinchman, L., Ranjan, A., Smith, D. L., Higbee, A. J., Ulbrich, A., Coon, J. J., Deshpande, R., Bukhman, Y. V., McIlwain, S.,

Ong, I. M., Myers, C. L., Boone, C., Landick, R., Ralph, J., Kabbage, M. & Ohya, Y. (2015) Plant-derived antifungal agent poacic acid targets β-1,3-glucan. *Proceedings of the National Academy of Sciences*, 112(12), E1490-7.

Pusztahelyi, T. (2018) Chitin and chitin-related compounds in plant-fungal interactions. *Mycology*, 9(3), 189-201.

Qiao, Y., Shi, J., Zhai, Y., Hou, Y. & Ma, W. (2015) Phytophthora effector targets a novel component of small RNA pathway in plants to promote infection. *Proceedings of the National Academy of Sciences*, 112(18), 5850-5855.

Raimi, O. G., Hurtado-Guerrero, R., Borodkin, V., Ferenbach, A., Urbaniak, M. D., Ferguson, M. A. J. & van Aalten, D. M. F. (2020) A mechanism-inspired UDP-N-acetylglucosamine pyrophosphorylase inhibitor. *RSC Chemical Biology*, 1(1), 13-25.

Ram, A. F., Arentshorst, M., Damveld, R. A., vanKuyk, P. A., Klis, F. M. & van den Hondel, C. A. (2004) The cell wall stress response in *Aspergillus niger* involves increased expression of the glutamine: fructose-6-phosphate amidotransferase-encoding gene (gfaA) and increased deposition of chitin in the cell wall. *Microbiology*, 150(10), 3315-3326.

Reyes-Chilpa, R., Quiroz-Vázquez, R., Jiménez-Estrada, M., Navarro-Oca a, A. & Cassani-Hernández, J. (1997) Antifungal activity of selected plant secondary metabolites against Coriolus versicolor. *Journal of Tropical Forest Products*, 3, 110-113.

Rubin, A. E., Gotlieb, D., Gisi, U. & Cohen, Y. (2008) Mutagenesis of *Phytophthora infestans* for resistance against carboxylic acid amide and phenylamide fungicides. *Plant Disease*, 92(5), 675-683.

Ruiz-Herrera, J. (1991) Biosynthesis of β-glucans in fungi. *Antonie Van Leeuwenhoek*, 60, 73-81.

Sánchez-Vallet, A., Mesters, J. R. & Thomma, B. P. H. J. (2015) The battle for chitin recognition in plant-microbe interactions. *FEMS Microbiology Reviews*, 39(2), 171-183.

Sass, G., Larwood, D. J., Martinez, M., Chatterjee, P., Xavier, M. O. & Stevens, D. A. (2021) Nikkomycin Z against disseminated coccidioidomycosis in a murine model of sustained-release dosing. *Antimicrobial Agents and Chemotherapy*, 65(10), e00285-

21.

Schornack, S., van Damme, M., Bozkurt, T. O., Cano, L. M., Smoker, M., Thines, M., Gaulin, E., Kamoun, S. & Huitema, E. (2010) Ancient class of translocated oomycete effectors targets the host nucleus. *Proceedings of the National Academy of Sciences*, 107(40), 17421-17426.

Sharma, M., Guleria, S. & Kulshrestha, S. (2016) Diacylglycerol acyl transferase: A pathogenicity related gene in *Colletotrichum gloeosporioides*. *Journal of Basic Microbiology*, 56(11), 1308-1315.

Shearer, B. L., Crane, C. E., Barrett, S. & Cochrane, A. (2007) Phytophthora cinnamomi invasion, a major threatening process to conservation of flora diversity in the South-west Botanical Province of Western Australia. *Australian Journal of Botany*, 55(3), 225-238.

Teixeira, P. J. P. L., Thomazella, D. P. d. T., Reis, O., do Prado, P. F. V., do Rio, M. C. S., Fiorin, G. L., José, J., Costa, G. G. L., Negri, V. A., Mondego, J. M. C., Mieczkowski, P. & Pereira, G. A. G. (2014) High-resolution transcript profiling of the atypical biotrophic interaction between theobroma cacao and the fungal pathogen Moniliophthora perniciosa. *The Plant Cell*, 26(11), 4245-4269.

Vetting, M. W., de Carvalho, L. P. S., Yu, M., Hegde, S. S., Magnet, S., Roderick, S. L. & Blanchard, J. S. (2005) Structure and functions of the GNAT superfamily of acetyltransferases. *Archives of Biochemistry and Biophysics*, 433(1), 212-226.

Wang, W. & Jiao, F. (2019) Effectors of Phytophthora pathogens are powerful weapons for manipulating host immunity. *Planta*, 250(2), 413-425.

Whisson, S. C., Boevink, P. C., Moleleki, L., Avrova, A. O., Morales, J. G., Gilroy, E. M., Armstrong, M. R., Grouffaud, S., Van West, P. & Chapman, S. (2007) A translocation signal for delivery of oomycete effector proteins into host plant cells. *Nature*, 450(7166), 115-118.

Win, J., Morgan, W., Bos, J., Krasileva, K. V., Cano, L. M., Chaparro-Garcia, A., Ammar, R., Staskawicz, B. J. & Kamoun, S. (2007) Adaptive evolution has targeted the C-terminal domain of the RXLR effectors of plant pathogenic oomycetes. *The Plant*

Cell, 19(8), 2349-2369.

Tables

Table 1: List of top 30 downregulated DEGs with the corresponding protein ID, Log2Fold Change, adjusted p-value (padj) and functional annotations.

Protein ID	log2FC	padj	Functional Annotation
KAG6622322.1	-23.3353	3.87E-09	Calcyphosin-like protein
KAG6622338.1	-8.38478	0.002678	unc-50 protein
KAG6613497.1	-6.919	3.12E-05	Retroelement pol Polyprotein
KAG6615902.1	-6.71818	0.046065	Integrase catalytic core protein
KAG6608851.1	-6.47299	0.003018	Retroelement pol Polyprotein
KAG6590634.1	-6.15688	0.000928	Copia protein
KAG6595982.1	-6.01053	0.001253	putative secreted RxLR effector protein
KAG6612259.1	-5.92609	2.54E-05	protease inhibitor EpiC2B
KAG6613604.1	-5.6432	0.002733	Retroelement pol Polyprotein
KAG6614963.1	-5.63882	0.000665	Retrotransposon protein
KAG6574682.1	-5.62002	1.43E-15	hypothetical protein
KAG6579966.1	-5.42575	1.43E-14	Cobalamin synthesis protein
KAG6612162.1	-5.40537	9.77E-10	aFGF intracellular-binding protein
KAG6613369.1	-5.28642	8.23E-05	hypothetical protein
KAG6610911.1	-5.26556	0.001545	hypothetical protein
KAG6622826.1	-5.25893	0.003498	proline-rich protein
KAG6623903.1	-5.22637	0.001421	hypothetical protein
KAG6623874.1	-5.13882	9.19E-16	Cobalamin synthesis protein
KAG6572718.1	-5.04325	0.004524	white protein
KAG6617508.1	-5.00851	5.06E-05	hypothetical protein
KAG6594291.1	-4.98331	4.34E-21	L-threonine dehydratase biosynthetic IlvA
KAG6614061.1	-4.96275	0.001025	hypothetical protein
KAG6613170.1	-4.95452	0.00636	Crinkler (CRN) family protein
KAG6615130.1	-4.95335	1.59E-09	Glutamate carboxypeptidase
KAG6595898.1	-4.93365	1.23E-06	Sodium-dependent phosphate transporter
KAG6610912.1	-4.8872	0.040587	Retroelement pol Polyprotein
KAG6608978.1	-4.85598	0.000485	hypothetical protein
KAG6614377.1	-4.85141	0.001602	putative endo-1,(4)-beta-glucanase
KAG6609570.1	-4.82796	0.000248	Myrosinase-binding protein
KAG6613760.1	-4.81225	8.74E-06	Mucin-like protein

Table 2: List of top 30 upregulated DEGs with the corresponding protein ID, Log2Fold Change, adjusted p-value (padj) and functional annotations.

Protein ID	log2FC	padj	Functional Annotation
KAG6613123.1	22.56985	1.22E-08	Isoflavone reductase P3
KAG6610067.1	21.7577	4.61E-08	Pyruvate phosphate dikinase
KAG6617769.1	19.73987	7.16E-07	Acetyl-CoA acetyltransferase
KAG6578248.1	9.565242	0.007921	Pyruvate kinase
KAG6594255.1	5.890289	0.040342	uracil phosphoribosyl transferase
KAG6582922.1	5.610758	0.016474	Sugar transport protein 10
KAG6614528.1	5.514496	0.000238	SCP-like extracellular protein
KAG6611444.1	5.416848	0.002562	dynein heavy chain%2C outer arm
KAG6622325.1	5.412445	0.013327	VAC14 family protein
KAG6610450.1	5.308665	0.009006	hypothetical protein
KAG6619968.1	4.881998	0.005366	hypothetical protein
KAG6584710.1	4.730613	1.15E-10	putative alcohol dehydrogenase
KAG6621840.1	4.72586	0.00269	Glycerol-3-phosphate dehydrogenase
KAG6584580.1	4.713004	8.12E-11	putative alcohol dehydrogenase
KAG6614730.1	4.676789	2.78E-15	hypothetical protein
KAG6585049.1	4.546233	2.20E-12	putative GPI anchor protein
KAG6582919.1	4.541638	4.97E-08	Sugar transport protein 10
KAG6592499.1	4.422977	7.82E-05	putative 12-oxophytodienoate reductase
KAG6613699.1	4.357397	9.30E-08	Spore coat protein A
KAG6603080.1	4.341581	1.69E-10	putative alcohol dehydrogenase
KAG6614770.1	4.256183	0.001357	hypothetical protein
KAG6614798.1	4.153145	0.041629	hypothetical protein
KAG6574732.1	4.109083	9.37E-07	multidrug resistance protein ABC superfamily
KAG6613016.1	4.104363	6.08E-08	Carbohydrate-binding protein
KAG6616503.1	4.06894	5.28E-12	Zinc finger-type protein
KAG6608922.1	3.999881	0.042395	Calcium release-activated calcium channel
KAG6614543.1	3.952407	0.000616	hypothetical protein
KAG6577917.1	3.948197	0.003181	hypothetical protein
KAG6615245.1	3.907756	0.021525	major facilitator superfamily
KAG6583000.1	3.856625	0.013536	putative polysaccharide lyase

Table 3: Summary of annotated downregulated and upregulated genes according to biological processes, cellular components, and molecular functions of all DEGs.

		Down DEGs	Up DEGs	Total
Gene		2057	565	2622
Annotated genes		806	332	1138
GO Terms	Biological	320	128	448
	Cellular	142	63	205
	Function	693	277	970
	Total	1155	468	1623

Table 4: List of differentially expressed genes involved in UDP-GlcNAc pathway with their corresponding protein ID, Log2Fold Change, adjusted p-value (padj) and functional annotations.

Protein ID	Log_2FC	padj	Functional annotation
KAG6576217.1	-2.04	0.000000000204	Phosphoacetylglucosamine mutase (AGMI/PGM)
KAG6618307.1	-0.714	0.013644775	Glutamine-fructose-6-phosphate aminotransferase (GFAT)
KAG6614601.1	0.85	0.000103243	UDP-sugar pyrophosphorylase 1 (UAP1)
KAG6608751.1	1.91	0.00000039	Gcn5-related n-acetyltransferase (GNAT)
KAG6608741.1	-2.03	0.001044927	Gcn5-related n-acetyltransferase (GNAT)

Table 5: List of differentially expressed genes that code for putative glycosylphosphatidylinositol (GPI) anchored proteins with the corresponding protein ID, Log2Fold Change, adjusted p-value (padj) and functional annotations.

Protein ID	Log_2FC	padj	Functional annotation
KAG6580123.1	-3.65	0.001284601	putative GPI-anchored protein
KAG6613240.1	-1.97	0.007394577	putative GPI-anchored protein
KAG6594176.1	-1.84	0.000000529	GPI ethanolamine phosphate transferase 2
KAG6578026.1	-1.56	0.003864265	GPI-anchored protein
KAG6578108.1	2.61	0.000000786	putative GPI anchor protein

KAG6579792.1	3.02	0.000000243	putative GPI anchor protein
KAG6585048.1	3.21	0.000000000749	putative GPI anchor protein
KAG6585049.1	4.55	0.000000000000022	putative GPI anchor protein

Table 6: List of differentially expressed genes that encode membrane-associated proteins of different cellular organelles with their corresponding protein ID, Log2Fold Change, adjusted p-value (padj) and functional annotations.

Protein ID	**Log_2FC**	**padj**	**Functional annotation**
KAG6614965.1	2.11	0.001001391	Membrane-associated eicosanoid/glutathione metabolism (MAPEG) protein
KAG6616100.1	1.82	0.044965212	Peroxisomal membrane protein 4
KAG6615018.1	1.50	0.003467476	MAPEG protein
KAG6572530.1	-1.55	0.000195917	vesicle-associated membrane protein 7b
KAG6616282.1	-1.57	0.00000069	Peroxisomal membrane protein 4
KAG6580351.1	-1.66	2.7E-21	putative membrane protein
KAG6611693.1	-1.66	0.000195917	putative Endonuclease Reverse transcriptase
KAG6576467.1	-1.77	0.000000127	plasma-membrane proton-efflux P-type ATPase
KAG6616294.1	-1.82	0.000141616	Peroxisomal membrane protein 4
KAG6618563.1	-1.84	0.000000000147	putative membrane protein
KAG6576503.1	-1.85	0.000000135	Plasma membrane protein
KAG6590999.1	-1.97	0.002741917	putative Endonuclease Reverse transcriptase
KAG6597871.1	-2.05	0.000000819	Plasma membrane protein
KAG6580088.1	-2.66	0.000000856	putative vacuolar membrane protein
KAG6597762.1	-3.09	0.00000339	putative haustorium-specific membrane protein
KAG6577840.1	-3.51	0.00000009	putative membrane protein

Supplementary Figures

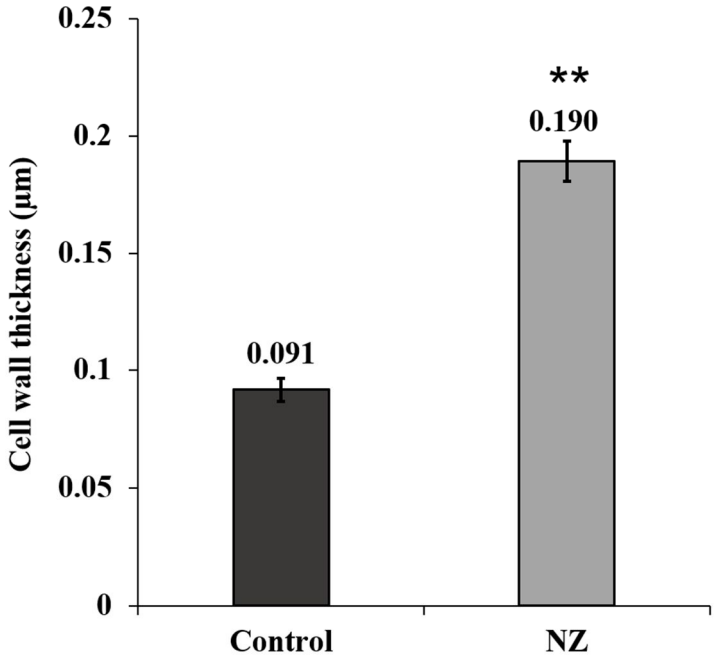

Supplementary Figure 1: Effect of nikkomycin Z on cell wall thickness of hyphal cells of *P. cinnamomi* exposed to 500 µM inhibitor for 48 h.

Data are presented as the mean ± SEM (biological replicates, N = 3). '**' denotes $p \leq 0.01$.

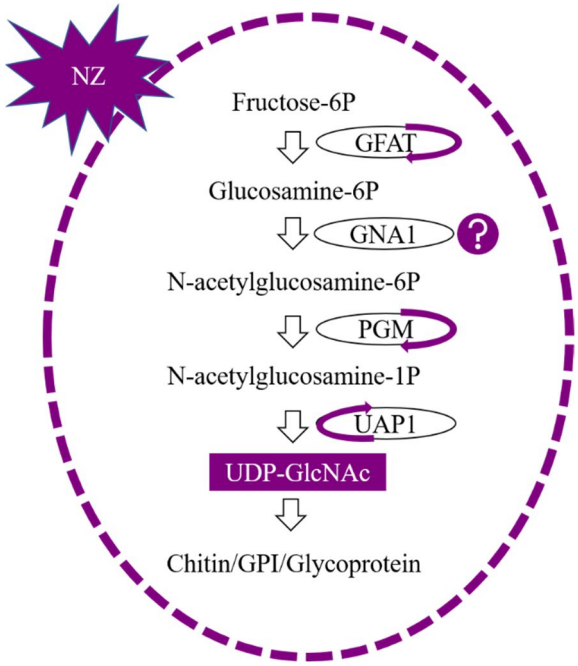

Supplementary Figure 2: Nikkomycin Z affects the UDP-GlcNAc biosynthesis pathway. Nikkomycin Z changes the gene expression level of Glutamine: fructose-6-phosphate aminotransferase (*Gfat*), Phosphoacetylglucosamine mutase (*Pgm/Agm1*), and UDP-GlcNAc pyrophosphorylase (*Uap1*), which are essential enzymes regulating the UDP-GlcNAc pathway. Nikkomycin Z treatment causes upregulation of genes of *Uap1* and downregulation of genes of *Gfat* and *Agm1*/*Pgm* which are denoted using upward or downward 'purple colored arrows'. The expression of *Gna1* is not directly affected but the 'question mark' denotes that gene expression of GCN5-related acetyl transferase family (*Gnat*s) was upregulated which is a gene family for *Gna1*.

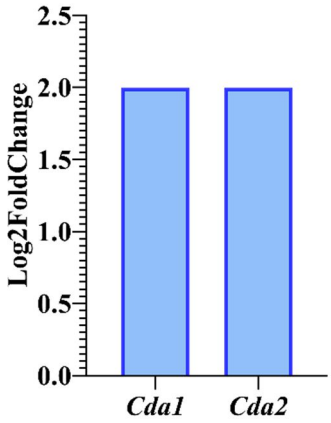

Supplementary Figure 3: Gene expression analysis by RNA-Seq of chitin deacetylases (*Cda 1* and *2*) in *P. cinnamomi* hyphae grown in the presence of 500 µM nikkomycin Z. Number of biological replicates = 5.

Supplementary File 1

A total of 3 putative chitin deacetylase genes was found in the *P. cinnamomi* genome. The identified protein sequences are listed, with the protein domain PF01522 found in polysaccharide deacetylases highlighted in yellow.

P. cinnamomi **CDA1 KAG6623988.1: 311aa**

MAELSVTRDLVGYGACGLDPKWPGGKKLALQFVLNYEEGGENCLLNGDAASEHLL
SDIVGAAPYVGQRHMNMESLYEYGSRAGFWRLHRAFTERQLPLTVYAVGLALEQNP
EAARAMKDAGWEVASHGYRWIDYQNVDEATEREHIRKTVAIHEKLLGARPVGIYQG
KPNVNTRRLVVEEGGFLYDADAYNDDLPYWNTQFGRPHLVIPYTLNNNDMKFVSA
QGFNSGDQFFTYLKDAFDVLLAEGRAGQPKMMSVGLHCRVVGHPGRIAALLRFLDY
VQSFQDVWICKREEIARHWYKTHYPQDAAASKL

P. cinnamomi **CDA2 KAG6594148.1: 225aa**

MHRAFTERQLPLTVYAVGLALEQNLEAARAMKDAGWEVASHGYRWIDYQNVDEA
TEREHIRKTVAIHEKLLGARPVGIYQGKPNVNTRRLVVEEGGFLYDADAYNDDLPY
WNTQFGRPHLVIPYTLNNNDMKFVSAQGFNSGDQFFTYLKDAFDVLLAEGRAGQPK
MMSVGLHCRVVGHPGRIAALLRFLDYVQSFQDVWICKREEIARHWYKTHYPQDAA
ASKL

P. cinnamomi **CDA3 KAG6623774.1: 319aa**

MATSSPAPPLLLLSLSLAACTCVAGPVDAPSSAMSGPAAAQIAGLCVFAAAGAFLAS
VYLLPRWLLRLVEWNSHPSVLWSVRTSARVCALTIDDAPSAATPAILDVLREHQVRA
TFFVISGRIPGHEDVLRRIVREGHALANHLTEDRASVLDELHVFEQKLQECDRAIAEF
QPSPDDQEPLETQQLLLQHKALGPDAVQPVLDVKEHDVGANRPRGKWMRPASGWF
TTPMREITARHGYRICLGSVYPHDAQIRSETVNSLHLRARTSCGSVIIVHDRSWTVGV
LKTALPELTRKFSFVSLDELVTYNERKPATKVTI

Chapter 4

Global transcriptomic analysis of the *Phytophthora cinnamomi* response to treatment with the plant defensin NaD1

Statement of Authorship

Title of Paper	**Global transcriptomic analysis of the *Phytophthora cinnamomi* response to treatment with the plant defensin NaD1**
Publication status	Unpublished and unsubmitted work written in manuscript style

Principal Author

Name of Principal Author	Amena Khatun		
Contribution to the Paper	Performed RNA extraction, conducted analysis and interpretation of RNA-Seq data, wrote and edited the manuscript.		
Overall percentage (%)	70%		
Certification	This paper reports on original research I conducted during the period of my Higher Degree by Research candidature and is not subject to any obligations or contractual agreements with a third party that would constrain its inclusion in this thesis. I am the primary author of this paper.		
Signature		Date	29/06/2023

Co-author Contributions

By signing the Statement of Authorship, each author certifies that:

i. The candidate's stated contribution to the publication is accurate (as detailed above)
ii. Permission is granted for the candidate in include the publication in the thesis, and
iii. The sum of all co-author contributions is equal to 100% less the candidate's stated contribution.

Name of Co-Author	Julian Schwerdt		
Contribution to the paper	Conducted analysis of RNA-Seq data, edited and reviewed the manuscript. I hereby certify that the Statement of Authorship is accurate		
Signature		Date	29/06/2023

Name of Co-Author	Vincent Bulone		
Contribution to the paper	Conceived the project, designed experiments, revised and edited the manuscript; corresponding author. I hereby certify that the Statement of Authorship is accurate.		
Signature		Date	29/06/2023

Global transcriptomic analysis of the *Phytophthora cinnamomi* response to treatment with the plant defensin NaD1

Amena Khatun, Julian Schwerdt[§] and Vincent Bulone[§,*]

School of Agriculture, Food and Wine, The University of Adelaide, Waite Campus, Urrbrae, South Australia 5064, Australia

[§]Present address: *College of Medicine and Public Health, Flinders University, Bedford Park South Australia 5042, South Australia, Australia*

[*]*To whom correspondence should be addressed: vincent.bulone@flinders.edu.au*

Abstract

The substantial impact of the oomycete genus *Phytophthora* on global food production and ecosystem is well-known. Efficient disease management strategies are necessary for these plant pathogens. At the same time, resistant cultivars and fungicides become ineffectual due to the development of new resistant pathogenic strains and their adverse impacts on the environment and human health. In nature, plants produce and use antimicrobial peptides (AMPs) against pathogenic microorganisms to keep themselves healthy, which can be considered a tool to design new biocontrol agents against the genus *Phytophthora*. We have previously reported that AMPs like *Nicotiana alata* defensin 1 (NaD1) are effective against *P. cinnamomi,* but the anti-oomycete mechanism remains unknown. Here, we performed a global transcriptomic analysis in *P. cinnamomi* using the RNA-Seq technique under the treatment of NaD1, the first known plant AMP tested against oomycetes. Four thousand one hundred ninety-four genes were differentially expressed (DEGs), including 1266 significantly upregulated genes and 333 significantly down-regulated genes (adjusted p-value < 0.05; Log2FoldChange > 1). Genes encoding voltage-gated ion channel activity, ion transporters, elicitin, GPI anchored protein, and RxLR effectors were significantly down-regulated among these DEGs. In contrast, genes associated with ergosterol biosynthesis, aminoacyl-tRNA ligase activity, and acyl/acetyltransferase activity were significantly upregulated. Gene Ontology enrichment analysis revealed that the related significant child terms belonged to molecular functions, which

were mainly involved in the growth, development, pathogenicity, and ion transport systems of *P. cinnamomi*. The result showed that NaD1 induces extensively complex responses in *P. cinnamomi*. The study provides evidence that NaD1 may inhibit mycelial growth and sporangia development by affecting multiple targets in *P. cinnamomi*. This transcriptional profiling also provides further understanding of the biological activity and mode of action of NaD1 against *P. cinnamomi*, which will contribute to developing novel biocontrol strategies for the genus *Phytophthora*.

Keywords: Antimicrobial peptides; NaD1; *Phytophthora cinnamomic*; RNA-Seq; transcriptomic analysis.

Introduction

The United Nations expects the human population to exceed 9 billion by 2050 and 11.5 billion by the turn of the century (Cole *et al.*, 2018). The challenge in achieving food security is enormous and remains complicated by human-induced climate change, war, and diverse global megatrends. Increasing agricultural productivity is fundamental to addressing this problem; however, intensifying fertilisers and pesticides can have severe environmental impacts. Microbial pathogens and other pests are responsible for roughly 25% loss in agricultural yield globally (Savary *et al.*, 2019). The use of pesticides for chemical control of crop diseases is essential for ensuring global food production, but it comes with potential ecotoxicological risks that cannot be ignored (Zubrod *et al.*, 2019). To mitigate the negative impact and intrinsic toxicity of these compounds, specific requirements have been imposed on pesticide registration by countries such as the European Union and the United States so that the exposure of toxic chemicals to the environment is limited. As a result, biocontrol agents such as plant-produced antimicrobial peptides (AMPs) have garnered significant attention as non-toxic future antimicrobial control measures (Chen *et al.*, 2021).

To date, ~900 AMPs have been discovered in bacteria, fungi, insects, mammals, and plants (Bakare *et al.*, 2022; Degenkolb *et al.*, 2003; Hancock, 2001). AMPs are crucial components of innate immunity systems as they disrupt the cell membrane (lipid bilayer) of pathogenic cells and prevent infection (Jenssen *et al.*, 2006; van der Weerden *et al.*, 2013). In plants, defensins are the most prominent family of AMPs, consisting of cysteine-rich cationic peptides typically composed of 45-54 amino acids. These peptides play a vital role in protecting the host plant from various microbial pathogens (Berkut *et al.*, 2014).

One such type of plant defensins is the *Nicotiana alata* Defensin 1 (NaD1), which is expressed in the flower of *N. alata* (Lay *et al.*, 2003). NaD1 can enter the cytoplasm through cell wall disruption in filamentous fungi like *Fusarium oxysporum* f.sp. *vasinfectum* and *Candida albicans* (Hayes *et al.*, 2013; Van Der Weerden *et al.*, 2008). In fungi, the mechanism of action of NaD1 involves three steps: initial attachment to the outer layer of the cell, internalisation to the cytoplasm, and subsequent production of reactive oxygen species (Hayes *et al.*, 2018). NaD1 has also been shown to inhibit mycelial growth in the *Phytophthora* species of the fungi-analogue oomycetes (Khatun *et al.*, 2023a), which comprise pathogens that can have devastating effects on trees and crops worldwide and are therefore considered both agronomically and ecologically important. However, the precise mechanisms by which NaD1 inhibits growth in *Phytophthora* remain unresolved.

Next-generation sequencing technologies have enabled the identification of the physiological and metabolic responses of microorganisms to antimicrobial compounds. RNA-Seq is a comprehensive and sensitive technique that offers significant advantages for gene expression studies, including profiling differentially expressed genes (DEGs) and their associated pathways (Nagalakshmi *et al.*, 2008; Nookaew *et al.*, 2012; Wang *et al.*, 2009). This technique has already been used to identify the physiological and metabolic responses of *Phytophthora* species in the presence of different chemical control agents (Gisi *et al.*, 2009; Hao *et al.*, 2020).

Conducting a global analysis of how NaD1 modifies gene expression in *Phytophthora* can provide insight into the unknown inhibitory mechanisms of NaD1. RNA-Seq has been used to identify the physiological and metabolic responses of *Phytophthora* to various chemical control agents, such as the response of *Phytophthora infestans* to the fungicide fluopicolide — where it was suggested that the mode of action of the fungicide is linked to the disruption of Golgi bodies and endoplasmic reticulum (Gisi *et al.*, 2009; Hao *et al.*, 2020). Another study used RNA-Seq to identify the mechanism by which the fungicide dimethomorph inhibited *Phytophthora parasitica*; it revealed significantly altered expression of genes related to cell wall biosynthesis, phosphate ion transporters, cell membrane permeability, and oxidative stress (Hao *et al.*, 2019). *Phytophthora cinnamomi* is considered among the top 10 devastating plant pathogenic oomycetes, yet remains understudied (Kamoun *et al.*, 2015). Here, we aimed to investigate the response of *P. cinnamomi* to the plant defensin NaD1 by utilising global transcriptomic analysis, leveraging a recently published whole genome assembly using third generation sequencing platforms (Engelbrecht *et al.*, 2021).

Materials and Methods

Culture of *Phytophthora cinnamomi*

Phytophthora cinnamomi (DAR 77502) was obtained from the Plant Pathology & Mycology Herbarium in New South Wales, Australia. Mycelial cultures were maintained on potato dextrose agar (PDA) at 25°C in dark conditions. For RNA extraction, mycelium was prepared for the target treatment by growing *P. cinnamomi* on PDA medium on which sterilized poppy seeds were evenly distributed. After 5 days of culture at 25°C in the dark, individual seeds covered by mycelium were transferred in each well of a 24-well plate (Corning Inc, US) containing 500 µl potato dextrose broth (PDB) per well. For NaD1 exposure, the peptide, which was generously provided by Prof. Marilyn Anderson (La Trobe University, Melbourne, Australia), was first prepared as a concentrated stock solution of 1 mM in sterilized ultrapure water and stored at – 20°C. Working dilutions of NaD1 were freshly prepared before mycelial treatment. Based on our previous study, a 50 µM concentration of NaD1 was selected, which can inhibit mycelial growth by 75% (Khatun *et al.*, 2023a). The PDB medium in each of the wells containing the poppy seed inoculum was supplemented with NaD1 and grown at 25°C in dark conditions for 48 h prior to RNA extraction and purification for RNA-Seq experiments.

RNA extraction and purification, and transcriptomic analysis by RNA-Seq

The *P. cinnamomi* mycelium grown as described above was washed with sterilised ultrapure water thrice and immediately ground using liquid nitrogen and a micro-pestle in a 1.5 mL tube. RNA was extracted using the Spectrum^{TM} Plant Total RNA Kit (Sigma-Aldrich, ST. Louis, MO, USA) according to the manufacturer's instructions. About 50 µL of extracted RNA solution was transferred into a sterilised 1.5 mL tube and 5.5 µL of 10X DNase buffer and 1 µL of DNase I (New England Biolabs, Ipswich, MA, USA) were added and the mixture was incubated at 37 °C for 15 min. Following incubation, 1 µL of 0.5 M EDTA was added and the samples were incubated at 75°C for 10 min. RNA quality was confirmed by agarose gel electrophoresis and spectrophotometry using a Thermo Scientific Nanodrop (Thermo Fisher Scientific, Waltham, MA, USA). The extracted RNA was further purified and concentrated using an RNA Clean & Concentrator Kit (Zymo Research, Irvine, CA, USA) and the final quality of RNA was checked using an Agilent 2100 Bioanalyzer (Agilent Technologies, CA) (Table 1). A total of five biological replicates were prepared for both the control and NaD1 treatment groups.

RNA samples were processed on a Novaseq 6000 S1 Lane (2x100 bp, v1.5 chemistry) at the South Australian Genomics Centre (SAGC) using their fee-for-service facility. The Nugen Universal Plus mRNA-seq kit was used to prepare Stranded polyA libraries. The Illumina protocol 15048776 v15 was followed for denaturation and clustering (on-board). RNA sequencing reads were quality-checked using FASTQC (https://www.bioinformatics.babraham.ac.uk/projects/fastqc/). Reads were mapped to the *P. cinnamomi* reference genome ASM1869171v1 using STAR 2.7.8a in 2-pass mode (Dobin *et al.*, 2012). Sequence contamination was assessed using DecontaMiner with default databases (Sangiovanni *et al.*, 2019). Gene count values and SAM/BAM file manipulation was determined using featureCounts (Liao *et al.*, 2013), Samtools (Danecek *et al.*, 2021) and BamTools (Barnett *et al.*, 2011), respectively. The DESeq2 pipeline was deployed to detect differentially expressed genes (DEGs) with count matrix data derived from featureCounts. Genes with adjusted p-value (<0.05) and expression fold changes of more than 1 or less than −1 were considered differentially expressed.

Functional term enrichment was performed on the DEGs to identify the impact of NaD1 on molecular functions and enzymatic pathways using topGO, with goexpress and goana also used to comprehend the data (Alexa *et al.*, 2006; Reti *et al.*, 2021; Rue-Albrecht *et al.*, 2016). As P. cinnamomi is a non-model organism an annotation database (OrgDb) was built using the AnnotationForge package. This enabled downstream GO analyses as these methods require a global functional annotation to achieve statistical power. GO enrichment maps, gene concept networks and graphs of enriched terms were constructed using the R package, clusterProfiler; specifically, enrichGO with qvaluecutoff (effectively the adjusted p-value) set to 0.05 and Benjamin-Hochberg p-value adjustment, was used to construct an enriched term set with visualisation and graphing performed with internal clusterProfiler functions and ggplot.

Results and Discussion

Assessment of genome quality

Since a good quality genome is a prerequisite for mapping transcript data, successful RNA-Seq data analysis largely depends on the choice of reference sequences (Kukurba & Montgomery, 2015; Yandell & Ence, 2012). Therefore, we chose the most contiguous draft assembly of our target organism, *P. cinnamomi* (ftp://ftp.ncbi.nlm.nih.gov/genomes/all/GCA/018/691/715/GCA_018691715.1_ASM1869171v1), comprising 133 scaffolds and 19,981 annotated genes with a total length of 109.7 Mb (Engelbrecht *et al.*, 2021). Assessing the representation of highly conserved eukaryotic core

genes, and the contiguity of scaffold sequences, are essential factors for determining assembly quality (Lander *et al.*, 2001; Manni *et al.*, 2021). The selected *P. cinnamomi* assembly was assessed by Benchmarking Universal Single-Copy Orthologs (BUSCO) to evaluate genic completeness and to contrast with previous sequencing projects (Longmuir *et al.*, 2017; Rands, 1922; Simão *et al.*, 2015; Studholme *et al.*, 2016). The assembly was shown to have a BUSCO completeness score of 97.5%, substantially higher than the 86.4% of Rands isolate (Rands, 1922) and the four alternative assemblies currently published (ranging from 91.5% to 97.4%) (Longmuir *et al.*, 2017; Studholme *et al.*, 2016). In addition, the assembly had an N50 (the length at which half of the assembled genome is contained in contigs) of 1.18 Mb, indicating a more contiguous assembly than prior projects (Engelbrecht *et al.*, 2021; Longmuir *et al.*, 2017; Studholme *et al.*, 2016). Therefore, given the relative strength of the above metrics, this assembly was selected as reference for the RNA-Seq read alignments.

It is worth noting that the genome of *P. cinnamomi* is highly plastic and has resulted in significant variation in assembly size due to isolate heterozygosity and large repetitive sequence content (Engelbrecht *et al.*, 2021). Repetitive sequences in genome assemblies generally interfere with sequence read mapping, and can complicate RNA-Seq sequencing experiments like those conducted here. Additionally, robust gene and functional annotation remains difficult and laborious with complications common in non-model organisms, like *P. cinnamomi*. In our previous study, we identified three voltage-gated calcium channel (*Vgcc*) genes (Protein ID: KAG6615340, KAG6622298, and KAG6604562), which were imprecisely predicted to encode 'L-type voltage-gated calcium channel' proteins (Khatun *et al.*, 2023a). We re-annotated exon structure using Fgenesh+ (http://www.softberry.com/berry.phtml?topic=fgenes_plus&group=programs&subgroup=gfs) and predicted function using BLAST homology and InterProScan (Camacho *et al.*, 2009; Jones *et al.*, 2014). These VGCCs are critical membrane-embedded transporters in eukaryotes and play a key role in calcium ion transport through the plasma membrane. To date, among all *Phytophthora* genome studied, only the *Vgcc* genes of *P. infestans* have been comprehensively annotated. Since homology to *P. infestans* did not inform the annotation of the selected *P. cinnamomi* assembly, the VGCC was characterised broadly as a 'Voltage-gated Ion Channel Superfamily', i.e., the superfamily of ion transporters such as potassium, calcium, and sodium transporters. Therefore, the present annotation lacks ion specificity. In addition, it has been found that superficial or incorrect functional annotation of genic regions is linked with incorrect Gene Ontology (GO) assignment (Andorf *et al.*, 2007; Brenner, 1999; Devos & Valencia, 2001; Jones *et al.*, 2007). Our investigation presented here found that GO:1990454 is a child term representing an 'L-type voltage-gated calcium channel complex' that should be associated with

our identified *Vgcc* genes encoding KAG6615340, KAG6622298, and KAG6604562. However, our GO enrichment analysis showed that these genes belong to the GO term GO:0005216, monoatomic ion channel activity and GO:0008324, monoatomic cation transmembrane transporter activity (Supplementary file 1), which are parent terms of GO:1990454. This analysis highlights the difficulty in achieving high functional annotation precision. Conversely, other enzyme family annotations have proved accurate. In our previous study we analysed four cellulose synthase, two chitin synthase, five glucan synthase, three chitin deacetylase genes, and four genes encoding enzymes from the hexosamine biosynthetic pathway (Khatun *et al.*, 2023a; Khatun *et al.*, 2023b). Each of these genomic loci were manually curated using homology methods, Fgenesh++ and phylogenetic validation with existing functional annotations shown to be correct. Therefore, with judicious manual curation and the awareness of annotation pitfalls, a global analysis of enzyme pathways was considered feasible.

Identification and analysis of *P. cinnamomi* differential gene expression in response to NaD1 exposure

To investigate the impact of NaD1 treatment on *P. cinnamomi*, we analysed the genes that are differentially expressed between the control and treated samples. Approximately 70% of sequence reads produced from all samples were successfully mapped to the *P. cinnamomi* genome (Table 2). Principal component analysis (PCA) was used to visualise and assess the variation in gene expression among samples treated with NaD1 and the untreated controls. The first and second principal components (PCA1 and PCA2) accounted for 51% and 27% of the total variance in the dataset, respectively. Samples from different treatment groups (presence or absence of NaD1) comprised two loose clusters (Figure 1). RNA quality was acceptable (Table 1), and no evidence of contamination was found during assessment using DecontaMiner with default databases (Sangiovanni *et al.*, 2019), so the pattern of variation between samples may be indicative of inherent underlying biological variability.

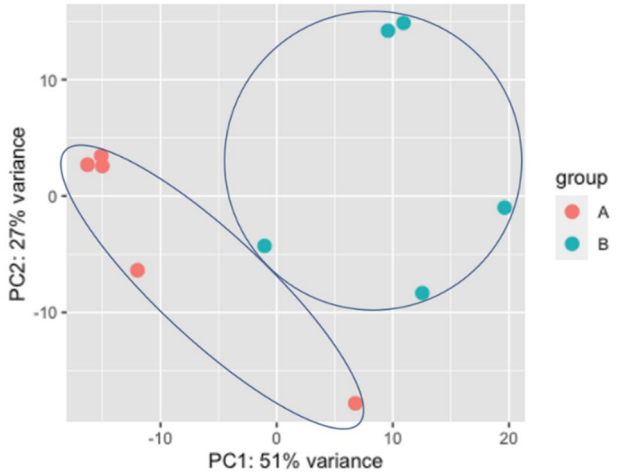

Figure 1: Score plot (PC1 vs PC2) of principal component analysis (PCA) of extracted RNA from mycelial cells of *P. cinnamomi* grown A) in the absence of NaD1 (control), and B) in the presence of 50 µM NaD1.

Our study reveals that 4194 genes were differentially expressed in the presence of NaD1. However, with an adjusted p-value ≤ 0.05 and log2 (Fold Change) ≥ ±1, the entire DEG set was reduced to 1599 genes, of which 1266 DEGs were downregulated, and 333 were upregulated. Several uncharacterised genes were present in the top 20 up and down-regulated genes (Tables 3 and 4). This is not surprising given that the genomic resources for *P. cinnamomi* remain at an early stage. No predicted gene sequences were found for these uncharacterised genes using FGENESH, which reflects the fragmented nature of the assembly with significant scope for improving contiguity.

The analysis of the top 20 upregulated genes in response to NaD1 revealed that the highest upregulated DEG encodes acetyl-CoA acetyltransferase (ACAT), which is involved in the ergosterol biosynthesis pathway (Soto *et al.*, 2011). This enzyme plays a vital role in the normal growth and development of fungi and oomycetes (Jin *et al.*, 2012). The approximately 20-fold upregulation of the gene encoding ACAT in *P. cinnamomi* during treatment with NaD1 could be linked with maintaining cell viability during mycelial growth inhibition (Khatun *et al.*, 2023a). The remaining proteins encoded by the top 20 upregulated genes are predicted to be involved in various fundamental-to-life functions, including: conversion of phosphoenolpyruvate into pyruvate; transport of divalent ions across cell membranes; regulation of alcohol metabolism; scavenging of reactive molecules like oxidase; transport of vacuolar amino acids; hydrolysis of glycosidic bonds; enabling metal ion binding activity;

splicing pre-mRNA; DNA-templated transcription, and DNA binding. These highly upregulated genes may be involved in a compensatory mechanism that helps maintain cell viability in response to NaD1 treatment (Table 3, Figure 2) (Edenberg, 2007; Magagnin *et al.*, 1993; Murphy *et al.*, 2011; Nguyen Trung *et al.*, 2022; Niegowski & Eshaghi, 2007; Sato *et al.*, 2021).

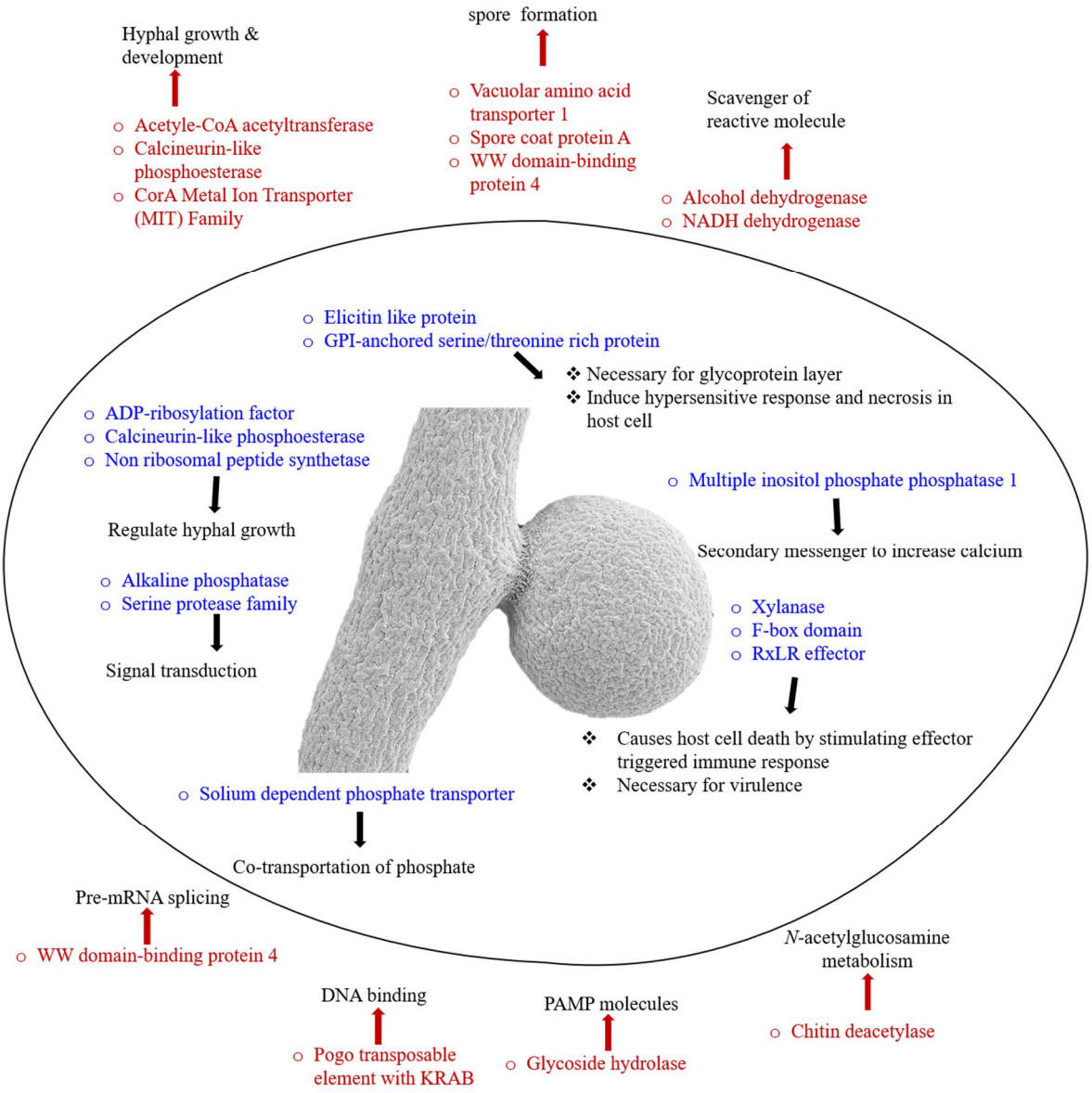

Figure 2: Schematic overview of the proposed responses of *P. cinnamomi* exposed NaD1, based on the differentially expressed genes (DEGs) identified by RNA-Seq.

Red coloured proteins indicate NaD1 treatment caused upregulation of their gene expression and blue coloured proteins indicates NaD1 treatment caused downregulation of their gene expression. The functions/roles of the genes are indicated by red/blue coloured arrows.

In addition, we have analysed the function and role of annotated genes that are differentially expressed in the top-20 downregulated list (Table 4, Figure 2). Previous research shows that significantly down-regulated loci include ADP-ribosylation factor, calcineurin-like phosphoesterase, nonribosomal peptide synthetase, multiple inositol polyphosphate phosphatase 1 — all of which play a key role in hyphal growth of fungi and oomycetes (Ah-Fong *et al.*, 2017; Michelsen *et al.*, 2015; Oide & Turgeon, 2020; Stearns *et al.*, 1990). Calcineurin-like phosphoesterase and multiple inositol polyphosphate phosphatase 1 are considered necessary for calcium homeostasis of *P. cinnamomi* and regulate cell growth and pathogenesis. They are among the most promising antifungal targets considered in recent years (Juvvadi *et al.*, 2014; Juvvadi *et al.*, 2017). In addition, two sodium-dependent phosphate transporters were found to be the top second and third downregulated genes. These genes have been shown to play vital roles in Na+/Pi- co-transportation in mammals, lower eukaryotes and bacteria (Murer *et al.*, 2004) (Magagnin *et al.*, 1993). Phosphate is a well-known essential nutrient for supplying energy, cell-signalling, and, most importantly, nucleotide biosynthesis in living organisms (Takeda *et al.*, 2000). It is plausible that the downregulation of these genes (log2FoldChange > -3) in our treated *P. cinnamomi* mycelia powerfully contributes to the slower hyphal growth observed in our previous study (Khatun *et al.*, 2023a).

Beyond modifying the expression of genes associated with fundamental organismal viability, several of the top 20 downregulated DEGs are essential for virulence and pathogenicity (Table 4, Figure 2). The well-documented effect of NaD1 to fungal pathogenicity is through its interaction with the cell wall (Van Der Weerden *et al.*, 2010). This has not been shown for oomycetes and here we show that NaD1 affects the critical *P. cinnamomi* genes, such as genes encoding KAG6610888.1, KAG6610748.1, KAG6583257.1, and KAG6617362.1 related to cell wall structure of *Phytophthora.* We observe the downregulation of GPI-anchored serine-threonine rich protein (KAG6580123.1, negative log2FC of -3.70) which plays an essential role in binding glucans to glycoproteins and thus influences the architecture of the cell wall for both fungi and oomycetes (Boisramé *et al.*, 2011; Kharel *et al.*, 2021). In our previous study, we have shown that NaD1 significantly alters the linkages between cell wall glucans of *P. cinnamomi*. Therefore, it can be proposed that the downregulation of genes encoding GPI-anchored serine-threonine may keep roles in modifying cell wall structure of *P. cinnamomi*. Nevertheless, additional research is necessary to validate this hypothesis.

Additional direct alterations to infective mechanisms are observed with the differential regulation of two genes predicted to encode elicitin proteins (KAG6613241.1 and KAG6613240.1). These genes are well characterised in the literature and are secreted by

Phytophthora species that induce necrosis and hypersensitive response (HR) in *Solanaceae* and *Cruciferae* families (Kharel *et al.*, 2021; Yu, 1995). Both are GPI-anchored and are considered promising antifungal targets (Mutz & Roemer, 2016). Other downregulated genes highlight the extent by which pathogenicity is affected, namely: xylanases; F-box domain proteins; and RxLR effector proteins, all of which play vital roles in pathogenicity and virulence (Lai & Liou, 2018; Morgan & Kamoun, 2007; Wu *et al.*, 2021). Finally, we observe the differential expression of a serine protease and alkaline phosphatase, both proteins mediate signal transduction but the former additionally is associated with protein maturation in fungi, and thus implicated in the evasion of host immune response (Muszewska *et al.*, 2017; Pang *et al.*, 2016).

Identification of differentially expressed *P. cinnamomi* metabolic pathways in response to NaD1 treatment

To comprehend the global effect of NaD1 on *P. cinnamomi* gene expression we performed Gene Ontology (GO) enrichment analysis. Gene Ontology is a standardised framework for comprehending the biomolecular function of a set of genes — for the work presented here, this is all expressed transcripts — using a hierarchical graph of terms that broadly correspond to enzyme pathways and expression networks. In total, 22 GO terms were found to be significantly enriched compared to the background (Figure 3 and 4).

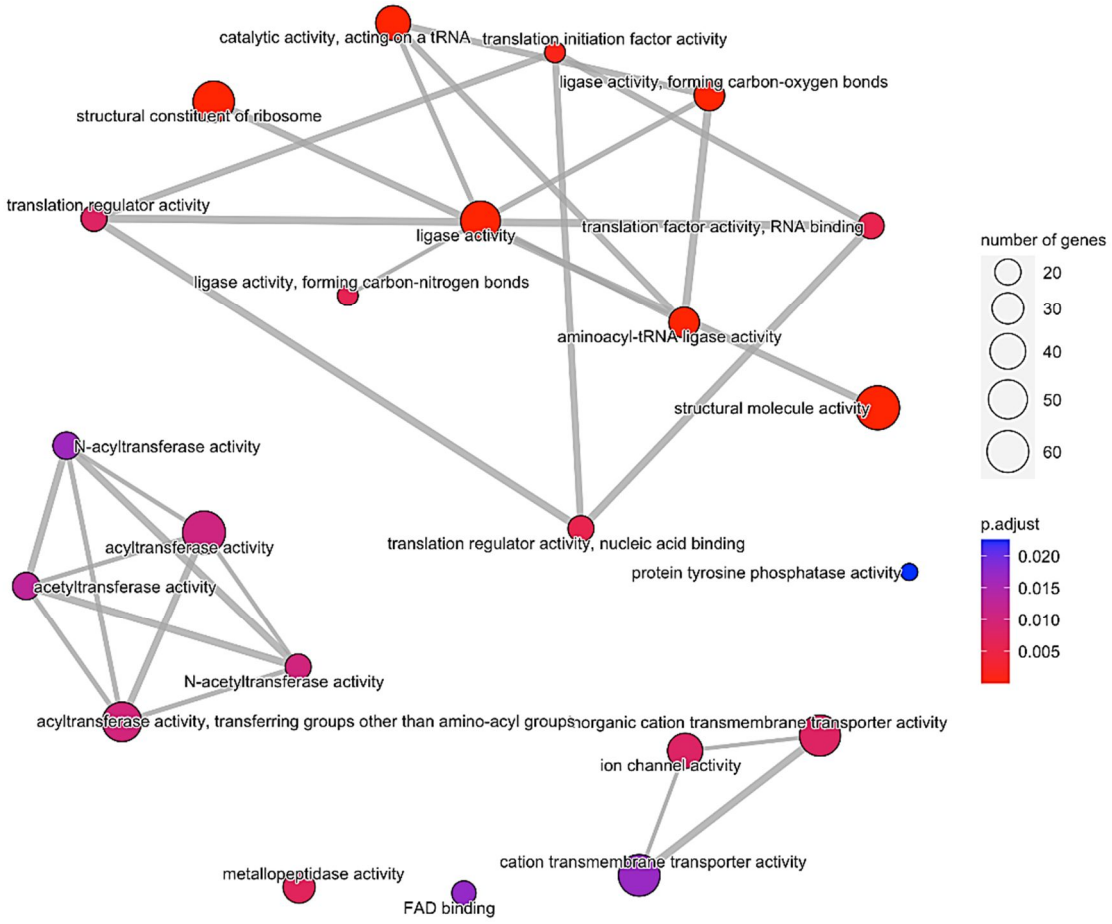

Figure 3: Gene concept network showing the relationships among enriched GO terms and the relationship of genes to GO terms hyphal cells of *P. cinnamomi* exposed to NaD1. The larger the size of the circles, the higher the number of DEGs.

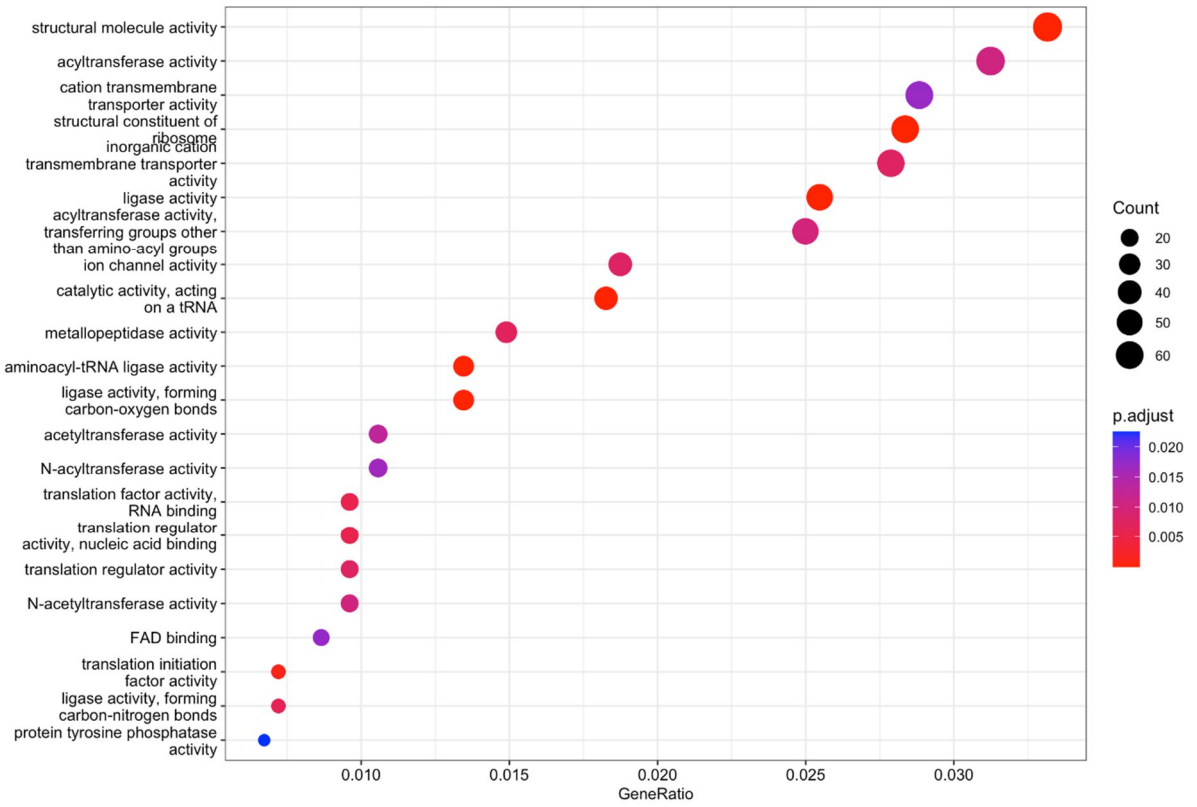

Figure 4: Top 22 enriched Gene Ontology terms of differentially expressed genes (DEGs) compared to the total number of genes recorded in hyphal cells of *P. cinnamomi*. The larger the size of the circles, the higher the number of DEGs.

These terms broadly cohere to several larger functional clusters, primarily: ligase activity, acyltransferase activity and ion channel activity. 'Ligase activity' is a large cluster that includes a total of 11 significantly enriched GO terms: GO:0016874, ligase activity; GO:0005198, structural molecule activity; GO:0003735, structural constituent of ribosome; GO:0016875, ligase activity forming carbon-oxygen bonds; GO:0004812, aminoacyl-tRNA ligase activity; GO:0140101, catalytic activity acting on a tRNA; GO:0003743, translation initiation factor activity; GO:0008135, translation factor activity and RNA binding; GO:0090079, translation regulator activity and nucleic acid binding, GO:0016879: ligase activity, forming carbon-nitrogen bonds, and GO:0045182: translation regulator activity (Figures 3 and 5). A significant cohort of differentially expressed ligase genes in the GO-enrichment data were upregulated.

The second significant cluster of network analysis is acyl/acetyl-transferase activity that includes a total of 5 significantly enriched GO terms (Figures 3-5), such as: GO:0016746, acyltransferase activity; GO:0016747, acyltransferase activity, transferring groups other than amino-acyl groups; GO:0008080, N-acetyltransferase activity; GO:0016407, acetyltransferase

activity; and GO:0016410. N-acyltransferase activity. The majority of differentially expressed genes encoding acetyl- and acyl-transferase enzymes were upregulated (Figure 3).

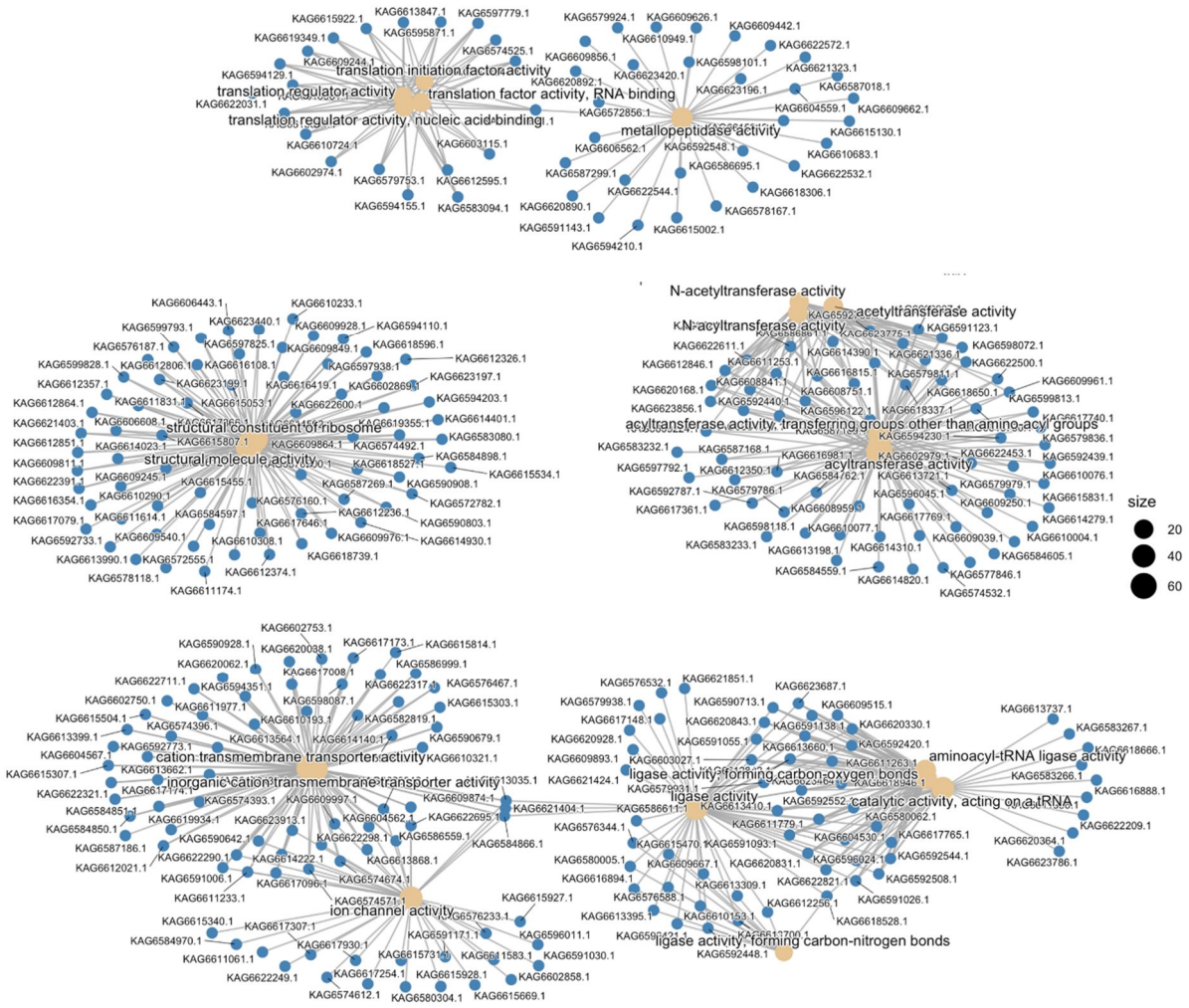

Figure 5: Enrichment map showing significant relationships between enriched GO terms (as per GO hierarchical graph) in the mycelium of *P. cinnamomi* exposed to NaD1.

Thirdly, we observe enrichment of the 'ion channel activity' cluster, which includes three significantly enriched GO terms: GO:0005216, ion channel activity; GO:0008324, cation transmembrane transporter activity; and GO:0022890, inorganic cation transmembrane transporter activity (Figures 3-5). Investigation of specific DEGs within each GO term revealed that 'ligase activity' and 'acyltransferase activity' were predominately upregulated, whereas those annotated as 'ion channel activity' were mainly downregulated. Figure 5 shows the relationships between enriched GO terms present in *P. cinnamomi* expression data and the specific gene products themselves. When considered alongside the GO term hierarchy (Figure 6) we observe a deep disruption to biochemical pathways, with GO clusters connected by numerous DEGs.

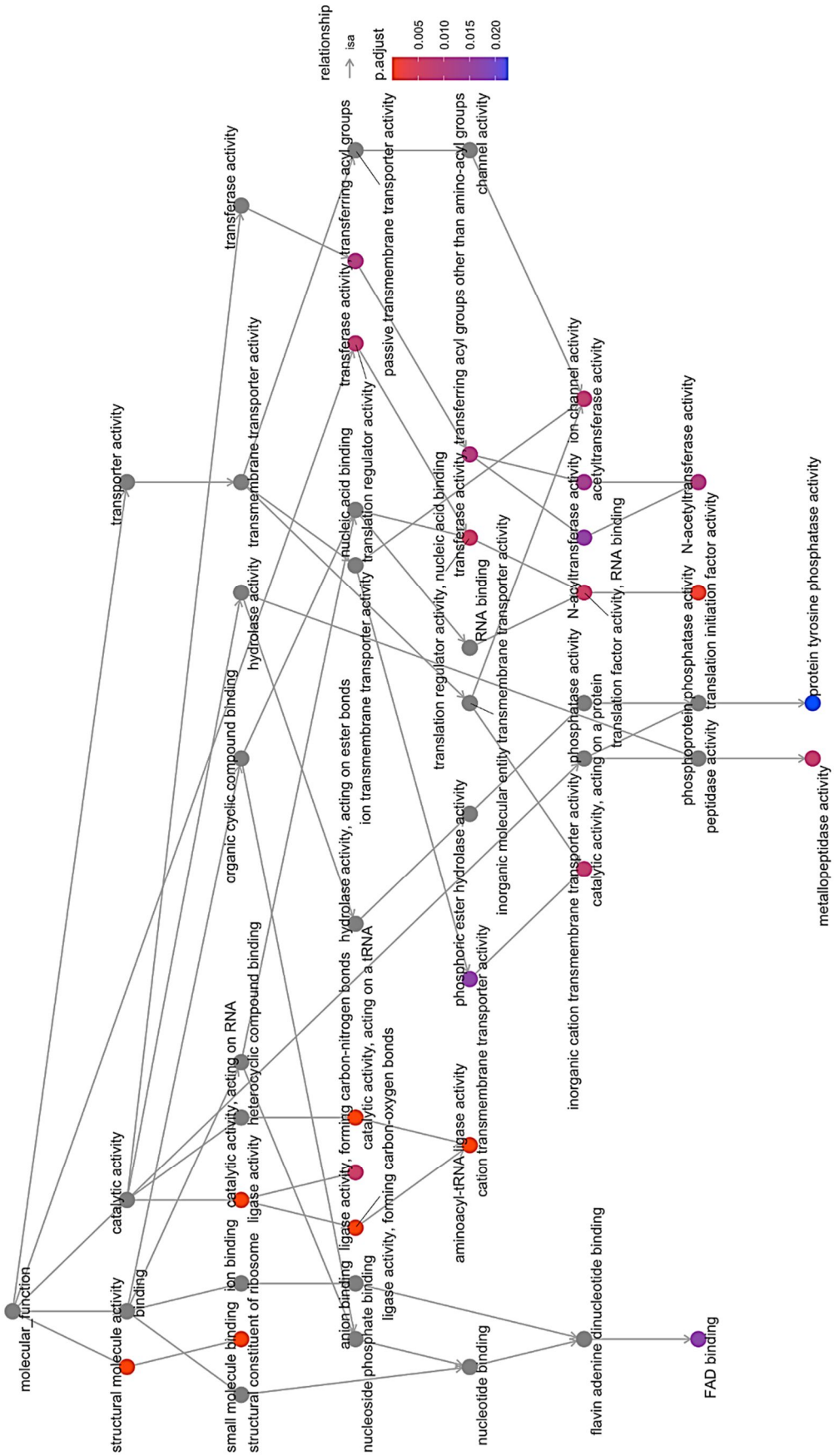

Figure 6: Network visualisation for predicted enriched GO term interactions and expression levels of genes due to differential responses to the NaD1 treatment of *P. cinnamomi* hyphal cells.

Upregulation of genes associated with tRNA ligase activity and acyl/acetyl-transferase activity suggests a compensatory mechanism for core survival and viability of *P. cinnamomi* in response to NaD1 treatment

Both ligases and acyl/acetyl-transferases are involved in a wide range of essential biochemical processes within cells. Indeed, ligases are involved in DNA replication/repair and protein modification, whilst acyl- and acetyltransferases are involved in metabolism, modification of protein function and gene regulation. To better understand how these pathways are modified in response to NaD1, we investigated specific genes within relevant GO terms.

Within ligases we observed several species of tRNA ligase enzymes (also known as aminoacyl-tRNA synthetase) were upregulated during our NaD1 treatment. These enzymes play a crucial role in charging tRNAs with specific amino acids, necessary for protein synthesis and cellular metabolism. Broadly, the upregulation of aminoacyl ligase-related genes appears to be linked to reprogramming cellular metabolism in response to the stress provoked by NaD1 treatment (Popow *et al.*, 2012).

Further modification of protein synthesis pathways are evident with 59 ribosome associated genes differentially expressed in the NaD1 treated samples (GO:0003735) (Figures 3 and 4, Supplementary file 1). Additionally, we observe the upregulation of 15 genes within the 'translation initiation factors (GO:0003743)' term and 20 genes assigned to 'translation factor activity, RNA binding (GO:0008135)' (Figures 3 and 4, Supplementary file 1). Both RNA binding proteins and translation initiation factors play a vital role in mRNA translation and gene expression (Hao *et al.*, 2020; Oliveira *et al.*, 2017). Enrichment of these GO terms in the expression profile of the mycelium of *P. cinnamomi* exposed to NaD1 indicates significant response to NaD1 stress through a substantial increase in overall gene transcription and protein synthesis.

Five GO terms covered the spread of differentially expressed acetyl- and acyltransferase genes in our data. The gene concept network shows them as functionally interrelated (Figure 3). Acetyl- and acyltransferase enzymes transfer acetyl or acyl group from a donor molecule as in, e.g., the acyl-coenzyme A or acetyl coenzyme A compounds pivotal to the Krebs cycle, to an acceptor molecule (such as a polypeptide chain), through an activity broadly called acylation. Acylation regulates several aspects of critical cellular processes, such as post-translational modifications and epigenetic changes to switch genes "on" and "off" (Drazic *et al.*, 2016). *N*-Acetyltransferases play significant role in modulating biological functions by modifying protein fine structure and regulating protein-protein interactions (Aksnes *et al.*, 2016). When

phytopathogenic fungi produce toxins to attack plants, their *N*-acetyltransferases are marshalled to detoxify the offending compounds (Ahmad *et al.*, 2021; Karagianni *et al.*, 2015; Sharma *et al.*, 2020). Likewise, acyltransferases play a crucial role in regulating the responses of *Phytophthora melonis* to biotic and abiotic stresses, e.g., protection from the oxidative stress of chilling temperatures (2 °C) (Ahmad *et al.*, 2021). We observed that the majority of DEGs encoding *N*-acetyltransferases were upregulated in *P. cinnamomi* in the presence of NaD1, which may indicate a defence response of *Phytophthora* to external toxins.

In fungi, a higher accumulation of intracellular reactive oxygen species (RoS) was observed in the presence of NaD1 (Van Der Weerden *et al.*, 2008). Accordingly, it can be hypothesised that *P. cinnamomi* attempts to shield the cell from oxidative stress perhaps by increasing the expression of acyltransferases such as acetyl-Co A acetyltransferase, as these enzymes are implicated in reducing susceptibility to RoS (Figures 2-4). It is consistent then that the acetyl-CoA acetyltransferase gene is the highest upregulated gene in the NaD1 treated mycelium of *P. cinnamomi* (Table 3, Supplementary file 1). However, given the enzymes central role in organismal viability other possible causes for over-expression must be considered (Zhang *et al.*, 2020). More directly, we observe that NADH dehydrogenase and alcohol dehydrogenase are significantly upregulated (Table 3), both of which are known to be involved in playing protective roles against oxidative stresses (DafaAlla *et al.*, 2021; Garavito *et al.*, 2019; Voulgaris *et al.*, 2012).

In our previous study, we demonstrated that NaD1 has the ability to impede the growth of hyphae and hinder the development of sporangia in *P. cinnamomi*. Building upon these findings, our current study proposes that the upregulation of ligase activity (specifically tRNA and aminoacyl ligases), translation initiation factors activity, acyltransferase activity, and acetyl-CoA acetyltransferase activity (Figure 3) serve as compensatory mechanisms (Figure 2). These mechanisms aim to maintain critical factors associated with the protein translation process, protein synthesis, oxidative stress, cellular viability, functional processes, and overall survival (optimal growth) of *P. cinnamomi*, particularly under stress induced by NaD1.

Downregulation of voltage-gated ion channels in response to NaD1 treatment

Voltage-gated ion channels (VIC) play a crucial role in maintaining cellular functions by regulating the flow of K^+, Na^+ and Ca^{2+} (Bezanilla, 2005; Zhao & Tombola, 2021; Zheng & Mackrill, 2016). The GO enrichment analyses presented here show that NaD1 significantly alters ion channel activity in *P. cinnamomi* (Figure 3). Enriched GO terms in this functional class include inorganic cation transmembrane transporter activity, ion channel activity, and

cation transmembrane transporter activity, with 58, 39, and 60 associated genes, respectively. The DEGs under these assigned GO terms primarily encode: VIC superfamily genes, the zinc (Zn2)-iron (Fe2) permease (ZIP) family, ATP synthases, calcium permeable stress-gated cation channel 1, putative sodium-dependent phosphate transporters, the metal ion (Mn^2-iron) transporter (NRAMP) family, a transmembrane protein, V-Type H^+-translocating pyrophosphatases, tRNA methyltransferases, the CorA metal ion transporter (MIT) family, a potassium/sodium hyperpolarisation-activated cyclic nucleotide-gated channel 4, necrosis-inducing protein NPP1 type, and calcium-translocating P-type ATPase (PMCA).

These genes were both up and downregulated significantly following treatment with NaD1 (Supplementary file 1). Our study found DEGs encoding members of the VIC superfamily to be exclusively downregulated without any compensatory upregulation. In our previous study, we identified three of these as putative voltage-gated calcium channel (*Vgcc*) genes encoding KAG6615340.1, KAG6604562.1, and KAG6622298.1, based on their GPHH motif and High Field Strength (HFS) site compared to other eukaryotic organisms (Khatun *et al.*, 2023a). We also observed the downregulation of three other genes encoding calcium channel subunit MID1, calcium-permeable stress-gated cation channel 1, and calcium-translocating P-type ATPase (PMCA) (Khatun *et al.*, 2023a), which are essential factors for maintaining calcium homeostasis in fungi and oomycetes (Lange & Peiter, 2019; Zheng & Mackrill, 2016). Using homology searches against other eukaryotic organisms in sequence databases, we identified additional genes that encode sodium channel proteins (KAG6622290.1, KAG6609874.1) and potassium voltage-gated channel proteins (KAG6617096.1, KAG6623946.1). Among these, only one DEG encoding a sodium channel (KAG6609874.1) was significantly downregulated under the 'ion channel activity' cluster (Figures 2 and 3).

Altogether, our data reveal that, among all ion channels, only calcium channels were strongly affected by NaD1. This finding is supported by our initial study, where we observed a lower level of intracellular calcium ions in the NaD1-treated hyphae of *P. cinnamomi* (Khatun *et al*., 2023a). It is noteworthy to mention that calcium is a crucial second messenger for controlling most of the physiological processes in all cellular organisms (Zheng & Mackrill, 2016). Indeed, previous studies have highlighted the importance of calcium in maintaining apical dominance of hyphal growth, cytokinesis, formation of zoospores, germination of cysts, appressorium formation, and sporogenesis in oomycetes (Bircher & Hohl, 1999; Connolly *et al.*, 1999; Donaldson & Deacon, 1992; Jackson & Hardham, 1996; Kerwin & Washino, 1986; Morris *et al.*, 2011). Similarly, we observed significantly altered hyphal growth under exposure to NaD1 (Khatun *et al.*, 2023a), which could be linked to the affected cellular calcium homeostasis

(Figures 2 and 3). The calcium channel subunit MID1 has been identified and characterised in *P. parasitica* and has been shown to play an essential role in the asexual development of this species (Hwu *et al.*, 2017). Interestingly, we observed the absence of sporangia production under NaD1 treatment (Khatun *et al.*, 2023a), which may directly or indirectly relate to the significant downregulation of the gene encoding MID1. The DEG encoding PMCA, a plasma membrane-bound Ca^{2+} ATPase that controls calcium ion homeostasis by regulating calcium efflux, was also found to be downregulated (Brini & Carafoli, 2011). In summary, it is conceivable that the effects of NaD1 on different ion channels, mainly calcium transporters, may be phenotypically relevant to the observed reduced growth, suppression of apical dominance, and absence of sporangia in *P. cinnamomi*.

Conclusion

Our study reports the effects of NaD1 on *P. cinnamomi* using a dataset generated by the DESeq2 pipeline of RNA-Seq data. It offers a comprehensive view of the transcriptomic deviations of *P. cinnamomi* cells exposed to NaD1. Significant changes in gene expression levels associated with voltage-gated ion channels, P-type ATPase, calcium channel subunit MID1, aminoacyl ligase, and acyl/acetyltransferase enzymes in *P. cinnamomi* provide insight into the mode of action of NaD1. The DEG dataset will also provide helpful candidate genes for the functional analysis of the plant defensin NaD1 to control *Phytophthora* species, including *P. cinnamomi.* The data from this study represents a novel contribution to the literature related to the mode of action of antimicrobial peptides like NaD1 against *Phytophthora* species.

Acknowledgments

The fee-for-service facility of the South Australian Genomics Centre (SAGC) was used for library construction and RNA sequencing. This work was supported by a grant to V.B. from the Australian Research Council (grant # DP180103974).

References

Ah-Fong, A. M. V., Kim, K. S. & Judelson, H. S. (2017) RNA-seq of life stages of the oomycete *Phytophthora infestans* reveals dynamic changes in metabolic, signal transduction, and pathogenesis genes and a major role for calcium signaling in development. *BMC Genomics*, 18(1), 198.

Ahmad, A., Akram, W., Bashir, Z., Shahzadi, I., Wang, R., Abbas, H. M. K., Hu, D., Ahmed, S., Xu, X., Li, G. & Wu, T. (2021) Functional and structural analysis of a novel acyltransferase from pathogenic *Phytophthora melonis*. *ACS Omega*, 6(3), 1797-1808.

Aksnes, H., Drazic, A., Marie, M. & Arnesen, T. (2016) First things first: vital protein marks by N-terminal acetyltransferases. *Trends in Biochemical Sciences*, 41(9), 746-760.

Alexa, A., Rahnenführer, J. & Lengauer, T. (2006) Improved scoring of functional groups from gene expression data by decorrelating GO graph structure. *Bioinformatics*, 22(13), 1600-1607.

Andorf, C., Dobbs, D. & Honavar, V. (2007) Exploring inconsistencies in genome-wide protein function annotations: a machine learning approach. *BMC Bioinformatics*, 8, 1-12.

Bakare, O. O., Gokul, A., Fadaka, A. O., Wu, R., Niekerk, L.-A., Barker, A. M., Keyster, M. & Klein, A. (2022) Plant antimicrobial peptides (PAMPs): Features, applications, production, expression, and challenges. *Molecules*, 27(12), 3703.

Barnett, D. W., Garrison, E. K., Quinlan, A. R., Strömberg, M. P. & Marth, G. T. (2011) BamTools: a C++ API and toolkit for analyzing and managing BAM files. *Bioinformatics*, 27(12), 1691-1692.

Berkut, A. A., Usmanova, D. R., Peigneur, S., Oparin, P. B., Mineev, K. S., Odintsova, T. I., Tytgat, J., Arseniev, A. S., Grishin, E. V. & Vassilevski, A. A. (2014) Structural similarity between defense peptide from wheat and scorpion neurotoxin permits rational functional design. *Journal of Biological Chemistry*, 289(20), 14331-14340.

Bezanilla, F. (2005) Voltage-gated ion channels. *IEEE Transactions on NanoBioscience*, 4(1), 34-48.

Bircher, U. & Hohl, H. (1999) A role for calcium in appressorium induction in *Phytophthora palmivora*. *Botanica Helvetica*, 109(1), 55-65.

Boisramé, A., Cornu, A., Da Costa, G. & Richard, M. L. (2011) Unexpected role for a serine/threonine-rich domain in the Candida albicans Iff protein family. *Eukaryotic Cell*, 10(10), 1317-30.

Brenner, S. E. (1999) Errors in genome annotation. *Trends in Genetics*, 15(4), 132-133.

Brini, M. & Carafoli, E. (2011) The plasma membrane Ca^{2+} ATPase and the plasma membrane sodium calcium exchanger cooperate in the regulation of cell calcium. *Cold Spring Harbor Perspectives in Biology*, 3(2).

Camacho, C., Coulouris, G., Avagyan, V., Ma, N., Papadopoulos, J., Bealer, K. & Madden, T. L. (2009) BLAST+: architecture and applications. *BMC Bioinformatics*, 10(1), 421.

Chen, E. H., Weng, C. W., Li, Y. M., Wu, M. C., Yang, C. C., Lee, K. T., Chen, R. P. & Cheng, C. P. (2021) De novo design of antimicrobial peptides with a special charge pattern and their application in combating plant pathogens. *Frontiers in Plant Science*, 12, 753217.

Cole, M. B., Augustin, M. A., Robertson, M. J. & Manners, J. M. (2018) The science of food security. *Npj Science of Food*, 2(1), 14.

Connolly, M. S., Williams, N., Heckman, C. A. & Morris, P. F. (1999) Soybean isoflavones trigger a calcium influx in *Phytophthora sojae*. *Fungal Genetics and Biology*, 28(1), 6-11.

DafaAlla, T. E. I., Abdalla, M., El-Arabey, A. A., Eltayb, W. A. & Mohapatra, R. K. (2021) Botrytis cinerea alcohol dehydrogenase mediates fungal development, environmental adaptation and pathogenicity. *Journal of Biomolecular Structure and Dynamics*, 1-13.

Danecek, P., Bonfield, J. K., Liddle, J., Marshall, J., Ohan, V., Pollard, M. O., Whitwham, A., Keane, T., McCarthy, S. A., Davies, R. M. & Li, H. (2021) Twelve years of SAMtools and BCFtools. *GigaScience*, 10(2).

Degenkolb, T., Berg, A., Gams, W., Schlegel, B. & Gräfe, U. (2003) The occurrence of peptaibols and structurally related peptaibiotics in fungi and their mass spectrometric identification via diagnostic fragment ions. *Journal of Peptide Science*, 9(11-12), 666-678.

Devos, D. & Valencia, A. (2001) Intrinsic errors in genome annotation. *Trends in Genetics*, 17(8), 429-431.

Dobin, A., Davis, C. A., Schlesinger, F., Drenkow, J., Zaleski, C., Jha, S., Batut, P., Chaisson, M. & Gingeras, T. R. (2012) STAR: ultrafast universal RNA-seq aligner. *Bioinformatics*, 29(1), 15-21.

Donaldson, S. P. & Deacon, J. W. (1992) Role of calcium in adhesion and germination of zoospore cysts of Pythium: a model to explain infection of host plants. *Microbiology*, 138(10), 2051-2059.

Drazic, A., Myklebust, L. M., Ree, R. & Arnesen, T. (2016) The world of protein acetylation. *Biochimica et Biophysica Acta (BBA)-Proteins and Proteomics*, 1864(10), 1372-1401.

Edenberg, H. J. (2007) The genetics of alcohol metabolism: role of alcohol dehydrogenase and aldehyde dehydrogenase variants. *Alcohol Research & Health*, 30(1), 5-13.

Engelbrecht, J., Duong, T. A., Prabhu, S. A., Seedat, M. & van den Berg, N. (2021) Genome of the destructive oomycete *Phytophthora cinnamomi* provides insights into its pathogenicity and adaptive potential. *BMC Genomics*, 22(1), 302.

Garavito, M. F., Narvaez-Ortiz, H. Y., Pulido, D. C., Löffler, M., Judelson, H. S., Restrepo, S. & Zimmermann, B. H. (2019) *Phytophthora infestans* dihydroorotate dehydrogenase is a potential target for chemical control - a comparison with the enzyme from solanum tuberosum. *Frontiers in Microbiology*, 10, 1479.

Gisi, U., Chet, I. & Gullino, M. L. (2009) Recent developments in management of plant diseases.

Hancock, R. E. W. (2001) Cationic peptides: effectors in innate immunity and novel antimicrobials. *The Lancet Infectious Diseases*, 1(3), 156-164.

Hao, K., Lin, B., Nian, F., Gao, X., Wei, Z., Luo, G., Lu, Y., Lan, M., Yang, J. & Wu, G. (2019) RNA-seq analysis of the response of plant-pathogenic oomycete *Phytophthora parasitica* to the fungicide dimethomorph. *Revista Argentina de Microbiología*, 51(3), 268-277.

Hao, P., Yu, J., Ward, R., Liu, Y., Hao, Q., An, S. & Xu, T. (2020) Eukaryotic translation initiation factors as promising targets in cancer therapy. *Cell Communication and Signaling*, 18(1), 175.

Hayes, B. M. E., Bleackley, M. R., Anderson, M. A. & van der Weerden, N. L. (2018) the plant defensin nad1 enters the cytoplasm of *Candida Albicans* via endocytosis. *Journal of Fungi (Basel)*, 4(1).

Hayes, B. M. E., Bleackley, M. R., Wiltshire, J. L., Anderson, M. A., Traven, A. & Weerden, N. L. v. d. (2013) Identification and mechanism of action of the plant defensin NaD1 as a new member of the antifungal drug arsenal against *Candida albicans*. *Antimicrobial Agents and Chemotherapy*, 57(8), 3667-3675.

Hwu, F. Y., Lai, M. W. & Liou, R. F. (2017) PpMID1 Plays a role in the asexual development and virulence of *Phytophthora parasitica*. *Frontiers in Microbiology*, 8, 610.

Jackson, S. L. & Hardham, A. R. (1996) A transient rise in cytoplasmic free calcium is required to induce cytokinesis in zoosporangia of *Phytophthora cinnamomi*. *European Journal of Cell Biology*, 69(2), 180-8.

Jenssen, H., Hamill, P. & Hancock, R. E. W. (2006) Peptide antimicrobial agents. *Clinical Microbiology Reviews*, 19(3), 491-511.

Jin, H., Song, Z. & Nikolau, B. J. (2012) Reverse genetic characterization of two paralogous acetoacetyl CoA thiolase genes in Arabidopsis reveals their importance in plant growth and development. *The Plant Journal*, 70(6), 1015-1032.

Jones, C. E., Brown, A. L. & Baumann, U. (2007) Estimating the annotation error rate of curated GO database sequence annotations. *BMC Bioinformatics*, 8(1), 1-9.

Jones, P., Binns, D., Chang, H.-Y., Fraser, M., Li, W., McAnulla, C., McWilliam, H., Maslen, J., Mitchell, A., Nuka, G., Pesseat, S., Quinn, A. F., Sangrador-Vegas, A., Scheremetjew, M., Yong, S.-Y., Lopez, R. & Hunter, S. (2014) InterProScan 5: genome-scale protein function classification. *Bioinformatics*, 30(9), 1236-1240.

Juvvadi, P. R., Lamoth, F. & Steinbach, W. J. (2014) Calcineurin as a multifunctional regulator: Unraveling novel functions in fungal stress responses, hyphal growth, drug resistance, and pathogenesis. *Fungal Biology Reviews*, 28(2), 56-69.

Juvvadi, P. R., Lee, S. C., Heitman, J. & Steinbach, W. J. (2017) Calcineurin in fungal virulence and drug resistance: Prospects for harnessing targeted inhibition of calcineurin for an antifungal therapeutic approach. *Virulence*, 8(2), 186-197.

Kamoun, S., Furzer, O., Jones, J. D. G., Judelson, H. S., Ali, G. S., Dalio, R. J. D., Roy, S. G., Schena, L., Zambounis, A., Panabières, F., Cahill, D., Ruocco, M., Figueiredo, A., Chen, X.-R., Hulvey, J., Stam, R., Lamour, K., Gijzen, M., Tyler, B. M., Grünwald, N. J., Mukhtar, M. S., Tomé, D. F. A., Tör, M., Van Den Ackerveken, G., McDowell, J., Daayf, F., Fry, W. E., Lindqvist-Kreuze, H., Meijer, H. J. G., Petre, B., Ristaino, J., Yoshida, K., Birch, P. R. J. & Govers, F. (2015) The Top 10 oomycete pathogens in molecular plant pathology. *Molecular Plant Pathology*, 16(4), 413-434.

Karagianni, E. P., Kontomina, E., Davis, B., Kotseli, B., Tsirka, T., Garefalaki, V., Sim, E., Glenn, A. E. & Boukouvala, S. (2015) Homologues of xenobiotic metabolizing N-acetyltransferases in plant-associated fungi: Novel functions for an old enzyme family. *Scientific Reports*, 5(1), 1-14.

Kerwin, J. L. & Washino, R. K. (1986) Oosporogenesis by *Lagenidium giganteum*: induction and maturation are regulated by calcium and calmodulin. *Canadian Journal of Microbiology*, 32(8), 663-672.

Kharel, A., Islam, M. T., Rookes, J. & Cahill, D. (2021) How to unravel the key functions of cryptic oomycete elicitin proteins and their role in plant disease. *Plants (Basel)*, 10(6).

Khatun, A. Selva, C., Schwerdt, J., Betts, N., Yu, L. & Bulone, V. (2023a) The plant defensin NaD1 inhibits the growth of Phytophthora species by interfering with cell wall structure and calcium transport. [*Manuscript to be submitted*]

Khatun, A., Schwerdt, J. Selva, C., Betts, N., Yu, L. & Bulone, V. (2023b) Analysis of the effect of the chitin synthase inhibitor nikkomycin Z on Phytophthora species. [*Manuscript to be submitted*]

Kukurba, K. R. & Montgomery, S. B. (2015) RNA sequencing and analysis. *Cold Spring Harbor Protocols*, 2015(11), 951-69.

Lai, M.-W. & Liou, R.-F. (2018) Two genes encoding GH10 xylanases are essential for the virulence of the oomycete plant pathogen *Phytophthora parasitica*. *Current Genetics*, 64(4), 931-943.

Lander, E. S., Linton, L. M., Birren, B., Nusbaum, C., Zody, M. C., Baldwin, J., Devon, K., Dewar, K., Doyle, M., FitzHugh, W., Funke, R., Gage, D., Harris, K., Heaford, A., Howland, J., Kann, L., Lehoczky, J., LeVine, R., McEwan, P., McKernan, K., Meldrim,

J., Mesirov, J. P., Miranda, C., Morris, W., Naylor, J., Raymond, C., Rosetti, M., Santos, R., Sheridan, A., Sougnez, C., Stange-Thomann, Y., Stojanovic, N., Subramanian, A., Wyman, D., Rogers, J., Sulston, J., Ainscough, R., Beck, S., Bentley, D., Burton, J., Clee, C., Carter, N., Coulson, A., Deadman, R., Deloukas, P., Dunham, A., Dunham, I., Durbin, R., French, L., Grafham, D., Gregory, S., Hubbard, T., Humphray, S., Hunt, A., Jones, M., Lloyd, C., McMurray, A., Matthews, L., Mercer, S., Milne, S., Mullikin, J. C., Mungall, A., Plumb, R., Ross, M., Shownkeen, R., Sims, S., Waterston, R. H., Wilson, R. K., Hillier, L. W., McPherson, J. D., Marra, M. A., Mardis, E. R., Fulton, L. A., Chinwalla, A. T., Pepin, K. H., Gish, W. R., Chissoe, S. L., Wendl, M. C., Delehaunty, K. D., Miner, T. L., Delehaunty, A., Kramer, J. B., Cook, L. L., Fulton, R. S., Johnson, D. L., Minx, P. J., Clifton, S. W., Hawkins, T., Branscomb, E., Predki, P., Richardson, P., Wenning, S., Slezak, T., Doggett, N., Cheng, J. F., Olsen, A., Lucas, S., Elkin, C., Uberbacher, E., Frazier, M., et al (2001) Initial sequencing and analysis of the human genome. *Nature*, 409(6822), 860-921.

Lange, M. & Peiter, E. (2019) Calcium Transport Proteins in Fungi: The phylogenetic diversity of their relevance for growth, virulence, and stress resistance. *Frontiers in Microbiology*, 10, 3100.

Lay, F. T., Brugliera, F. & Anderson, M. A. (2003) Isolation and properties of floral defensins from ornamental tobacco and petunia. *Plant Physiology*, 131(3), 1283-1293.

Liao, Y., Smyth, G. K. & Shi, W. (2013) featureCounts: an efficient general purpose program for assigning sequence reads to genomic features. *Bioinformatics*, 30(7), 923-930.

Longmuir, A. L., Beech, P. L. & Richardson, M. F. (2017) Draft genomes of two Australian strains of the plant pathogen, *Phytophthora cinnamomi*. *F1000Res*, 6, 1972.

Magagnin, S., Werner, A., Markovich, D., Sorribas, V., Stange, G., Biber, J. & Murer, H. (1993) Expression cloning of human and rat renal cortex Na/Pi cotransport. *Proceedings of the National Academy of Sciences of the United States of America*, 90(13), 5979-5983.

Manni, M., Berkeley, M. R., Seppey, M. & Zdobnov, E. M. (2021) BUSCO: Assessing genomic data quality and beyond. *Current Protocols*, 1(12), e323.

Michelsen, C. F., Watrous, J., Glaring, M. A., Kersten, R., Koyama, N., Dorrestein, P. C. & Stougaard, P. (2015) Nonribosomal peptides, key biocontrol components for

Pseudomonas fluorescens In5, isolated from a Greenlandic suppressive soil. *mBio*, 6(2), e00079.

Morgan, W. & Kamoun, S. (2007) RXLR effectors of plant pathogenic oomycetes. *Current Opinion in Microbiology*, 10(4), 332-338.

Morris, E. J. S., Jackson, S. L. & Garrill, A. (2011) An investigation of the effects of Ca^{2+} channel inhibitors on branching and chemotropism in the oomycete *Achlya bisexualis*: Support for a role for Ca2+ in apical dominance. *Fungal Genetics and Biology*, 48(5), 512-518.

Murer, H., Forster, I. & Biber, J. (2004) The sodium phosphate cotransporter family SLC34. *Pflugers Archiv: European journal of physiology*, 447(5), 763-767.

Murphy, C., Powlowski, J., Wu, M., Butler, G. & Tsang, A. (2011) Curation of characterized glycoside hydrolases of Fungal origin. *Database*, 2011.

Muszewska, A., Stepniewska-Dziubinska, M. M., Steczkiewicz, K., Pawlowska, J., Dziedzic, A. & Ginalski, K. (2017) Fungal lifestyle reflected in serine protease repertoire. *Scientific Reports*, 7(1), 9147.\

Mutz, M. & Roemer, T. (2016) The GPI anchor pathway: a promising antifungal target? *Future Medicinal Chemistry*, 8(12), 1387-1391.

Nagalakshmi, U., Wang, Z., Waern, K., Shou, C., Raha, D., Gerstein, M. & Snyder, M. (2008) The transcriptional landscape of the yeast genome defined by RNA sequencing. *Science*, 320(5881), 1344-1349.

Nguyen Trung, M., Kieninger, S., Fandi, Z., Qiu, D., Liu, G., Mehendale, N. K., Saiardi, A., Jessen, H., Keller, B. & Fiedler, D. (2022) stable isotopomers of myo-inositol uncover a complex minpp1-dependent inositol phosphate network. *ACS Central Science*, 8(12), 1683-1694.

Niegowski, D. & Eshaghi, S. (2007) The CorA family: structure and function revisited. *Cellular and Molecular Life Sciences*, 64(19-20), 2564-74.

Nookaew, I., Papini, M., Pornputtapong, N., Scalcinati, G., Fagerberg, L., Uhlén, M. & Nielsen, J. (2012) A comprehensive comparison of RNA-Seq-based transcriptome analysis from

reads to differential gene expression and cross-comparison with microarrays: a case study in *Saccharomyces cerevisiae*. *Nucleic Acids Research*, 40(20), 10084-10097.

Oide, S. & Turgeon, B. G. (2020) Natural roles of nonribosomal peptide metabolites in fungi. *Mycoscience*, 61(3), 101-110.

Oliveira, C., Faoro, H., Alves, L. R. & Goldenberg, S. (2017) RNA-binding proteins and their role in the regulation of gene expression in Trypanosoma cruzi and Saccharomyces cerevisiae. *Genetics and Molecular Biology*, 40(1), 22-30.

Pang, Z., Chen, L., Mu, W., Liu, L. & Liu, X. (2016) Insights into the adaptive response of the plant-pathogenic oomycete *Phytophthora capsici* to the fungicide flumorph. *Scientific Reports*, 6(1), 24103.

Popow, J., Schleiffer, A. & Martinez, J. (2012) Diversity and roles of (t)RNA ligases. *Cellular and Molecular Life Sciences*, 69(16), 2657-70.

Rands, R. D. (1922) Streepkanker van kaneel, veroorzaakt door phytophthora cinnamomi n. SP. *Mededelingen van het Instituut voor Plantenziekten*, 54, 53.

Reti, D., O'Brien, A., Wetzel, P., Tay, A., Bauer, D. C. & Wilson, L. O. W. (2021) GOANA: A Universal high-throughput web service for assessing and comparing the outcome and efficiency of genome editing experiments. *The CRISPR Journal,* 4(2), 243-252.

Rue-Albrecht, K., McGettigan, P. A., Hernández, B., Nalpas, N. C., Magee, D. A., Parnell, A. C., Gordon, S. V. & MacHugh, D. E. (2016) GOexpress: an R/Bioconductor package for the identification and visualisation of robust gene ontology signatures through supervised learning of gene expression data. *BMC Bioinformatics*, 17(1), 126.

Sangiovanni, M., Granata, I., Thind, A. S. & Guarracino, M. R. (2019) From trash to treasure: detecting unexpected contamination in unmapped NGS data. *BMC Bioinformatics*, 20(4), 168.

Sato, A., Kimura, T., Hondo, K., Kawano-Kawada, M. & Sekito, T. (2021) The vacuolar amino acid transport system is a novel, direct target of GATA transcription factors. *Bioscience, Biotechnology, and Biochemistry*, 85(3), 587-599.

Savary, S., Willocquet, L., Pethybridge, S. J., Esker, P., McRoberts, N. & Nelson, A. (2019) The global burden of pathogens and pests on major food crops. *Nature Ecology & Evolution*, 3(3), 430-439.

Sharma, S., Ahmed, M. & Akhter, Y. (2020) Fungal acetyltransferases structures, mechanisms and inhibitors: A review. *International Journal of Biological Macromolecules*, 157, 626-640.

Simão, F. A., Waterhouse, R. M., Ioannidis, P., Kriventseva, E. V. & Zdobnov, E. M. (2015) BUSCO: assessing genome assembly and annotation completeness with single-copy orthologs. *Bioinformatics*, 31(19), 3210-2.

Soto, G., Stritzler, M., Lisi, C., Alleva, K., Pagano, M. E., Ardila, F., Mozzicafreddo, M., Cuccioloni, M., Angeletti, M. & Ayub, N. D. (2011) Acetoacetyl-CoA thiolase regulates the mevalonate pathway during abiotic stress adaptation. *Journal of Experimental Botany*, 62(15), 5699-5711.

Stearns, T., Kahn, R. A., Botstein, D. & Hoyt, M. A. (1990) ADP ribosylation factor is an essential protein in *Saccharomyces cerevisiae* and is encoded by two genes. *Molecular and Cellular Biology*, 10(12), 6690-9.

Studholme, D. J., McDougal, R. L., Sambles, C., Hansen, E., Hardy, G., Grant, M., Ganley, R. J. & Williams, N. M. (2016) Genome sequences of six Phytophthora species associated with forests in New Zealand. *Genomics Data*, 7, 54-6.

Takeda, E., Taketani, Y., Morita, K., Tatsumi, S., Katai, K., Nii, T., Yamamoto, H. & Miyamoto, K.-i. (2000) Molecular mechanisms of mammalian inorganic phosphate homeostasis. *Advances in Enzyme Regulation*, 40(1), 285-302.

van der Weerden, N. L., Bleackley, M. R. & Anderson, M. A. (2013) Properties and mechanisms of action of naturally occurring antifungal peptides. *Cellular and Molecular Life Sciences*, 70(19), 3545-3570.

Van Der Weerden, N. L., Hancock, R. E. & Anderson, M. A. (2010) Permeabilization of fungal hyphae by the plant defensin NaD1 occurs through a cell wall-dependent process. *Journal of Biological Chemistry*, 285(48), 37513-37520.

Van Der Weerden, N. L., Lay, F. T. & Anderson, M. A. (2008) The plant defensin, NaD1, enters the cytoplasm of *Fusarium oxysporum* hyphae. *Journal of Biological Chemistry*, 283(21), 14445-14452.

Voulgaris, I., O'Donnell, A., Harvey, L. M. & McNeil, B. (2012) Inactivating alternative NADH dehydrogenases: enhancing fungal bioprocesses by improving growth and biomass yield? *Scientific Reports*, 2(1), 322.

Wang, Z., Gerstein, M. & Snyder, M. (2009) RNA-Seq: a revolutionary tool for transcriptomics. *Nature Reviews Genetics*, 10(1), 57-63.

Wu, T., Fan, C. L., Han, L. T., Guo, Y. B. & Liu, T. B. (2021) Role of f-box protein cdc4 in fungal virulence and sexual reproduction of *Cryptococcus neoformans*. *Frontiers in Cellular and Infection Microbiology*, 11, 806465.

Yandell, M. & Ence, D. (2012) A beginner's guide to eukaryotic genome annotation. *Nature Reviews Genetics*, 13(5), 329-342.

Yu, L. M. (1995) Elicitins from Phytophthora and basic resistance in tobacco. *Proceedings of the National Academy of Sciences of the United States of America*, 92(10), 4088-4094.

Zhang, Y., Wei, W., Fan, J., Jin, C., Lu, L. & Fang, W. (2020) *Aspergillus fumigatus* mitochondrial acetyl coenzyme a acetyltransferase as an antifungal target. *Applied and Environmental Microbiology*, 86(7).

Zhao, C. & Tombola, F. (2021) Voltage-gated proton channels from fungi highlight role of peripheral regions in channel activation. *Communications Biology*, 4(1), 261.

Zheng, L. & Mackrill, J. J. (2016) Calcium signaling in oomycetes: An evolutionary perspective. *Frontiers in Physiology*, 7, 123.

Zubrod, J. P., Bundschuh, M., Arts, G., Brühl, C. A., Imfeld, G., Knäbel, A., Payraudeau, S., Rasmussen, J. J., Rohr, J., Scharmüller, A., Smalling, K., Stehle, S., Schulz, R. & Schäfer, R. B. (2019) Fungicides: An overlooked pesticide class? *Environmental Science & Technology*, 53(7), 3347-3365.

Tables

Table 1: Quality of extracted RNA for Next-Generation Sequencing

Treatment group	Amount (ng)	RIN*	Index	Mean Size (bp)	Total Reads Passed Filter (Million)
Control replicate 1	410	7.1	TCCTGGTA +AGGATCTG	362	71.6
Control replicate 2	405	6.9	CATCAACC +TTCAGGAG	363	64.8
Control replicate 3	678	6.5	AGCAGACA +CATCCTCT	369	76.7
Control replicate 4	711	7.3	GAAGACTG +TCATGGTG	363	65.3
Control replicate 5	305	8.2	TCTAGTCC +GATTACCG	362	63.5
NaD1 replicate 1	150	7	CTCGACTT +ACACACTC	363	61
NaD1 replicate 2	420	7.1	CTAGCTCA +CCTCAGTT	361	77.9
NaD1 replicate 3	477	6.6	TCCAACTG +CTGACACA	340	68.9
NaD1 replicate 4	358	7.3	GACATCTC +GTGTGACA	363	75.9
NaD1 replicate 5	170	7.3	ACTGCACT +GACGATCT	364	71.9

*NB. Some RINs can be underestimated due to software optimised for mammals.

Table 2: Profile of the RNA sequence data

Treatment group	Sample group	Input reads	Uniquely mapped reads	Uniquely mapped reads (%)	Number of reads mapped to multiple loci	% of reads mapped to multiple loci
Control replicate 1	21_00887	61747499	44528805	72.11%	11450245	18.54%
Control replicate 2	21_00873	55964366	40789570	72.88%	9766260	17.45%
Control replicate 3	21_00888	66292747	47851661	72.18%	12625037	19.04%
Control replicate 4	21_00889	56302406	41242738	73.25%	9939660	17.65%
Control replicate 5	21_00876	54754548	40403616	73.79%	9152609	16.72%
NaD1 replicate 1	21_00877	52628866	38444266	73.05%	8849515	16.81%
NaD1 replicate 2	21_00878	67132897	48946662	72.91%	11780824	17.55%
NaD1 replicate 3	21_00890	59209066	40592786	68.56%	10423005	17.60%
NaD1 replicate 4	21_00891	65491242	47811005	73.00%	10913043	16.66%
NaD1 replicate 5	21_00881	62035731	45297236	73.02%	9768315	15.75%

Table 3: Top 20 upregulated genes/proteins of *P. cinnamomi* cells exposed to NaD1

Locus_tag	Log2(FC)	adjusted p-value	Protein ID	Functional Annotation
gene-IUM83_09676	20.8204	2.96E-06	KAG6617769.1	Acetyl-CoA acetyltransferase
gene-IUM83_00853	19.73148	1.24E-05	KAG6610067.1	pyruvate phosphate dikinase
gene-IUM83_16488	8.597457	0.046912	KAG6578248.1	Pyruvate kinase
gene-IUM83_12385	3.310159	0.013799	KAG6592499.1	putative 12-oxophytodienoate reductase
gene-IUM83_04254	3.064091	3.80E-06	KAG6613399.1	CorA Metal Ion Transporter (MIT) Family
gene-IUM83_04670	2.855177	0.006733	KAG6616895.1	Transmembrane protein
gene-IUM83_05877	2.799457	1.44E-05	KAG6620132.1	hypothetical protein
gene-IUM83_17565	2.767826	0.000368	KAG6603080.1	putative alcohol dehydrogenase
gene-IUM83_04227	2.724299	4.76E-05	KAG6614730.1	hypothetical protein
gene-IUM83_06994	2.702762	0.00066	KAG6603002.1	NADH dehydrogenase
gene-IUM83_10497	2.651484	0.009212	KAG6578097.1	Pogo transposable element with KRAB
gene-IUM83_08703	2.631214	2.30E-05	KAG6614868.1	putative 12-oxophytodienoate reductase
gene-IUM83_16705	2.628195	0.000484	KAG6586822.1	Vacuolar amino acid transporter 1
gene-IUM83_04299	2.625984	0.004815	KAG6613699.1	Spore coat protein A
gene-IUM83_11186	2.545523	0.012639	KAG6591005.1	Glycoside hydrolase

gene-IUM83_01783	2.528657	0.004815	KAG6623988.1	Urate catabolism protein/ Chitin deacetylase 1
gene-IUM83_01544	2.527221	1.69E-10	KAG6618292.1	Calcineurin-like phosphoesterase
gene-IUM83_19169	2.525306	0.002374	KAG6595893.1	WW domain-binding protein 4
gene-IUM83_19986	2.499015	2.28E-05	KAG6595769.1	Pogo transposable element with KRAB domain-like
gene-IUM83_18128	2.333121	0.000205	KAG6586688.1	hypothetical protein

Table 4: Top 20 downregulated genes/proteins of *P. cinnamomi* hyphal cells exposed to NaD1

Locus_tag	log2FC	adjusted p-value	Protein ID	Functional Annotation
gene-IUM83_02504	-6.23864	3.19E-05	KAG6617508.1	hypothetical protein
gene-IUM83_19166	-5.5606	1.74E-06	KAG6595898.1	Sodium-dependent phosphate transporter
gene-IUM83_05866	-5.21492	5.17E-05	KAG6619934.1	putative sodium-dependent phosphate transporter
gene-IUM83_10814	-4.69524	2.62E-10	KAG6574682.1	hypothetical protein
gene-IUM83_16934	-4.66096	3.66E-09	KAG6613241.1	elicitin-like protein
gene-IUM83_16935	-4.42239	4.15E-08	KAG6613240.1	putative GPI-anchored elicitin INL11b-like protein
gene-IUM83_15438	-4.12206	0.007551	KAG6572820.1	Serine protease family S33
gene-IUM83_13110	-4.10442	2.55E-06	KAG6616673.1	F-box domain

gene-IUM83_03957	-4.04517	0.000226	KAG6614602.1	Calcineurin-like phosphoesterase
gene-IUM83_10281	-3.9881	5.49E-21	KAG6614038.1	Nonribosomal peptide synthetase
gene-IUM83_09652	-3.9683	0.000162	KAG6617893.1	Secreted RxLR effector peptide protein
gene-IUM83_06260	-3.87305	0.002925	KAG6623326.1	Alkaline phosphatase
gene-IUM83_04004	-3.85439	0.009814	KAG6614770.1	hypothetical protein
gene-IUM83_15117	-3.7941	9.98E-07	KAG6580391.1	Multiple inositol polyphosphate phosphatase 1
gene-IUM83_04398	-3.77366	2.84E-10	KAG6613614.1	hypothetical protein
gene-IUM83_15118	-3.71231	3.69E-08	KAG6580334.1	Multiple inositol polyphosphate phosphatase 1
gene-IUM83_15781	-3.7075	0.004714	KAG6580123.1	putative GPI-anchored serine-threonine rich hypothetical protein
gene-IUM83_09638	-3.66456	7.54E-05	KAG6617879.1	Secreted RxLR effector peptide protein
gene-IUM83_05937	-3.64065	2.87E-06	KAG6583183.1	ADP-ribosylation factor
gene-IUM83_19347	-3.61392	0.042856	KAG6599635.1	putative xylanase

Supplementary File

Supplementary File 1: List of differentially expressed genes (DEGs) under each enriched Gene Ontology Term.

eGOr.ID	eGOr.Description
GO:0016874	ligase activity
GO:0003735	structural constituent of ribosome
GO:0004812	aminoacyl-tRNA ligase activity
GO:0016875	ligase activity, forming carbon-oxygen bonds
GO:0005198	structural molecule activity
GO:0140101	catalytic activity, acting on a tRNA
GO:0003743	translation initiation factor activity
GO:0008135	translation factor activity, RNA binding
GO:0090079	translation regulator activity, nucleic acid binding
GO:0016879	ligase activity, forming carbon-nitrogen bonds
GO:0008237	metallopeptidase activity
GO:0022890	inorganic cation transmembrane transporter activity
GO:0045182	translation regulator activity
GO:0005216	ion channel activity
GO:0016747	acyltransferase activity, transferring groups other than amino-acyl groups
GO:0008080	N-acetyltransferase activity
GO:0016746	acyltransferase activity
GO:0016407	acetyltransferase activity
GO:0016410	N-acyltransferase activity
GO:0008324	cation transmembrane transporter activity
GO:0071949	FAD binding
GO:0004725	protein tyrosine phosphatase activity

GO:0022890 **inorganic cation transmembrane transporter activity**			
Protein ID	**Log2(FC)**	**Functional annotation**	**Padj**
KAG6584866.1	0.883072182	ATP synthase F1 delta subunit	0.002260951
KAG6613035.1	0.518831165	ATP synthase F1 gamma subunit	0.050194366
KAG6621404.1	0.731141935	ATP synthase subunit beta mitochondrial	0.023958696
KAG6599825.1	0.517649512	ATP synthase subunit d	0.001316683
KAG6620062.1	0.572982333	ATP synthase subunit mitochondrial	0.01966957
KAG6591006.1	-1.563751015	calcium channel subunit mid1	0.00235635
KAG6574674.1	0.68628794	Calcium permeable stress-gated cation channel 1	0.036002122
KAG6574571.1	-1.031519704	Calcium permeable stress-gated cation channel 1	0.019469581
KAG6620038.1	-1.098638247	Calcium-translocating P-type ATPase PMCA-type	0.088640305
KAG6613399.1	3.064090829	CorA Metal Ion Transporter (MIT) Family	0.0000038
KAG6610321.1	-1.647481703	CorA Metal Ion transporter (MIT) Family	0.0031377
KAG6617174.1	-0.552741582	Ctr copper transporter	0.044385082
KAG6582819.1	0.682373398	H - or Na -translocating F-type V-type and A-type ATPase (F-ATPase) Superfamily	0.051502053
KAG6617173.1	-0.606746386	hypothetical protein	0.013870179
KAG6611233.1	-2.496163074	hypothetical protein	0.000294724
KAG6613438.1	-0.620102705	magnesium transporter nipa	0.001314646
KAG6602753.1	0.515158656	Metal Ion (Mn2 -iron) transporter (Nramp) Family	0.04852251
KAG6611977.1	0.381407274	Metal Ion (Mn2 -iron) Transporter (Nramp) Family	0.032585864
KAG6590642.1	0.294594216	Mucolipidin	0.041438021
KAG6590928.1	-0.753905138	Necrosis inducing protein NPP1 type	0.028256316
KAG6622711.1	-0.466154357	NIPA protein 2	0.067554686
KAG6592773.1	0.5994487	Phospho Lipase D	0.052193509
KAG6576467.1	-0.65693191	plasma-membrane proton-efflux P-type ATPase	0.097688458
KAG6614222.1	-0.832144637	Potassium/sodium hyperpolarization-activated cyclic nucleotide-gated channel 4	0.044744795
KAG6617008.1	0.395697623	P-type ATPase (P-ATPase) Superfamily	0.090259805
KAG6586999.1	-1.073560146	putative copper-transporting ATPase	0.045998199
KAG6613662.1	-1.158800659	putative sodium-dependent phosphate transporter	0.0000334
KAG6613564.1	-1.877376151	putative sodium-dependent phosphate transporter	0.000181995
KAG6619934.1	-5.214918745	putative sodium-dependent phosphate transporter	0.0000517

KAG6623913.1	-1.55931485	putative transmembrane protein	0.02690057
KAG6610193.1	-0.475590338	sodium/hydrogen exchanger 3	0.086826456
KAG6595898.1	-5.560601557	Sodium-dependent phosphate transporter	0.00000174
KAG6584850.1	-1.143561297	Transmembrane protein	0.002180839
KAG6602750.1	-1.198325766	Transmembrane protein	0.000618386
KAG6584851.1	-1.489498017	Transmembrane protein	0.0000285
KAG6609997.1	-1.902631434	tRNA methyltransferase	0.000543358
KAG6622290.1	-0.935380109	Voltage-gated Ion Channel	0.009223103
KAG6617096.1	-0.520532402	Voltage-gated Ion Channel (VIC) Superfamily	0.08560639
KAG6623946.1	-0.766215316	Voltage-gated Ion Channel (VIC) Superfamily	0.058097921
KAG6622695.1	-0.824226059	Voltage-gated Ion Channel (VIC) Superfamily	0.093393378
KAG6604562.1	-1.451862781	Voltage-gated Ion Channel (VIC) Superfamily	0.001759972
KAG6613868.1	-1.561419227	Voltage-gated Ion Channel (VIC) Superfamily	0.012986595
KAG6622298.1	-2.036346785	Voltage-gated Ion Channel (VIC) Superfamily	0.000174551
KAG6609874.1	-2.150584816	Voltage-gated Ion Channel (VIC) Superfamily	0.017162192
KAG6586559.1	-2.996455263	Voltage-gated Ion Channel (VIC) Superfamily	0.002218298
KAG6615504.1	0.832009131	V-type ATPase A subunit	0.023959956
KAG6590679.1	1.252250101	V-type H(+)-translocating pyrophosphatase	0.007623708
KAG6604567.1	0.542399462	V-type H(+)-translocating pyrophosphatase	0.041700426
KAG6614140.1	0.794917981	V-type proton ATPase subunit H	0.004167896
KAG6612021.1	1.797691785	Zinc (Zn2)-Iron (Fe2) Permease (ZIP) Family	0.00701598
KAG6574396.1	1.573098603	Zinc (Zn2)-Iron (Fe2) Permease (ZIP) Family	0.000607035
KAG6574393.1	1.457120911	Zinc (Zn2)-Iron (Fe2) Permease (ZIP) Family	0.014001052
KAG6598087.1	1.195305877	Zinc (Zn2)-Iron (Fe2) Permease (ZIP) Family	0.005000462
KAG6622317.1	-0.670945584	Zinc (Zn2)-Iron (Fe2) Permease (ZIP) Family	0.047734778
KAG6622321.1	-0.811057451	Zinc (Zn2)-Iron (Fe2) Permease (ZIP) Family	0.042102744
KAG6594351.1	-0.954155038	Zinc (Zn2)-Iron (Fe2) Permease (ZIP) Family	0.035487875
KAG6615307.1	-1.031211792	Zinc (Zn2)-Iron (Fe2) Permease (ZIP) Family	0.083511334
KAG6615303.1	-2.189072717	Zinc (Zn2)-Iron (Fe2) Permease (ZIP) Family	9.11E-09

GO:0005216 ion channel activity			
Protein ID	**Log2(FC)**	**Functional annotation**	**Padj**
KAG6584866.1	0.883072182	ATP synthase F1 delta subunit	0.002260951
KAG6613035.1	0.518831165	ATP synthase F1 gamma subunit	0.050194366
KAG6621404.1	0.731141935	ATP synthase subunit beta mitochondrial	0.023958696
KAG6591006.1	-1.563751015	calcium channel subunit mid1	0.00235635
KAG6574674.1	0.68628794	Calcium permeable stress-gated cation channel 1	0.036002122
KAG6574571.1	-1.031519704	Calcium permeable stress-gated cation channel 1	0.019469581
KAG6622249.1	-0.584013873	Chloride Channel (ClC) Family	0.046918685
KAG6591171.1	-0.944220072	Chloride Channel (ClC) Family	0.000236539
KAG6591030.1	-0.952778237	Chloride Channel (ClC) Family	0.000194045
KAG6615927.1	-1.95711689	Chloride Channel (ClC) Family	0.001322377
KAG6602858.1	-2.11985853	Chloride Channel (ClC) Family	0.004771896
KAG6615928.1	-0.916811176	chloride channel family	0.006677969
KAG6596011.1	0.354739018	eukaryotic porin	0.023613257
KAG6611583.1	0.506575672	hypothetical protein	0.04149123
KAG6584970.1	0.466558392	hypothetical protein	0.021353712
KAG6574612.1	-1.536562937	hypothetical protein	0.005835515
KAG6611233.1	-2.496163074	hypothetical protein	0.000294724
KAG6590642.1	0.294594216	Mucolipidin	0.041438021
KAG6614222.1	-0.832144637	Potassium/sodium hyperpolarization-activated cyclic nucleotide-gated channel 4	0.044744795
KAG6623913.1	-1.55931485	putative transmembrane protein	0.02690057
KAG6611061.1	0.463355989	putative voltage-dependent anion-selective channel protein	0.098660744
KAG6609997.1	-1.902631434	tRNA methyltransferase	0.000543358
KAG6622290.1	-0.935380109	Voltage-gated Ion Channel	0.009223103
KAG6576233.1	-0.456920755	Voltage-gated Ion Channel (VIC) Superfamily	0.080879225
KAG6617096.1	-0.520532402	Voltage-gated Ion Channel (VIC) Superfamily	0.08560639
KAG6617307.1	-0.697758032	Voltage-gated Ion Channel (VIC) Superfamily	0.042783725
KAG6617930.1	-0.731920589	Voltage-gated Ion Channel (VIC) Superfamily	0.015274872
KAG6623946.1	-0.766215316	Voltage-gated Ion Channel (VIC) Superfamily	0.058097921
KAG6615669.1	-0.802812124	Voltage-gated Ion Channel (VIC) Superfamily	0.001631154
KAG6622695.1	-0.824226059	Voltage-gated Ion Channel (VIC) Superfamily	0.093393378
KAG6580304.1	-1.208827601	Voltage-gated Ion Channel (VIC) Superfamily	0.005745826

KAG6604562.1	-1.451862781	Voltage-gated Ion Channel (VIC) Superfamily	0.001759972
KAG6615731.1	-1.48576453	Voltage-gated Ion Channel (VIC) Superfamily	0.017559821
KAG6613868.1	-1.561419227	Voltage-gated Ion Channel (VIC) Superfamily	0.012986595
KAG6615340.1	-1.81247536	Voltage-gated Ion Channel (VIC) Superfamily	0.00111306
KAG6617254.1	-1.822851888	Voltage-gated Ion Channel (VIC) Superfamily	0.010548129
KAG6622298.1	-2.036346785	Voltage-gated Ion Channel (VIC) Superfamily	0.000174551
KAG6609874.1	-2.150584816	Voltage-gated Ion Channel (VIC) Superfamily	0.017162192
KAG6586559.1	-2.996455263	Voltage-gated Ion Channel (VIC) Superfamily	0.002218298

GO:0008324 **cation transmembrane transporter activity**			
Protein ID	**Log2(FC)**	**Functional annotation**	**Padj**
KAG6584866.1	0.883072182	ATP synthase F1 delta subunit	0.002260951
KAG6613035.1	0.518831165	ATP synthase F1 gamma subunit	0.050194366
KAG6621404.1	0.731141935	ATP synthase subunit beta mitochondrial	0.023958696
KAG6599825.1	0.517649512	ATP synthase subunit d	0.001316683
KAG6620062.1	0.572982333	ATP synthase subunit mitochondrial	0.01966957
KAG6591006.1	-1.563751015	calcium channel subunit mid1	0.00235635
KAG6574674.1	0.68628794	Calcium permeable stress-gated cation channel 1	0.036002122
KAG6574571.1	-1.031519704	Calcium permeable stress-gated cation channel 1	0.019469581
KAG6620038.1	-1.098638247	Calcium-translocating P-type ATPase PMCA-type	0.088640305
KAG6587186.1	0.897249125	Cation Diffusion Facilitator (CDF) Family	0.005868922
KAG6615814.1	-0.959281503	Cation Diffusion Facilitator (CDF) Family	0.065540873
KAG6613399.1	3.064090829	CorA Metal Ion Transporter (MIT) Family	0.0000038
KAG6610321.1	-1.647481703	CorA Metal Ion transporter (MIT) Family	0.0031377
KAG6617174.1	-0.552741582	Ctr copper transporter	0.044385082
KAG6582819.1	0.682373398	H - or Na -translocating F-type V-type and A-type ATPase (F-ATPase) Superfamily	0.051502053
KAG6617173.1	-0.606746386	hypothetical protein	0.013870179
KAG6611233.1	-2.496163074	hypothetical protein	0.000294724
KAG6613438.1	-0.620102705	magnesium transporter nipa	0.001314646

KAG6602753.1	0.515158656	Metal Ion (Mn2 -iron) transporter (Nramp) Family	0.04852251
KAG6611977.1	0.381407274	Metal Ion (Mn2 -iron) Transporter (Nramp) Family	0.032585864
KAG6590642.1	0.294594216	Mucolipidin	0.041438021
KAG6590928.1	-0.753905138	Necrosis inducing protein NPP1 type	0.028256316
KAG6622711.1	-0.466154357	NIPA protein 2	0.067554686
KAG6592773.1	0.5994487	PhosphoLipase D	0.052193509
KAG6576467.1	-0.65693191	plasma-membrane proton-efflux P-type ATPase	0.097688458
KAG6614222.1	-0.832144637	Potassium/sodium hyperpolarization-activated cyclic nucleotide-gated channel 4	0.044744795
KAG6617008.1	0.395697623	P-type ATPase (P-ATPase) Superfamily	0.090259805
KAG6586999.1	-1.073560146	putative copper-transporting ATPase	0.045998199
KAG6613662.1	-1.158800659	putative sodium-dependent phosphate transporter	0.0000334
KAG6613564.1	-1.877376151	putative sodium-dependent phosphate transporter	0.000181995
KAG6619934.1	-5.214918745	putative sodium-dependent phosphate transporter	0.0000517
KAG6623913.1	-1.55931485	putative transmembrane protein	0.02690057
KAG6610193.1	-0.475590338	sodium/hydrogen exchanger 3	0.086826456
KAG6595898.1	-5.560601557	Sodium-dependent phosphate transporter	0.00000174
KAG6584850.1	-1.143561297	Transmembrane protein	0.002180839
KAG6602750.1	-1.198325766	Transmembrane protein	0.000618386
KAG6584851.1	-1.489498017	Transmembrane protein	0.0000285
KAG6609997.1	-1.902631434	tRNA methyltransferase	0.000543358
KAG6622290.1	-0.935380109	Voltage-gated Ion Channel	0.009223103
KAG6617096.1	-0.520532402	Voltage-gated Ion Channel (VIC) Superfamily	0.08560639
KAG6623946.1	-0.766215316	Voltage-gated Ion Channel (VIC) Superfamily	0.058097921
KAG6622695.1	-0.824226059	Voltage-gated Ion Channel (VIC) Superfamily	0.093393378
KAG6604562.1	-1.451862781	Voltage-gated Ion Channel (VIC) Superfamily	0.001759972
KAG6613868.1	-1.561419227	Voltage-gated Ion Channel (VIC) Superfamily	0.012986595
KAG6622298.1	-2.036346785	Voltage-gated Ion Channel (VIC) Superfamily	0.000174551
KAG6609874.1	-2.150584816	Voltage-gated Ion Channel (VIC) Superfamily	0.017162192
KAG6586559.1	-2.996455263	Voltage-gated Ion Channel (VIC) Superfamily	0.002218298
KAG6615504.1	0.832009131	V-type ATPase A subunit	0.023959956

KAG6590679.1	1.252250101	V-type H(+)-translocating pyrophosphatase	0.007623708
KAG6604567.1	0.542399462	V-type H(+)-translocating pyrophosphatase	0.041700426
KAG6614140.1	0.794917981	V-type proton ATPase subunit H	0.004167896
KAG6612021.1	1.797691785	Zinc (Zn2)-Iron (Fe2) Permease (ZIP) Family	0.00701598
KAG6574396.1	1.573098603	Zinc (Zn2)-Iron (Fe2) Permease (ZIP) Family	0.000607035
KAG6574393.1	1.457120911	Zinc (Zn2)-Iron (Fe2) Permease (ZIP) Family	0.014001052
KAG6598087.1	1.195305877	Zinc (Zn2)-Iron (Fe2) Permease (ZIP) Family	0.005000462
KAG6622317.1	-0.670945584	Zinc (Zn2)-Iron (Fe2) Permease (ZIP) Family	0.047734778
KAG6622321.1	-0.811057451	Zinc (Zn2)-Iron (Fe2) Permease (ZIP) Family	0.042102744
KAG6594351.1	-0.954155038	Zinc (Zn2)-Iron (Fe2) Permease (ZIP) Family	0.035487875
KAG6615307.1	-1.031211792	Zinc (Zn2)-Iron (Fe2) Permease (ZIP) Family	0.083511334
KAG6615303.1	-2.189072717	Zinc (Zn2)-Iron (Fe2) Permease (ZIP) Family	9.11E-09

GO:0016747 **acyltransferase activity, transferring groups other than amino-acyl groups**			
Protein ID	**Log2(FC)**	**Functional annotation**	**Padj**
KAG6617769.1	20.82039518	Acetyl-CoA acetyltransferase	0.00000296
KAG6608751.1	1.727688707	Gcn5-related n-acetyltransferase	0.000047
KAG6579786.1	1.509105927	Diacylglycerol O-acyltransferase	0.033366089
KAG6608907.1	1.403831294	putative isomerase	0.000928341
KAG6609039.1	1.25599066	putative enoyl-[acyl-carrier-protein] reductase [NADH]	0.001143451
KAG6608841.1	1.252777732	Gcn5-related n-acetyltransferase	0.000607035
KAG6584827.1	1.214413612	gnat family protein	0.023068438
KAG6592787.1	1.177490378	Elongation of very long chain fatty acids protein	0.002950925
KAG6613721.1	1.144831723	diacylglycerol o	0.002258954
KAG6618337.1	1.100647528	arginine biosynthesis Arg mitochondrial	0.00000287
KAG6610077.1	1.060323404	beta-ketoacyl-acyl-carrier-protein synthase II	0.000486024
KAG6620168.1	0.972777887	leucine carboxyl methyltransferase 2-like	0.002074097
KAG6591123.1	0.910209278	GNAT family acetyltransferase	0.016503126
KAG6596122.1	0.849362513	N-terminal acetyltransferase complex ARD1 subunit	0.001376635
KAG6622500.1	0.816691362	UDP-3-O-[3-hydroxymyristoyl] glucosamine N-acyltransferase	0.006079672

KAG6602979.1	0.81555252	acetyl-CoA acetyltransferase	0.000672356
KAG6614390.1	0.806654047	n-alpha-acetyltransferase 40	0.047699592
KAG6592789.1	0.789947607	homoserine O-acetyltransferase	0.042107321
KAG6617740.1	0.74462148	Acetyl-CoA acetyltransferase	0.057273701
KAG6622611.1	0.723624003	elongator complex protein 3	0.014700198
KAG6609961.1	0.721468083	2-amino-3-ketobutyrate coenzyme A ligase	0.005785598
KAG6618650.1	0.601016182	putative acetyltransferase (GNAT) family	0.056189271
KAG6598072.1	0.581217715	amino-acid N-acetyltransferase	0.012546503
KAG6586861.1	0.576377455	Palmitoyltransferase ZDHHC7	0.070396175
KAG6621336.1	0.518562971	N-alpha-acetyltransferase 40	0.064489517
KAG6609250.1	0.517932315	Diacylglycerol O-acyltransferase 2	0.005287181
KAG6612350.1	0.48170325	putative dihydrolipoamide succinyltransferase	0.001659606
KAG6622453.1	0.434902906	putative palmitoyltransferase	0.062994694
KAG6592440.1	0.432764466	N-acetyltransferase 5	0.094492606
KAG6611253.1	0.430851522	Histone acetyltransferase	0.046830932
KAG6610076.1	0.413883438	beta-ketoacyl-acyl-carrier-protein synthase II	0.039713463
KAG6616981.1	0.413027254	putative palmitoyltransferase	0.005868922
KAG6609224.1	0.398714715	Longevity-assurance protein (LAC1)	0.035600237
KAG6623856.1	0.35074429	n-acetyltransferase 9	0.05185958
KAG6594230.1	0.349665392	putative palmitoyltransferase	0.079523533
KAG6623775.1	0.316289492	putative histone acetyltransferase	0.010841315
KAG6579979.1	-0.298412212	palmitoyltransferase ZDHHC11	0.099537402
KAG6574609.1	-0.481031511	Fatty acyl-CoA reductase	0.044695811
KAG6599813.1	-0.52204169	protein S-acyltransferase 23	0.029333945
KAG6608959.1	-0.5486525	putative transmembrane protein	0.055455754
KAG6592439.1	-0.623547889	Acyltransferase family	0.020126335
KAG6616815.1	-0.659891839	n-alpha-acetyltransferase 60-like	0.025333533
KAG6612846.1	-0.808028683	histone acetyltransferase	0.012299907
KAG6610780.1	-1.280064057	Maltose O-acetyltransferase	0.0000743
KAG6584762.1	-1.425563697	peptidylprolyl isomerase domain and wd repeat-containing protein 1	0.003256392
KAG6614310.1	-1.589864251	ribosomal protein	0.000186869
KAG6579811.1	-1.66225801	Heparan-alpha-glucosaminide N-acetyltransferase	0.014494016
KAG6596045.1	-1.848934555	Omega-hydroxypalmitate O-feruloyl transferase	0.001180413
KAG6579836.1	-1.945223967	2-acylglycerol O-acyltransferase 2	0.023613257
KAG6598118.1	-2.179985323	Homoserine O-acetyltransferase	0.01077936
KAG6587169.1	-2.186531076	Shikimate O-hydroxycinnamoyltransferase	0.024187915
KAG6587168.1	-2.2168439	Agmatine coumaroyltransferase-2	0.069575058

GO:0008080 **N-acetyltransferase activity**

Protein ID	Log2(FC)	Functional annotation	Padj
KAG6608751.1	1.727688707	Gcn5-related n-acetyltransferase	0.000047
KAG6608907.1	1.403831294	putative isomerase	0.000928341
KAG6608841.1	1.252777732	Gcn5-related n-acetyltransferase	0.000607035
KAG6584827.1	1.214413612	gnat family protein	0.023068438
KAG6618337.1	1.100647528	arginine biosynthesis ArgJ mitochondrial	0.00000287
KAG6620168.1	0.972777887	leucine carboxyl methyltransferase 2-like	0.002074097
KAG6591123.1	0.910209278	GNAT family acetyltransferase	0.016503126
KAG6596122.1	0.849362513	N-terminal acetyltransferase complex ARD1 subunit	0.001376635
KAG6614390.1	0.806654047	n-alpha-acetyltransferase 40	0.047699592
KAG6622611.1	0.723624003	elongator complex protein 3	0.014700198
KAG6618650.1	0.601016182	putative acetyltransferase (GNAT) family	0.056189271
KAG6598072.1	0.581217715	amino-acid N-acetyltransferase	0.012546503
KAG6621336.1	0.518562971	N-alpha-acetyltransferase 40	0.064489517
KAG6592440.1	0.432764466	N-acetyltransferase 5	0.094492606
KAG6611253.1	0.430851522	Histone acetyltransferase	0.046830932
KAG6623856.1	0.35074429	n-acetyltransferase 9	0.05185958
KAG6623775.1	0.316289492	putative histone acetyltransferase	0.010841315
KAG6616815.1	-0.659891839	n-alpha-acetyltransferase 60-like	0.025333533
KAG6612846.1	-0.808028683	histone acetyltransferase	0.012299907
KAG6579811.1	-1.66225801	Heparan-alpha-glucosaminide N-acetyltransferase	0.014494016

GO:0016746 acyltransferase activity			
Protein ID	**Log2(FC)**	**Functional annotation**	**Padj**
KAG6617769.1	20.82039518	Acetyl-CoA acetyltransferase	0.00000296
KAG6597792.1	1.973100992	Lipoamide acyltransferase component of branched-chain alpha-keto acid dehydrogenase complex	1.67E-09
KAG6608751.1	1.727688707	Gcn5-related n-acetyltransferase	0.000047
KAG6579786.1	1.509105927	Diacylglycerol O-acyltransferase	0.033366089
KAG6608907.1	1.403831294	putative isomerase	0.000928341
KAG6609039.1	1.25599066	putative enoyl-[acyl-carrier-protein] reductase [NADH]	0.001143451
KAG6608841.1	1.252777732	Gcn5-related n-acetyltransferase	0.000607035
KAG6584827.1	1.214413612	gnat family protein	0.023068438
KAG6592787.1	1.177490378	Elongation of very long chain fatty acids protein	0.002950925
KAG6613721.1	1.144831723	diacylglycerol o	0.002258954
KAG6618337.1	1.100647528	arginine biosynthesis ArgJ mitochondrial	0.00000287

KAG6610077.1	1.060323404	beta-ketoacyl-acyl-carrier-protein synthase II	0.000486024
KAG6610004.1	0.990298579	2-isopropylmalate synthase	0.001345115
KAG6617361.1	0.986140474	citrate (Si)-synthase eukaryotic	0.000319905
KAG6620168.1	0.972777887	leucine carboxyl methyltransferase 2-like	0.002074097
KAG6591123.1	0.910209278	GNAT family acetyltransferase	0.016503126
KAG6583233.1	0.899810172	putative transglutaminase elicitor	0.070396175
KAG6583232.1	0.870686844	Transglutaminase elicitor M81C	0.002090932
KAG6596122.1	0.849362513	N-terminal acetyltransferase complex ARD1 subunit	0.001376635
KAG6622500.1	0.816691362	UDP-3-O-[3-hydroxymyristoyl] glucosamine N-acyltransferase	0.006079672
KAG6602979.1	0.81555252	acetyl-CoA acetyltransferase	0.000672356
KAG6614390.1	0.806654047	n-alpha-acetyltransferase 40	0.047699592
KAG6592789.1	0.789947607	homoserine O-acetyltransferase	0.042107321
KAG6617740.1	0.74462148	Acetyl-CoA acetyltransferase	0.057273701
KAG6614279.1	0.728405587	ATP-citrate synthase	0.002267733
KAG6622611.1	0.723624003	elongator complex protein 3	0.014700198
KAG6609961.1	0.721468083	2-amino-3-ketobutyrate coenzyme A ligase	0.005785598
KAG6574532.1	0.685499636	1-acyl-sn-glycerol-3-phosphate acyltransferase	0.002107181
KAG6618650.1	0.601016182	putative acetyltransferase (GNAT) family	0.056189271
KAG6598072.1	0.581217715	amino-acid N-acetyltransferase	0.012546503
KAG6586861.1	0.576377455	Palmitoyltransferase ZDHHC7	0.070396175
KAG6613198.1	0.550416091	Lysocardiolipin acyltransferase	0.016483629
KAG6614820.1	0.525079901	Choline/Carnitine O-acyltransferase	0.03515814
KAG6621336.1	0.518562971	N-alpha-acetyltransferase 40	0.064489517
KAG6609250.1	0.517932315	Diacylglycerol O-acyltransferase 2	0.005287181
KAG6584605.1	0.501113586	Lysophosphatidylcholine acyltransferase	0.002681113
KAG6612350.1	0.48170325	putative dihydrolipoamide succinyltransferase	0.001659606
KAG6622453.1	0.434902906	putative palmitoyltransferase	0.062994694
KAG6592440.1	0.432764466	N-acetyltransferase 5	0.094492606
KAG6611253.1	0.430851522	Histone acetyltransferase	0.046830932
KAG6610076.1	0.413883438	beta-ketoacyl-acyl-carrier-protein synthase II	0.039713463
KAG6616981.1	0.413027254	putative palmitoyltransferase	0.005868922
KAG6609224.1	0.398714715	Longevity-assurance protein (LAC1)	0.035600237
KAG6623856.1	0.35074429	n-acetyltransferase 9	0.05185958
KAG6594230.1	0.349665392	putative palmitoyltransferase	0.079523533
KAG6623775.1	0.316289492	putative histone acetyltransferase	0.010841315
KAG6579979.1	-0.298412212	palmitoyltransferase ZDHHC11	0.099537402

KAG6574609.1	-0.481031511	Fatty acyl-CoA reductase	0.044695811
KAG6599813.1	-0.52204169	protein S-acyltransferase 23	0.029333945
KAG6608959.1	-0.5486525	putative transmembrane protein	0.055455754
KAG6592439.1	-0.623547889	Acyltransferase family	0.020126335
KAG6616815.1	-0.659891839	n-alpha-acetyltransferase 60-like	0.025333533
KAG6584559.1	-0.773179533	putative glutathione gamma-glutamylcysteinyltransferase	0.049541918
KAG6612846.1	-0.808028683	histone acetyltransferase	0.012299907
KAG6610780.1	-1.280064057	Maltose O-acetyltransferase	0.0000743
KAG6615831.1	-1.288135401	elicitor-like transglutaminase	0.001161075
KAG6584762.1	-1.425563697	peptidylprolyl isomerase domain and wd repeat-containing protein 1	0.003256392
KAG6614310.1	-1.589864251	ribosomal protein	0.000186869
KAG6577846.1	-1.622462991	Elicitor-like transglutaminase M81-like protein	0.005805819
KAG6579811.1	-1.66225801	Heparan-alpha-glucosaminide N-acetyltransferase	0.014494016
KAG6596045.1	-1.848934555	Omega-hydroxypalmitate O-feruloyl transferase	0.001180413
KAG6579836.1	-1.945223967	2-acylglycerol O-acyltransferase 2	0.023613257
KAG6598118.1	-2.179985323	Homoserine O-acetyltransferase	0.01077936
KAG6587169.1	-2.186531076	Shikimate O-hydroxycinnamoyltransferase	0.024187915
KAG6587168.1	-2.2168439	Agmatine coumaroyltransferase-2	0.069575058

GO:0016407 acetyltransferase activity			
Protein ID	**Log2(FC)**	**Functional annotation**	**Padj**
KAG6608751.1	1.727688707	Gcn5-related n-acetyltransferase	0.000047
KAG6608907.1	1.403831294	putative isomerase	0.000928341
KAG6608841.1	1.252777732	Gcn5-related n-acetyltransferase	0.000607035
KAG6584827.1	1.214413612	gnat family protein	0.023068438
KAG6618337.1	1.100647528	arginine biosynthesis Arg mitochondrial	0.00000287
KAG6620168.1	0.972777887	leucine carboxyl methyltransferase 2-like	0.002074097
KAG6591123.1	0.910209278	GNAT family acetyltransferase	0.016503126
KAG6596122.1	0.849362513	N-terminal acetyltransferase complex ARD1 subunit	0.001376635
KAG6614390.1	0.806654047	n-alpha-acetyltransferase 40	0.047699592
KAG6622611.1	0.723624003	elongator complex protein 3	0.014700198
KAG6609961.1	0.721468083	2-amino-3-ketobutyrate coenzyme A ligase	0.005785598
KAG6618650.1	0.601016182	putative acetyltransferase (GNAT) family	0.056189271

KAG6598072.1	0.581217715	amino-acid N-acetyltransferase	0.012546503
KAG6621336.1	0.518562971	N-alpha-acetyltransferase 40	0.064489517
KAG6592440.1	0.432764466	N-acetyltransferase 5	0.094492606
KAG6611253.1	0.430851522	Histone acetyltransferase	0.046830932
KAG6623856.1	0.35074429	n-acetyltransferase 9	0.05185958
KAG6623775.1	0.316289492	putative histone acetyltransferase	0.010841315
KAG6616815.1	-0.659891839	n-alpha-acetyltransferase 60-like	0.025333533
KAG6612846.1	-0.808028683	histone acetyltransferase	0.012299907
KAG6610780.1	-1.280064057	Maltose O-acetyltransferase	0.0000743
KAG6579811.1	-1.66225801	Heparan-alpha-glucosaminide N-acetyltransferase	0.014494016

GO:0016410 N-acyltransferase activity			
Protein ID	**Log2(FC)**	**Functional annotation**	**Padj**
KAG6608751.1	1.727688707	Gcn5-related n-acetyltransferase	0.000047
KAG6608907.1	1.403831294	putative isomerase	0.000928341
KAG6608841.1	1.252777732	Gcn5-related n-acetyltransferase	0.000607035
KAG6584827.1	1.214413612	gnat family protein	0.023068438
KAG6618337.1	1.100647528	arginine biosynthesis ArgJ mitochondrial	0.00000287
KAG6620168.1	0.972777887	leucine carboxyl methyltransferase 2-like	0.002074097
KAG6591123.1	0.910209278	GNAT family acetyltransferase	0.016503126
KAG6596122.1	0.849362513	N-terminal acetyltransferase complex ARD1 subunit	0.001376635
KAG6622500.1	0.816691362	UDP-3-O-[3-hydroxymyristoyl] glucosamine N-acyltransferase	0.006079672
KAG6614390.1	0.806654047	n-alpha-acetyltransferase 40	0.047699592
KAG6622611.1	0.723624003	elongator complex protein 3	0.014700198
KAG6618650.1	0.601016182	putative acetyltransferase (GNAT) family	0.056189271
KAG6598072.1	0.581217715	amino-acid N-acetyltransferase	0.012546503
KAG6621336.1	0.518562971	N-alpha-acetyltransferase 40	0.064489517
KAG6592440.1	0.432764466	N-acetyltransferase 5	0.094492606
KAG6611253.1	0.430851522	Histone acetyltransferase	0.046830932
KAG6609224.1	0.398714715	Longevity-assurance protein (LAC1)	0.035600237
KAG6623856.1	0.35074429	n-acetyltransferase 9	0.05185958
KAG6623775.1	0.316289492	putative histone acetyltransferase	0.010841315
KAG6616815.1	-0.659891839	n-alpha-acetyltransferase 60-like	0.025333533
KAG6612846.1	-0.808028683	histone acetyltransferase	0.012299907

KAG6579811.1	-1.66225801	Heparan-alpha-glucosaminide N-acetyltransferase	0.014494016

GO:0016874 ligase activity			
Protein ID	**Log2(FC)**	**Functional annotation**	**Padj**
KAG6609667.1	1.910249	carbamoyl-phosphate synthase large subunit	1.69E-08
KAG6613395.1	1.163331	argininosuccinate synthase	0.001561035
KAG6604530.1	1.147124	Phenylalanine-tRNA ligase	0.001894553
KAG6576532.1	1.114854	acetate-CoA ligase	0.068489541
KAG6576588.1	1.114161	Formate-tetrahydrofolate ligase	0.000433684
KAG6609515.1	0.934739	proline-tRNA ligase	0.000179696
KAG6591138.1	0.912751	tyrosine-tRNA ligase	0.001199729
KAG6596024.1	0.907942	lysine-tRNA ligase	0.013660558
KAG6618528.1	0.888005	Aspartyl/glutamyl-tRNA (Asn/Gln) amidotransferase A subunit	0.002869785
KAG6584866.1	0.883072	ATP synthase F1 delta subunit	0.002260951
KAG6613410.1	0.873776	asparagine-tRNA ligase	0.002025774
KAG6579938.1	0.855394	propionyl-CoA carboxylase beta chain mitochondrial	0.00353378
KAG6579931.1	0.838084	methionine-tRNA ligase	0.006587038
KAG6592421.1	0.837153	adenylosuccinate synthetase	0.044728946
KAG6620831.1	0.824299	tryptophan-tRNA ligase	0.017559821
KAG6612256.1	0.816184	phosphoribosylformylglycinamidine synthase	0.067426222
KAG6611263.1	0.816052	Nucleotidylyl transferase superfamily protein	0.000716758
KAG6590713.1	0.811863	glutamate-tRNA ligase	0.007683211
KAG6613660.1	0.806421	arginine-tRNA ligase	0.003767797
KAG6586611.1	0.789167	aspartyl/glutamyl-tRNA (Asn/Gln) amidotransferase B subunit	0.025114149
KAG6620330.1	0.783033	leucine-tRNA ligase	0.008653193
KAG6623687.1	0.778196	lysine-tRNA ligase	0.011377001
KAG6616894.1	0.743836	Glutamate-cysteine ligase catalytic subunit	0.00844809
KAG6591026.1	0.741236	valine-tRNA ligase	0.008447158
KAG6621404.1	0.731142	ATP synthase subunit beta mitochondrial	0.023958696
KAG6592544.1	0.722002	glutamine-tRNA ligase	0.028253599
KAG6615470.1	0.720729	asparagine synthase (glutamine-hydrolyzing)	0.056162803
KAG6592552.1	0.717367	arginine-tRNA ligase	0.027685664
KAG6591093.1	0.711551	glycyl-tRNA synthetase	0.007745073
KAG6610153.1	0.702283	tRNA (Ile)-lysidine synthetase	0.004831135
KAG6609893.1	0.700021	Ubiquitin-activating enzyme (E1)	0.032468054
KAG6580005.1	0.69203	Glutathione synthetase	0.048375531
KAG6576344.1	0.685754	hypothetical protein	0.080456198
KAG6592420.1	0.669118	Isoleucine-tRNA ligase	0.016320741

KAG6617148.1	0.667921	methylcrotonoyl-CoA carboxylase beta chain mitochondrial	0.093669864
KAG6603027.1	0.628998	tryptophan-tRNA ligase	0.091434037
KAG6591055.1	0.627885	methionine-tRNA ligase	0.029333754
KAG6618946.1	0.584481	alanine-tRNA ligase	0.013113534
KAG6623464.1	0.569455	Threonine-tRNA ligase	0.017237587
KAG6620843.1	0.550514	proline-tRNA ligase	0.033108505
KAG6611779.1	0.550307	serine-tRNA ligase	0.071695911
KAG6621424.1	0.527013	putative ubiquitin activating enzyme E1 family	0.056246059
KAG6613035.1	0.518831	ATP synthase F1 gamma subunit	0.050194366
KAG6592448.1	0.517246	adenylosuccinate synthetase	0.011438443
KAG6621851.1	0.502873	putative DNA ligase	0.04883535
KAG6617765.1	0.456175	glycine-tRNA ligase	0.08345258
KAG6612842.1	0.408624	phenylalanine-tRNA ligase alpha subunit	0.071190849
KAG6580062.1	0.394592	histidine-tRNA ligase	0.050287169
KAG6613700.1	0.345309	NAD+ synthetase	0.089112217
KAG6592508.1	0.274782	cysteine-tRNA ligase	0.096557193
KAG6613309.1	-0.67186	nicotinate phosphoribosyltransferase	0.036474733
KAG6622821.1	-0.93693	glutamate-tRNA ligase	0.082473645
KAG6620928.1	-1.17285	DNA ligase	0.037947979

GO:0003735 structural constituent of ribosome			
Protein ID	**Log2(FC)**	**Functional annotation**	**Padj**
KAG6623197.1	1.18654	ribosomal protein L7/L12	0.000083
KAG6594203.1	1.073917	ribosomal protein L32	0.0008
KAG6621403.1	1.029151	ribosomal protein S18	0.004714
KAG6602869.1	0.980887	ribosomal protein L19	0.013414
KAG6616419.1	0.918828	ribosomal protein L25 Ctc-form	0.000484
KAG6616108.1	0.909812	Ribosomal protein L11	0.023311
KAG6609849.1	0.903287	50S ribosomal protein L4	0.001797
KAG6597825.1	0.856494	ribosomal protein L22	0.028748
KAG6623440.1	0.852306	Mitochondrial 39-S ribosomal protein L47	0.037948
KAG6574492.1	0.83568	ribosomal protein L1	0.044343
KAG6614023.1	0.832554	ribosomal protein L24	0.005146
KAG6584597.1	0.831995	39s ribosomal protein mitochondrial-like	0.003686
KAG6611614.1	0.818419	Mitochondrial/chloroplast ribosomal protein 36a	0.000666
KAG6616354.1	0.815372	40S ribosomal protein S26	0.002915
KAG6587269.1	0.782116	28S ribosomal protein S34 mitochondrial	0.001561
KAG6606608.1	0.768675	Ribosomal protein S2	0.000573
KAG6612374.1	0.763834	hypothetical protein	0.022687
KAG6611831.1	0.759822	50s ribosomal protein l24	0.035952
KAG6594110.1	0.756065	ribosomal protein L9	0.000835
KAG6609540.1	0.755066	ribosomal protein L13	0.002073
KAG6584898.1	0.74816	ribosomal protein L36	0.056636

KAG6576160.1	0.747466	50S ribosomal protein L3	0.086254
KAG6576187.1	0.71619	40S ribosomal protein S3a	0.000053
KAG6612851.1	0.699722	40S ribosomal protein S20	0.026015
KAG6617646.1	0.686449	40S ribosomal protein S2	0.019081
KAG6614401.1	0.677796	30S ribosomal protein S17	0.020965
KAG6618739.1	0.667841	60S ribosomal protein L4	0.001864
KAG6590803.1	0.663108	Ribosomal protein L21	0.013719
KAG6590908.1	0.658434	Ribosomal protein L13	0.025456
KAG6609928.1	0.657927	60S ribosomal protein L6	0.008955
KAG6597938.1	0.654569	40S ribosomal protein S6	0.00347
KAG6614930.1	0.636814	30S ribosomal protein S9	0.036918
KAG6617366.1	0.621173	40S ribosomal protein S8	0.019639
KAG6609245.1	0.613139	60S ribosomal protein L35a-4	0.019178
KAG6615455.1	0.609042	60S ribosomal protein L31	0.021224
KAG6609811.1	0.607582	60S ribosomal protein L27	0.067193
KAG6610290.1	0.593172	60S ribosomal protein L9	0.032795
KAG6615807.1	0.587403	archaeal ribosomal protein S17P	0.027669
KAG6599793.1	0.582136	putative ribosomal protein L23	4.84E-05
KAG6609976.1	0.577867	ribosomal protein L22	0.082478
KAG6606443.1	0.575921	40S ribosomal protein	0.053078
KAG6622391.1	0.568986	60S ribosomal protein L18-2	0.053988
KAG6612357.1	0.55624	60S ribosomal protein L11	0.019895
KAG6623199.1	0.549962	60S ribosomal protein	0.013887
KAG6612236.1	0.535573	60S ribosomal protein L5	0.040069
KAG6618596.1	0.519936	60S ribosomal protein L13	0.057274
KAG6612784.1	0.515845	40S ribosomal protein S15	0.088263
KAG6572555.1	0.493078	60S ribosomal protein L21-1	0.089898
KAG6619355.1	0.488806	60S ribosomal protein	0.066785
KAG6622600.1	0.480073	50S ribosomal protein L36e	0.082474
KAG6583080.1	0.466481	40s ribosomal protein s13	0.072469
KAG6612806.1	0.463766	60S ribosomal protein L22	0.034257
KAG6609864.1	0.442219	Ribosomal protein L37a	0.007778
KAG6572782.1	0.438244	60S ribosomal protein L23a	0.039228
KAG6618527.1	0.417534	Ribosomal protein L28	0.09746
KAG6615053.1	0.409327	40S ribosomal protein S17	0.032085
KAG6610308.1	0.385367	60S ribosomal protein L38	0.022937
KAG6599828.1	0.383207	ribosomal-ubiquitin protein RPL40	0.092111
KAG6612864.1	0.337719	ubiquitin-40s ribosomal protein s27a	0.044826

GO:0004812 **aminoacyl-tRNA ligase activity**			
Protein ID	**Log2(FC)**	**Functional annotation**	**Padj**
KAG6604530.1	1.147124	Phenylalanine-tRNA ligase	0.001895
KAG6609515.1	0.934739	proline-tRNA ligase	0.00018
KAG6591138.1	0.912751	tyrosine-tRNA ligase	0.0012
KAG6596024.1	0.907942	lysine-tRNA ligase	0.013661

KAG6613410.1	0.873776	asparagine-tRNA ligase	0.002026
KAG6579931.1	0.838084	methionine-tRNA ligase	0.006587
KAG6620831.1	0.824299	tryptophan-tRNA ligase	0.01756
KAG6611263.1	0.816052	Nucleotidylyl transferase superfamily protein	0.000717
KAG6590713.1	0.811863	glutamate-tRNA ligase	0.007683
KAG6613660.1	0.806421	arginine-tRNA ligase	0.003768
KAG6620330.1	0.783033	leucine-tRNA ligase	0.008653
KAG6623687.1	0.778196	lysine-tRNA ligase	0.011377
KAG6591026.1	0.741236	valine-tRNA ligase	0.008447
KAG6592544.1	0.722002	glutamine-tRNA ligase	0.028254
KAG6592552.1	0.717367	arginine-tRNA ligase	0.027686
KAG6591093.1	0.711551	glycyl-tRNA synthetase	0.007745
KAG6592420.1	0.669118	Isoleucine-tRNA ligase	0.016321
KAG6603027.1	0.628998	tryptophan-tRNA ligase	0.091434
KAG6591055.1	0.627885	methionine-tRNA ligase	0.029334
KAG6618946.1	0.584481	alanine-tRNA ligase	0.013114
KAG6623464.1	0.569455	Threonine-tRNA ligase	0.017238
KAG6620843.1	0.550514	proline-tRNA ligase	0.033109
KAG6611779.1	0.550307	serine-tRNA ligase	0.071696
KAG6617765.1	0.456175	glycine-tRNA ligase	0.083453
KAG6612842.1	0.408624	phenylalanine-tRNA ligase alpha subunit	0.071191
KAG6580062.1	0.394592	histidine-tRNA ligase	0.050287
KAG6592508.1	0.274782	cysteine-tRNA ligase	0.096557
KAG6622821.1	-0.93693	glutamate-tRNA ligase	0.082474

GO:0016875 **ligase activity, forming carbon-oxygen bonds**			
Protein ID	**Log2(FC)**	**Functional annotation**	**Padj**
KAG6604530.1	1.147124	Phenylalanine-tRNA ligase	0.001895
KAG6609515.1	0.934739	proline-tRNA ligase	0.00018
KAG6591138.1	0.912751	tyrosine-tRNA ligase	0.0012
KAG6596024.1	0.907942	lysine-tRNA ligase	0.013661
KAG6613410.1	0.873776	asparagine-tRNA ligase	0.002026
KAG6579931.1	0.838084	methionine-tRNA ligase	0.006587
KAG6620831.1	0.824299	tryptophan-tRNA ligase	0.01756
KAG6611263.1	0.816052	Nucleotidylyl transferase superfamily protein	0.000717
KAG6590713.1	0.811863	glutamate-tRNA ligase	0.007683
KAG6613660.1	0.806421	arginine-tRNA ligase	0.003768
KAG6620330.1	0.783033	leucine-tRNA ligase	0.008653
KAG6623687.1	0.778196	lysine-tRNA ligase	0.011377
KAG6591026.1	0.741236	valine-tRNA ligase	0.008447
KAG6592544.1	0.722002	glutamine-tRNA ligase	0.028254
KAG6592552.1	0.717367	arginine-tRNA ligase	0.027686
KAG6591093.1	0.711551	glycyl-tRNA synthetase	0.007745
KAG6592420.1	0.669118	Isoleucine-tRNA ligase	0.016321

KAG6603027.1	0.628998	tryptophan-tRNA ligase	0.091434
KAG6591055.1	0.627885	methionine-tRNA ligase	0.029334
KAG6618946.1	0.584481	alanine-tRNA ligase	0.013114
KAG6623464.1	0.569455	Threonine-tRNA ligase	0.017238
KAG6620843.1	0.550514	proline-tRNA ligase	0.033109
KAG6611779.1	0.550307	serine-tRNA ligase	0.071696
KAG6617765.1	0.456175	glycine-tRNA ligase	0.083453
KAG6612842.1	0.408624	phenylalanine-tRNA ligase alpha subunit	0.071191
KAG6580062.1	0.394592	histidine-tRNA ligase	0.050287
KAG6592508.1	0.274782	cysteine-tRNA ligase	0.096557
KAG6622821.1	-0.93693	glutamate-tRNA ligase	0.082474

GO:0005198 structural molecule activity			
Protein ID	**Log2(FC)**	**Functional annotation**	**Padj**
KAG6617079.1	2.3024	tubulin alpha chain	0.054655
KAG6592733.1	1.472125	SF-assemblin	0.01972
KAG6623197.1	1.18654	ribosomal protein L7/L12	0.000083
KAG6594203.1	1.073917	ribosomal protein L32	0.0008
KAG6621403.1	1.029151	ribosomal protein S18	0.004714
KAG6602869.1	0.980887	ribosomal protein L19	0.013414
KAG6616419.1	0.918828	ribosomal protein L25 Ctc-form	0.000484
KAG6616108.1	0.909812	Ribosomal protein L11	0.023311
KAG6609849.1	0.903287	50S ribosomal protein L4	0.001797
KAG6597825.1	0.856494	ribosomal protein L22	0.028748
KAG6623440.1	0.852306	Mitochondrial 39-S ribosomal protein L47	0.037948
KAG6574492.1	0.83568	ribosomal protein L1	0.044343
KAG6614023.1	0.832554	ribosomal protein L24	0.005146
KAG6584597.1	0.831995	39s ribosomal protein mitochondrial-like	0.003686
KAG6611614.1	0.818419	Mitochondrial/chloroplast ribosomal protein 36a	0.000666
KAG6616354.1	0.815372	40S ribosomal protein S26	0.002915
KAG6587269.1	0.782116	28S ribosomal protein S34 mitochondrial	0.001561
KAG6613990.1	0.779787	tubulin alpha chain	0.036002
KAG6606608.1	0.768675	Ribosomal protein S2	0.000573
KAG6612374.1	0.763834	hypothetical protein	0.022687
KAG6611831.1	0.759822	50s ribosomal protein l24	0.035952
KAG6594110.1	0.756065	ribosomal protein L9	0.000835
KAG6609540.1	0.755066	ribosomal protein L13	0.002073
KAG6584898.1	0.74816	ribosomal protein L36	0.056636
KAG6576160.1	0.747466	50S ribosomal protein L3	0.086254
KAG6576187.1	0.71619	40S ribosomal protein S3a	0.000053
KAG6612851.1	0.699722	40S ribosomal protein S20	0.026015
KAG6617646.1	0.686449	40S ribosomal protein S2	0.019081
KAG6614401.1	0.677796	30S ribosomal protein S17	0.020965

KAG6618739.1	0.667841	60S ribosomal protein L4	0.001864
KAG6590803.1	0.663108	Ribosomal protein L21	0.013719
KAG6590908.1	0.658434	Ribosomal protein L13	0.025456
KAG6609928.1	0.657927	60S ribosomal protein L6	0.008955
KAG6597938.1	0.654569	40S ribosomal protein S6	0.00347
KAG6612326.1	0.653613	coatomer subunit beta	0.008955
KAG6614930.1	0.636814	30S ribosomal protein S9	0.036918
KAG6617366.1	0.621173	40S ribosomal protein S8	0.019639
KAG6609245.1	0.613139	60S ribosomal protein L35a-4	0.019178
KAG6615455.1	0.609042	60S ribosomal protein L31	0.021224
KAG6609811.1	0.607582	60S ribosomal protein L27	0.067193
KAG6610290.1	0.593172	60S ribosomal protein L9	0.032795
KAG6615807.1	0.587403	archaeal ribosomal protein S17P	0.027669
KAG6599793.1	0.582136	putative ribosomal protein L23	4.84E-05
KAG6609976.1	0.577867	ribosomal protein L22	0.082478
KAG6606443.1	0.575921	40S ribosomal protein	0.053078
KAG6622391.1	0.568986	60S ribosomal protein L18-2	0.053988
KAG6612357.1	0.55624	60S ribosomal protein L11	0.019895
KAG6623199.1	0.549962	60S ribosomal protein	0.013887
KAG6612236.1	0.535573	60S ribosomal protein L5	0.040069
KAG6618596.1	0.519936	60S ribosomal protein L13	0.057274
KAG6612784.1	0.515845	40S ribosomal protein S15	0.088263
KAG6610233.1	0.502021	Coatomer subunit gamma	0.043856
KAG6572555.1	0.493078	60S ribosomal protein L21-1	0.089898
KAG6619355.1	0.488806	60S ribosomal protein	0.066785
KAG6611174.1	0.483062	beta-tubulin	0.070456
KAG6622600.1	0.480073	50S ribosomal protein L36e	0.082474
KAG6583080.1	0.466481	40s ribosomal protein s13	0.072469
KAG6612806.1	0.463766	60S ribosomal protein L22	0.034257
KAG6615534.1	0.447258	nucleoporin-like protein	0.028993
KAG6609864.1	0.442219	Ribosomal protein L37a	0.007778
KAG6572782.1	0.438244	60S ribosomal protein L23a	0.039228
KAG6578118.1	0.437328	Coatomer subunit beta	0.033576
KAG6618527.1	0.417534	Ribosomal protein L28	0.09746
KAG6615053.1	0.409327	40S ribosomal protein S17	0.032085
KAG6610308.1	0.385367	60S ribosomal protein L38	0.022937
KAG6599828.1	0.383207	ribosomal-ubiquitin protein RPL40	0.092111
KAG6614592.1	0.362325	putative nuclear pore glycoprotein	0.071605
KAG6612864.1	0.337719	ubiquitin-40s ribosomal protein s27a	0.044826
KAG6576200.1	-1.36975	nuclear pore complex protein NUP98A isoform X3	0.000295

GO:0140101 catalytic activity, acting on a tRNA			
Protein ID	**Log2(FC)**	**Functional annotation**	**Padj**
KAG6604530.1	1.147124	Phenylalanine-tRNA ligase	0.001895
KAG6609515.1	0.934739	proline-tRNA ligase	0.00018
KAG6620364.1	0.919973	putative queuine tRNA-ribosyltransferase domain-containing protein	0.00026
KAG6591138.1	0.912751	tyrosine-tRNA ligase	0.0012
KAG6596024.1	0.907942	lysine-tRNA ligase	0.013661
KAG6618528.1	0.888005	Aspartyl/glutamyl-tRNA (Asn/Gln) amidotransferase A subunit	0.00287
KAG6618666.1	0.883641	tRNA-intron endonuclease	0.00137
KAG6613410.1	0.873776	asparagine-tRNA ligase	0.002026
KAG6579931.1	0.838084	methionine-tRNA ligase	0.006587
KAG6620831.1	0.824299	tryptophan-tRNA ligase	0.01756
KAG6611263.1	0.816052	Nucleotidylyl transferase superfamily protein	0.000717
KAG6590713.1	0.811863	glutamate-tRNA ligase	0.007683
KAG6613660.1	0.806421	arginine-tRNA ligase	0.003768
KAG6620330.1	0.783033	leucine-tRNA ligase	0.008653
KAG6623687.1	0.778196	lysine-tRNA ligase	0.011377
KAG6591026.1	0.741236	valine-tRNA ligase	0.008447
KAG6592544.1	0.722002	glutamine-tRNA ligase	0.028254
KAG6592552.1	0.717367	arginine-tRNA ligase	0.027686
KAG6591093.1	0.711551	glycyl-tRNA synthetase	0.007745
KAG6583267.1	0.689783	putative tRNA-dihydrouridine synthase	0.039175
KAG6592420.1	0.669118	Isoleucine-tRNA ligase	0.016321
KAG6622209.1	0.666381	proline-trna ligase associated domain containing protein	0.097809
KAG6623786.1	0.665101	peptidyl-tRNA hydrolase	0.010606
KAG6603027.1	0.628998	tryptophan-tRNA ligase	0.091434
KAG6591055.1	0.627885	methionine-tRNA ligase	0.029334
KAG6583266.1	0.599308	tRNA-dihydrouridine synthase	0.076722
KAG6618946.1	0.584481	alanine-tRNA ligase	0.013114
KAG6623464.1	0.569455	Threonine-tRNA ligase	0.017238
KAG6620843.1	0.550514	proline-tRNA ligase	0.033109
KAG6611779.1	0.550307	serine-tRNA ligase	0.071696
KAG6616888.1	0.461728	tRNA-dihydrouridine synthase	0.005625
KAG6617765.1	0.456175	glycine-tRNA ligase	0.083453
KAG6612842.1	0.408624	phenylalanine-tRNA ligase alpha subunit	0.071191
KAG6580062.1	0.394592	histidine-tRNA ligase	0.050287
KAG6611956.1	0.372153	tRNA-intron endonuclease	0.084068
KAG6592508.1	0.274782	cysteine-tRNA ligase	0.096557
KAG6613737.1	-0.5248	Exonuclease mut-7	0.068734
KAG6622821.1	-0.93693	glutamate-tRNA ligase	0.082474

GO:0003743 **translation initiation factor activity**			
Protein ID	**Log2(FC)**	**Functional annotation**	**Padj**
KAG6610661.1	0.894803	eukaryotic translation initiation factor 3	0.023858
KAG6594129.1	0.866604	Eukaryotic translation initiation factor 3 subunit G	0.001624
KAG6610724.1	0.743249	putative eukaryotic initiation factor 4E	0.053597
KAG6597779.1	0.706441	Eukaryotic translation initiation factor 3 subunit C	0.023972
KAG6603115.1	0.671173	Eukaryotic translation initiation factor 3 subunit J	9.45E-05
KAG6614344.1	0.623085	Eukaryotic translation initiation factor 3 subunit I	0.011652
KAG6612595.1	0.616435	putative ligatin	0.050526
KAG6595871.1	0.516699	putative eukaryotic translation initiation factor 3 subunit E-interacting protein	0.093393
KAG6615922.1	0.501539	Eukaryotic translation initiation factor 3 subunit E	0.08761
KAG6613847.1	0.487207	rna-binding protein	0.02961
KAG6619349.1	0.474835	eukaryotic translation initiation factor 4e	0.001161
KAG6613851.1	0.451769	Eukaryotic translation initiation factor 2 subunit beta	0.05186
KAG6579753.1	0.437859	eukaryotic translation initiation factor 1A X-chromosomal	0.014385
KAG6618621.1	0.39907	Eukaryotic translation initiation factor 3 subunit H	0.006678
KAG6609244.1	0.388053	eukaryotic initiation factor 4e	0.028484

GO:0008135 **translation factor activity, RNA binding**			
Protein ID	**Log2(FC)**	**Functional annotation**	**Padj**
KAG6603115.1	0.671173	Eukaryotic translation initiation factor 3 subunit J	9.45E-05
KAG6619349.1	0.474835	eukaryotic translation initiation factor 4e	0.001161
KAG6594129.1	0.866604	Eukaryotic translation initiation factor 3 subunit G	0.001624
KAG6618621.1	0.39907	Eukaryotic translation initiation factor 3 subunit H	0.006678
KAG6614344.1	0.623085	Eukaryotic translation initiation factor 3 subunit I	0.011652
KAG6579753.1	0.437859	eukaryotic translation initiation factor 1A X-chromosomal	0.014385
KAG6574525.1	0.763114	putative elongation factor 1-gamma	0.018558
KAG6610661.1	0.894803	eukaryotic translation initiation factor 3	0.023858
KAG6597779.1	0.706441	Eukaryotic translation initiation factor 3 subunit C	0.023972
KAG6609244.1	0.388053	eukaryotic initiation factor 4e	0.028484
KAG6613847.1	0.487207	rna-binding protein	0.02961

KAG6612595.1	0.616435	putative ligatin	0.050526
KAG6622031.1	0.869654	elongation factor 1-alpha	0.055748
KAG6613851.1	0.451769	Eukaryotic translation initiation factor 2 subunit beta	0.05186
KAG6610724.1	0.743249	putative eukaryotic initiation factor 4E	0.053597
KAG6594155.1	0.657719	translation elongation factor IF5A	0.054988
KAG6583094.1	0.917204	translation elongation factor Ts	0.06885
KAG6602974.1	0.531821	Peptide chain release factor 2	0.08465
KAG6615922.1	0.501539	Eukaryotic translation initiation factor 3 subunit E	0.08761
KAG6595871.1	0.516699	putative eukaryotic translation initiation factor 3 subunit E-interacting protein	0.093393

GO:0090079 **translation regulator activity, nucleic acid binding**			
Protein ID	**Log2(FC)**	**Functional annotation**	**Padj**
KAG6603115.1	0.671173	Eukaryotic translation initiation factor 3 subunit J	9.45E-05
KAG6619349.1	0.474835	eukaryotic translation initiation factor 4e	0.001161
KAG6594129.1	0.866604	Eukaryotic translation initiation factor 3 subunit G	0.001624
KAG6618621.1	0.39907	Eukaryotic translation initiation factor 3 subunit H	0.006678
KAG6614344.1	0.623085	Eukaryotic translation initiation factor 3 subunit I	0.011652
KAG6579753.1	0.437859	eukaryotic translation initiation factor 1A X-chromosomal	0.014385
KAG6574525.1	0.763114	putative elongation factor 1-gamma	0.018558
KAG6610661.1	0.894803	eukaryotic translation initiation factor 3	0.023858
KAG6597779.1	0.706441	Eukaryotic translation initiation factor 3 subunit C	0.023972
KAG6609244.1	0.388053	eukaryotic initiation factor 4e	0.028484
KAG6613847.1	0.487207	rna-binding protein	0.02961
KAG6612595.1	0.616435	putative ligatin	0.050526
KAG6622031.1	0.869654	elongation factor 1-alpha	0.055748
KAG6613851.1	0.451769	Eukaryotic translation initiation factor 2 subunit beta	0.05186
KAG6610724.1	0.743249	putative eukaryotic initiation factor 4E	0.053597
KAG6594155.1	0.657719	translation elongation factor IF5A	0.054988
KAG6583094.1	0.917204	translation elongation factor Ts	0.06885
KAG6602974.1	0.531821	Peptide chain release factor 2	0.08465
KAG6615922.1	0.501539	Eukaryotic translation initiation factor 3 subunit E	0.08761
KAG6595871.1	0.516699	putative eukaryotic translation initiation factor 3 subunit E-interacting protein	0.093393

GO:0016879 **ligase activity, forming carbon-nitrogen bonds**			
Protein ID	**Log2(FC)**	**Functional annotation**	**Padj**
KAG6609667.1	1.910249	carbamoyl-phosphate synthase large subunit	1.69E-08
KAG6576588.1	1.114161	Formate-tetrahydrofolate ligase	0.000434
KAG6613395.1	1.163331	argininosuccinate synthase	0.001561
KAG6618528.1	0.888005	Aspartyl/glutamyl-tRNA (Asn/Gln) amidotransferase A subunit	0.00287
KAG6610153.1	0.702283	tRNA (Ile)-lysidine synthetase	0.004831
KAG6616894.1	0.743836	Glutamate-cysteine ligase catalytic subunit	0.008448
KAG6592448.1	0.517246	adenylosuccinate synthetase	0.011438
KAG6586611.1	0.789167	aspartyl/glutamyl-tRNA (Asn/Gln) amidotransferase B subunit	0.025114
KAG6613309.1	-0.67186	nicotinate phosphoribosyltransferase	0.036475
KAG6580005.1	0.69203	Glutathione synthetase	0.048376
KAG6592421.1	0.837153	adenylosuccinate synthetase	0.044729
KAG6615470.1	0.720729	asparagine synthase (glutamine-hydrolyzing)	0.056163
KAG6612256.1	0.816184	phosphoribosylformylglycinamidine synthase	0.067426
KAG6613700.1	0.345309	NAD+ synthetase	0.089112
KAG6576344.1	0.685754	hypothetical protein	0.080456

GO:0045182 **translation regulator activity**			
Protein ID	**Log2(FC)**	**Functional annotation**	**Padj**
KAG6603115.1	0.671173	Eukaryotic translation initiation factor 3 subunit J	9.45E-05
KAG6619349.1	0.474835	eukaryotic translation initiation factor 4e	0.001161
KAG6594129.1	0.866604	Eukaryotic translation initiation factor 3 subunit G	0.001624
KAG6618621.1	0.39907	Eukaryotic translation initiation factor 3 subunit H	0.006678
KAG6614344.1	0.623085	Eukaryotic translation initiation factor 3 subunit I	0.011652
KAG6579753.1	0.437859	eukaryotic translation initiation factor 1A X-chromosomal	0.014385
KAG6574525.1	0.763114	putative elongation factor 1-gamma	0.018558
KAG6610661.1	0.894803	eukaryotic translation initiation factor 3	0.023858
KAG6597779.1	0.706441	Eukaryotic translation initiation factor 3 subunit C	0.023972
KAG6609244.1	0.388053	eukaryotic initiation factor 4e	0.028484
KAG6613847.1	0.487207	rna-binding protein	0.02961
KAG6612595.1	0.616435	putative ligatin	0.050526
KAG6622031.1	0.869654	elongation factor 1-alpha	0.055748
KAG6613851.1	0.451769	Eukaryotic translation initiation factor 2 subunit beta	0.05186

KAG6610724.1	0.743249	putative eukaryotic initiation factor 4E	0.053597
KAG6594155.1	0.657719	translation elongation factor IF5A	0.054988
KAG6583094.1	0.917204	translation elongation factor Ts	0.06885
KAG6602974.1	0.531821	Peptide chain release factor 2	0.08465
KAG6615922.1	0.501539	Eukaryotic translation initiation factor 3 subunit E	0.08761
KAG6595871.1	0.516699	putative eukaryotic translation initiation factor 3 subunit E-interacting protein	0.093393

Chapter 5

Conclusion, contribution to knowledge and future directions

Conclusion

The *Phytophthora* genus presently includes more than 120 known pathogenic species (Kroon *et al*., 2012), representing a significant threat to the agriculture sector and natural ecosystems. New pathogenic *Phytophthora* species are continuously being identified, increasing concerns about emerging phytopathogens and effective disease management. Cell walls regulate the interaction of oomycetes with the environment, and represent promising targets for disease control. However, the cell wall biology of *Phytophthora* species remains poorly characterized. Indeed, little is known about the genes responsible for the biosynthesis of cell wall polysaccharides, the role of these genes in cell survival, and the mode of interaction between *Phytophthora*'s cell walls and plant antimicrobial peptides (AMPs). To increase our understanding of the effectiveness of AMPs against oomycetes and their interaction with the cell wall, the present work aimed to investigate the impact of the AMP NaD1 and the chitin synthase inhibitor nikkomycin Z on several *Phytophthora* species, with a strong focus on cell wall biosynthesis and *P. cinnamomi* as a case study.

The carbohydrate components of the *Phytophthora* cell wall are not well studied. Previous work provided insight into the cell wall composition of *P. infestans* and *P. parasitica* (Mélida *et al*., 2013), but the cell wall of many phytopathogenic species within this genus still remains to be studied (Goodwin, 1997). The present investigation of the cell wall carbohydrates of *P. cinnamomi* is consistent with previous reports and confirms cellulose and other glucans as the major components (**Chapter 2**). We also identified previously uncharacterised *Phytophthora* cell wall biosynthetic genes, including cellulose synthase (*CesA*), glucan synthase (*fks*) and chitin synthase (*chs*) genes, and were able to correlate gene expression patterns to the *P. cinnamomi* phenotypes observed in hyphal cells grown in the presence of NaD1 and nikkomycin z.

AMPs form part of a plant's defence system and can be found in various plant tissues such as roots, seeds, flowers, stems, and leaves. These peptides have been shown to be greatly effective against plant pathogens (Chen *et al.*, 2021), and demonstrate potential to tackle increased disease resistance in different crop families (Iqbal *et al.*, 2019). Furthermore, there is an increased interest in using AMPs as an alternative to chemical fungicides (Iqbal *et al.*, 2019). The AMP *Nicotiana alata* defensin 1 (NaD1) has been demonstrated to inhibit phytopathogenic fungi and to bind to chitin and glucans in fungal cell walls (Bleackley *et al.*, 2019). This study shows that NaD1 restricts the growth of all four *Phytophthora* species tested, and alters the morphology and apical dominance of growing hyphae (**Chapter 2**). This effect is likely due to dysregulation of intracellular calcium homeostasis and can be rescued with addition of exogenous calcium ions. Bioinformatic analysis enabled the identification of four putative voltage-gated calcium channels in *P. cinnamomi* that will be targeted for further studies (**Chapter 2**). Global transcriptomic analysis of *P. cinnamomi* suggests that NaD1 acts on the cell wall, but also on many other vital cellular processes. The data provide a more detailed understanding of the mode of action and the effects of NaD1 in *P. cinnamomi* (**Chapter 4**).

Since chitin is absent in *Phytophthora*'s cell walls, the presence and function of chitin synthase genes in these species remain unclear. Interestingly, the chitin synthase inhibitor nikkomycin Z showed inhibitory effects on the hyphal growth of all four tested species and altered the monosaccharide composition and glycosidic linkage composition in *P. cinnamomi*'s hyphal cells (**Chapter 3**). Based on transcriptomic analysis by RNA sequencing, we propose that nikkomycin Z acts on fundamental pathways, such as the hexosamine biosynthetic pathway, peptidase activity, and acyltransferase activity (**Chapter 3**).

In conclusion, this research demonstrates that the AMP NaD1 and nikkomycin Z can act as control agents for *Phytophthora* species. It also identifies putative candidate genes and their products as potential targets for *Phytophthora* disease management, thus providing the foundation to successfully tackle *Phytophthora* diseases.

Contribution to knowledge

Assessing the efficacy of the plant antimicrobial peptide NaD1 to control *Phytophthora* species through microscopic, biochemical, and genomic approaches, together with global transcriptomics is expected to provide new opportunities for controlling oomycete diseases. These discoveries hold the potential to mitigate agricultural and ecological losses through the development of inhibitors that target oomycete cell walls, novel biocontrol agents that target essential biological pathways, and transgenic plant varieties engineered to possess enhanced disease resistance. The outcomes of this study contribute to the fundamental understanding of NaD1's effects on cell wall biosynthesis and other regulatory pathways that are involved in hyphal growth and asexual reproduction. Additionally, this study provides novel insights into the genome-wide transcriptional changes in *P. cinnamomi* caused by NaD1 and nikkomycin Z.

Future directions

Inhibiting oomycetes by targeting the cell wall

Even though oomycete cell walls represent an ideal target for developing new inhibitors, this area remains largely unexplored. We have observed that a plant AMP inhibits the growth and asexual reproduction of four well-known pathogenic *Phytophthora* species. Although NaD1 did not completely kill the pathogens, we have identified several cell wall genes which have been affected. In particular, three cellulose synthase genes (*CesA*) and two glucan synthase genes (*fks*) were found to be lowly expressed in NaD1-treated *P. cinnamomi* hyphal cells. Further studies could focus on addressing the connection between NaD1 and these cell wall genes. Based on our findings, genome editing approaches (CRISPR/Cas9) could be helpful to characterise the function of these cell wall biosynthetic genes and their role in determining oomycete cell wall integrity, pathogenicity, and susceptibility to NaD1. The elucidation of the

role of cell wall biosynthetic genes in disease establishment and progression holds potential for the development of innovative disease control strategies.

Additionally, although attempts to generate zoospores from *P. cinnamomi* under *in vitro* conditions were unsuccessful in this study, it would be valuable to begin developing methods for assessing the effects of NaD1 and other potential AMPs on zoospores. A combination of microscopic, genomic, and transcriptomic approaches can be used for this purpose.

Innovative biocontrol strategies: exploring new pathways

This study offers a comprehensive overview of the transcriptional changes that occurred in the hyphal cells of *P. cinnamomi* exposed to the plant defensin NaD1 or the cell wall inhibitor nikkomycin Z. In the case of NaD1, altered expression of genes involved in calcium transport, tRNA ligase activity and acyl/acetyl-transferase activity was predominant. For nikkomycin Z, many genes related to the uridine diphosphate N-acetylglucosamine pathway, acylation-related enzymes, effector proteins, and chitin deacetylases were found to be affected. These pathways and genes have been demonstrated to be vital for the survival of pathogenic fungi, their integrity and pathogenicity (Fang *et al.*, 2013; Gascuel *et al.*, 2016; Hu *et al.*, 2007; Lockhart *et al.*, 2020; Sharma *et al.*, 2016).

Future studies should focus on these unexplored pathways in oomycetes to provide a thorough understanding of how the corresponding genes and proteins could be exploited for the development of innovative biocontrol methods. Moreover, future exploration using transformed *Phytophthora* cells that express fluorescent tagged proteins developed by the Judelson lab could help in understanding the effects of NaD1 at the cellular level (Ah-Fong *et al*., 2018)

Transgenic plant varieties with enhanced disease resistance

To date, the antimicrobial activities of plant defensins have mostly been demonstrated against pathogenic fungi. For example, NaD1 shows robust antifungal activity against *Botrytis cinerea*, *Candida albicans*, *Aspergillus niger*, *Saccharomyces cerevisiae* and *Fusarium oxysporum*

(Hayes *et al.*, 2013; Lay & Anderson, 2005; Poon *et al.*, 2014). For this reason, recent studies focused on developing resistant plant varieties by expressing genes coding for AMP synthesis for increased disease resistance against pathogenic fungi (Seo *et al.*, 2014). For example, a study showed that transgenic pepper plants expressing the plant defensin J1-1 gained strong resistance against the anthracnose fungus by reducing lesion formation and colonisation by the fungus (Seo *et al.*, 2014). Our research has demonstrated the anti-oomycete activity of the plant defensin NaD1 in species from the *Phytophthora* genus. This knowledge provides the foundation for developing transgenic plant varieties resistant to pathogenic oomycetes as a novel approach for disease control.

References

Ah-Fong, A.M.V., Kagda, M., & Judelson, H.S. (2018) Illuminating Phytophthora Biology with Fluorescent Protein Tags. In Ma, W., Wolpert, T. (eds) In *Plant Pathogenic Fungi and Oomycetes. Methods in Molecular Biology*, New York: Humana Press, 119-129.

Bleackley, M. R., Dawson, C. S., Payne, J. A. E., Harvey, P. J., Rosengren, K. J., Quimbar, P., Garcia-Ceron, D., Lowe, R., Bulone, V., van der Weerden, N. L., Craik, D. J. & Anderson, M. A. (2019) The interaction with fungal cell wall polysaccharides determines the salt tolerance of antifungal plant defensins. *The Cell Surface*, 5, 100026.

Chen, E. H.-L., Weng, C.-W., Li, Y.-M., Wu, M.-C., Yang, C.-C., Lee, K.-T., Chen, R. P.-Y. & Cheng, C.-P. (2021) De novo design of antimicrobial peptides with a special charge pattern and their application in combating plant pathogens. *Frontiers in Plant Science*, 12, 753217.

Fang, W., Du, T., Raimi, O. G., Hurtado-Guerrero, R., Urbaniak, M. D., Ibrahim, A. F., Ferguson, M. A., Jin, C. & van Aalten, D. M. (2013) Genetic and structural validation of A spergillus fumigatus UDP-N-acetylglucosamine pyrophosphorylase as an antifungal target. *Molecular Microbiology*, 89(3), 479-493.

Gascuel, Q., Buendia, L., Pecrix, Y., Blanchet, N., Muños, S., Vear, F. & Godiard, L. (2016) RXLR and CRN Effectors from the sunflower downy mildew pathogen *Plasmopara halstedii* induce hypersensitive-like responses in resistant sunflower lines. *Frontiers in Plant Science*, 7, 1887.

Goodwin, S. B. (1997) The population genetics of phytophthora. *Phytopathology*, 87(4), 462-73.

Hayes, B. M., Bleackley, M. R., Wiltshire, J. L., Anderson, M. A., Traven, A. & van der Weerden, N. L. (2013) Identification and mechanism of action of the plant defensin NaD1 as a new member of the antifungal drug arsenal against *Candida albicans*. *Antimicrobial Agents and Chemotherapy*, 57(8), 3667-75.

Hu, W., Sillaots, S., Lemieux, S., Davison, J., Kauffman, S., Breton, A., Linteau, A., Xin, C., Bowman, J. & Becker, J. (2007) Essential gene identification and drug target prioritization in *Aspergillus fumigatus*. *PLoS Pathogens*, 3(3), e24.

Iqbal, A., Khan, R. S., Shehryar, K., Imran, A., Ali, F., Attia, S., Shah, S. & Mii, M. (2019) Antimicrobial peptides as effective tools for enhanced disease resistance in plants. *Plant Cell, Tissue and Organ Culture (PCTOC)*, 139(1), 1-15.Lay, F. T. & Anderson, M. A. (2005) Defensins--components of the innate immune system in plants. *Current Protein & Peptide Science*, 6(1), 85-101.

Lockhart, D. E. A., Stanley, M., Raimi, O. G., Robinson, D. A., Boldovjakova, D., Squair, D. R., Ferenbach, A. T., Fang, W. & van Aalten, D. M. F. (2020) Targeting a critical step in fungal hexosamine biosynthesis. *Journal of Biological Chemistry*, 295(26), 8678-8691.

Mélida, H., Sandoval-Sierra, J. V., Diéguez-Uribeondo, J. & Bulone, V. (2013) Analyses of extracellular carbohydrates in oomycetes unveil the existence of three different cell wall types. *Eukaryotic Cell*, 12(2), 194-203.

Poon, I. K. H., Baxter, A. A., Lay, F. T., Mills, G. D., Adda, C. G., Payne, J. A. E., Phan, T. K., Ryan, G. F., White, J. A., Veneer, P. K., van der Weerden, N. L., Anderson, M. A., Kvansakul, M. & Hulett, M. D. (2014) Phosphoinositide-mediated oligomerization of a defensin induces cell lysis. *eLife*, 3, e01808.

Seo, H.-H., Park, S., Park, S., Oh, B.-J., Back, K., Han, O., Kim, J.-I. & Kim, Y. S. (2014) Overexpression of a defensin enhances resistance to a fruit-specific anthracnose fungus in pepper. *PloS One*, 9(5), e97936.

Sharma, M., Guleria, S. & Kulshrestha, S. (2016) Diacylglycerol acyl transferase: A pathogenicity related gene in *Colletotrichum gloeosporioides*. *Journal of Basic Microbiology*, 56(11), 1308-1315.

Appendix

Career and Research Skills Training (CaRST)

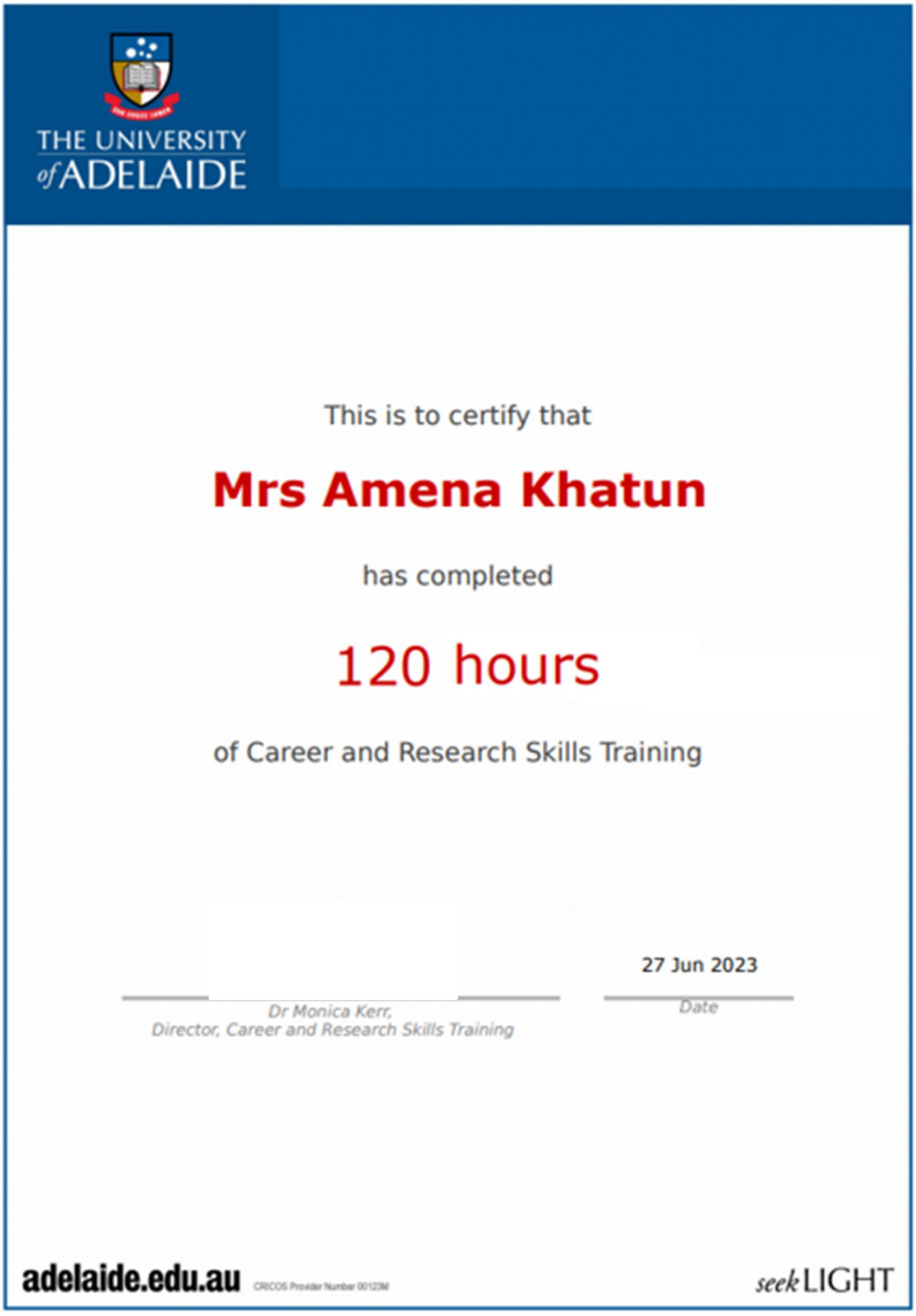

THE UNIVERSITY of ADELAIDE

This is to certify that

Mrs Amena Khatun

has completed

120 hours

of Career and Research Skills Training

27 Jun 2023

Dr Monica Kerr,
Director, Career and Research Skills Training

Date

adelaide.edu.au CRICOS Provider Number 00123M

seekLIGHT